



4
2010



This is to certify that the
dissertation entitled

Genetic analysis of tocopherol functions in *Arabidopsis* at low
temperatures

presented by

Wan Song

has been accepted towards fulfillment
of the requirements for the

Ph.D. degree in Genetics

Major Professor's Signature

12/17/09

Date

GENETIC ANALYSIS OF TOCOPHEROL FUNCTIONS IN *ARABIDOPSIS*
AT LOW TEMPERATURES

By

Wan Song

A DISSERTATION

Submitted to
Michigan State University
in partial fulfillment of the requirements
for the degree of

DOCTOR OF PHILOSOPHY

Genetics

2009

ABSTRACT

GENETIC ANALYSIS OF TOCOPHEROL FUNCTIONS IN *ARABIDOPSIS* AT LOW TEMPERATURES

By

Wan Song

Tocopherols (vitamin E) are lipid-soluble antioxidants that are synthesized only by photosynthetic organisms. Molecular dissection of the tocopherol biosynthetic pathway in *Arabidopsis* and *Synechocystis* and the availability of various mutants containing different amounts and compositions of tocopherols have greatly facilitated studies directed at elucidating tocopherol functions in photosynthetic organisms. Blockage in phloem source-to-sink transportation is a common phenotype shared by multiple tocopherol-deficient plant species but the molecular mechanism behind the phenomenon has remained enigmatic. The phenotype in *Arabidopsis thaliana* tocopherol deficient *vte2* mutant is inducible under low temperature (LT) treatment and thus provides an ideal system to study the relevant tocopherol functions. A series of events occurs in *vte2* mutant, including abnormal transfer cell wall development, vascular callose deposition, impaired photoassimilate export capacity, sugar and starch accumulation, which eventually led to growth inhibition during LT adaptation. A forward genetic screen for mutations that suppress the *vte2* LT-induced phenotypes was undertaken in order to understand the genetic basis of the *vte2* phenotype and determine links between tocopherol deficiency and the *vte2* LT-induced phenotypes. Seven independent *sve* (*suppressor of vte2 low temperature-induced phenotype*) lines were identified from EMS mutagenized *vte2* population and three lines were selected for further detailed analysis and molecular cloning based on biochemical characterization of the primary *sve* lines.

sve1 completely suppressed all *vte2* LT phenotypes and was found to be a novel allele of *fad2*, the endoplasmic reticulum-localized oleate desaturase. *sve2* showed partial suppression and was found to be a new allele of *trigalactosyldiacylglycerol1* (*tgdl*), a component of the ER-to-plastid lipid ATP-binding cassette (ABC) transporter. Introduction of *tgdl2*, *tgdl3*, and *tgdl4* mutations into the *vte2* background similarly suppressed the *vte2* LT phenotypes, indicating a key role for lipid transport in this process. *sve7* partially suppressed all *vte2* LT phenotypes without impacting fatty acid and lipid metabolism at permissive temperature. Analyses of the acyl composition of ER- and plastid-derived lipids before and after LT treatment demonstrated the elevation of 18:2 in phosphatidylcholine is an early and key component in *vte2* LT-induced responses as all suppressors attenuated this change. Identification and characterization of *sve* loci highlights the involvement of ER lipid metabolism in tocopherol function in plants. A global transcript profiling study was carried out to further investigate the transcriptional effect of tocopherol deficiency and understand the *vte2* LT-induced phenotypes. By comparing *vte2* and wild type under different time period of LT treatment, it was shown that tocopherol deficiency had no effect on gene expression at permissive conditions but affected a limited number of specific genes after 48h of LT treatment. Based on gene expression profiles, tocopherol deficiency appeared to result in some degree of oxidative stress response and influenced the expression of genes involved in cell wall modification and solute transport in LT-treated *vte2*. Statistical analyses also highlighted several potentially important target genes for future studies. These results together provide new insights into tocopherol functions in LT adaptation in plants.

ACKNOWLEDGEMENTS

First of all I would like to express my deep and sincere gratitude to my advisor Dr. Dean DellaPenna, professor of Department of Biochemistry and Molecular Biology, Michigan State University. Dean gave me the opportunity to work in his lab for the past five years and provided me with many helpful suggestions, important advice and constant encouragement during the course of this work. I have not only learned how to solve various problems and get smarter avoiding making the same mistakes the next time but also from his management of time and handling of multitasks how to be an good and efficient scientist. I am also grateful for his great support during my breastfeeding and allowing me to occupy a separate office during my manuscript and thesis writing.

I would also like to thank my past and present guidance committee. Dr. Andreas Weber, Dr. Rob Last, Dr. John Ohlrogge and Dr. Markus Pauly for their guidance, encouragement and help through my graduate research.

Special thanks are due to Hiroshi Maeda, for his direct guidance during my rotation period in the lab and his continuous support and friendship through the end of my thesis research. His enthusiasm towards scientific research has greatly influenced me.

I would like to thank the former and present members of the DellaPenna Lab, especially Laura Ullrich, for her patience, kindness and help in genetics; Scott Sattler for providing the EMS mutagenized *vte2* seed and helpful suggestions; Joonyul Kim for his help in the protein alignment analysis; Payam Mehrshahi and Sabrina Jorge for their great support and friendship; Laurent Mene-Saffrane for his generosity in sharing of new ideas and all the other former and present members of the DellaPenna lab, Naoko Kobayashi,

Eun-Ha Kim, Holly Little, Maria Magallanes, Jiying Li for their friendship and assistance. Sincere thanks are extended to all former and present members of Dr. Christoph Benning's lab, especially Changcheng Xu and Eric Moellering for their great technical assistance in lipid analysis and helpful discussions.

My special appreciation goes to my mother, Sizhen Yao, my sisters and my brother, though living far away in another country, they always support and encourage me to focus on scientific research.

I would like to express my heartiest thanks to my friends, Carlene Meijer and Herb Meijer, for their kindness, affection and encouragement; Feng Shi, Ailing Zhou, Xiangrong Guo, Xiaohua Wang, and for sharing the parental tips and their friendships have made me feel that I am not too far away from my parents and country.

Finally, I would like to express special thanks to my husband Zhiyuan Jia. He took the responsibility of taking care of our son and kept me away from most of family responsibilities so that I could concentrate on completing this dissertation in the last few months and supported mentally during the course of this work. Without his help and encouragement, this study would not have been completed.

TABLE OF CONTENTS

LIST OF TABLES	VIII
LIST OF FIGURES	X
CHAPTER 1 LITERATURE REVIEW	1
 TOCOPHEROLS.....	1
 PLANT ADAPTATION TO LOW TEMPERATURE STRESS	12
 AIM OF THIS STUDY	22
 TABLES AND FIGURES.....	24
CHAPTER 2 GENETIC SCREEN AND PRELIMINARY CHARACTERIZATION OF SUPPRESSOR OF <i>VTE2</i> LOW TEMPERATURE-INDUCED PHENOTYPES	30
 ABSTRACT.....	30
 INTRODUCTION	32
 RESULTS	37
 DISCUSSION.....	43
 MATERIALS AND METHODS	47
 TABLES AND FIGURES.....	50
CHAPTER 3 CLONING OF <i>ARABIDOPSIS SVE</i> (SUPPRESSORS OF <i>VTE2</i> LOW TEMPERATURE-INDUCED PHENOTYPE) MUTANTS HIGHLIGHT THE INVOLVEMENT OF TOCOPHEROLS IN LIPID METABOLISM.....	65
 ABSTRACT.....	65
 RESULTS	69
 DISCUSSION	78
 MATERIALS AND METHODS	84
 TABLES AND FIGURES.....	88
CHAPTER 4 MICROARRAY ANALYSIS OF THE LOW TEMPERATURE RESPONSE OF THE <i>ARABIDOPSIS VTE2</i> MUTANT	118
 ABSTRACT.....	118
 INTRODUCITON	120
 RESULTS	123
 DISCUSSION	134
 MATERIALS AND METHODS	137
 TABLES AND FIGURES.....	142
CHAPTER 5 SUMMARY AND FUTURE PERSPECTIVES	161

APPENDIX.....	171
TOCOPHEROLS PLAY A CRUCIAL ROLE IN LOW TEMPERATURE ADAPTATION AND PHLOEM LOADING IN <i>ARABIDOPSIS</i>	171
LITERATURE CITED	255

LIST OF TABLES

Table 1.1 Phenotypes of lipid metabolism mutants at low temperature conditions.	24
Table 2.1 A summary of the primary <i>sve</i> lines identified from suppressor screens.	50
Table 2.2 Leaf fatty acid composition of the primary <i>sve</i> lines, <i>Col</i> , <i>vte2</i> and <i>vte1</i> at permissive conditions.....	52
Table 2.3 Leaf fatty acid composition of four primary <i>sve</i> lines and <i>Col</i> , <i>vte2</i> and <i>vte1</i> after 14 d of LT treatment.....	53
Table 3.1 Leaf fatty acid composition of <i>sve1vte2</i> , <i>sve2vte2</i> and <i>sve7vte2</i> compared with <i>Col</i> , <i>vte2</i> and <i>vte1</i>	88
Table 3.2 Leaf fatty acid composition and photoassimilate export capacity of <i>sve1vte2</i> backcross populations.	89
Table 3.3 Acyl compositions of PC, PE, DGDG, MGDG in indicated genotypes before LT treatment	90
Table 3.4 Acyl compositions of PC, PE, DGDG, MGDG in indicated genotypes after 14d LT treatment	94
Table 4.1 The 49 genes significantly upregulated in <i>vte2</i> relative to <i>Col</i> at 48h of LT treatment.....	142
Table 4.2 The 28 genes significantly downregulated in <i>vte2</i> relative to <i>Col</i> at 48h of LT treatment	144
Table 4.3 Genes containing W box sequence (C/T)TGAC(T/G) in the 1000bp upstream regions.....	145
Table 4.4 Common 12 genes between the 77 significantly different genes in 48h-LT-treated <i>vte2</i> plant and 744 significantly different genes in 3-d-old <i>vte2</i> seedling.	146
Table A.1 Tocopherol and DMPBQ Content in Leaves of Wild Types and Tocopherol Biosynthetic Mutants Grown Under Permissive Conditions.....	209

Table A.2 Content of Photosynthetic Pigments and Tocopherols of Col and the <i>vte2</i> and <i>vte1</i> Mutants After HL1800 Treatment at 22°C.....	210
Table A.3 Yields and Abortion Rates of Seed Produced During Low Temperature (7.5°C) Treatment.....	211
Table A.4 Content of Photosynthetic Pigments and Tocopherols of Col and the <i>vte2</i> and <i>vte1</i> Mutants Grown at Permissive condition.....	212
Table A.5 Content of Individual Photosynthetic Pigments of Col and the <i>vte2</i> Mutant During Low Temperature (7.5°C) Treatment.....	213

LIST OF FIGURES

Figure 1.1 Structure of tocopherols.	25
Figure 1.2 Tocopherol biosynthetic pathway and locations of mutations in <i>Arabidopsis thaliana</i>	27
Figure 1.3 An abbreviated diagram of two pathways of glycerolipid biosynthesis in <i>Arabidopsis</i> leaves.	28
Figure 2.1 Suppressor screening scheme.	54
Figure 2.2 An example flat from the first round of suppressor screening.	55
Figure 2.3 An example image of the second round of suppressor screening.	56
Figure 2.4 Whole plant phenotype of primary lines of <i>sve1vte2-sve7vte2</i> compared with Col, <i>vte2</i> and <i>vte1</i> before LT treatment.	57
Figure 2.5 Whole plant phenotype of the primary lines <i>sve1vte2-sve7vte2</i> compared with Col, <i>vte2</i> and <i>vte1</i> after LT treatment.	58
Figure 2.6 Leaf total soluble sugar content in primary <i>sve1vte2-sve7vte2</i> lines compared with Col, <i>vte2</i> and <i>vte1</i>	59
Figure 2.7 Total ¹⁴ CO ₂ fixation after 7 d of LT treatment of primary <i>sve1vte2-sve7vte2</i> lines compared with Col, <i>vte2</i> and <i>vte1</i>	60
Figure 2.8 Percent exudation of primary <i>sve1vte2-sve7vte2</i> lines compared with Col, <i>vte2</i> and <i>vte1</i>	61
Figure 2.9 Callose deposition in primary <i>sve1vte2-sve7vte2</i> lines compared with Col, <i>vte2</i> and <i>vte1</i> after 3 d of LT treatment.	62
Figure 2.10 Callose deposition in primary <i>sve1vte2-sve7vte2</i> lines compared with Col, <i>vte2</i> , and <i>vte1</i> after 7 d of LT treatment.	63
Figure 2.11 Molar ratios of linoleic acid (18:2) and linolenic acid (18:3) in primary suppressor lines of <i>sve3vte2</i> , <i>sve4vte2</i> , <i>sve6vte2</i> , <i>sve7vte2</i> compared with Col, <i>vte2</i> and <i>vte1</i> after 14 d of LT treatment.	64
Figure 3.1 Whole plant phenotypes of LT treated Col, <i>vte2</i> , <i>sve1vte2</i> , <i>sve2vte2</i> , <i>sve7vte2</i> , and the F1 progeny of <i>sve1vte2</i> , <i>sve2vte2</i> , <i>sve7vte2</i> × <i>vte2</i>	98
Figure 3.2 A demonstration of leaf phenotypes of F2 population from <i>sve1vte2</i> × <i>vte2</i> backcross.	99

Figure 3.3 LT phenotypes of <i>sve1vte2</i> , <i>sve2vte2</i> and <i>sve7vte2</i> compared with Col, <i>vte2</i> and <i>vte1</i>	100
Figure 3.4 Complementation test of <i>sve1vte2</i> and <i>fad2-1vte2</i>	102
Figure 3.5 <i>sve2</i> carries a single recessive mutation in <i>TGD1</i>	105
Figure 3.6 Complementation test of <i>sve2vte2</i> and <i>tgdlvte2</i>	107
Figure 3.7 <i>tgd2</i> , <i>tgd3</i> and <i>tgd4</i> also suppress the <i>vte2</i> LT phenotypes.....	109
Figure 3.8 <i>tgd</i> mutations impact differently on <i>vte2</i> LT-induced callose deposition.	111
Figure 3.9 Correlation of individual lipid species with photoassimilate export capacity.	112
Figure 3.10 Callose deposition in leaf vascular tissues of the indicated genotypes after 7 d of LT treatment.	114
Figure 3.11 Multiple sequence alignment of relevant regions of FAD2 (A) and TGD1 (B) from representative photosynthetic organisms.	115
Figure 3.12 Callose deposition in the indicated genotypes after 7 d LT treatment.	116
Figure 3.13 Scattered plot of photoassimilate export capacity versus leaf total sugar content.....	117
Figure 4.1 RNA degradation plot for the 18 arrays used in this study.	147
Figure 4.2 QC plot of 3': 5' ratios for control genes, percentage of present gene calls and background levels.	148
Figure 4.3 Box plot of all perfect match (pm) intensities (Log2) of unnormalized 18 array data set.	150
Figure 4.4 Histogram of kernel density estimates of all perfect match (pm) probe intensities (Log2) of unnormalized 18 array data set.....	151
Figure 4.5 Box plot of all perfect match probe intensities (Log2) of quantile normalized array data.....	152
Figure 4.6 Histogram of kernel density estimates of all perfect match probe intensities (Log2) of quantile normalized 18 array data set.....	153
Figure 4.7 Cluster dendrogram of a correlation matrix for all-against-all chip comparisons.	154
Figure 4.8 A gene tree of the 77 significantly different genes in 48h-LT-treated <i>vte2</i> relative to Col.....	155

Figure 4.9 Normalized expression levels of <i>Msr</i> genes in Col (gray) and <i>vte2</i> (purple) at different time points of LT treatment.....	156
Figure 4.10 A heat map of expression of the significantly upregulated 49 genes in 48h LT-treated <i>vte2</i> under different conditions.	157
Figure 4.11 Whole plant phenotype of Col, <i>vte2</i> , <i>gsl4</i> , <i>gsl4vte2</i> , <i>gsl11</i> , <i>gsl11vte2</i>	159
Figure 4.12 Vascular callose deposition in Col, <i>vte2</i> , <i>gsl4</i> , <i>gsl4vte2</i> , <i>gsl11</i> and <i>gsl11vte2</i> after 3 d of LT treatment.....	160
Figure 5.1 A genetic model of <i>vte2</i> responses under LT treatment.....	170
Figure A.1 Tocopherol Biosynthetic Pathway and <i>vte</i> Mutations in <i>Arabidopsis thaliana</i>	215
Figure A.2 Phenotypic and Photosynthetic Responses of Col and the <i>vte2</i> and <i>vte1</i> Mutants to HL stress.	216
Figure A.3 Visible Phenotype of <i>vte</i> Mutants During Extended Low Temperature Treatment.	221
Figure A.4 Tocopherol, Lipid Peroxide, Anthocyanin, and Photosynthetic Pigment Content of Col and the <i>vte2</i> Mutant During Four Weeks of Low Temperature Treatment.	223
Figure A.5 Photosynthetic Status of Col and the <i>vte2</i> Mutant During Four Weeks of Low Temperature Treatment.....	226
Figure A.6 Changes in Starch and Soluble Sugar levels in Col and the <i>vte2</i> Mutant During Four Weeks of Low Temperature Treatment.	229
Figure A.7 Diurnal Changes in Starch and Soluble Sugar levels in Col and the <i>vte2</i> Mutant During the First Four Days of Low Temperature Treatment.	231
Figure A.8 Biochemical Phenotypes in Mature and Young Leaves of Col, and the <i>vte2</i> and <i>vte1</i> Mutants After Four Weeks of Low Temperature Treatment.....	233
Figure A.9 Translocation and Export of ¹⁴ C Labeled Photoassimilates in Low Temperature-Treated Col and the <i>vte2</i> and <i>vte1</i> Mutants.....	235
Figure A.10 Aniline Blue Positive Fluorescence in Leaves of Col and the <i>vte2</i> Mutant During Low Temperature Treatment.	240
Figure A.11 Aniline Blue Positive Fluorescence in Leaves of the <i>vte2</i> Mutant at Various Light Intensities under Permissive and Low Temperature Conditions.....	242

Figure A.12 Cellular Structure and Immunodetection of Callose in Col and <i>vte2-1</i> Before and After 14 Days of Low Temperature Treatment.....	244
Figure A.13 Cellular Structure and Immunodetection of Callose in <i>vte2-1</i> After 3 Days of Low Temperature Treatment.	246
Figure A.14 Phenotypes of the <i>vte2</i> Mutant and Col During HL, Drought and Salinity Stress.	247
Figure A.15 Phenotypic and Photosynthetic Responses of Col and the <i>vte2</i> and <i>vte1</i> Mutants to HL stress.	250
Figure A.16 Aniline Blue Positive Fluorescence in Leaves of the <i>vte2</i> and <i>vte1</i> Mutant During Low Temperature Treatment.	252

Images in this dissertation are presented in color

CHAPTER 1 LITERATURE REVIEW

TOCOPHEROLS

Structure, physiochemical and physical properties

Vitamin E is a collective term for a group of eight amphipathic compounds derived from tocopherols and tocotrienols (α -, β -, γ -, and δ -tocopherol and α -, β -, γ -, and δ -tocotrienol). All tocopherol and tocotrienols (“tocochromanols”) possess a chromanol ring head and 16-carbon hydrophobic side chain tail (Figure 1.1). The fully saturated 16-carbon side chain of tocopherols is derived from phytol while 16-carbon side chain of tocotrienols is derived from geranylgeranyl and contains three double bonds at C-3', C-7' and C-11'. The α -, β -, γ -, δ - isomer of tocochromanols designate the number and position of methyl substituents attached to the chromanol head group (Schneider, 2005).

The physiochemical roles of tocochromanols as non-enzymatic antioxidants are well established. Tocochromanols are can quench singlet oxygen $^1\text{O}_2$ and scavenge a variety of reactive oxygen species (ROS) and free radicals, including the superoxide anion radical (O_2^-), hydrogen peroxide (H_2O_2), and the hydroxyl radical ($\text{HO}\cdot$) (Brigelius-Flohe and Traber, 1999; Wang and Quinn, 2000). The chromanol hydroxyl group is critical for the antioxidant activity of tocochromanols as it allows donation of a hydrogen atom from this group (KamalEldin and Appelqvist, 1996). Donation of the chromanol ring hydrogen generates the tocochromanol radical, which is relatively long lived and stable and can be converted to tocochromanol by direct interaction with redox-active reagents like ascorbate or other reductants (Liebler, 1993). In contrast, other aromatic antioxidants must donate two hydrogen atoms to attain a stable state (Liebler and Burr, 2000). As they

are localized within membranes, tocopherols primarily act as potent lipid-soluble antioxidants to prevent free radical damage of polyunsaturated fatty acids (PUFAs) acyl chains. The oxidation reactions by the free radicals can start a very destructive chain reaction of lipid peroxidation. By reacting rapidly with fatty acid peroxy radicals, the primary products of lipid peroxidation, and converting the lipid peroxy radicals to lipid hydroperoxides, tocopherols terminate the propagation of lipid peroxidation chain reactions (Burton and Ingold, 1981; Schneider, 2005). The lipid hydroperoxides produced are enzymatically or non-enzymatically converted to relatively inert hydroxy fatty acids or other products.

The physical roles of tocopherols in membranes are less well appreciated. Various biophysical techniques have shown that the ring hydroxyl of tocopherols interact with the polar head groups of lipids while the prenyl chain anchors the molecule firmly within the phospholipid bilayer orienting the chromanol ring moiety towards the lipid-water interface of the phospholipid bilayer (Erin et al., 1983; Gorbunov et al., 1991; Salgado et al., 1993; Atkinson et al., 2008). However, the orientation and depth of chromanol head group of tocopherols in the lipid bilayer is yet to be determined (Fukuzawa, 2008). Studies have shown that tocopherols spontaneously and dynamically associate with unsaturated lipids (Stillwell et al., 1992). In addition, when incorporated into membranes, α -tocopherol assumes a negative curvature that is even higher than cholesterol (Chen and Rand, 1997; Bradford et al., 2003; Atkinson et al., 2008), and as such may have significant effects on membrane curvature stress and processes such as vesicle fusion (Churchward et al., 2005). The matching curvatures between α -tocopherol (negative) and lysolipids (positive) also contribute to the well-known property of

tocopherols in countering the detergent-like, membrane-destabilizing effects of lysolipids (Erin et al., 1986). These physical properties underlie the phenomena that tocopherols preferentially partition into PUFA-enriched membrane domains (SanchezMigallon et al., 1996) and potentially into those membrane domains sensitive to aspects of lipid packing and curvature stress (Atkinson et al., 2008). Therefore, although tocopherols are usually relatively minor membrane component, they may be able to exert a significant structural role via localized effects.

Tocopherols in animals

Vitamin E is an essential nutrient for humans and animals that must be obtained through the diet. Vitamin E is taken up as the free alcohol by the intestine, secreted into chylomicrons and then taken up by the liver. Although all tocopherols are taken up and transported to the liver with similar kinetics (Brigelius-Flohe and Traber, 1999), in the liver, α -tocopherol is specifically bound and transferred by α -tocopherol transfer protein (α TTP) (Hosomi et al., 1997) and secreted into very-low-density lipoprotein (VLDL). Metabolism of VLDL results in the delivery of α -tocopherol into low-density lipoprotein (LDL) and high-density lipoprotein (HDL) (Traber et al., 2004). Chemically, all tocopherols have similar antioxidant activity but differ in biological activity as vitamin E by orders of magnitude due largely to the preferential retaining of α -tocopherol by the body. α -tocopherol is thus the biologically most active form of vitamin E, accounting for over 90% of the vitamin E activity found in tissues (Cohn, 1997).

Vitamin E was first discovered as early as in 1922 as a micronutrient that was indispensable for reproduction in female rats (Evans and Bishop, 1922). Since then, symptoms of vitamin E deficiency have been produced experimentally in different animal

species, e.g. muscular dystrophy and encephalomalacia in chickens (Shih et al., 1977) and neurologic lesions in rats and monkeys (Towfighi, 1981). In addition, lack of a functional α TTP gene causes delayed onset of ataxia and retinal degeneration in mice (Yokota et al., 2001) and an autosomal recessive neurodegenerative disease called ataxia with isolated vitamin E deficiency (AVED) with symptoms such as hyporeflexia, ataxia, limitation of upward gaze and profound muscle weakness in humans (Gotoda et al., 1995). The precise molecular mechanisms of these vitamin E deficiency symptoms, especially the role of α -tocopherol in the interplay between nerves and muscles, remain elusive. While the mechanism for this is still not elucidated, in almost every major chronic disease, free radical oxidative damage has been implicated (Pratico et al., 1998; Yokota et al., 2001; Ahuja et al., 2004) and numerous studies suggest that activity of vitamin E as scavenger of reactive metabolites of oxygen and as an inhibitor of lipid peroxidation in membrane may play a mechanistic role in its impact on chronic diseases (Brigelius-Flohe and Traber, 1999).

Increasing evidence is suggesting that in addition to its antioxidant role, vitamin E also exerts biological effects through non-antioxidant mechanisms. Several studies have shown that individual tocopherols have physiological activities beyond their action as antioxidants. α -, but not β - tocopherol, was found to specifically inhibit the enzymatic activity of protein kinase C (PKC), an important player in cellular signaling in vascular smooth muscle cells leading to growth arrest (Boscoboinik et al., 1991), probably by upregulating cytosolic protein phosphatase 2A (PP_{2A}) which leads to increased dephosphorylation and inactivation of PKC (Ricciarelli et al., 1998). α -tocopherol was also shown to specifically modulate expression of various genes, including the SR-A and

CD36 scavenger receptors (specific receptors for oxidized low density lipoprotein) in smooth muscle cells (Ricciarelli et al., 2000), collagenase in human skin fibroblasts (Ricciarelli et al., 1999) as well as α -tropomyosin (an actin-binding protein important for muscle contraction) (Aratri et al., 1999). γ -tocopherol also possesses unique features as it specifically inhibits cyclooxygenase activity and thus has anti-inflammatory properties (Jiang et al., 2001). All these effects are unrelated to the antioxidant activities of the molecules, and possibly reflect specific interactions of the individual tocopherols with enzymes, structural proteins, lipids, or transcription factors (Zingg and Azzi, 2004).

Tocopherol biosynthesis and distribution in plants

Vitamin E compounds are exclusively produced by photosynthetic organisms, including all plants, algae and most cyanobacteria (Dasilva and Jensen, 1971; Grusak and DellaPenna, 1999; Horvath et al., 2006). In most dicotyledonous species, tocopherols are the principle vitamin E components in leaves and seeds while tocotrienols are found in high amounts in seeds of certain cereal species (DellaPenna, 2005a).

The biosynthetic pathway of tocopherols in *Arabidopsis* has been elucidated from radiotracer studies in isolated chloroplasts and cyanobacteria in the early 1970's (Whistanc and Threlfal, 1970). During the last 10 years, the enzymes of the core pathway have been isolated by the combined approaches of genomics, genetics and biochemical analyses (Shintani and DellaPenna, 1998; DellaPenna, 1999; Collakova and DellaPenna, 2001; Porfirova et al., 2002; Shintani et al., 2002; Cheng et al., 2003; Sattler et al., 2003b; DellaPenna, 2005b, a). As shown in Figure 1.2, tocopherols are biosynthesized from two converging pathways, with the head group (homogentisic acid, HGA) produced from tyrosine catabolism via the shikimate pathway (Herrmann and Weaver, 1999), and the tail

group (phytyl diphosphate, PDP) synthesized via the non-mevalonate 2-C-methyl-D-erythritol 4-phosphate/deoxy-xylulose phosphate (MEP/DOXP) pathway in plastids (Schwender et al., 1996). In addition, an enzyme encoding a phytol kinase activity (encoded by *VTE5*) was recently identified to provide an alternative source of PDP from chlorophyll hydrolysis for tocopherol synthesis (Valentin et al., 2006). The first committed step is catalyzed by homogentisate prenyl transferase (HPT, encoded by *VTE2*), condensing PDP with HGA to produce 2-methyl-6-phytyl-1,4-benzoquinol (MPBQ), the first intermediate for the synthesis of all forms of tocopherols. MPBQ can be methylated by MPBQ methyl transferase (MT1, encoded by *VTE3*) to produce 2,3-dimethyl-6-phytyl-1,4-benzoquinol (DMPBQ). Tocopherol cyclase (TC, encoded by *VTE1*) can act on either MPBQ or DMPBQ to produce δ -tocopherol or γ -tocopherol, respectively. The final production of β -tocopherol or α -tocopherol is catalyzed by a second methyl transferase, γ -tocopherol methyltransferase (γ TMT, encoded by *VTE4*) from δ -tocopherol and γ -tocopherol, respectively. In Arabidopsis, α -tocopherol predominates in photosynthetic tissues while γ -tocopherol is the major tocopherol in seed (Grusak and DellaPenna, 1999). Identification of the genes and rate-limiting activities for vitamin E biosynthesis have greatly facilitated engineering efforts to dramatically elevate vitamin E levels in crop species (Collakova and DellaPenna, 2003a; DellaPenna and Last, 2006).

There are large variations in the content and compositions of vitamin E in different plants and tissues (Grusak and DellaPenna, 1999). Generally 10 to 50 μg vitamin E /g FW exists in unstressed leaves, with the predominant form being α -tocopherol. Seeds are highly variable and contain many forms of tocotrienols or tocopherols (α , β , γ , δ), with a

much wider range of content (300–2000 µg vitamin E /g oil(DellaPenna and Last, 2006). Many studies indicate that tocopherols and tocotrienols are localized in plastids (Lichtenthaler et al., 1981; Fryer, 1992; Kruk and Strzalka, 1995; Munne-Bosch and Alegre, 2002). Though plastid envelopes are the primary sites of tocopherol synthesis, roughly equal amount of α -tocopherol is found in envelopes (Lichtenthaler et al., 1981; Arango and Heise, 1998) and thylakoid membranes, which include plastoglobuli (Lichtenthaler et al., 1981; Wise and Naylor, 1987; Havaux, 1998). In addition, high levels of tocopherols (as much as 38% of the total seed tocopherol content) have been reported in oil bodies of soybean, oat and sunflower, which are extraplastidic organelles derived from the ER (Yamauchi and Matsushita, 1976; Fisk et al., 2006; White et al., 2006). Extra-plastidic localization of low amounts of α -tocopherol has also been reported in vacuoles isolated from barley leaves, mitochondria in spinach leaves and microsomal membranes in iron-supplemented soybean roots (Dilley and Crane, 1963; Rautenkranz et al., 1994; Caro and Puntarulo, 1996). These studies have provided evidence that while tocopherols are certainly synthesized in plastids their localization is not necessarily restricted to this organelle.

Tocopherol functions in plants

The fully characterized tocopherol biosynthetic pathway and availability of various mutants defective in specific steps of the core pathway (*vte1* through *vte4*, Figure 1.2) (Porfirova et al., 2002; Cheng et al., 2003; Sattler et al., 2003b; Sattler et al., 2004) have greatly facilitated functional studies of tocopherols in plants and begun to uncover the multi-facet functions (Dormann, 2007; Maeda and DellaPenna, 2007). The *Arabidopsis* *vte1* mutant, which lacks all forms of tocopherols but accumulate equivalent amounts of

redox active biosynthetic intermediate DMPBQ, and *vte2* mutant, which lacks all forms of tocopherols as well as DMPBQ, have been particularly useful in this regard. Both *vte2* and *vte1* have been shown to have significantly reduced seed longevity compared to wild type and this is directly related to the antioxidant function of tocopherols. In addition, *vte2* mutants have severe seedling developmental defects, including impaired cotyledon expansion and reduced root growth, and contain massive amounts of non-enzymatic lipid peroxidation products, including lipid peroxides, lipid hydroperoxides, malondialdehyde (MDA) and phytoprostanes, in comparison to wild type (Sattler et al., 2004; Sattler et al., 2006). These combined results clearly indicate that a principle function of tocopherols in plants is to protect PUFAs from nonenzymatic oxidation during seed storage, germination, and early seedling development.

In mature photosynthetic tissues, tocopherols have long been assumed to provide photoprotection (Fryer, 1992; Munne-Bosch and Alegre, 2002) since the chloroplast is one of the major locations where ROS are produced (Knox and Dodge, 1985; Robinson, 1988). Consistent with this theory is the observation that tocopherol levels tend to increase in response to various abiotic stresses including high-intensity light (Collakova and DellaPenna, 2003b; Muller-Moule et al., 2003), cold (Maeda et al., 2006), drought (Munne-Bosch and Alegre, 2000), heat (Bergmuller et al., 2003), osmotic (Abbasi et al., 2007) and heavy metals (Collin et al., 2008). However, after germination *vte2* and *vte1* mutant plants are indistinguishable from wild type, suggesting tocopherols are not vital in *Arabidopsis* plants under optimal growth conditions (22/18°C, 120 $\mu\text{E m}^{-2} \text{s}^{-1}$) (Maeda et al., 2006). Similarly, *vte2* plants were similarly indistinguishable from wild type plants under drought and salt stress conditions (Maeda et al., 2006). Even when placed under

severe photooxidative stress conditions, the extent of bleaching and photoinhibition in *vte2* and *vte1* was similar to wild type (Porfirova et al., 2002; Havaux et al., 2005; Kanwischer et al., 2005; Maeda et al., 2006). Significant differences were only observed when high intensity light was combined with low temperature (Havaux et al., 2005), indicating a more limited role for tocopherols in photoprotection than had been assumed. In tobacco, *VTE2*-RNAi lines containing <5% of WT tocopherol levels exhibited increased lipid peroxidation, enhanced chlorosis and reduced fresh weight under salt or sorbitol stress while those with >5% of WT tocopherol levels were indistinguishable from WT (Abbasi et al., 2007). These combined results suggest that the tocopherol threshold at which oxidative damage is observed is quite low and that the protective roles of tocopherols in various oxidative stresses may be both stress- and species-specific.

In contrast, when *vte2* plants are subjected to non-freezing low temperature (LT) treatment (3~12°C with 15~200 $\mu\text{E m}^{-2} \text{s}^{-1}$), they show severely inhibited growth compared with wild type (Maeda et al., 2006). The visible phenotypes of *vte2* plants during the long-term low temperature treatment include inhibited growth, purple color in mature leaves, shorter siliques, more aborted seeds and reduced seed yield (Maeda et al., 2006). *vte1* shows an intermediate phenotype between *vte2* and wild type, suggesting DMPBQ can partially replace the functions of tocopherols at LT conditions. Detailed LT time course experiments defined a series of biochemical and physiological events occur before visible phenotypes between *vte2* and wild type are observed. After as short as 6 h of LT treatment, photoassimilate export capacity from source (mature leaves) to sink tissues (young leaves and roots) was impaired in *vte2*. This coincided with initiation of callose deposition in leaf vasculature tissues in *vte2*. After 60 h of treatment, the amount

of soluble sugars in mature leaves of *vte2* became significantly higher than in wild type. After 14 d of LT treatment, the accumulation of starch and anthocyanins in *vte2* also became significantly higher than in wild type. At two weeks of LT treatment, *vte2* started to show a small but significant decrease in quantum yield of photosystem II electron transport (Φ_{PSII}), indicating a suppression of photochemistry. After 28 d, besides the obvious inhibited growth, *vte2* plants also contained significantly less chlorophylls and carotenoids and Φ_{PSII} was decreased further. Interestingly these phenotypes occurred in LT-treated *vte2* without photoinhibition, as the maximum efficiency of photosystem II (Fv/Fm) was identical in both *vte2* and wild type during 4 weeks at LT. Furthermore, the levels of lipid peroxides as measure by FOX assay were identical in *vte2* and wild type during the LT treatment (Maeda et al., 2006). Oxidized lipid profiling further confirmed that there is no significant production of oxidized lipid species in LT-treated *vte2* relative to wild type (Maeda et al., 2008), indicating that *vte2* plants are not experiencing severe oxidative stress during low temperature treatment. These results together suggest an important role of tocopherols in LT adaptation in plants that is independent of their antioxidant roles.

Studies in plants other than *Arabidopsis* have also provided data pertinent to the functional roles of tocopherols. The maize *sxd1* (*sucrose export defective 1*) mutant, now known to be a mutant in the maize *VTE1* (tocopherol cyclase) ortholog, was reported to have a defect in photoassimilate translocation and accumulate carbohydrate and anthocyanins in mature leaves under normal growth conditions (Russin et al., 1996; Stitt, 1996; Provencher et al., 2001; Hofius et al., 2004). The potato *VTE1*-RNAi lines also display constitutive carbohydrate and anthocyanin accumulation in mature leaves,

although the phenotype was only present in lines with >99% reduction in total tocopherols (Hofius et al., 2004). In both *sxd1* and the potato *VTE1*-RNAi lines, callose was constitutively deposited in the vasculature of mature leaves (Botha et al., 2000; Hofius et al., 2004). However, the tobacco *VTE1*-RNAi line did not show similar phenotypes either at normal or moderate LT (15°C) conditions (Abbasi et al., 2009), which may be related with the ultra chilling-sensitivity of the species. Taken together, the observed phenotypes of *Arabidopsis vte2*, and to a lesser degree *Arabidopsis vte1*, though visible only under low temperature conditions, resemble the visible and biochemical phenotypes of the maize and potato plants defective in *VTE1* at normal temperatures, indicating such functions of tocopherols may be conserved in plants.

Because tocopherols are synthesized in chloroplasts and photoassimilate translocation is mediated through transporters at the plasma membrane, an intercellular signaling function of tocopherols in plants was proposed (Munne-Bosch and Alegre, 2002; Sattler et al., 2003b; Munne-Bosch and Falk, 2004; Munne-Bosch, 2005b), but evidence supporting such functions and the mechanism underlying the phenomenon is far from being established. A recent study discovered that although the leaf fatty acid compositions of *vte2* and the wild type are identical at permissive conditions, 14 d LT-treated *vte2* had significantly higher and lower linoleic acid (18:2) and linolenic acid (18:3), respectively, relative to wild type, predominantly in ER-derived lipids (Maeda et al., 2008). In addition, introduction of *fad2* and *fad6*, mutations in the ER and plastidic localized oleate desaturases, respectively, suppressed the LT phenotypes of *vte2* to different degrees (Maeda et al., 2008). These new findings suggested a link between tocopherol deficiency and extraplastidic LT responses of *vte2*. Further studies on the

effects of tocopherol deficiency on lipid metabolism could lead to a better understanding of the roles of tocopherols in phloem loading and LT adaptation in plants.

PLANT ADAPTATION TO LOW TEMPERATURE STRESS

Exposure to low temperatures frequently occurs in nature and is one of the most important factors affecting plant performance and distribution. Cold-hardy species, including *Arabidopsis*, can increase their freezing tolerance by a period of pre-exposure to low but non-freezing temperatures, a process known as cold adaptation or cold acclimation (Thomashow, 1999; Xin and Browse, 2000). Low temperature causes significant changes in the cell biophysics, and the acclimation process facilitates changes to plant cell structure, metabolism, and biochemistry that help a plant to efficiently operate under the new, colder conditions. During cold acclimation, multiple regulatory and biochemical mechanisms are triggered to optimize growth at LT conditions, and it has been difficult to determine which processes are directly affected or affected most severely by LT, and differential responses between species generate complex indirect effects. A number of genes and cell processes that respond to cold acclimation have been described, yet there are many aspects of the cold acclimation process that have yet to be explained.

LT perception and signal transduction

Plants first need to perceive the LT and transduce the signal to alter the expression of appropriate genes to combat the diverse stresses that LT imposes on living cells. Molecular and mutational analyses of temperature signaling in *Synechocystis* PCC6803 demonstrate the existence of at least two temperature sensors. One of the two component

regulators, Hik33, is activated by reduced membrane fluidity, allowing the autophosphorylation of Hik33 and the subsequent transfer of a phosphate group to Hik19 and finally to the response regulator Rev1 (Suzuki et al., 2000; Suzuki et al., 2001). In higher plants, however, the cellular elements that sense LT and initiate the first stages of LT signaling are not yet identified and details of the early LT-signaling pathway are missing.

As the most external surface of the plant cell, the cell wall is the first element to receive a stress signal and begin the signal transmission to the cell interior (Baluska et al., 2003). The cell wall is intimately associated with both the plasma membrane and cytoskeleton and communication across the cell wall-plasma membrane-cytoskeleton continuum facilitates the transmission of cell wall and plasma membrane modifications to microtubules (Nguema-Ona et al., 2007). Indeed, two of the earliest LT responses are rigidification of the plasma membrane and remodeling of the cytoskeleton. Chilling caused depolymerization and disassembly of microtubules (Wang and Nick, 2001). This initial, partial disassembly of microtubules was shown to trigger efficient cold acclimation (Orvar et al., 2000; Abdrakhamanova et al., 2003). Microtubule activity can then mediate Ca^{2+} channel opening since disassembly of microtubules results in increased activity of voltage-dependent Ca^{2+} channels (Thion et al., 1996). Cell wall proteins, including kinases, extensins (Yoshida et al., 2001) and arabinogalactan proteins with glycosyl phosphatidylinositol (GPI) anchors (Humphrey et al., 2007) have also been proposed to be potential temperature sensors.

Transient influx of Ca^{2+} into the cytosol is another early event occurring in plants in response to various abiotic stresses (Monroy and Dhindsa, 1995; Xiong et al., 2002). It

was proposed that the opening of Ca^{2+} channels and Ca^{2+} influx occur immediately following membrane and cytoskeleton changes, which in turn triggers protein kinases and cold-specific signal transduction cascades, leading to the activation of cold-induced genes and the acquisition of freezing tolerance (Murata and Los, 1997; Sangwan et al., 2001; Wasteneys and Galway, 2003). The cytosolic Ca^{2+} burst is shown to be required for regulating several cold-inducible genes (Monroy et al., 1993; Knight et al., 1996; Polisensky and Braam, 1996; Tahtiharju et al., 1997). Recently, calmodulin binding transcription activators (CAMRA) were shown to bind to a regulatory element in the CBF2 gene promoter (Doherty et al., 2009), providing evidence for a link between calcium signaling and cold induction of CBF pathway, a key signaling pathway in LT adaptation.

Signaling pathways in low temperature adaptation

Extensive changes occur in the transcriptome during cold acclimation. Systematic analysis of expression profiles of large numbers of genes using whole genome arrays demonstrated that 45% of Arabidopsis transcripts could change in response to low temperature (Zarka et al., 2003; Vogel et al., 2005). In a recent thorough transcript profiling study using Affymetrix GeneChips that contain 24,000 genes, as many as 939 genes were determined to be cold-regulated after 24h of cold treatment at 0°C (Lee et al., 2005).

Multiple regulatory pathways operate in LT adaptation. The best understood system is the C-repeat Binding Factor (CBF)-dependent signaling pathway (Thomashow, 2001). In Arabidopsis low temperature is believed to activate the Inducer of CBF Expression-1 (ICE1), a bHLH (basic helix-loop-helix) transcription factor, which stimulates the

transcription of the *CBF* genes (Chinnusamy et al., 2003). The CBF1, 2, and 3 transcription activators are expressed rapidly in response to LT (within 15 min), binding to the C-repeat (CRT)/dehydration response element (DRE) present in the promoters of cold-regulated (COR) and other cold-responsive genes, inducing CBF-targeted genes (CBF-regulon), which contributes to an increase in freezing tolerance (Thomashow et al., 1997). The CBF transcription factors are the major regulators of cold acclimation (Cook et al., 2004) and it was shown that about 10-15% of all the cold-regulated genes belong to the CBF regulon (Hannah, et al. 2005). Other transcription factors, including AtMYB15 (Agarwal et al., 2006) and ZAT12 (Vogel et al., 2005), can negatively regulate the expression of CBF genes. In addition, studies are identifying other regulatory pathways that also activate during LT stress. For instance, the *eskimo1* mutant possesses constitutive freezing tolerance under both acclimated and non-acclimated conditions without constitutively expressing COR genes. The *ESKIMO 1 (ESK1)* gene product controls transcription of a set of stress responsive genes that overlap with salt, osmotic stress and abscisic acid (ABA) induced genes and are largely independent of the genes regulated by cold acclimation and CBF (Xin and Browse, 1998).

Effect of LT on plant carbohydrate metabolism

Traditional targeted metabolite studies have established correlations between LT adaptation and the presence and abundance of certain metabolites. More recently, metabolite profiling has emerged as an important tool in this regard and the rapid non-targeted identification and quantification of a wide array of metabolites made it possible to gain a thorough insight of the metabolic state of the plant and understand the effects of low temperature stress on plant metabolism (Cook et al., 2004; Wang et al., 2006; Kaplan

et al., 2007). The non-targeted metabolite profiling approach revealed that extensive changes in the metabolome occur in plants at low temperatures and expanded the inventory of metabolites and pathways linked with cold acclimation (Cook et al., 2004; Gray and Heath, 2005; Hannah et al., 2006; Kaplan et al., 2007). About 60% of metabolites were shown to be affected by low temperature with central carbohydrate metabolism being a particularly prominent component of the metabolome reprogramming at low temperature (Cook et al., 2004).

It is well known that low temperatures inhibit phloem transport (Giaquinta and Geiger, 1973; Chamberlain and Spanner, 1978; Krapp and Stitt, 1995; Strand et al., 1997). Optimal rates of photosynthesis require an appropriate balance between the rates of carbon fixation, sucrose synthesis and sucrose export (Stitt, 1991). Photosynthesis is strongly inhibited in *Arabidopsis* leaves shifted to LT and this inhibition is associated with the reduced expression of nuclear-encoded photosynthetic genes (Strand et al., 1997). In the time period of hours to days, LT stress inhibits sucrose synthesis, inducing accumulation of phosphorylated intermediates and Pi-limitation of photosynthesis. In the longer term of weeks to months, carbon metabolism in photosynthetic organs is reprogrammed and redirected into a variety of sugar phosphates and free sugars (Leegood and Furbank, 1986; Sharkey et al., 1986; Stitt et al., 1988). Studies with *Arabidopsis* showed that a sequence of events reverses the inhibition of sucrose synthesis and photosynthesis as the plants acclimate to low temperatures. Full acclimation occurs in leaves that developed at LT with the recovery of photosynthetic activity, which has been shown to be associated with a strong increase in the activities of enzymes of the Calvin cycle and of the sucrose biosynthetic pathway. These acclimative changes also result in a

pronounced shift in partitioning of newly fixed carbon into sucrose (Strand et al., 1999; Hurry et al., 2000; Hurry et al., 2002). The sugars accumulated in cold-acclimated plants were proposed to be important in osmoregulation or cryoprotection. Indeed, accumulation of about 15 metabolites involving in central carbohydrate metabolism, including xylose, glucose, fructose, galactose, sucrose and raffinose, were identified to be significantly correlated with acclimated freezing tolerance (Hannah et al., 2006).

Plant glycerolipid biosynthesis and ER-plastid lipid trafficking

Two parallel pathways, prokaryotic and eukaryotic, operate in plant cells for glycerolipid biosynthesis and PUFA production (Figure 1.3). All acyl chains of membrane and storage lipid synthesis are produced in the plastid (Ohlrogge and Browse, 1995). Glycerolipid synthesis starts with two sequential acylations of glycerol-3-phosphate (G3P) catalyzed by G3P acyltransferase (GPAT) and lyso-phosphatidic acid (LPA) acyltransferase (LPAAT) producing phosphatidic acid (PA). PA is used to synthesize phosphatidylglycerol (PG) in all plants and a portion of the plastidic glycolipids in some plants via the prokaryotic pathway (Ohlrogge and Browse, 1995). Plastid localized acyl-lipid desaturases, including FAD4, FAD5, FAD6, FAD7 and FAD8, act on the initial 18:1/16:0 molecular species of PG or glycerolipids to produce the highly unsaturated species that are characteristic of chloroplasts (Harwood, 1996). Alternatively, the 18:1 is hydrolyzed and the resultant acyl-ACP thioesters are exported from the plastid to enter the ER-localized eukaryotic pathway (Roughan and Slack, 1982; Browse et al., 1986; Somerville and Browse, 1991). The determination of the membrane phospholipid composition is completed in the ER compartment by the action of microsomal acyl-lipid desaturases FAD2 and FAD3, and acyltransferases.

Phosphatidylcholine (PC) is the major extraplastidic phospholipid in multi-cellular plants and main site of acyl desaturation for production of all other molecular species. The diacylglycerol backbones of PE, PS, PI and storage TAG are also produced by the eukaryotic pathway. The proportion of nascent FA incorporated into the eukaryotic and prokaryotic pathways vary among plants and different tissues. In leaves of *Arabidopsis*, a typical “16:3” plant, the flux of acyl chains into leaf glycerolipids is approximately 62% eukaryotic and 38% prokaryotic, with about half of the galactolipid (plastidic) DAG moieties contributed by the eukaryotic pathway (Browse et al., 1986).

The separation of glycerolipid synthesis activities makes it necessary for lipid transfer between ER and plastid (Figure 1.3). Reversible exchange of lipids exists between the eukaryotic and prokaryotic pathways (Browse and Somerville, 1991; Miquel and Browse, 1992). The eukaryotic pathway produces the “DAG moiety” for plastid glycolipid synthesis (Slack et al., 1977). Either PA (Ohlrogge and Browse, 1995; Awai et al., 2006), diacylglycerol (DAG), or lyso-PC (Mongrand et al., 2000; Andersson et al., 2004) has been hypothesized as the transfer molecule, however, the exact nature of the lipid molecule transferred from the ER to the outer envelope of the plastid remains unclear. Studies on the four *Arabidopsis trigalactosyldiacylglycerol* (*tgd1-4*) mutants in recent years shed light on the process of ER-plastid lipid trafficking (Xu et al., 2005; Awai et al., 2006; Lu et al., 2007a; Xu et al., 2008). A distinct processive galactolipid: galactolipid galactosyltransferase was presumed to be induced, producing the diagnostic oligogalactoglycerolipids accumulating in these mutants. TGD1, TGD2 and TGD3 have been proposed to form an ABC lipid transporter complex in the inner chloroplast envelope membrane responsible for phosphatidic acid (PA) transfer through the inner

envelope membrane (Xu et al., 2005; Awai et al., 2006; Lu et al., 2007a) whereas TGD4 likely associates with the ER membrane and transfers lipids between the ER and outer plastid envelop membranes (Xu et al., 2008).

The recent demonstration of membrane contact sites (MCRs) between the ER and plastid in leaf mesophyll cells, so called PLAMs for plastid associated membranes (Andersson et al., 2007), provides a physical mechanism for the transfer of lipids between the plastid and the ER (Figure 1.3). PLAMs are likely the plastidic structural and functional equivalent of mitochondria associated membranes (MAMs, (Ruby et al., 1969; Pichler et al., 2001; Choi et al., 2006; Goetz and Nabi, 2006) and plasma membrane associated membranes (PAMs, (Pichler et al., 2001), ER membrane associations with mitochondria and the plasma membrane, respectively, that are involved in non-vesicular transport of hydrophobic molecules such as lipids and sterols (Hajnoczky et al., 2002; Levine, 2004). Transfer lipid molecules may not have to traverse the hydrophilic cytosol at all, but may travel through a PLAM which may allow direct transfer of lipid molecules between the ER and plastid membrane systems.

In addition to transfer of lipids between subcellular components, numerous studies in mammalian, yeast and bacterial systems showed that the acyl chains of phospholipids are subjected to acyl editing or remodeling, which involves the deacylation and reacylation of glycerolipids without net lipid synthesis (Macdonald and Sprecher, 1991; Schmid et al., 1995; Boumann et al., 2003; Kol et al., 2004; de Kroon, 2007; Tanaka et al., 2008). Recently, lipid remodeling has also been shown in leaves of pea and *Brassica napus* and germinating embryos of soybean. Newly synthesized saturated or monounsaturated fatty acids from plastids are exchanged with PUFAs in PC through an acyl editing process

(Figure 1.3), producing initial molecular species of PC containing mixtures of previously synthesized PUFA with newly synthesized FA (Williams et al., 2000; Bates et al., 2007; Bates et al., 2009). Acyl editing may play an important role in fine-tuning the fatty acid composition and optimizing membrane properties in plants under ever-changing growth conditions and may act as a mechanism to allow enrichment of PUFAs for TAG synthesis in oilseeds (Bates et al., 2009).

Effect of LT on plant lipid metabolism and lipid metabolism mutants

Normal functioning of integral membrane proteins such as transporters and receptor proteins depends on maintaining the fluidity of the membrane, which is strongly influenced at a given temperature by its lipid composition (reviewed in (Hazel, 1995). One of the best-documented responses of plants to chilling stress is that activities of fatty acid desaturase enzymes increase (Williams et al., 1992; Palta et al., 1993; Weiss et al., 1993), resulting in an increase in polyunsaturated acyl chains of membrane lipids during LT acclimation (Nishida and Murata, 1996; Welts et al., 2002). This kind of modification promotes membrane fluidity at lower temperatures by decreasing the temperature at which the membrane lipids experience a gradual phase change from fluid to semi-crystalline and reduce, which in some cases may eliminate the propensity of cellular membranes to undergo freezing-induced non-bilayer phase formation (Uemura et al., 1995).

The importance of membrane lipid composition in temperature tolerance has also been defined by transgenic studies and mutational analyses (Orvar et al., 2000; Sung et al., 2003). Overexpressing *Arabidopsis FAD7* under the control of 35S promoter caused a decrease in dienoic fatty acids and an increase in trienoic fatty acids in tobacco, resulting

in reduced low-temperature-induced chlorosis in young seedlings (Kodama et al., 1994; Kodama et al., 1995). Similarly, in transgenic tobacco plants expressing a Δ -9 cyanobacterial desaturase which introduces a cis-double bond at carbon 9 of both 16- and 18- carbon saturated fatty acids of various membrane lipids, the saturated fatty acid level was greatly decreased, resulting in a significant increase in chilling resistance (IshizakiNishizawa et al., 1996). Enhanced cold tolerance was observed in transgenic tobacco expressing a chloroplast *FAD7* gene under the control of a cold-inducible promoter which resulted in a higher survival rate during a long-term exposure to cold stress (0-3.5°C) (Khodakovskaya et al., 2006). Conversely, tobacco plants with the *FAD7* gene silenced had a lower trienoic fatty acid content than the wild type and were better able to acclimate to higher temperatures (Murakami et al., 2000).

Mutants affecting fatty acid and lipid metabolism in *Arabidopsis* (Figure 1.3) have also provided important insight into the involvement of membrane lipid in LT adaptation. Five lipid mutants were found to be indistinguishable from wild type at normal growth conditions and have differing impacts at low temperatures (Table 1.1). The most dramatic LT mutant phenotypes were observed in *fab1* and *fad2*. *fab1* mutants show reduced photosynthetic capacity, chlorophyll and chloroplast glycerolipids after 7-10 d, and eventually dies after 5 to 7 weeks at 2°C (Wu and Browse, 1995; Wu et al., 1997), while *fad2* leaves gradually deteriorate, displaying patches of necrosis and extensive accumulation of anthocyanins at 6°C and eventually leading to death of the whole plants (Miquel et al., 1993). The other three mutants, *fad5*, *fad6*, and the triple mutant *fad3fad7fad8*, have more moderate phenotypes under LT conditions. *fad5* and *fad6* develop chlorotic leaves when grown at 5°C with a 20-30% growth reduction and 70%

reduction in thylakoid membrane content (Kunst et al., 1989; Hugly and Somerville, 1992). When *fad3fad7fad8* is subjected to short term LT, there is only a slight reduction in Φ_{PSII} , but under prolonged LT it shows decreased chlorophyll content and also a reduction in thylakoid membrane content (McConn and Browse, 1996; Routaboul and Browse, 2002). Surprisingly, a suppressor of *fab1* which rescued the collapse of photosynthetic function and allowed survival of *fab1* plants at 2°C was found to be a new allele of *fad5* (Barkan et al., 2006). *fab1fad5* suppressors remained viable after 16 weeks in the cold, were able to resume growth following a return to 22°C and subsequently produced viable seed. The further increase in lipid saturation in the suppressor *fab1fad5* challenged the assumptions on the role of thylakoid unsaturation in photosynthetic function and suggested the involvement of physical properties of different lipid species and importance of lipid composition for the LT adaptation in plants.

AIM OF THIS STUDY

This thesis research involves a detailed characterization of the LT-induced phenotypes in *vte2* from multiple perspectives. During my rotation and first year of my thesis research, I collaborated with a senior fellow graduate student (Hiroshi Maeda) to assess aspects of the *vte2* LT phenotypes in detail. I independently assessed the diurnal changes of leaf soluble sugars and starch levels during the short term time courses of LT treatment and also participated in the assessment of changes in other biochemical and physiological parameters, including anthocyanins, tocopherols, carotenoids, lipid peroxides, and chlorophyll fluorescence [maximum photosynthesis efficiency (F_v/F_m) and quantum yield of PSII (Φ_{PSII})]. These time course measurements allowed a

biochemical order for the responses of *vte2* to LT to be defined, with vascular callose deposition and defective photoassimilate export capacity appearing first (6h of LT treatment), followed by the elevated soluble sugars (60h), accumulation of starch and anthocyanins (14d) and the distinctive growth inhibition (28d) in *vte2*. This work resulted in a manuscript detailing these LT-induced phenotypes in *vte2* published in *Plant Cell* in 2006 on which I was the second author (Maeda et al., 2006). This collaborative work laid the foundation and logic for a suppressor screen to identify and understand the links between tocopherol deficiency and the *vte2* LT phenotypes. This screen became the major focus of the work described in this thesis.

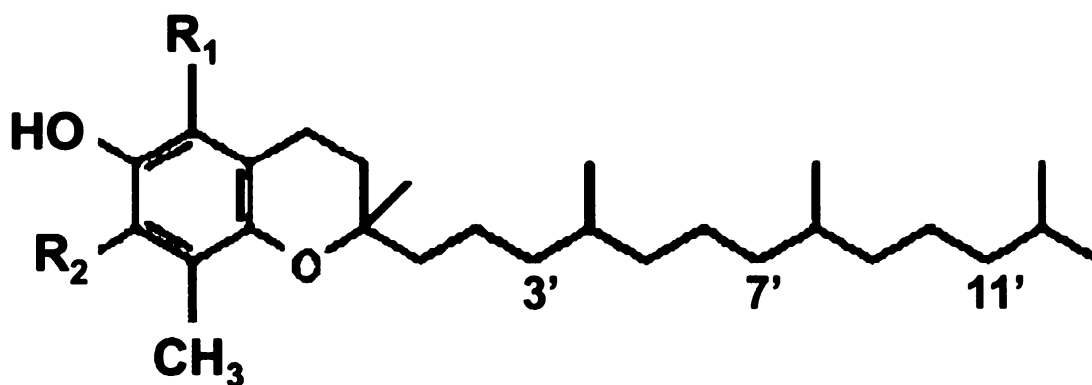
In fall 2005, I launched an unbiased genetic screen for second-site mutations that alleviate the *vte2* LT-induced phenotypes. Chapter 2 details the screening, identification and preliminary biochemical, genetic and physiological analyses of a large number of primary suppressors. Seven *sve* (*suppressors of vte2* LT-induced phenotypes) loci were defined from which three were selected for molecular cloning efforts detailed in Chapter 3. Chapter 3 provides the detailed characterization of these three *sve* loci (*sve1*, *sve2* and *sve7*) and demonstration of the molecular identities of *sve1* and *sve2*, which together have provided strong genetic evidence supporting roles for tocopherols in ER lipid metabolism.

Chapter 4 describes an effort initiated in 2006 to further investigate the influence of tocopherol deficiency on global gene expression and determine whether the transcriptional responses could further our understanding of the differing responses of *vte2* and *Col* during LT treatment. Statistical analysis and insights gained from the transcriptional profiling studies are detailed in Chapter 4.

TABLES AND FIGURES

Table 1.1 Phenotypes of lipid metabolism mutants at low temperature conditions.

Mutant	Deficient enzyme(s)	Effect on lipids	Phenotype at normal conditions	LT (°C)	Phenotype at LT conditions	Citation
<i>fab1</i>	3-ketoacyl-acyl carrier protein synthase II	~40% increase in 16:0	Similar to WT (both at 22°C and 12°C)	2	Reduced photosynthetic capacity, chlorophyll, and chloroplast glycerolipids; Eventually die	Wu and Browse, 1995; Wu et al., 1997
<i>fad2</i>	ER ω -6 desaturase	Substantial decrease in 18:2 and increase in 18:1 in all the major ER lipids	Similar to WT	6	Necrotic leaves with anthocyanin accumulation; Eventually die	Miquel et al., 1993
<i>fad5</i>	Chloroplast 16:0 δ -7 desaturase	Absence of 16:3- δ -7,10,13	Similar to WT (slight chlorophyll reduction)	5	Chlorotic leaves; reduced growth and thylakoid membrane content	Kunst et al., 1989
<i>fad6</i>	Chloroplast ω -6 desaturase	Substantial decrease in 18:3 and 16:3 and increase in 18:1 and 16:1				Hugly and Somerville, 1992
<i>fad3/</i> <i>fad7/</i> <i>fad8</i>	ER (<i>fad3</i>) and chloroplast (<i>fad7/8</i>) ω -3 desaturases	Completely deficient in 18:3 and 16:3	Similar to WT (slight chlorophyll reduction and being infertile)	4	Short term: reduced Φ_{PSII} ; Long term: decreased chlorophyll and thylakoid membrane content	Routaboul and Browse, 2002



Form	R ₁	R ₂
α-	CH ₃	CH ₃
β-	CH ₃	H
γ-	H	CH ₃
δ-	H	H

Figure 1.1 Structure of tocopherols.

α-, β-, γ- and δ- tocopherols differ by the number and position of methyl groups on the chromanol ring. α-tocopherol has a fully methylated chromanol ring while β- and γ-tocopherol contains two methyl groups and δ-tocopherol contains only one methyl group.

Tocotrienols have the same basic structure except for the presence of double bonds on the isoprenoid side-chain at C-3', C-7' and C-11' positions.

Figure 1.2 Tocopherol biosynthetic pathway and locations of mutations in *Arabidopsis thaliana*.

MPBQ, 2-methyl-6-phytyl-1,4-benzoquinol; DMPBQ, 2,3-dimethyl-6-phytyl-1,4-benzoquinol; PK, Phytol kinase; HPT, Homogentisate phtyl transferase; TC, tocopherol cyclase; MT, MPBQ methyltransferase; γ -TMT, γ -tocopherol methyltransferase; *vte1*, *vte2*, *vte3*, *vte4* and *vte5*, mutants of TC, HPT, MT1, γ -TMT and PK, respectively. Bold arrows indicate the major biosynthetic flux leading to accumulation of α -tocopherol in leaves.

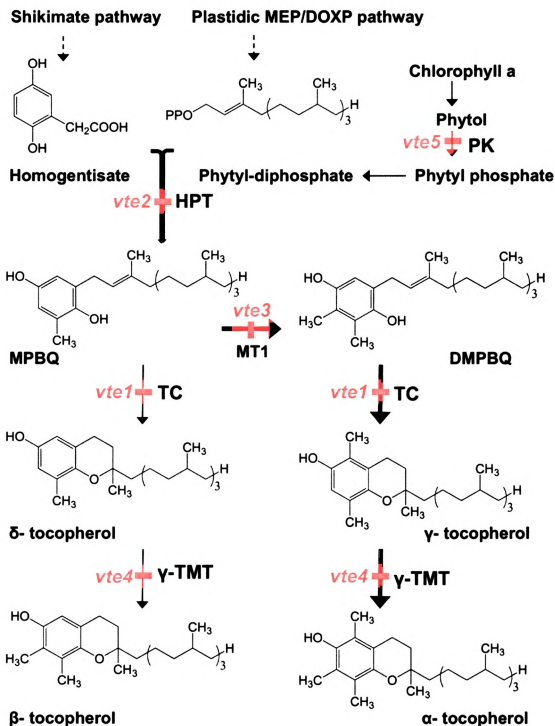


Figure 1.2

Figure 1.3 An abbreviated diagram of two pathways of glycerolipid biosynthesis in *Arabidopsis* leaves.

Adapted from Browse and Somerville (1991) and Benning (2009). For clarity, only the pathways, genes and processes relevant to the work in this thesis are shown. Abbreviations for the lipid structures: fatty acids - X:Y, a fatty acid group containing X carbon atoms and Y cis double bonds; t16:1, trans-hexadecenoic acid; G3P, glycerol-3-phosphate; LPA, lysophosphatidic acid; PA, phosphatidic acid; DAG, diacylglycerol; PG, phosphatidylglycerol; MGDG, monogalactosyldiacylglycerol; DGDG, digalactosyldiacylglycerol; SL, sulfoquinosyldiacylglycerol; PC, phosphatidylcholine; PE, phosphatidylethanolamine; PI, phosphatidylinositol. Acyl editing is shown in which PC is constantly turned over to LPC and newly exported fatty acids are exchanged between the PC and the acyl-CoA pools. TGD4 is associated with the endoplasmic reticulum (ER) and TGD1, TGD2, TGD3 are components of a transporter complex in the inner envelope membrane. The exact nature and transporting mechanism of the lipid precursor returned to the plastid is not known. Both acyl editing and ER-plastid lipid trafficking could occur in the plastid envelope ER-contact sites (PLAMs).

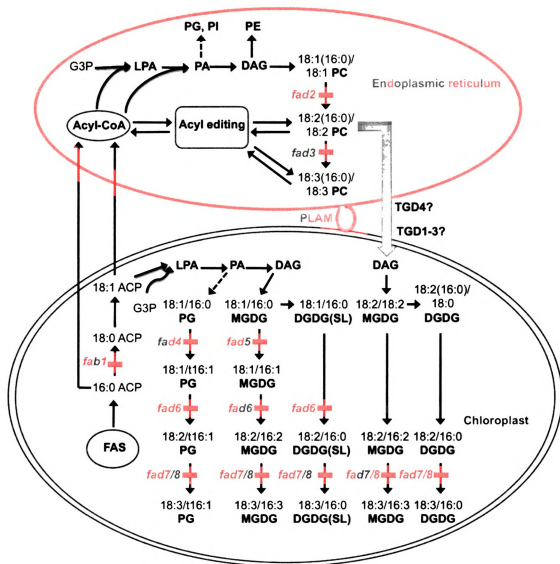


Figure 1.3

CHAPTER 2 GENETIC SCREEN AND PRELIMINARY CHARACTERIZATION OF SUPPRESSOR OF *VTE2* LOW TEMPERATURE-INDUCED PHENOTYPES

ABSTRACT

Tocopherols (vitamin E) are lipid-soluble antioxidants that are synthesized only by photosynthetic organisms (plants, algae and some cyanobacteria). Molecular dissection of the tocopherol biosynthetic pathway in *Arabidopsis* and *Synechocystis* has allowed the isolation of mutants containing different amounts and compositions of tocopherols and made possible studies directed at elucidating their functions in photosynthetic organisms. Studies with the tocopherol-deficient *Arabidopsis thaliana* *vte2* mutant demonstrated an important role for tocopherols in transfer cell wall development and achievement of full photoassimilate export capacity during low temperature (LT) adaptation. In order to understand the genetic basis of the *vte2* phenotype and determine the missing links between tocopherol deficiency and the *vte2* LT-induced phenotypes, a genetic screen for mutations that suppress the *vte2* LT-induced phenotypes was undertaken. This chapter describes the primary genetic screen, identification and genetic determination of the number of suppressor loci. Seven independent *sve* (*suppressor of vte2 low temperature-induced phenotype*) lines were identified from approximately 12,000 EMS mutagenized M₂ *vte2* plants screened under low temperature conditions. Due to long time period required for backcrossing and evaluation of allelism tests (4 weeks at permissive conditions and 4 weeks at LT to determine suppression), primary mutants representing individual from different pools were subjected to physiological and biochemical analysis to gain insight into their impact on the *vte2* LT phenotype and to provide data for

selecting a limited number of lines for detailed study. Biochemical characterization of the primary *sve* lines demonstrated they have differing impacts on sugar accumulation, photoassimilate export capacity and vascular-specific callose deposition in the *vte2* background at LT. Significantly, five of the primary *sve* lines altered fatty acid composition before or in response to LT treatment reinforcing an important role for lipid metabolism in the initiation and development of the *vte2* LT phenotypes. Preliminary characterization of the primary *sve* lines in this chapter allowed three lines (*sve1vte2*, *sve2vte2* and *sve7vte2*) to be selected and prioritized for further backcrossing, detailed analysis, and cloning described in Chapter 3.

INTRODUCTION

Tocopherols (vitamin E) are amphipathic molecules consisting of a chromanol ring head group and a phytyl-derived side chain (Figure 1.1) (Schneider, 2005). The best characterized function of tocopherols in animal systems is their role as lipid-soluble antioxidants that prevent free radical damage of membrane polyunsaturated fatty acids (PUFAs) (Burton and Ingold, 1981; Liebler and Burr, 1992; Bramley et al., 2000; Schneider, 2005). Studies have also shown that tocopherols can affect membrane properties due to their physical structure and interactions with specific lipid acyls (Kagan, 1989; Wang and Quinn, 2000; Atkinson et al., 2008). In addition, in animals specific tocopherols also appear to have functions that are independent of their antioxidant activities such as the stimulation of protein phosphatase A₂ and thereby inhibition of protein kinase C activities by α -tocopherol but not γ -tocopherol (Boscoboinik et al., 1991; Tasinato et al., 1995; Ricciarelli et al., 1998) and inhibition of cyclooxygenase-2 activity and hence prostaglandin E₂ synthesis by γ -tocopherol but not α -tocopherol (Jiang et al., 2000).

Tocopherols are essential dietary component for humans and animals and are produced exclusively by photosynthetic organisms: higher plants, algae and some photosynthetic bacteria (Grusak and DellaPenna, 1999). The molecular genetic dissection of the complete tocopherol biosynthetic pathway in *Arabidopsis thaliana* and *Synechocystis* sp. PCC6803 in recent years (Shintani and DellaPenna, 1998; DellaPenna, 1999; Collakova and DellaPenna, 2001; Porfirova et al., 2002; Shintani et al., 2002; Cheng et al., 2003; Sattler et al., 2003b; DellaPenna, 2005b, a; DellaPenna and Pogson, 2006) allowed manipulation of tocopherol content and composition in plant tissues and

also enabled studies of the biological functions of tocopherols in photosynthetic organisms (Maeda and DellaPenna, 2007).

Tocopherols are localized in plastids where their primary function has long been assumed to be protecting polyunsaturated fatty acids (PUFAs) from oxidative damage (Knox and Dodge, 1985; Robinson, 1988; Fryer, 1992; Munne-Bosch and Alegre, 2002), an assumption based largely on correlations of increased tocopherol levels in response to various abiotic stresses (DeLong and Steffen, 1997; Munne-Bosch and Alegre, 2000; Collakova and DellaPenna, 2003b; Abbasi et al., 2007; Collin et al., 2008). *vitamin E deficient (vte)* mutants have been pivotal in defining tocopherol functions in plants. The *Arabidopsis vte2* mutant, which is deficient in homogentisate phytyl transferase and lacks all forms of tocopherols and pathway intermediates, had significantly reduced seed longevity and produced excessive amounts of lipid peroxidation byproducts during germination (Sattler et al., 2004; Sattler et al., 2006), consistent with tocopherols playing an important role in protecting PUFAs in seed from oxidation. The *vte1* mutant, which is deficient in tocopherol cyclase activity, also lacks all tocopherols but unlike *vte2* accumulates the redox active pathway intermediate dimethylphytylbenzoquinone (DMPBQ). *vte1* has only modestly reduced seed viability and is otherwise indistinguishable from wild type (WT) (Sattler et al., 2004), suggesting the DMPBQ accumulated by *vte1* suppresses these tocopherol-deficient seed phenotypes.

In contrast to the clear situation in seeds of tocopherol deficient plants, studies of their mature photosynthetic tissues have been equivocal. For example, when placed under severe photooxidative stress conditions, the extent of bleaching and photoinhibition in *vte2* and *vte1* was similar to WT (Porfirova et al., 2002; Havaux et al., 2005; Kanwischer

et al., 2005; Maeda et al., 2006). Significant differences were only observed when high intensity light was combined with low temperature, indicating a more limited role for tocopherols in photoprotection than had been assumed. Similarly, *vte2* and WT were indistinguishable under drought and salt stress conditions (Maeda et al., 2006). In tobacco, VTE2-RNAi lines containing <5% of WT tocopherol levels exhibited increased lipid peroxidation, enhanced chlorosis and reduced fresh weight under salt or sorbitol stress while those with >5% WT tocopherol levels were indistinguishable from WT (Abbasi et al., 2007). These combined results suggest that the tocopherol threshold at which oxidative damage is observed is quite low and that the protective roles of tocopherols in various oxidative stresses may be both stress- and species-specific.

In contrast to the variable results observed for stress responses of tocopherol deficient plant species, a phenotype observed in mature plants of most tocopherol deficient species is a disturbance of carbohydrate metabolism in source leaves. The maize *sxd1* (*sucrose export defective1*) mutant was initially identified due to a constitutive defect in photoassimilate translocation and carbohydrate and anthocyanins accumulation in mature leaves under normal growth conditions (Russin et al., 1996; Provencher et al., 2001). The *SXD1* gene was subsequently shown to encode tocopherol cyclase (*VTE1*; (Sattler et al., 2003b). Similarly, VTE1:RNAi lines of potato display constitutive carbohydrate and anthocyanin accumulation in mature leaves, although the phenotype was only present in lines with >99% reduction in total tocopherols (Hofius et al., 2004). In both *sxd1* and the potato *VTE1*:RNAi lines, callose was constitutively deposited in the vasculature of mature leaves (Botha et al., 2000; Hofius et al., 2004). In *Arabidopsis*, tocopherol-deficient mutants are indistinguishable from WT at permissive temperatures

but develop defective photoassimilate export capacity, sugar accumulation and vascular callose deposition upon exposure to non-freezing low temperature (LT) treatment (Maeda et al., 2006). *vte1* shows an intermediate phenotype between *vte2* and wild type, suggesting DMPBQ partially replaces the functions of tocopherols at LT conditions. These results demonstrated that tocopherols are required for the development of full photoassimilate transport capacity at LT in *Arabidopsis*. Importantly, the inducible nature of these phenotypes in *Arabidopsis* provides a unique platform to study this aspect of tocopherol function (Maeda et al., 2006).

It was initially hypothesized that LT-treated *vte2* mutants might be under severe photo-oxidative stress considering the lack of antioxidant protection in the absence of tocopherols. However, lipid hydroperoxide contents measured using the FOX assay (Jiang et al., 1992; Wolff, 1994) were below background levels in both *vte2* and WT during the long term LT treatment (Maeda et al., 2006). Zeaxanthin and antheraxanthin, two xanthophyll cycle carotenoids known to be induced during photooxidative stress (Demmig-Adams and Adams, 2002; Bouvier et al., 2005), were not detected in either WT or *vte2*. Furthermore, under normal growth conditions and also during LT treatment, maximum photosystem II (PSII) efficiency (F_v/F_m) in both WT and *vte2* was maintained at approximately 0.85, the typical F_v/F_m value for healthy *Arabidopsis* plants (Krause and Weis, 1984). In addition, a recent mass spectrometry (MS)-based lipid profiling did not detect any significant production of lipid peroxidation products (Maeda et al., 2008). These results together indicate that *vte2* plants are not experiencing severe oxidative stress during low temperature treatment (Maeda et al., 2006).

The *vte2* LT-induced phenotypes, especially the significant carbohydrate accumulation in mature leaves, have raised many intriguing questions: How does the lack of tocopherols cause carbohydrate accumulation under LT conditions? Do any other changes occur prior to elevation of soluble sugar accumulation in *vte2* after 60 hours of low temperature treatment? What role, if not as an antioxidant, does tocopherols play in plants experiencing low temperature stress conditions?

To search for the missing links between the lack of tocopherols in *vte2* and altered carbohydrate metabolism at LT and begin to understand the phenotypes of *vte2*, I have undertaken a genetic screen for second site mutations that can suppress some or all of the *vte2* phenotypes. As a forward genetic tool, a suppression screen is essentially unbiased, in contrast to reverse genetic studies, which may be based on incorrect or biased assumptions and hypotheses. Suppressor screening has been successfully applied to many systems and has given unexpected insights into complicated genetic pathways, regulatory networks, and gene interactions (Li et al., 1999; Carpinelli et al., 2004; Eriksson et al., 2004; Collins and Cohen, 2005). Although more time-consuming than reverse genetic screens, this screen approach is especially suitable for this study because we lacked sufficient knowledge to propose obvious targets for reverse genetic approaches. The overall aim of the suppressor screen is to identify genes whose mutation allow restoration of a wild type or near wild type phenotype in the presence of the *vte2* mutation. Characterization and identification of the suppressor mutants at different developmental and treatment stages will help to dissect the complex process whereby tocopherols regulate carbohydrate metabolism at low temperatures.

Ethyl methane sulfonate (EMS), an alkylating agent that primarily produces GC→AT transitions, was chosen to induce mutations since it is able to generate a greater diversity and density of mutations than insertional mutagenesis (Jander et al., 2002). As EMS typically introduces hundreds of mutations in each plant line, it is possible to identify mutations in any given gene by screening fewer plants than in insertional mutagenesis (Feldman, 1994). Compared to activation tagging (Weigel et al., 2000), which mainly produces gain-of-function mutations, EMS induces point mutations that primarily results in a total or partial loss of function. It is therefore possible to dissect the genetic pathway involved in *vte2* phenotype by analyzing the non-redundant mutants that disrupt such a pathway.

RESULTS

Suppressor screen identified 7 independent suppressor loci

Previous studies have shown that exposing 4-week-old *vte2* plants grown at permissive conditions to 7°C results in rapid induction of callose deposition in phloem transfer cells, decreased photoassimilate export and increased levels of soluble sugars, starch and anthocyanins in source tissues culminating in plants that are somewhat smaller than wild type (Maeda et al., 2006). When 2-week-old plants grown at permissive conditions are treated for 4 weeks at 7°C, these same biochemical changes occur but the size difference between wild type and *vte2* is greatly exaggerated (e.g. see Figure 2.5). Therefore the primary mutagenesis screen was performed for second site mutations that attenuate this severe reduction in plant size of 2-week-old *vte2* after 4 weeks of LT treatment. All subsequent biochemical characterization was performed using LT

treatment of 4-week-old plants grown at permissive conditions to obtain sufficient experimental materials and allow direct comparison to previous results (Maeda et al., 2006; Maeda et al., 2008). Suppressor screens were performed on M₂ plants, in which homozygous recessive mutations can be detected. Approximately 12,000 M₂ plants from 10 separate M₁ pools were screened (the suppressor screening scheme is depicted in Figure 2.1) and the M₂ plants were allowed to grow for two weeks at permissive conditions before being transferred to low temperature conditions. After four weeks of low temperature treatment, when the visible phenotypes between *vte2* and Col were readily distinguishable, a total of 97 individuals that were larger in plant size and had less purple color in leaves than *vte2-1*, were selected as putative suppressor lines (an example screening flat is shown in Figure 2.2). Two sets of plants were screened and the putative suppressors lines labeled as 01-XXX from set 1 and 02-XXX from set 2. Because the *vte2-1* mutation is a G to A transition converting a Trp (TGG) to a premature stop codon (TGA) and the primary target of EMS is guanines, it is highly unlikely that the stop codon would be converted to that encoding an amino acid by EMS mutagenesis. Hence, all the suppressors should still be deficient in HPT activity and thus lack tocopherols. When tocopherol analysis was performed on each putative suppressor by HPLC (Sattler et al., 2003b), three lines were identified that had wild type levels of tocopherols and lacked the *vte2-1* polymorphism. These three lines most likely represent wild type seed contamination and were discarded.

To confirm that the suppression phenotype is heritable, 10-15 M₃ progeny from the putative 94 suppressor lines were screened a second time (Figure 2.1) under the same LT treatment (an example of screening pots is shown in Figure 2.3). Ultimately, 29 lines

originating from seven M₁ pools were identified that clearly inherited the suppressor phenotype and were carried on for further analysis. The 29 suppressor lines obtained from different pools, their various nomenclatures and their general biochemical and developmental traits are listed in Table 2.1. Pool 4 and 9 had the most suppressor isolates, with 10 and 7 isolated, respectively.

To determine how many independent loci are represented by the 29 suppressor lines, allelism tests were carried out by crossing representative lines from each M₁ pool, and in selected cases between lines within an M₁ pool, and comparing the F₁ progeny with their respective parental suppressor lines, and Col and *vte2*. Evidence of allelism is provided by the inability to complementation and the occurrence of suppression phenotypes similar to both parents in the F₁ progeny. Efforts were made to perform the crosses that would provide most information about allelism between suppressors from the different pools. Suppressors from the same pool were invariably found to be allelic and likely descended from the same M₁ plant while suppressor lines from separate pools were found to be non-allelic. Therefore the representative members from each of the 7 pools were named “*sve1* to *sve7*”, respectively, for the “*suppressor of vte2 low temperature-induced phenotype 1-7*” (Table 2.1). It is important to stress that these are primary suppressors (denoted “primary *sve* line”) and had not yet been backcrossed. The remainder of this chapter describes physiological and biochemical analysis with these primary *sve* lines that was performed to gain information into their nature while in parallel the lines were being backcrossed at least twice during a 9~12 month period to provide “clean” genetic lines for detailed analysis in Chapter 3. Each representative primary *sve* line, *vte2*, *vte1* and Col had similar plant size and morphology before LT treatment (Figure 2.4). However,

after prolonged LT treatment, all primary *sve* lines exhibited enhanced growth and reduced purple coloration of leaves relative to *vte2*, with the exception of *sve6vte2*, which although was larger than Col, had leaf coloration similar to *vte2* (Figure 2.5).

The primary sve loci show a range of suppression in sugar accumulation and photoassimilate export capacity

Previously *vte2*, and to a lesser extent *vte1*, were found to accumulate sugars and starch in mature leaves in response to LT treatment (Maeda et al., 2006). Since the suppressors were selected primarily on the basis of plant size and lack of visible purple coloration in the leaves, they may not necessarily suppress all other aspects of the *vte2* LT phenotypes such as soluble sugar and starch accumulation. To test if the primary *sve* loci affected the LT-inducible sugar accumulation phenotype of *vte2*, the leaf soluble sugar content of each line was measured after two weeks of LT treatment (Figure 2.6). The suppressors were found to have various degrees of suppression in soluble sugar accumulation with the *sve1vte2* and *sve2vte2* primary suppressor lines completely suppressing the *vte2* sugar accumulation phenotype to the level of Col while the other lines, with the exception of *sve6vte2*, showed at least a partial suppression. Primary suppressor *sve6vte2* contained sugar levels nearly equivalent to *vte2* but had a plant size similar to Col, suggesting carbohydrate accumulation and the *vte2* growth phenotype can be genetically uncoupled.

To investigate any impact of the primary *sve* lines on the impairment of photoassimilate export in LT-treated *vte2*, photoassimilate export capacities were also measured in all genotypes after 7 days of LT treatment. $^{14}\text{CO}_2$ incorporation under LT conditions was similar in all suppressor lines, *vte2*, *vte1* and Col indicating that neither

the primary *sve* nor *vte* mutations significantly impacts the rate of carbon fixation in leaves (Figure 2.7). Consistent with a prior report (Maeda et al., 2006), after 7 days of LT treatment *vte2* exhibited a dramatic reduction in ¹⁴C-labeled photoassimilate export to a level 15% that of Col (Figure 2.8). This phenotype was partially suppressed in *vte1* to a level 35% that of Col. The seven primary *sve* lines exhibited varying degrees of suppression of the *vte2* LT-induced photoassimilate export phenotype (Figure 2.8). *sve1vte2* and *sve2vte2* fully suppressed, *sve6vte2* did not suppress, and suppression in *sve3vte2*, *sve4vte2*, *sve5vte2* and *sve7vte2* was to a level similar or slightly higher than that in *vte1*.

The primary sve lines display varying degrees of suppression in callose deposition

To investigate whether any of the primary *sve* lines have altered callose deposition compared to *vte2*, two and four week-old *sve* plants were subjected to LT treatment and aniline-blue positive fluorescence in leaf vascular tissues was examined and compared to Col, *vte2* and *vte1*. The most obvious differences in callose deposition were apparent after 3 days of LT treatment (Figure 2.9). Primary *sve1vte2*, *sve2vte2* and *sve5vte2* lines completely suppressed callose deposition while primary *sve3vte2*, *sve4vte2* and *sve7vte2* lines showed partial suppression to levels less than or similar to *vte1*. Callose deposition was not suppressed in *sve6vte2* and was indistinguishable from or even stronger than *vte2*. After 7 days of LT treatment, *sve1vte2* and *sve2vte2* still showed almost complete suppression of callose deposition while the other *sve* lines showed strong aniline-blue fluorescence indistinguishable from *vte2* (Figure 2.10).

Five of the primary sve lines show changes in fatty acid composition before or after LT treatment

Recently it was shown (Maeda et al., 2008) that the levels of linolenic acid (18:3) and linoleic acid (18:2) in *vte2* leaves were significantly lower and higher than Col, respectively, after two weeks of LT treatment. Furthermore, *fad2* and *fad6*, the respective ER- or chloroplast- localized ω 6-desaturase mutants (Miquel and Browse, 1992; Falcone et al., 1994), were crossed to *vte2*, and the double mutants unexpectedly were found to suppress both the morphological and biochemical phenotypes of the *vte2* mutant at low temperatures completely (*fad2vte2*) or partially (*fad6vte2*) (Maeda et al., 2008). Because of these findings, we assessed the fatty acid (FA) composition of the primary *sve* lines. To test whether any of the primary *sve* lines impacted fatty acid composition before LT treatment, they and Col, *vte2* and *vte1* were grown at permissive conditions for four weeks and their leaf fatty acid composition was assessed by analyzing the corresponding fatty acid methyl esters using gas chromatograph (GC). Under permissive conditions primary *sve3vte2*, *sve4vte2*, *sve6vte2* and *sve7vte2* lines had leaf fatty acid compositions indistinguishable from Col, *vte2* and *vte1* (Table 2.2). Three other suppressors (primary *sve1vte2*, *sve2vte2*, and *sve5vte2* lines) had fatty acid compositions significantly different from Col (or *vte2*) under permissive conditions. In comparison to both Col and *vte2*, all three lines had lower 18:3 and higher oleic acid (18:1) levels with the 18:1 level in *sve1vte2* being particularly high and nearly 4-fold that in Col. The level of 18:2 was also severely reduced in *sve1vte2* and moderately elevated in *sve2vte2* and *sve5vte2*. Based on the FA compositions in plants grown under permissive conditions, the suppressors were categorized into two groups. Group I comprises the primary lines *sve1vte2*, *sve2vte2*,

sve5vte2 from pools 1, 2 and 4, respectively, and all have altered FA compositions. Group II includes suppressor lines from the rest of the four pools and they possess normal leaf FA compositions compared with Col (and *vte2*) at permissive conditions (Table 2.1).

To further investigate if the LT-induced PUFA changes observed in *vte2* were affected in *vte1* and the primary *sve* lines that showed fatty acid compositions similar to Col under permissive conditions (e.g. *sve3vte2*, *sve4vte2*, *sve6vte2* and *sve7vte2*), four-week-old plants were transferred from permissive to LT conditions for an additional two weeks and fatty acid compositions analyzed by GC (Table 2.3). The LT-dependent PUFA changes in these lines fell into two groups: primary suppressors *sve4vte2*, *sve6vte2* and *vte1* had *vte2*-like PUFA changes and 18:3 and 18:2 levels not significantly different from *vte2*, while the PUFA changes in primary lines *sve3vte2* and *sve7vte2* were more similar to Col and had 18:3 and 18:2 levels significantly different from *vte2* (Figure 2.11). These results suggest that the primary lines *sve3vte2* and *sve7vte2* have suppressed the LT-induced PUFA changes occurring in *vte2*.

DISCUSSION

LT treatment induced a series of responses in the tocopherol-deficient *vte2* mutant, and to a lesser extent the *vte1* mutant, that were absent from wild type, including callose deposition and altered transfer cell wall development in vascular parenchyma cells and impairment in photoassimilate export followed by soluble sugar accumulation and growth inhibition (Maeda et al., 2006). In this study, we employed a forward genetic approach to identify a suite of suppressors of the LT-induced *vte2* phenotypes in an attempt to genetically define and dissect the pathway involved in the response of tocopherol-deficient *Arabidopsis* mutants to LT treatment.

At least seven independent primary *sve* suppressor loci were identified based on allelism tests and comparative biochemical characterization. This chapter reported characterization of the primary suppressor lines. These data were used to select three *sve* lines to target for future analysis and attempted cloning (Chapter 3). The growth inhibition of LT-treated *vte2* was at least partially suppressed in all the primary *sve* lines (Figure 2.5) while other *vte2*-dependent responses were differentially impacted. The primary *sve1vte2* and *sve2vte2* lines completely suppressed all LT-inducible *vte2* phenotypes, including elevated sugar accumulation (Figure 2.6), reduced photoassimilate export (Figure 2.8), and callose deposition (Figure 2.9). Primary *sve3vte2*, *sve4vte2*, *sve5vte2* and *sve7vte2* lines showed a partial suppression of sugar accumulation and photoassimilate export, similar to the levels observed in *vte1*. These four lines also had partial or near total suppression of callose deposition after 3 days of LT treatment (Figure 2.9), but by 7 days of LT callose deposition in these lines was indistinguishable from *vte2* (Figure 2.10). The primary *sve6vte2* was unique in suppressing growth inhibition (Figure 2.5) but not impacting any other *vte2*-dependent responses (Figure 2.8, Figure 2.9) indicating that growth inhibition can be genetically uncoupled from and is downstream of the other LT-induced *vte2* phenotypes.

Consistent with the observations of Maeda et al (2008), *vte2* leaves show a fatty acid composition identical to Col under permissive conditions (Table 2.2) but have higher 18:2 and correspondingly lower 18:3 levels relative to Col in response to LT treatment (Table 2.3). Interestingly, three primary suppressor lines, *sve1vte2*, *sve2vte2* and *sve5vte2* had fatty acid compositions that differed from Col or *vte2* prior to LT treatment (Table 2.2). This result suggests that the constitutive alteration of fatty acids or membrane lipids

in these lines prevents the initiation and development of *vte2* LT-induced phenotypes. The fatty acid composition of the other four primary suppressor lines, *sve3vte2*, *sve4vte2*, *sve6vte2* and *sve7vte2* were indistinguishable from Col under permissive conditions but the responses of these suppressors to LT treatment fell in two distinct groups (Figure 2.12, Table 2.3). LT-treated *sve3vte2* and *sve7vte2* had fatty acid compositions most similar to LT-treated Col, indicating these two lines suppress the *vte2*-dependent, LT-induced PUFA changes, while LT-treated *sve4vte2* and *sve6vte2* showed PUFA composition changes similar to LT-treated *vte2* and thus genetically uncoupled *vte2*-dependent, LT-induced PUFA changes from the other *vte2* phenotypes. The fact that five out of seven primary *sve* lines affect fatty acid composition either prior to (*sve1vte2*, *sve2vte2* and *sve5vte2*) or after LT treatment (*sve3vte2* and *sve7vte2*) implies that LT-induced PUFA changes is an important event involved in initiation and development of LT phenotypes in *vte2* and membrane lipid metabolism may play an early and central role in the functions of tocopherols during LT adaptation.

Based on the physiological and biochemical analyses on the primary *sve* lines, three lines (*sve1vte2*, *sve2vte2* and *sve7vte2*), were selected for further detailed genetic, physiological, biochemical analyses and molecular cloning (Chapter 3). The primary lines of *sve1vte2* and *sve2vte2* almost completely suppressed all of the *vte2* LT phenotypes, including growth inhibition, sugar accumulation, photoassimilate export and callose deposition (Figure 2.5, Figure 2.6, Figure 2.8 and Figure 2.9). In addition, both of these lines have altered leaf fatty acid composition at permissive temperature (Table 2.1), which may prove useful as a convenient selectable marker during genetic backcrossing and mapping. More importantly, the biochemical processes which are disrupted in

sve1vte2 and *sve2vte2* may identify important links between tocopherol deficiency, the abnormal fatty acid alteration and photoassimilate export defect in LT-treated *vte2*. *sve7vte2*, the third suppressor line, had a strong, though incomplete, suppression of all the *vte2* LT phenotypes (Figure 2.5, Figure 2.6, Figure 2.8 and Figure 2.9) and unlike *sve1vte2* and *sve2vte2*, did not display abnormal fatty acid composition at permissive temperature (Table 2.1). *sve7vte2* may have a distinctive suppression mechanism from that of *sve1vte2* and *sve2vte2* and thus it would be interesting to define the gene involved. These three strongest suppressors lines selected for further studies should provide valuable insights into tocopherol functions in plants.

MATERIALS AND METHODS

EMS mutagenesis

Mutagenesis was performed by exposing 52.4 mg of *vte2-1* mutant seed to 0.3% ethylmethane sulfonate (EMS) for 15 hours at room temperature. The seed were then rinsed 10 times with distilled water over a 2h period, stratified for 5 days and separated into 10 pools. Each M₁ pool was grown independently and the individual M₂ seed pools collected and used for suppressor screening.

Suppressor screening and low temperature treatment

For the first round suppressor screening, approximately 1200 seed from each of 10 M₂ pool were surface sterilized, stratified for 5 days at 4°C, and then sown evenly on soil along with a few seed of Columbia-0, *vte1-1* and *vte2-1* in each tray for comparison. Plants were grown at permissive conditions (22°C day/18°C night) under 12h of 100 $\mu\text{mol quanta m}^{-2}\text{s}^{-1}$ illumination for two weeks. The temperature was then adjusted to 7°C ($\pm <3^\circ\text{C}$) and illumination lowered to 75 $\mu\text{mol quanta m}^{-2}\text{s}^{-1}$ for 4 weeks at which time the visible phenotypes of *vte2-1* and Col-0 were readily distinguishable. 94 individual seedlings that were judged larger than *vte2-1* and do not contain tocopherols were selected as putative suppressors.

For the second round of suppressor screening, the putative suppressor lines were allowed to self and grow to maturity at permissive conditions to produce M₃ seed. About 15-20 progeny per line were re-screened as described above. 29 lines inheriting clearly larger plant phenotypes at LT were selected and carried through additional analyses.

Allelism tests were carried out by performing multiple crosses between selected suppressor lines from the same and different pools. 10-15 F₁ progeny plants were subjected to low temperature treatment as described above and their phenotypes compared with their parental lines, Col-0 and *vte2-1*.

Tocopherol analysis

To confirm the *vte2* background in each putative suppressor, a leaf disk (~ 0.5cm in diameter) was harvested from each plant, and lipids were extracted as described (Collakova and DellaPenna, 2001). 0.01% (w/v) butylated hydroxytoluene (BHT) was added for protecting lipids from oxidative damage and 0.5ug/ml tocol as an internal standard. The lipid phase is dried and resuspended in the solvent (Methanol with 0.01% w/v BHT) and used for reverse phase HPLC analysis to identify tocopherols as described previously (Collakova and DellaPenna, 2001).

Analysis of soluble sugars

Quantification of leaf soluble sugar levels was based on the enzyme assay developed by Jones et al (Jones et al., 1977) with minor modifications. A leaf disc (~ 0.5cm in diameter) from each plant was harvested at the end of the light cycle. The leaf punches were quickly weighed and the soluble sugars were extracted twice in 80°C 80% ethanol as previously described (Maeda et al., 2006). The extracts were combined, dried and redissolved in 200 uL of distilled water. Dilutions were made on samples with higher sugar contents and glucose, fructose and sucrose levels determined enzymatically as previously described (Jones et al., 1977; Maeda et al., 2006). The total sugar content is the sum of glucose, fructose and sucrose and expressed as % relative to *vte2* level.

¹⁴C photoassimilate labeling

¹⁴CO₂ labeling of photoassimilate and measurement of phloem exudation were performed as described (Maeda et al., 2006) with the exceptions that 10mM EDTA was used for exudation buffer and 0.05 mCi of NaH¹⁴CO₃ was used per labeling experiment. Phloem exudates were collected after 5 hours of exudation.

Fluorescence microscopy

Leaves from each plant were harvested at the end of the light cycle and prepared for aniline blue fluorescence microscopy as described (Maeda et al., 2006). At least 3 plants for each genotype (n ≥ 3) were analyzed. The camera (SPOT FlexColor “C” mount FX1520) settings for 3 d LT treated samples are: Exposure: 700 msec, Gain: 2, Gamma: 1.00 while those for 7 d LT treated samples are: Exposure: 900 msec, Gain: 4, Gamma: 1.40.

Analysis of fatty acid composition

Leaf punches from un-shaded mature leaf of each genotype were harvested and lipids extracted as previously described (Dormann et al., 1995) and used to prepare fatty acid methyl esters. The methyl esters were analyzed by gas-liquid chromatography using myristic acid as an internal standard as previously described (James and Dooner, 1990; Collakova and DellaPenna, 2001).

TABLES AND FIGURES

Table 2.1 A summary of the primary *sve* lines identified from suppressor screens.

Categorization of suppressors are based on fatty acid composition (Group), primary suppressor locus name (Locus), the corresponding M₁ pool from which the suppressors were identified (Pool), number of suppressor lines selected from each pool (Lines), the names of the suppressor lines (suppressors), the leaf fatty acid composition under permissive conditions (FA composition, 22°C) (refer to Table 2.2 for details), the type of changes (“Col” or “*vte2*”) in linoleic acid (18:2) and linolenic acid (18:3) after 14 d of LT treatment (18:2, 18:3 change, 7°C) (refer to Table 2.3 and Figure 2.11 for details), the type of carbohydrate accumulation and photoassimilate export capacity (Sugars and export) (“Col”, “*vte2*” or “intermediate”) in mature leaves after 14 d of LT treatment (refer to Figure 2.6 and Figure 2.8 for details), the type of callose deposition (“Col”, “*vte2*” or “intermediate”) after 3 d of LT treatment (refer to Figure 2.10 for details), and the plant size after 28 d of LT treatment (Size). Representative suppressor lines at each primary locus are marked with bold font

Table 2.1

Group	Locu s	Pool	Lines	Suppressors	FA composition (22°C)	18:2,18:3 change (7°C)	Sugars and export	Callose	Size
I (altered FA)	<i>sve1</i>	4	10	01-034, 01-035, 01-036, 02-004, 02-011, 02-017 , 02-018, 02-024, 02-025, 02-027	Dramatically higher 18:1, lower 18:2 and 18:3	NA	Col	Col	Col
	<i>sve2</i>	1	4	01-016, 01-037, 02-007, 02-008	Higher 18:1 and 18:2, lower 18:3	NA	Col	Col	Col
	<i>sve5</i>	10	4	01-050 , 01-003, 01-021, 02-001	Higher 18:1 and 18:2, lower 18:3	NA	Intermediate	Intermediate	Col
II (Normal FA)	<i>sve3</i>	10	4	01-050 , 01-003, 01-021, 02-001	Normal	Col	Intermediate	Intermediate	Col
	<i>sve7</i>	9	7	01-047, 02-003, 01-048, 01-012, 01-013, 02-014, 02-015	Normal	Col	Intermediate	Intermediate	Col
	<i>sve4</i>	3	2	01-032 , 01-033	Normal	<i>vte2</i>	Intermediate	Intermediate	Col
	<i>sve6</i>	7	1	01-051	Normal	<i>vte2</i>	<i>vte2</i>	<i>vte2</i>	Col

Table 2.2 Leaf fatty acid composition of the primary *sve* lines, Col, *vte2* and *vte1* at permissive conditions

Genotype	Fatty acid composition (mol %)									
	16:0	16:1	16:2	16:3	18:0	18:1	18:2	18:3		
Col	17.9 ±1.1	3.1 ±0.3	0.8 ±0.2	5.8 ±0.4	1.2 ±0.2	6.8 ±0.3	19.0 ±0.9	45.3 ±1.8		
<i>vte2</i>	18.2 ±1.0	3.2 ±0.3	0.8 ±0.2	6.0 ±0.5	1.3 ±0.3	7.0 ±0.9	19.9 ±1.3	43.6 ±2.3		
<i>vte1</i>	17.9 ±1.9	3.3 ±0.3	0.8 ±0.2	5.8 ±0.8	1.2 ±0.3	6.9 ±0.7	18.6 ±1.9	45.5 ±3.8		
<i>sve1vte2</i>	12.4 ±0.7**	3.0 ±0.3	0.9 ±0.0	6.2 ±0.6	0.7 ±0.1**	29.6 ±1.2**	5.6 ±0.2**	41.5 ±1.6**		
<i>sve2vte2</i>	19.7 ±0.5**	3.5 ±0.3	1.0 ±0.0*	5.0 ±0.5*	1.5 ±0.1*	9.5 ±0.5**	24.4 ±0.5**	35.5 ±0.3**		
<i>sve3vte2</i>	19.4 ±1.5	3.4 ±0.4	0.7 ±0.1	6.1 ±0.6	1.4 ±0.0	6.8 ±0.1	18.8 ±0.2	43.4 ±1.3		
<i>sve4vte2</i>	18.9 ±2.1	3.5 ±0.5	0.6 ±0.0	5.5 ±1.3	1.8 ±1.0	7.2 ±1.2	19.7 ±1.8	42.8 ±4.9		
<i>sve5vte2</i>	16.8 ±1.6	3.2 ±0.2	1.4 ±0.3*	3.6 ±0.7**	1.2 ±0.2	9.3 ±0.6**	26.6 ±1.8**	38.1 ±3.7*		
<i>sve6vte2</i>	17.6 ±1.2	3.0 ±0.3	0.9 ±0.2	6.3 ±0.5*	1.2 ±0.3	6.3 ±0.6	18.9 ±1.2	45.9 ±2.0		
<i>sve7vte2</i>	18.1 ±1.3	3.3 ±0.3	0.6 ±0.1	5.8 ±0.6	1.4 ±0.1	7.4 ±0.8	17.6 ±0.7*	45.8 ±2.1		

All lines were grown at permissive conditions for four weeks and leaf samples taken at the middle of the light cycle for fatty acid analyses. Data are means ± SD (n ≥ 5). Significant differences of each fatty acid relative to Col are indicated (* P < 0.05, ** P < 0.01, Student's t-test).

Table 2.3 Leaf fatty acid composition of four primary *sve* lines and Col, *vte2* and *vte1* after 14 d of LT treatment

Genotype	Fatty acid composition (mol %)									
	16:0	16:1	16:2	16:3	18:0	18:1	18:2	18:3		
Col	35.3 ± 0.8 ^a	2.7 ± 0.2 ^a	0.1 ± 0.1	0.9 ± 0.2	1.4 ± 0.1	5.4 ± 0.5	22.3 ± 0.8 ^a	31.9 ± 1.4 ^a		
<i>vte2</i>	32.7 ± 1.0 ^b	2.1 ± 0.1 ^b	0.0 ± 0.0	0.7 ± 0.1	1.2 ± 0.1	6.1 ± 0.4	30.9 ± 0.8 ^b	26.3 ± 1.4 ^b		
<i>vte1</i>	33.7 ± 0.6 ^b	2.1 ± 0.1 ^b	0.1 ± 0.0	0.7 ± 0.1	1.2 ± 0.0	5.8 ± 0.4	28.5 ± 0.3 ^{ab}	28.0 ± 0.4 ^b		
<i>sve3vte2</i>	30.3 ± 0.8 ^{ab}	2.3 ± 0.1 ^a	0.2 ± 0.0	1.2 ± 0.1 ^a	1.1 ± 0.1 ^b	6.7 ± 0.4 ^{ba}	25.9 ± 1.0 ^{ab}	32.3 ± 0.6 ^a		
<i>sve4vte2</i>	33.9 ± 0.5 ^b	2.5 ± 0.2 ^a	0.1 ± 0.0	0.6 ± 0.0	1.2 ± 0.0	6.8 ± 0.4 ^b	28.2 ± 0.6 ^{ab}	26.8 ± 0.3 ^b		
<i>sve6vte2</i>	33.1 ± 0.9 ^b	2.3 ± 0.1 ^a	0.1 ± 0.0	0.6 ± 0.1	1.2 ± 0.1 ^b	6.9 ± 0.5 ^b	28.8 ± 1.6 ^b	26.9 ± 0.4 ^b		
<i>sve7vte2</i>	33.2 ± 0.9 ^b	2.4 ± 0.1 ^a	0.0 ± 0.0	0.7 ± 0.1	1.1 ± 0.1 ^b	7.5 ± 0.7 ^{ba}	23.5 ± 0.9 ^a	31.6 ± 1.4 ^a		

All lines were grown at permissive conditions for four weeks, transferred to low temperature conditions for an additional 14 days and leaf samples taken at the middle of the light cycle for FAME analysis. Data are means ± SD (n ≥ 5). ^a and ^b indicate significant differences (P < 0.01) relative to *vte2* and Col, respectively (Student's t-test).

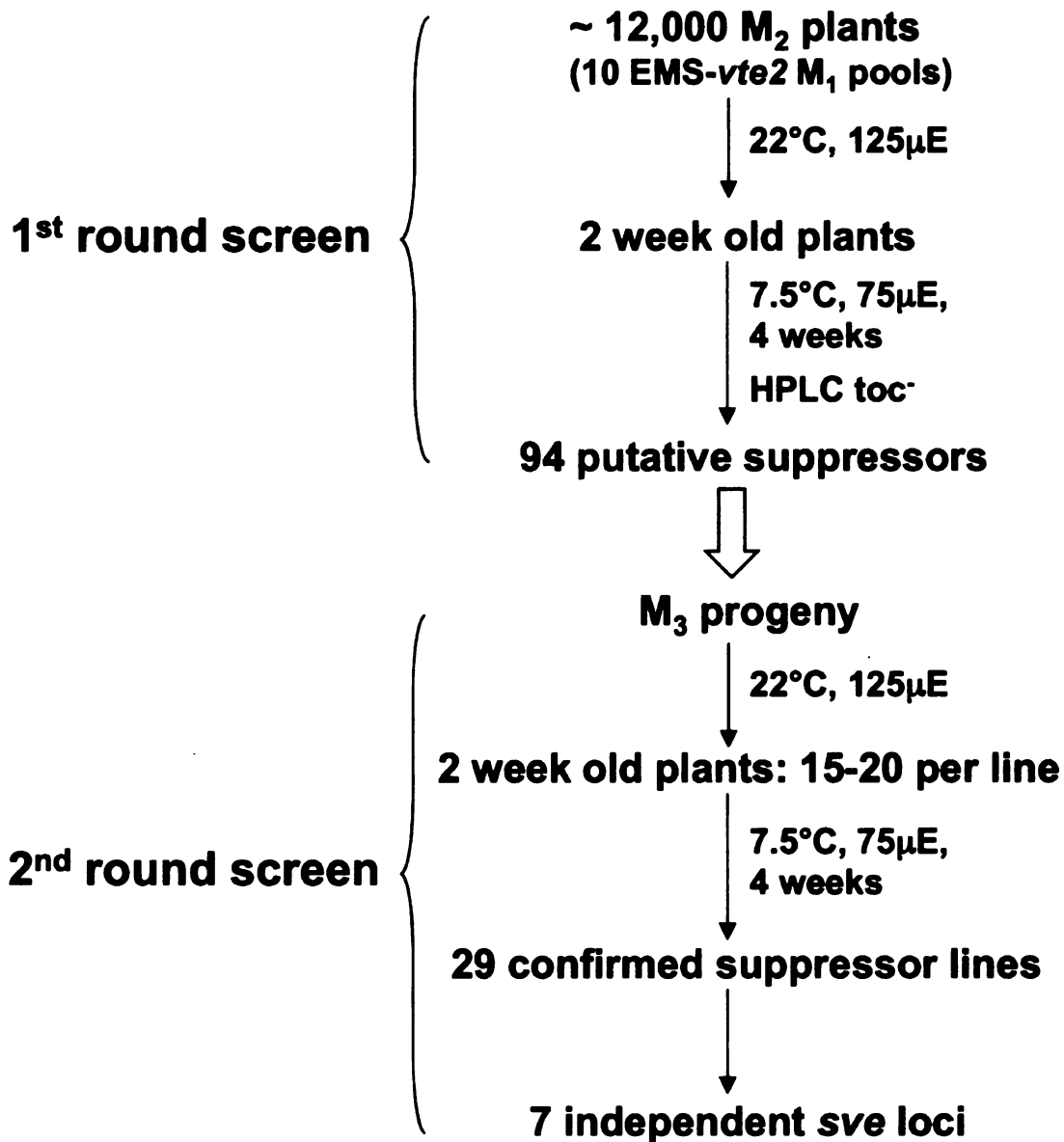


Figure 2.1 Suppressor screening scheme.

The first round of suppressor screening identified 94 putative suppressor lines of which 29 were confirmed in a second screen. Allelism tests grouped these into seven independent primary *sve* (*suppressor of vte2* LT-induced phenotype) lines.

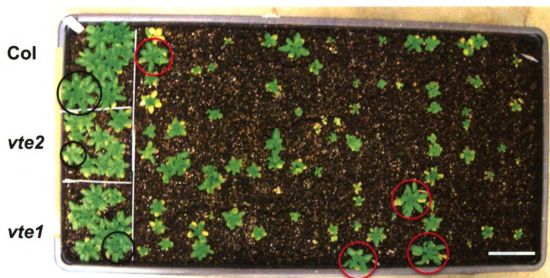


Figure 2.2 An example flat from the first round of suppressor screening.

About 200 M_2 plants from separate M_1 pools (in this image: pool 4) together with control genotypes (*Col*, *vte2* and *vte1*, marked with black circles) were planted in a flat and allowed to grow for two weeks under permissive conditions and then transferred to low temperature conditions. Pictures were taken after four weeks of low temperature treatment. Individuals that were larger in plant size and had less purple color in leaves than *vte2* were selected as candidate suppressor lines (e.g. the four plants marked with red circles). Size bar = 5 cm.



Figure 2.3 An example image of the second round of suppressor screening.

The 94 putative suppressors were reassessed under LT conditions. About 15-20 M_3 plants from each putative suppressor line (e.g. 01-013 and 01-16) were grown together with control genotypes (Col, *vte2*) for two weeks under permissive conditions and then transferred to LT conditions. Pictures are of plants after four weeks of low temperature treatment. 29 lines whose M_3 progeny inherited the suppressor phenotypes were confirmed and used for further analysis. Size bar = 2 cm.

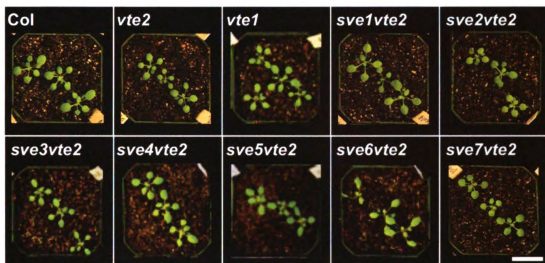


Figure 2.4 Whole plant phenotype of primary lines of *sve1vte2-sve7vte2* compared with Col, *vte2* and *vte1* before LT treatment.

Pictures were taken after growth under permissive growth conditions for two weeks. Size bar = 2 cm.

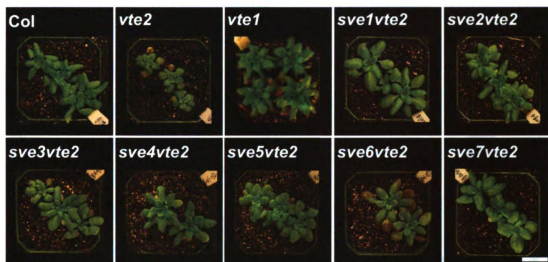


Figure 2.5 Whole plant phenotype of the primary lines *sve1vte2-sve7vte2* compared with Col, *vte2* and *vte1* after LT treatment.

All genotypes were grown for 2 weeks at permissive conditions and then transferred to LT conditions. Pictures were taken after four weeks of LT treatment. Size bar = 2 cm.

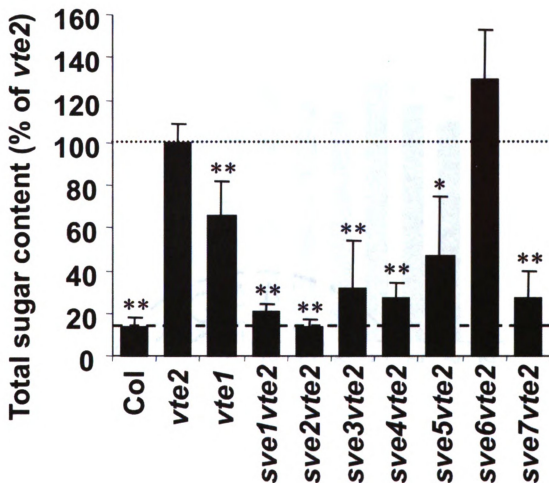


Figure 2.6 Leaf total soluble sugar content in primary *sve1vte2*-*sve7vte2* lines compared with Col, *vte2* and *vte1*.

All the plants were grown for 2 weeks at permissive conditions and then transferred to LT conditions. Sugar samples were taken from the 9-11th leaves of plants at the end of the light cycle after 2 weeks of LT treatment. Total sugar content is expressed relative to the *vte2* level. The dotted and dashed lines indicate the average sugar levels in *vte2* and Col, respectively. Data are means \pm SD (n = 5). Values significantly different from *vte2* are indicated by * (P < 0.05) or ** (P < 0.01) (Student's t-test).

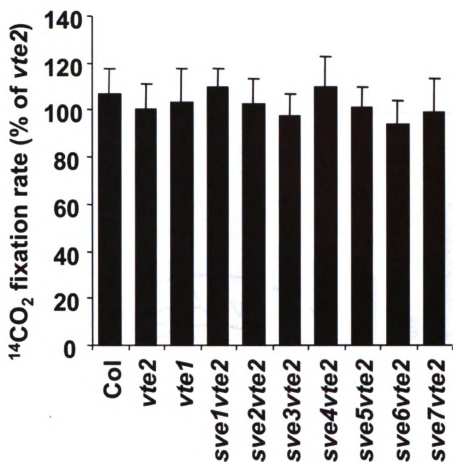


Figure 2.7 Total $^{14}\text{CO}_2$ fixation after 7 d of LT treatment of primary *sve1vte2-sve7vte2* lines compared with Col, *vte2* and *vte1*.

All lines were grown at permissive conditions for four weeks and transferred to low temperature conditions. $^{14}\text{CO}_2$ labeling was done at the middle of the light cycle after 7 d of LT treatment. Total fixed $^{14}\text{CO}_2$ is expressed as relative to *vte2*. Data are means \pm SD ($n \geq 5$).

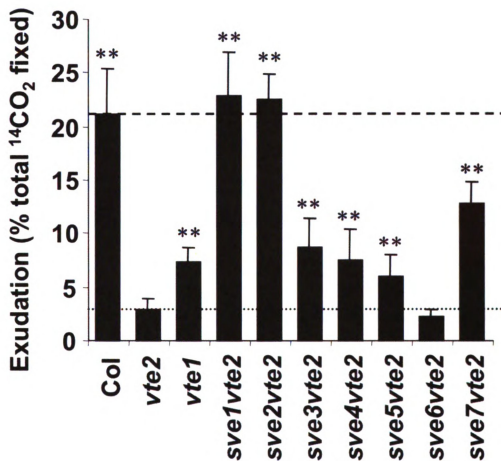


Figure 2.8 Percent exudation of primary *sve1vte2-sve7vte2* lines compared with Col, *vte2* and *vte1*.

All lines were grown at permissive conditions for 4 weeks and transferred to LT conditions. $^{14}\text{CO}_2$ labeling of an individual leaf was done at the middle of the light cycle following 7 d of LT treatment. Photoassimilate export capacity is expressed as the percentage exudation (after 5 hours) of total fixed $^{14}\text{CO}_2$. The dotted and dashed lines indicate the levels in *vte2* and Col, respectively. Data are means \pm SD ($n = 5$). Values significantly different from *vte2* are indicated by * ($P < 0.05$) or ** ($P < 0.01$) (Student's t-test).



Figure 2.9 Callose deposition in primary *sve1vte2*-*sve7vte2* lines compared with Col, *vte2* and *vte1* after 3 d of LT treatment.

All lines were grown on ½ MS plates for two weeks under permissive conditions and whole seedlings were fixed at the middle of the light cycle after 3 additional days of LT treatment. Aniline-blue positive fluorescence was examined in the lower portions of leaves ($n \geq 3$, size bar = 1 mm).

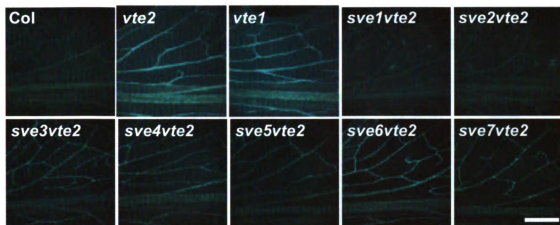


Figure 2.10 Callose deposition in primary *sve1vte2-sve7vte2* lines compared with Col, *vte2*, and *vte1* after 7 d of LT treatment.

All lines were grown on soil under permissive conditions for four weeks and leaves were fixed at the middle of the light cycle after an additional 7 days of low temperature treatment. Aniline-blue positive fluorescence was examined in the lower portions of leaves ($n \geq 3$, size bar = 1 mm).

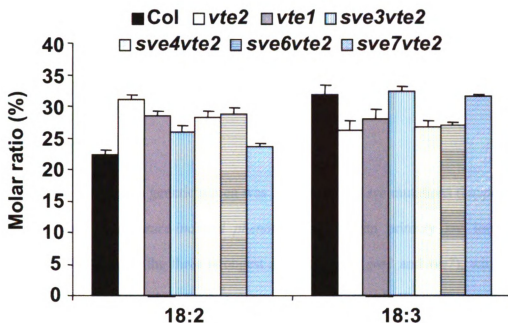


Figure 2.11 Molar ratios of linoleic acid (18:2) and linolenic acid (18:3) in primary suppressor lines of *sve3vte2*, *sve4vte2*, *sve6vte2*, *sve7vte2* compared with *Col*, *vte2* and *vte1* after 14 d of LT treatment.

Plants were grown under permissive conditions for 4 weeks and transferred to LT conditions. Leaf samples were taken at the middle of the light cycle for fatty acid analysis. *sve3vte2* (vertical bars), *sve4vte2* (dotted bars), *sve6vte2* (horizontal bars), *sve7vte2* (hatched bars), *Col* (black), *vte2* (white) and *vte1* (gray). Data are means \pm SD (n = 5).

CHAPTER 3 CLONING OF *ARABIDOPSIS SVE* (SUPPRESSORS OF *VTE2* LOW TEMPERATURE-INDUCED PHENOTYPE) MUTANTS HIGHLIGHT THE INVOLVEMENT OF TOCOPHEROLS IN LIPID METABOLISM

ABSTRACT

In the prior chapter, a genetic screen was carried out for *sve* mutations (*suppressors of the *vte2* low temperature-induced phenotype*) and seven primary *sve* loci were identified. In this chapter the three strongest *sve* loci (*sve1*, *sve2* and *sve7*), which had differing impacts on LT-induced sugar accumulation, photoassimilate export reduction and vascular-specific callose deposition in *vte2* were selected for further detailed analysis and molecular cloning. *sve1* completely suppressed all *vte2* LT phenotypes and was found to be a novel allele of *fad2*, the endoplasmic reticulum-localized oleate desaturase. *sve2* showed partial suppression and was found to be a new allele of *trigalactosyldiacylglycerol1 (tgd1)*, a component of the ER-to-plastid lipid ATP-binding cassette (ABC) transporter. Introduction of *tgd2*, *tgd3*, and *tgd4* mutations into the *vte2* background similarly suppressed the *vte2* LT phenotypes, indicating a key role for lipid transport in the suppression of the phenotype. *sve7* partially suppressed all *vte2* LT phenotypes without impacting fatty acid and lipid metabolism at permissive temperature. Analyses of the acyl composition of ER- and plastid-derived lipids before and after LT treatment demonstrated the elevation of 18:2 in phosphatidylcholine is an early and key component in *vte2* LT-induced responses as all suppressors attenuated this change and it was the only lipid species significantly correlated with the suppressor photoassimilate export capacity. Identification and characterization of *sve* loci highlights the involvement

of tocopherols in ER lipid metabolism in plants.

INTRODUCTION

Tocopherols are lipid-soluble antioxidants that are produced exclusively by photosynthetic organisms (Grusak and DellaPenna, 1999). In plants, tocopherols are synthesized in the plastid inner envelope (Soll et al., 1980a; Soll et al., 1980b) and the majority of tocopherols are localized in plastids (Wise and Naylor, 1987; Havaux, 1998) where their primary function has long been assumed to be protecting polyunsaturated fatty acids (PUFAs) from oxidative damage (Knox and Dodge, 1985; Robinson, 1988; Fryer, 1992; Munne-Bosch and Alegre, 2002). This was clearly shown to be a primary role of tocopherols in dormant seed and germinating seedlings as in their absence the seed PUFA pool suffers extreme non-enzymatic lipid peroxidation (Sattler et al., 2004; Sattler et al., 2006). However in photosynthetic tissues, the role of tocopherols in photoprotection was shown to be quite limited (Havaux et al., 2005; Maeda et al., 2006; Abbasi et al., 2009) and studies in other plants are suggesting the roles of tocopherols in various stresses may be both species and stress-specific (Maeda et al., 2006; Abbasi et al., 2007; Maeda et al., 2008).

Similar to the maize *sxd1* and potato *VTE1*-RNAi lines (Russin et al., 1996; Provencher et al., 2001; Hofius et al., 2004), the *Arabidopsis* tocopherol-deficient *vte2* mutants develop vascular callose deposition, defective photoassimilate export capacity, and sugar accumulation but only upon exposure to non-freezing low temperature (LT) treatment (Maeda et al., 2006), suggesting that a role for tocopherols in development of full photoassimilate transport capacity is evolutionarily conserved. A recent study showed that LT-treated *vte2* leaves have the levels of linolenic acid (18:3) and linoleic acid (18:2) significantly lower and higher than wild type, respectively (Maeda et al.,

2008). However, exhaustive analysis by chemical and MS-based lipid profiling failed to detect any significant differences in lipid peroxidation products in LT-treated *vte2* relative to wild type. In addition, mutations in ER ω -6 fatty acid desaturase *fad2* and to a lesser degree plastidial ω -6 fatty acid desaturase *fad6*, suppressed the *vte2* LT-induced phenotypes, whereas mutations decreasing or eliminating 18:3, the fatty acid most susceptible to oxidation (*fad3*, *fad7fad8*, *fad3fad7fad8*) did not (Maeda et al., 2008). While these experiments have excluded a role for lipid oxidation in the *vte2* LT phenotype, the results have also clearly indicated the involvement of PUFA metabolism. However, the cause and effect relationships between tocopherol deficiency, altered lipid metabolism and the LT-induced *vte2* phenotypes and the molecular mechanism underlying this phenomenon remain unclear.

The previous chapter described a forward genetic approach to identify elements linking tocopherol deficiency and carbohydrate metabolism in the LT-inducible *Arabidopsis vte2* system. Seven *sve* loci were identified but as it is impractical to move forward and carry out map-based cloning with all the primary *sve* lines, the three strongest lines (*sve1vte2*, *sve2vte2* and *sve7vte2*) were prioritized based on their unique features. The primary lines of *sve1vte2* and *sve2vte2* almost completely suppressed all of the *vte2* LT phenotypes (Figure 2.5, Figure 2.6, Figure 2.8 and Figure 2.9) and also have altered leaf fatty acid composition at permissive temperature (Table 2.2). *sve7vte2* showed a partial but strong suppression of all the *vte2* LT phenotypes (Figure 2.5, Figure 2.6, Figure 2.8 and Figure 2.9) and has a normal fatty acid composition before LT treatment (Table 2.2). In addition, following LT treatment, *sve7vte2* showed changes in fatty acids 18:2 and 18:3 similar to Col (Table 2.3, Figure 2.11) suggesting that *sve7vte2*

may suppress the LT-induced *vte2*-specific PUFA changes. The biochemical processes which are disrupted in *sve1vte2*, *sve2vte2* and *sve7vte2* are distinct and it is anticipated that the detailed biochemical analysis and molecular identification of these suppressor loci will reveal important links between tocopherol deficiency, fatty acid alterations and photoassimilate export defect in LT-treated *vte2* and thereby provide new insights into tocopherol functions and their apparent involvement in lipid metabolism in plants.

RESULTS

sve1, *sve2* and *sve7* are single recessive loci

Representative lines of the three strongest suppressors, *sve1vte2*, *sve2vte2*, and *sve7vte2* (Figure 2.5) were selected for further genetic analysis and backcrossing to remove other mutations in their backgrounds. F₁ progeny of *sve1vte2*, *sve2vte2* and *sve7vte2* backcrossed to *vte2* showed LT phenotypes indistinguishable from LT-treated *vte2* (Figure 3.1), consistent with the three *sve* loci being recessive. This was confirmed in F₂ progeny of an *sve1vte2* × *vte2* cross which segregated 89:32 for *vte2* and *sve1vte2* LT plant phenotypes, respectively (Chi square test, p=0.67) (Figure 3.2). Similarly, F₂ progeny of an *sve7vte2* × *vte2* segregated 50:18 for *vte2* and *sve7vte2* LT phenotypes, respectively (Chi square test, p=0.92) (data not shown). The two primary lines were backcrossed at least twice and *sve1vte2* and *sve7vte2* were selected based on their visibly distinguishable LT plant phenotype relative to *vte2* and further confirmed by their significantly lower sugar content (see later section). Segregation of *sve2* in backcrossed F₂ population turned out to be more complex because of at least two other unlinked mutations that resulted in yellowish leaf color and smaller plants and hence affected

sugar content and plant size making it difficult to select *sve2* based on the LT sugar phenotype (data not shown). Selection of *sve2* was achieved using its other biochemical phenotypes detailed in a later section. After segregating away the other mutations, unlike the primary *sve2* line which fully suppressed (Chapter 2 Figure 2.5, Figure 2.6, Figure 2.8 and Figure 2.9), the backcrossed *sve2* now partially suppressed the *vte2* LT phenotypes (see later sections).

sve loci show different degrees of *vte2* LT-induced phenotype suppression

When four-week-old *sve1vte2* and *sve7vte2* plants grown at permissive conditions were subjected to an additional 4 weeks of LT treatment, they remained green and were visibly similar to Col while *sve2vte2* plants showed a phenotype intermediate between Col and *vte2* (Figure 3.3 A).

To assess whether the *sve* mutations affect the carbohydrate accumulation and export phenotypes of LT-treated *vte2*, their soluble sugar contents and photoassimilate export capacities were measured and compared with *vte2*, Col and *vte1*. After two weeks of LT treatment, the soluble sugar level in *vte2* was nearly six times higher than Col (232 and 40 $\mu\text{mol/g}$ FW, respectively). *sve1vte2* had a sugar content identical to Col, while the levels in *sve2vte2* and *sve7vte2* were intermediate and similar to *vte1* (Figure 3.3 B). Photoassimilate export capacity was measured after 7 d of LT treatment, when the differences between *vte2* and Col were sufficiently large (5-fold) for an intermediate phenotype to be observed (Figure 3.3 C). The photoassimilate export capacity of *sve1vte2* was indistinguishable from Col, while *sve2vte2* and *sve7vte2* were significantly different from *vte2* and Col but similar to *vte1*. These results indicate that *sve1*, and to lesser extent

sve2 and *sve7*, suppressed both the carbohydrate accumulation and export phenotypes of LT-treated *vte2*.

To investigate whether *sve* lines altered the vasculature-specific callose deposition phenotype of LT-treated *vte2*, aniline-blue positive fluorescence was examined in response to LT treatment. Prior to LT treatment, all genotypes lacked callose deposition in the vasculature (data not shown). Callose deposition remained absent in Col at all LT treatment time points (Figure 3.3 D, Figure 3.10). After 3 d of LT treatment, the vasculature of *vte2* and to a lesser extent *vte1* contained significant levels of callose (Figure 3.3 D), which intensified after 7 d LT treatment (Figure 3.10). *sve1vte2* was indistinguishable from Col after 3 d LT treatment (Figure 3.3 D) and had very few spots of callose deposition after 7 d of LT treatment (Figure 3). After 3 d of LT treatment callose deposition was delayed and decreased in *sve2vte2* and *sve7vte2* to a degree lesser than *vte1* (Figure 3.3 D) but by 7 d of LT treatment was similar to both *vte2* and *vte1* (Figure 3.10).

sve1 and sve2 but not sve7 have constitutively altered fatty acid composition

A prior study showed that 14 d LT-treated *vte2* had significantly higher and lower linoleic acid (18:2) and linolenic acid (18:3), respectively, relative to Col and esterified primarily to phosphatidylcholine (PC) and phosphatidylethanolamine (PE) (Maeda et al., 2008). To test the hypothesis that PUFA metabolism might be affected by *sve* mutations, we assessed the leaf fatty acid composition of *sve* plants in comparison to Col, *vte2*, and *vte1* (Table 3.1). Under permissive conditions the fatty acid composition of Col, *vte2* and *vte1* was nearly indistinguishable. *sve7vte2* had slightly lower 18:2 and slightly higher 16:3 but was otherwise similar to Col. In contrast, the fatty acid compositions of *sve1vte2*

and *sve2vte2* were significantly different from Col. Both had elevated oleic acid (18:1) levels with that of *sve1vte2* nearly 5-fold that of Col. 18:2 was severely reduced and 16:0 moderately reduced in *sve1vte2* while both were moderately elevated in *sve2vte2*. The level of 18:3 was also reduced significantly in *sve2vte2*. These results indicate that *sve1* and *sve2* but not *sve7* significantly altered the fatty acid composition of *vte2* at permissive conditions.

sve1 is a novel mutant allele of the ER localized oleic acid desaturase *FAD2*

sve1 was the strongest suppressor isolated from the genetic screen (Figure 3.3) and had significantly altered fatty acid composition (Table 3.1). The fatty acid composition of F₁ progeny from an *sve1vte2* × *vte2* cross at permissive temperature was identical to Col and *vte2* and photoassimilate export capacity after 7 d LT treatment was reduced to *vte2* levels (Table 3.2). 32 F₂ progeny of this cross that suppressed the LT-induced *vte2* phenotype (Figure 3.2) also possessed a marked reduction in 18:2 and increase in 18:1 under permissive conditions, while 89 F₂ progeny that did not suppress the *vte2* LT phenotypes (Figure 3.2) had fatty acid compositions identical to Col and *vte2* (Table 3.2). These results confirmed that *sve1* is a single recessive locus and indicate its altered fatty acid phenotype cosegregates with suppression of the *vte2* LT phenotype.

The fatty acid composition in *sve1* suggested a defect in 18:1 to 18:2 desaturation and was remarkably similar to the fatty acid profile of *fatty acid desaturase 2* (*fad2*) mutants (Lemieux et al., 1990; Miquel and Browse, 1992). To test if *sve1* carries a mutation in *FAD2*, the coding and 1 kb upstream region of *FAD2* in *sve1vte2* was sequenced and compared to Col. The *FAD2* gene of *sve1vte2* contains a single point

mutation (G to A) that converts Ala335 to Thr335, a highly conserved residue in *FAD2* orthologs from evolutionary divergent photosynthetic organisms (Figure 3.11 A).

When *sve1vte2* was crossed to an independently generated *fad2-1vte2* double mutant (Maeda et al., 2008) to test for genetic complementation, the leaf fatty acid composition of F₁ progeny was nearly identical to both parents (Figure 3.4 A), indicating that *sve1* carries a mutation at the same locus as *fad2-1*. Furthermore, the F₁ progeny of this cross completely suppressed *vte2* LT phenotypes including photoassimilate export deficiency (Figure 3.4 B), callose deposition (Figure 3.4 C), and whole plant phenotype (Figure 3.4 D). These results indicate that the Ala335→Thr335 mutation in *FAD2* of *sve1vte2* is responsible for suppression of the *vte2* LT phenotypes.

sve2 is a novel mutant allele of the ABC lipid transporter component *TGD1*

sve2vte2 partially suppressed all *vte2* LT phenotypes to a degree similar to that of *vte1* (Figure 3.3) and also exhibited altered fatty acid composition under permissive conditions (Table 3.1). The fatty acid composition of F₁ progeny from a *sve2vte2* × *vte2* cross was identical to Col and *vte2* (Figure 3.5 A), consistent with the *sve2* mutation being recessive. The fatty acid profile of *sve2vte2* did not resemble previously reported *fad* mutants (Browse et al., 1993; Iba et al., 1993; Wallis and Browse, 2002). When the polar lipid composition of *sve2vte2*, Col and *vte2* was analyzed by thin layer chromatography, an additional spot was identified in *sve2vte2* that is characteristic of trigalactosyldiacylglycerol (TGDG) (Figure 3.5 B, (Xu et al., 2003b). Four *trigalactosyldiacylglycerol* (*tgd*) loci, *tgdl* to *tgd4*, have been isolated in *Arabidopsis* and found to accumulate TGDG due to defective lipid trafficking from the ER to plastid (Xu

et al., 2003b; Awai et al., 2006; Lu et al., 2007b; Xu et al., 2008). All *tgd* mutants exhibit changes in fatty acid compositions similar to *sve2vte2* (data not shown).

To test if *sve2* is allelic to any *tgd* locus, *sve2vte2* was crossed to each *tgd* mutant and the resulting F₁ progeny analyzed for polar lipid composition. Only the progeny of the *sve2vte2* × *tgd1* cross showed a TGDG band (Figure 3.5 B and data of others not shown), indicating the mutation giving rise to TGDG production in *sve2* is allelic to *tgd1*. Sequencing of the *TGD1* coding region in *sve2vte2* identified a single G to A mutation converting Ala319 to Thr319, a conserved residue in TGD1 orthologs from evolutionary divergent photosynthetic organisms (Figure 3.11 B). A CAPS marker was developed for the *sve2* (*tgd1*) allele and used to genotype F₂ progeny from an *sve2vte2* × *vte2* that were then scored for sugar content in response to LT treatment. The sugar content of 14 *sve2/sve2* progeny was significantly lower than that of *vte2* whereas that of the 22 *SVE2/sve2* and 10 *SVE2/SVE2* progeny were not (Figure 3.5 C), indicating that the *tgd1* point mutation in *sve2* is recessive and cosegregates with the *sve2vte2* suppression phenotype.

The previously characterized *tgd1-1* mutation (Xu et al., 2003a) was introduced into the *vte2* background and crossed to *sve2vte2* to test for complementation. The leaf sugar content (Figure 3.6 A), export capacity (Figure 3.6 B), callose deposition in mature leaves after 3 d LT treatment (Figure 3.6 C) and purple coloration in mature plants after prolonged LT treatment (Figure 3.6 D) of the resultant F₁ progeny were similar to both parents and significantly different from that of *vte2*, indicating that *tgd1* mutation in *sve2* is responsible for the suppression of the *vte2* LT phenotypes. Notably, the effect of

sve2vte2 on the above phenotypes is less dramatic than that of *tgdl-1vte2* indicating that *sve2* is a weaker allele of *tgdl*.

Three other tgd loci also suppress the vte2 LT- induced phenotypes

TGD1, 2 and 3 have been proposed to form an ABC lipid transporter complex that is responsible for phosphatidic acid (PA) transfer through the plastid inner envelope membrane (Xu et al., 2005; Awai et al., 2006; Lu et al., 2007a). TGD4 associates with the ER membrane and is hypothesized to transfer lipids between the ER and outer plastid envelop membranes (Xu et al., 2008). To test if the other *tgd* loci (*tgd2*, *tgd3* and *tgd4*) also suppress the *vte2* LT phenotypes, we introduced *tgd2-1* (Awai et al., 2006), *tgd3-1* (Lu et al., 2007b) and *tgd4-1* (Xu et al., 2008) into the *vte2* background and tested the single and corresponding double homozygous mutants for their LT phenotypes. After transfer of plants to LT conditions, all *tgd* single mutants were slightly paler than Col but had soluble sugar content and photoassimilate export capacity nearly identical to Col (Figure 3.7), indicating the *tgd* mutations alone did not impact LT adaptation. All *tgd vte2* double mutants were larger and had less purple coloration than *vte2*, suggesting partial suppression of the *vte2* LT phenotype (Figure 3.7 A), which was also apparent at the biochemical level. The soluble sugar levels of LT-treated *tgdlvte2*, *tgd2vte2*, *tgd3vte2* and *tgd4vte2* were significantly lower than *vte2*, at 38%, 42%, 48% and 76% of the *vte2* level, respectively (Figure 3.7 B) and their photoassimilate export capacity significantly higher than *vte2* at 64%, 66%, 56% and 44% of the Col level, respectively (Figure 3.7 C). These results indicate that all four *tgd* loci partially suppress the *vte2* LT phenotypes in the order *tgdl=tgd2 >tgd3 >tgd4*.

Callose deposition in single and double *tgd vte2* mutants was also assessed in

comparison to Col and *vte2* before and during LT treatment. Under permissive conditions, no significant deposition of callose was observed in any genotype (data not shown). After 3 d (Figure 3.8) and 7 d (Figure 3.12) of LT treatment the four *tgd* single mutants and Col lacked vascular callose deposition while in *vte2* vascular callose deposition was present throughout the leaf at 3 d (Figure 3.8) and intensified by 7 d (Figure 3.12). After 3 d LT treatment, *tgd1vte2* and *tgd2vte2* showed sporadic callose deposition in the primary veins of petioles and a significant reduction in deposition in the leaf blade relative to *vte2* (Figure 3.8). Callose deposition in *tgd3vte2* and *tgd4vte2* was also reduced but to a lesser degree and some callose deposition was also observed in the leaf blade (Figure 3.8). By 7 d LT treatment callose deposition in all the *tgd vte2* double mutants was indistinguishable from *vte2* (Figure 3.12). These time-course observations indicated that *tgd1vte2*, *tgd2vte2* and to a lesser extent *tgd3vte2* and *tgd4vte2* delayed the development of *vte2* LT-induced callose deposition.

sve lines alleviate the *vte2* LT-induced increase in phospholipid 18:2

Changes in the PUFA composition of ER-derived lipids have been shown to occur in LT-treated *vte2* leaves (Maeda et al., 2008). To investigate if the suite of *sve* lines impacts these changes, we separated the major groups of ER- and plastid- derived lipids [PC and PE, DGDG (digalactosyldiacylglycerol) and MGDG (monogalactosyldiacylglycerol), respectively] by thin layer chromatography (TLC) and assessed their acyl composition before and after 14 d of LT treatment. Under permissive conditions, *vte2*, *vte1*, *sve7vte2* and Col had identical fatty acid compositions in all lipid classes analyzed (Table 3.3), confirming that *vte2*, *vte1* and *sve7vte2* do not impact fatty acid content at permissive temperature. The four *tgd* mutants had higher 18:1 and lower

18:3 in both ER- and plastid- derived lipids, and *fad2* had 6-8 fold higher 18:1 and lower 18:2 in PC and PE, consistent with prior reports (Miquel and Browse, 1992; Xu et al., 2003a; Awai et al., 2006; Lu et al., 2007b; Xu et al., 2008). Introduction of *vte2* into *tgd* backgrounds had no impact on these profiles (Table 3.3). The fatty acid composition of *fad2vte2* was also similar to *fad2-1*, with minor exceptions (slightly higher PE-18:3 and DGDG-18:1 and slightly lower DGDG-16:3). These results reinforce that tocopherol deficiency *per se* has little or no impact on either ER- or plastidial fatty acid and lipid metabolism under permissive conditions.

After 14 d of LT treatment, all genotypes showed elevated 16:3 and 18:3 levels (Table 3.4), a phenomenon commonly observed in LT-treated plants (Williams et al., 1988; Johnson and Williams, 1989; Uemura and Steponkus, 1997), indicating that *vte2* did not affect this general LT-induced response of fatty acid desaturation. Col, *vte2*, *vte1* and *sve7vte2* showed identical changes in all fatty acids esterified to galactolipids. The compositions of fatty acids esterified to galactolipids in the four *tgd vte2* double mutants and *fad2vte2* were similar to the corresponding *tgd* and *fad2* single mutants, respectively (Table 3.4). These results indicate that tocopherol deficiency had little impact on plastid lipid metabolism under LT conditions.

In contrast, significant fatty acid composition changes occurred in 18 carbon PUFAs of ER-derived phospholipids under LT conditions (Table 3.4). Consistent with a prior report (Maeda et al., 2008), *vte2* showed significantly lower 18:3 and higher 18:2 levels in PC and PE relative to Col. These changes were intermediate in *vte1* indicating that the DMPBQ accumulated in this genotype partially suppressed these *vte2*-dependent LT PUFA changes. *sve7vte2* fully suppressed these changes and had PC and PE 18:2 and

18:3 levels indistinguishable from those of Col. The four *tgd vte2* double mutants also attenuated these *vte2*-dependent LT PUFA alterations and had PC and PE 18:2 and 18:3 levels similar to their corresponding single mutants. The extreme impact of *fad2* on 18 carbon PUFA content makes data interpretation challenging, but PC and PE 18:2 levels were identical in *fad2* and *fad2vte2*. Thus, a common theme that emerges from the suite of suppressors is that all alleviate the LT-induced increase in membrane phospholipid 18:2 that would otherwise occur in LT-treated *vte2*. When the levels of unsaturated 18 carbon fatty acids esterified to PC, PE, MGDG and DGDG after 14 d LT treatment were plotted against the LT photoassimilate export capacity of the suppressors (Figure 3.9 A), PC-18:2 was the only membrane lipid species that showed significant correlation (Figure 3.9 B), suggesting that PC-18:2 plays a central role in the induction and development of the *vte2* LT phenotype.

DISCUSSION

Tocopherol synthesis has been conserved during plant evolution but the biochemical and physiological functions of these compounds in plants remains the subject of debate (Grasses et al., 2001; Munne-Bosch and Alegre, 2002; Hofius et al., 2004; Havaux et al., 2005; Munne-Bosch, 2005a; Maeda et al., 2006; Abbasi et al., 2007; Dormann, 2007; Maeda and DellaPenna, 2007). Tocopherol deficient lines in maize and potato exhibit constitutive vascular callose deposition, carbohydrate accumulation in source leaves and impairment in photoassimilate translocation to sink tissues (Russin et al., 1996; Botha et al., 2000; Provencher et al., 2001). In tocopherol-deficient *Arabidopsis* mutants, such phenotypes are conditionally induced by LT treatment and identification of *sve*

suppressors in this study allowed us to genetically dissect this complex pathway and provide further insight into this novel aspect of tocopherol function.

All suppressor mutations, *sve1(fad2)*, *sve2(tgd1)*, *sve7*, *tdg2*, *tdg3*, *tdg4* and *vte1* fully or partially alleviated the growth inhibition of LT-treated *vte2* to degrees that correlated with their suppression of sugar accumulation, photoassimilate export impairment and callose deposition (Figures 3.3, 3.7 and 3.8). Given that none of the suppressors uncoupled growth inhibition from reduced photoassimilate export and soluble sugar accumulation, these phenotypes are tightly linked genetically. The facts that impaired photoassimilate export occurs immediately before soluble sugar accumulation in LT-treated *vte2* (Maeda et al., 2006) and that these two traits are negatively correlated across all suppressors ($R^2=-0.86$, Figure 3.13) strongly suggest that defective photoassimilate export is the direct cause of elevated sugar accumulation. The vascular-specific callose deposition and photoassimilate export block were almost completely eliminated by the strongest suppressor (*sve1vte2*) (Figure 3.3), while weaker suppressors partially attenuated callose deposition during the first 3 d but not 7 d of LT treatment (Figures 3.3, 3.7 and 3.8) and partially restored photoassimilate export. Because transfer cell wall proliferation is rapidly initiated and largely completed by 3 d of LT treatment (Maeda et al., 2006), the partial suppression of callose deposition by weaker *sve* loci [i.e. *sve2 (tgd1)*, *sve7*, *tdg2-4*] during this critical developmental time window is apparently sufficient to allow an intermediate level of photoassimilate export.

Prior and current studies consistently showed that under LT conditions *vte2* develops higher 18:2 and lower 18:3 levels in ER-derived lipids (Maeda et al., 2008). The identification of *sve1* and *sve2* as novel alleles of *fad2* (encoding ER oleate desaturase;

Figure 3.4, Table 3.2) and *tgdl* (a component of ABC transporter system responsible for ER to plastid lipid trafficking; Figures 3.5 and 3.6), respectively, provides genetic evidence for involvement of ER PUFA/lipid metabolism in the *vte2* LT phenotype. Furthermore, because mutations in the other transporter components (*TGD2*, *TGD3*, *TGD4*) also suppressed the *vte2* LT phenotype (Figures 3.7 and 3.8), we can conclude that it is the disruption of the ER-plastid lipid trafficking process, rather than a specific transporter component, that is responsible for the suppression of *vte2* LT phenotypes.

Previous radioactive tracer studies and lipidomic analyses demonstrated that the observed PUFA changes in LT-treated *vte2* were consistent with reduced conversion of 18:2 to 18:3 in the ER catalyzed by FAD3 (Maeda et al., 2008). However, because multiple changes were observed in LT-treated *vte2* relative to Col (e.g. elevated PC-18:2 and PE-18:2, decreased PC-18:3, PE-18:3 and DGDG-18:3) it was unclear which lipid species were critical for development of the *vte2* LT phenotype. The *vte2* suppressor lines isolated or generated in this study provide important insight into this question. The common biochemical phenotype shared by all *vte2* suppressing lines (i.e. *sve1*, *sve2*, *sve7*, *tdg2*, *tdg3*, *tdg4* and *vte1*) was found to be attenuation in the elevation of 18:2 in PC and PE that would otherwise occur in *vte2* at LT (Table 3.4). When the levels of 18 carbon fatty acids in individual lipid classes were plotted against the LT photoassimilate export capacity of various genotypes, only PC-18:2 levels were found to be significantly correlated ($R^2=0.73$, Figure 3.9). These results indicate that the increase in 18:2 esterified to PC plays a key role in the onset of the *vte2* LT phenotype.

Why would PC-18:2 be highly correlated with suppression of the *vte2* LT phenotype? In plants, ER-produced PC is a key intermediate in lipid metabolism: ER-

localized desaturases predominantly act upon PC (Arondel et al., 1992; Okuley et al., 1994); PC is the precursor to PA, diacylglycerol (DAG) and lyso-PC (Ohlrogge and Browse, 1995; Mongrand et al., 2000; Andersson et al., 2004); PC-18:2 species are the major donors of the DAG moiety for plastidic galactolipid synthesis (Slack et al., 1977; Browse et al., 1986; Somerville and Browse, 1991) and acyl chains of PC are in a constant state of remodeling or acyl editing (Williams et al., 2000; Bates et al., 2007; Bates et al., 2009). The rapid development of transfer cell walls in LT-treated *Arabidopsis* (i.e. during 3 d LT treatment, (Maeda et al., 2008) requires a highly-regulated supply of membrane lipids to the plasma membrane through ER-derived vesicles (Offler et al., 2002; Maeda et al., 2006; Maeda et al., 2008). In the absence of tocopherols, the fatty acid acyl composition of ER-derived lipids is suboptimal or unbalanced as manifested by increased PC- and PE-18:2 pools (Table 3.4), resulting in deformed vesicle formation, function and transfer cell wall development (Maeda 2006, 2008). The *sve1* mutation decreases the synthesis of 18:2 in the ER and may restore the unbalanced PUFA composition of ER-derived lipids used for transfer cell wall development. Likewise, *sve2* and all *tgd* mutations indirectly reduce ER 18:2 synthesis as indicated by their increased levels of PC- and PE-18:1 (Table 3.3, (Xu et al., 2003b; Awai et al., 2006; Lu et al., 2007b; Xu et al., 2008), leading to partial restoration of ER PUFA imbalance and suppression of *vte2* LT phenotypes.

It is difficult to envision how the absence of tocopherols influence ER lipid metabolism when tocopherols are synthesized and presumably localized in plastids (Soll et al., 1980a; Lichtenthaler et al., 1981; Soll, 1987; Vidi et al., 2006). However, the presence of high levels of tocopherols in ER-derived extraplastidic oil bodies (Yamauchi

and Matsushita, 1976; Fisk et al., 2006; White et al., 2006) is evidence that tocopherols are not necessarily restricted to plastids. The recent demonstration of ER/plastid membrane connection sites (plastid associated membranes or PLAMs) (Kjellberg et al., 2000; Andersson et al., 2007) and of an ER:plastid lipid transport system (Hartel et al., 2000; Benning, 2009) provide physical mechanisms whereby tocopherols could directly access components of the ER membrane and/or lipid biosynthetic machinery. Once one accepts that tocopherols have access to the ER compartment, several mechanisms for tocopherols impacting ER lipid metabolism become feasible.

In vitro studies have shown that tocopherols can stabilize membranes (Stillwell et al., 1996; Atkinson et al., 2008), possess a negative membrane curvature greater than cholesterol (Chen et al., 1997; Bradford et al., 2003) and, because they dynamically associate with PUFAs (Urano et al., 1988), may partition into more fluid membrane domains sensitive to curvature stress (Brown and London, 1998; Simons and Toomre, 2000). These properties would likely impact processes such as vesicle function and membrane fusion (Churchward et al., 2005), both of which are highly active in *Arabidopsis* transfer cells at LT (Aubert et al., 1996; Maeda et al., 2008; McCurdy et al., 2008). In animal systems tocopherol levels have also been shown to impact lipid and fatty acid metabolism (Okayasu et al., 1977; Buttriss and Diplock, 1988; Mahoney and Azzi, 1988; Bell et al., 2000) by directly affecting enzyme activities (Douglas et al., 1986; Chandra et al., 2002) or indirectly by affecting the association of enzymes with the membrane (Cachia et al., 1998; Brigelius-Flohe, 2009). Whether analogous biophysical or biochemical membrane processes are similarly affected in tocopherol deficient mutants in plants will require additional studies.

The *sve* lines characterized in this study provide genetic evidence for the sequence of physiological and biochemical events occurring in tocopherol deficient plants under LT and have defined elevated PC-18:2 lipid species as critical components of the *vte2* LT phenotype. The identification of *sve1* and *sve2* as mutations in genes encoding an ER fatty acid desaturase (FAD2) and a component of ER-plastid lipid transporter (TGD1) highlights an important role for tocopherols in regulating ER PUFA metabolism. Future studies focusing on the possible transport of tocopherols from plastid to extraplastidic membranes, role(s) of ER lipid PUFAs (especially PC-18:2) on transfer cell wall development and the mechanistic basis of tocopherol function in ER PUFA metabolism will eventually lead to a better understanding of these unanticipated tocopherol functions in plants.

MATERIALS AND METHODS

Plant growth and low temperature treatment

Seed were surface sterilized, stratified for 5 days at 4°C, and then planted in a vermiculite and soil mixture fertilized with 1× Hoagland solution, and grown in a chamber under permissive conditions (22°C day/18°C night) under 12h of 100 mmol quanta m⁻² s⁻¹ illumination for 4 weeks. For low temperature treatment, 4-week-old plants grown at permissive conditions were transferred at the beginning of the light cycle to low temperature conditions (12h day/12h night under 7± 3°C with light intensity of 75 mmol quanta m⁻² s⁻¹) for indicated time periods.

¹⁴C photoassimilate labeling and analysis of sugars and callose

¹⁴CO₂ labeling of photoassimilate and measurement of phloem exudation after 5h were as described (Maeda et al., 2006) except that exudation buffer contained 10mM EDTA and 0.05mCi of NaH¹⁴CO₃ was used per labeling experiment. Photoassimilate export capacity is the percent exudation of the total fixed ¹⁴CO₂ and is expressed as % of Col. Leaf glucose, fructose and sucrose analyses were performed as previously described (Maeda et al., 2006) and leaf total sugar content is the sum of glucose, fructose and sucrose contents and expressed as % of *vte2*. Callose staining and visualization were performed as described (Maeda et al., 2006).

Lipid and fatty acid composition analysis

Lipids were extracted and polar lipids analyzed on activated ammonium sulfate-impregnated silica gel TLC plates (Si250 with pre-adsorbent layer; Mallinckrodt Baker) as previously described (Dormann et al., 1995; Xu et al., 2005). Galactolipids were visualized with α -naphthol spray. For fatty acid composition analysis, total lipids or individual lipids isolated from TLC plates were converted to fatty acid methyl esters and analyzed by gas-liquid chromatography using myristic acid as internal standard (James and Dooner, 1990; Collakova and DellaPenna, 2001).

Generation of double mutants

tgdl-1, *tgdl-2*, *tgdl-3*, and *tgdl-4* mutants were kindly provided by Dr. Christoph Benning and introduced into the *vte2* background. F2 plants homozygous for *vte2* and one *tgdl* locus were identified and confirmed using published TLC, HPLC and genotyping methods (Collakova and DellaPenna, 2001; Xu et al., 2003b; Awai et al., 2006; Lu et al., 2007).

Genotyping analysis of sve2

For genotyping of *sve2*, a CAPs marker was developed based on the presence of the point mutation in *TGD1*. A 300 bp *TGD1* PCR fragment was amplified using primers 5'-CTGTTGGTATGGCTTCAA-3' and 5'-TTCAAAGAATCTCCAGCACCT-3'. The mutant produces bands of 220bp and 80bp when digested with *TaaI*.

Sequencing and sequence alignment analysis of FAD2 and TGD1

The genomic regions of *FAD2* in *sve1vte2* and *fad2-1*, and *TGD1* in *sve2vte2* were amplified in triplicate, pooled and used as sequencing templates. Mutations were

identified by comparison to the published *FAD2* and *TGD1* sequences. *FAD2* and *TGD1* protein sequences for alignments were obtained from cDNA or deduced from genomic sequence for: *Arabidopsis thaliana* (P46313, PF02405), *Oryza sativa* (TC267364, NP_001053506), *Picea abies* (CAC18722), *Physcomitrella patens* (Contig11227, XP_001763740), *Ostrecoccus tauri* (Ot17g02110), *Galdieria sulphuraria* (contig_818_Oct13_2005_g2.t1_Ga), *Chlorella vulgaris* (BAB78716), *Chlamydomonas reinhardtii* (TC40690, XP_001696522), *Prochlorococcus marinus* str. MIT 9313 (NC_005071), *Synechococcus* sp. PCC7002 (AAB61352) *Synechococcus elongatus* PCC 6301 (YP_171846), *Populus trichocarpa* (XP_002303003), *Picea sitchensis* (ABK25388). Sequences were aligned using the CLUSTAL X (1.81) multiple sequence alignment program.

Statistical analysis

For comparing three or more groups, one-way ANOVA as implemented in the CoStat program (Cohort Software, 1990. Berkeley, CA, USA) was used with genotype as the fixed effects. When significance was observed ($p < 0.05$), multiple pairwise comparisons were performed using the Tukey-Kramer test (Hsu, 1996), which allows for unequal sample sizes. Significance of the coefficient of determination (R^2) in Figure 7 was assessed using a t-test with $(n-2)$ degrees of freedom (n =number of genotypes).

Accession Numbers

Sequences can be found at TAIR or GenBank: *VTE1* (At4g32770), *VTE2* (At2g18950), *FAD2* (At3g12120), *TGD1* (At1g19800), *TGD2* (At3g20320), *TGD3* (At1g65410), *TGD4* (At3g06960). Information for *Arabidopsis* mutants is at TAIR. Seed

homozygous for *vte2* rapidly lose viability (see (Sattler et al., 2004)) and thus are maintained in the authors' lab and available upon request.

ACKNOWLEDGMENTS

We thank Dr. Scott Sattler for providing EMS mutagenized *vte2* seed, Dr. Christoph Benning for providing *tgd* mutant seed and members of the DellaPenna lab for their critical advice, discussions and manuscript review. This work was supported by NSF grant MCB-023529 to D.D.P.

TABLES AND FIGURES

Table 3.1 Leaf fatty acid composition of *sve1vte2*, *sve2vte2* and *sve7vte2* compared with Col, *vte2* and *vte1*. DAMNDAM

Genotype	Fatty acid composition (mol %)									
	16:0	16:1	16:2	16:3	18:0	18:1	18:2	18:3		
Col	16.3 ± 0.4	2.7 ± 0.2	0.5 ± 0.1	6.9 ± 0.3	1.3 ± 0.1	5.3 ± 0.5	17.4 ± 0.5	49.6 ± 1.1		
<i>vte2</i>	16.4 ± 0.7	2.8 ± 0.1	0.5 ± 0.0	7.0 ± 0.2	1.3 ± 0.1	5.2 ± 0.4	17.8 ± 0.6	48.9 ± 1.4		
<i>vte1</i>	16.5 ± 0.6	2.8 ± 0.1	0.6 ± 0.0	6.7 ± 0.3	1.3 ± 0.1	5.5 ± 0.3	16.9 ± 0.5	49.6 ± 1.0		
<i>Sve1vte2</i>	11.1 ± 0.4**	2.5 ± 0.1	0.5 ± 0.1	8.0 ± 0.3**	0.8 ± 0.1**	26.0 ± 2.0**	4.0 ± 0.3**	47.0 ± 2.3		
<i>Sve2vte2</i>	17.7 ± 1.0*	2.9 ± 0.2	0.8 ± 0.1**	6.2 ± 0.4*	1.7 ± 0.1**	7.3 ± 0.6**	23.4 ± 1.4**	39.9 ± 2.3**		
<i>Sve7vte2</i>	14.8 ± 1.2	2.8 ± 0.2	0.5 ± 0.1	8.2 ± 0.5**	1.6 ± 0.5	4.9 ± 0.6	15.6 ± 1.4*	51.6 ± 2.6		

88

All genotypes were grown at permissive conditions for 4 weeks when leaf samples were taken for fatty acid analysis at the middle of the light cycle. Data are means ±SD (n=5). Significant differences relative to Col are marked with * (P<0.05) or ** (P<0.01).

Table 3.2 Leaf fatty acid composition and photoassimilate export capacity of *sve/vte2* backcross populations.

Plant	Fatty acid composition (mol %)								Export capacity (% of Col)
	16:0	16:1	16:2	16:3	18:0	18:1	18:2	18:3	
Col	15.3 ±2.5	2.9 ±0.4	0.7 ±0.1	8.1 ±2.6	1.3 ±0.1	5.8 ±1.1	17.0 ±1.6	49.0 ±3.0	100.0 ±16.8
<i>vte2</i>	16.5 ±0.6	2.8 ±0.1	0.6 ±0.1	6.8 ±0.6	1.5 ±0.1	6.0 ±0.7	18.4 ±1.0	47.3 ±1.9	21.9 ±11.7**
<i>sve/vte2</i>	11.2 ±0.3*	2.6 ±0.1	0.6 ±0.0	8.0 ±0.2	0.8 ±0.1**	26.2 ±1.5**	4.7 ±0.2**	45.9 ±1.5	93.5 ±5.3
<i>sve/vte2</i> × <i>vte2</i>	15.6 ±1.2	2.9 ±0.3	0.5 ±0.0	7.5 ±0.5	1.2 ±0.1	7.5 ±0.2**	15.1 ±0.7	49.6 ±2.0	21.9 ±4.3**
F ₁									
32 F ₂ of <i>sve/vte2</i> × <i>vte2</i>	10.3 ±0.5*	2.5 ±0.3	0.7 ±0.1	8.5 ±0.5	0.8 ±0.1**	24.0 ±1.9**	5.0 ±0.4**	48.1 ±2.1	
89 F ₂ of <i>sve/vte2</i> × <i>vte2</i>	14.4 ±1.1	2.7 ±0.3	0.6 ±0.1	8.1 ±0.5	1.2 ±0.1*	5.9 ±1.3	15.3 ±1.3	51.8 ±2.4	

All genotypes were grown at permissive conditions for 4 weeks when leaf samples were taken for fatty acid analysis at the middle of the light cycle. Photoassimilate export capacity was assessed using mature leaves at the middle of the light cycle after 7 d of LT treatment. Data for Col, *vte2*, *sve/vte2* and *sve/vte2* × *vte2* are means ±SD (*n*=5). Significant differences relative to Col are marked by * (P < 0.05) or ** (P < 0.01).

Table 3.3 Acyl compositions of PC, PE, DGDG, MGDG in indicated genotypes before LT treatment

Lipid	Genotype	Fatty acid composition (mol%)							
		16:0	16:1	16:2	16:3	18:0	18:1	18:2	18:3
PC	<i>Col</i>	24.4 ± 2.5 ^{abc}	0.9 ± 0.2 ^{bcde}	0.1 ± 0.0	0.2 ± 0.2 ^d	3.5 ± 0.5 ^a	11.7 ± 0.5 ^f	33.6 ± 0.2 ^a	25.7 ± 2.6 ^{ab}
	<i>vte2</i>	25.7 ± 2.6 ^a	0.9 ± 0.1 ^{bcde}	0.1 ± 0.0	0.3 ± 0.1 ^d	4.2 ± 0.9 ^a	10.9 ± 1.3 ^f	33.7 ± 1.2 ^a	24.2 ± 2.9 ^{abc}
	<i>vte1</i>	24.4 ± 2.2 ^{abc}	0.9 ± 0.1 ^{bcde}	0.1 ± 0.0	0.3 ± 0.2 ^d	3.6 ± 0.2 ^a	11.1 ± 0.6 ^f	32.2 ± 1.0 ^{ab}	27.4 ± 2.4 ^a
	<i>sve7vte2</i>	25.2 ± 3.8 ^{ab}	0.9 ± 0.2 ^{bcd}	0.1 ± 0.0	0.3 ± 0.2 ^d	3.4 ± 0.7 ^{ab}	13.1 ± 0.9 ^f	31.4 ± 1.0 ^{ab}	25.7 ± 4.1 ^{ab}
	<i>tgdl</i>	18.0 ± 0.7 ^d	1.4 ± 0.2 ^a	0.1 ± 0.1	1.5 ± 0.2 ^{ab}	4.3 ± 0.6 ^a	32.8 ± 2.4 ^b	24.2 ± 1.0 ^d	17.7 ± 1.1 ^{def}
	<i>tgdlvte2</i>	18.7 ± 1.7 ^d	1.3 ± 0.0 ^{ab}	0.1 ± 0.1	1.5 ± 0.2 ^{ab}	4.3 ± 0.6 ^a	29.8 ± 1.1 ^{bc}	25.2 ± 0.6 ^d	19.0 ± 0.5 ^{cdef}
	<i>tgdl2</i>	19.3 ± 1.1 ^{bcd}	0.7 ± 0.0 ^{cde}	0.2 ± 0.2	1.6 ± 0.1 ^a	5.1 ± 0.3 ^a	27.6 ± 0.7 ^{bcd}	25.6 ± 0.6 ^d	19.9 ± 1.1 ^{bcdef}
	<i>tgdl2vte2</i>	17.8 ± 1.2 ^d	1.2 ± 0.2 ^{abc}	0.1 ± 0.1	1.6 ± 0.1 ^a	4.4 ± 0.6 ^a	28.1 ± 2.3 ^{bc}	24.3 ± 1.1 ^d	22.5 ± 1.2 ^{abcd}
	<i>tgdl3</i>	19.2 ± 1.2 ^{cd}	1.1 ± 0.2 ^{abc}	0.1 ± 0.1	1.5 ± 0.2 ^a	4.2 ± 0.5 ^a	26.2 ± 3.4 ^{cde}	26.9 ± 1.7 ^{cd}	20.7 ± 3.0 ^{bcde}
	<i>tgdl3vte2</i>	19.3 ± 0.4 ^{bcd}	0.9 ± 0.1 ^{bcde}	0.1 ± 0.1	1.3 ± 0.2 ^{abc}	4.2 ± 0.2 ^a	27.5 ± 2.5 ^{bcd}	27.2 ± 0.7 ^{cd}	19.6 ± 1.7 ^{bcdef}
	<i>tgdl4</i>	20.5 ± 1.4 ^{abcd}	1.0 ± 0.1 ^{abcd}	0.1 ± 0.1	1.1 ± 0.2 ^{bc}	5.2 ± 1.0 ^a	22.1 ± 0.4 ^{de}	29.7 ± 0.3 ^{bc}	20.5 ± 1.4 ^{bcde}
	<i>tgdl4vte2</i>	21.2 ± 1.0 ^{abcd}	0.9 ± 0.1 ^{bcd}	0.1 ± 0.0	0.9 ± 0.0 ^c	5.6 ± 2.0 ^a	21.3 ± 2.6 ^e	29.4 ± 2.1 ^{bc}	20.5 ± 1.5 ^{bcde}
	<i>fad2</i>	12.1 ± 1.3 ^e	0.6 ± 0.0 ^{de}	0.0 ± 0.0	0.1 ± 0.1 ^d	1.1 ± 0.1 ^{bc}	66.4 ± 1.1 ^a	3.9 ± 0.2 ^e	15.8 ± 0.3 ^{ef}
	<i>fad2vte2</i>	10.3 ± 0.8 ^e	0.5 ± 0.0 ^e	0.0 ± 0.0	0.1 ± 0.0 ^d	0.8 ± 0.0 ^c	71.4 ± 0.7 ^a	3.7 ± 0.3 ^e	13.2 ± 1.3 ^f

Table 3.3 (cont'd)

Lipid	Genotype	Fatty acid composition (mol%)							
		16:0	16:1	16:2	16:3	18:0	18:1	18:2	18:3
PE	<i>Col</i>	32.2 ±4.0 ^{ab}	0.6 ±0.1 ^b	0.0 ±0.0	0.3 ±0.1 ^c	2.8 ±0.2 ^{bcd}	4.3 ±0.5 ^c	36.5 ±2.2 ^a	23.3 ±1.5 ^c
	<i>vte2</i>	30.4 ±6.4 ^{ab}	0.6 ±0.1 ^b	0.0 ±0.0	0.2 ±0.1 ^c	3.3 ±0.7 ^{abc}	4.3 ±0.4 ^c	38.6 ±3.9 ^a	22.5 ±1.8 ^{cd}
	<i>vte1</i>	31.1 ±4.9 ^{ab}	0.6 ±0.0 ^{ab}	0.0 ±0.0	0.4 ±0.3 ^c	3.0 ±0.2 ^{bc}	5.5 ±2.5 ^{de}	35.1 ±1.8 ^a	24.2 ±1.4 ^c
	<i>sve7vte2</i>	34.0 ±5.2 ^a	0.6 ±0.0 ^b	0.0 ±0.0	0.3 ±0.2 ^c	2.6 ±0.4 ^{cd}	5.1 ±0.4 ^{de}	34.1 ±2.6 ^a	23.4 ±2.8 ^c
	<i>tgdl</i>	27.0 ±1.3 ^{abc}	0.9 ±0.2 ^a	0.1 ±0.1	1.2 ±0.1 ^{ab}	3.8 ±0.2 ^{abc}	13.6 ±1.1 ^b	39.2 ±2.2 ^a	14.2 ±0.9 ^c
	<i>tgdlvte2</i>	26.3 ±1.6 ^{abc}	0.8 ±0.1 ^{ab}	0.1 ±0.1	1.2 ±0.2 ^a	3.8 ±0.3 ^{abc}	12.0 ±1.2 ^{bc}	40.4 ±1.1 ^a	15.3 ±0.5 ^c
	<i>tgdl2</i>	27.8 ±0.6 ^{abc}	0.5 ±0.0 ^b	0.1 ±0.1	1.1 ±0.0 ^{ab}	4.5 ±0.2 ^{ab}	11.5 ±0.7 ^{bc}	40.0 ±0.1 ^a	14.5 ±0.2 ^c
	<i>tgdl2vte2</i>	26.9 ±1.5 ^{abc}	0.8 ±0.1 ^{ab}	0.1 ±0.1	1.2 ±0.3 ^{ab}	4.3 ±0.7 ^{ab}	12.2 ±0.6 ^{bc}	38.4 ±0.3 ^a	16.2 ±2.1 ^c
	<i>tgdl3</i>	30.8 ±3.3 ^{ab}	0.7 ±0.2 ^{ab}	0.0 ±0.1	1.0 ±0.2 ^{ab}	4.7 ±1.6 ^a	10.8 ±0.3 ^{bc}	38.0 ±3.4 ^a	13.8 ±2.0 ^c
	<i>tgdl3vte2</i>	30.4 ±0.8 ^{ab}	0.7 ±0.0 ^{ab}	0.1 ±0.1	0.8 ±0.0 ^{abc}	3.9 ±0.1 ^{abc}	11.3 ±0.5 ^{bc}	39.3 ±0.9 ^a	13.4 ±0.2 ^c
	<i>tgdl4</i>	30.7 ±3.1 ^{ab}	0.6 ±0.1 ^b	0.0 ±0.1	0.8 ±0.2 ^{abc}	4.3 ±0.6 ^{ab}	9.0 ±0.5 ^{cd}	38.7 ±2.3 ^a	15.9 ±0.8 ^c
	<i>tgdl4vte2</i>	29.6 ±3.0 ^{ab}	0.5 ±0.1 ^b	0.0 ±0.1	0.7 ±0.1 ^{abc}	4.0 ±0.4 ^{abc}	8.4 ±1.0 ^{cde}	39.5 ±3.1 ^a	17.3 ±1.2 ^{de}
	<i>fad2</i>	23.5 ±0.7 ^{bc}	0.9 ±0.1 ^a	0.0 ±0.0	0.6 ±0.3 ^{bc}	1.2 ±0.1 ^d	33.8 ±4.0 ^a	6.5 ±0.2 ^b	33.4 ±3.3 ^b
	<i>fad2vte2</i>	18.9 ±1.1 ^c	0.8 ±0.0 ^{ab}	0.0 ±0.0	0.6 ±0.1 ^{bc}	1.1 ±0.3 ^d	32.7 ±0.7 ^a	7.0 ±0.1 ^b	38.9 ±1.9 ^a

Table 3.3 (cont'd)

Lipid	Genotype	Fatty acid composition (mol%)							
		16:0	16:1	16:2	16:3	18:0	18:1	18:2	18:3
DGDG	<i>Col</i>	23.6 ± 7.3 ^{bcd}	2.9 ± 4.2	0.2 ± 0.1	1.4 ± 0.5 ^c	1.7 ± 0.3 ^{bc}	2.7 ± 0.6 ^{fg}	5.9 ± 1.2 ^{bcde}	61.6 ± 11.4 ^{ab}
	<i>vte2</i>	24.7 ± 2.5 ^{bcd}	2.4 ± 3.2	0.2 ± 0.1	1.2 ± 0.2 ^c	1.8 ± 0.2 ^{bc}	2.7 ± 0.3 ^{fg}	6.3 ± 1.7	60.7 ± 5.0 ^{ab}
	<i>vte1</i>	21.6 ± 2.3 ^{cd}	1.2 ± 0.9	0.2 ± 0.1	1.4 ± 0.2 ^c	1.8 ± 0.4 ^{bc}	2.4 ± 0.1 ^g	6.0 ± 1.0 ^{bcde}	65.5 ± 2.9 ^a
	<i>sve7vte2</i>	23.4 ± 9.3 ^{cd}	1.5 ± 1.6	0.1 ± 0.2	1.8 ± 0.5 ^c	1.4 ± 0.6 ^{cd}	2.3 ± 0.7 ^g	5.7 ± 1.7 ^{cde}	63.9 ± 12.2 ^a
	<i>tgdl</i>	45.5 ± 8.3 ^a	1.6 ± 0.9	0.2 ± 0.4	2.8 ± 0.8 ^c	2.7 ± 0.6 ^{ab}	9.2 ± 0.4 ^{ab}	7.9 ± 1.1	30.0 ± 7.1 ^d
	<i>tgdlvte2</i>	45.3 ± 8.5 ^a	1.3 ± 0.4	0.2 ± 0.3	3.2 ± 0.7 ^c	2.6 ± 0.4 ^{ab}	8.5 ± 1.3 ^{bc}	8.6 ± 0.9 ^{abcd}	30.2 ± 6.4 ^d
	<i>tgdl2</i>	40.9 ± 1.1 ^{abc}	0.5 ± 0.0	0.3 ± 0.4	3.0 ± 0.2 ^c	2.7 ± 0.0 ^{ab}	5.8 ± 0.1 ^{de}	10.6 ± 0.9 ^{ab}	36.1 ± 1.4 ^{cd}
	<i>tgdl2vte2</i>	46.2 ± 8.6 ^a	1.1 ± 0.5	0.1 ± 0.1	2.5 ± 0.6 ^c	3.0 ± 0.3 ^a	6.5 ± 0.9 ^{cde}	9.7 ± 2.4 ^{abc}	30.8 ± 5.8 ^d
	<i>tgdl3</i>	41.6 ± 7.8 ^{ab}	1.2 ± 0.6	0.2 ± 0.2	3.0 ± 0.6 ^c	2.5 ± 0.4 ^{abc}	6.9 ± 0.8 ^{bcde}	8.8 ± 2.5 ^{abcd}	35.9 ± 6.9 ^d
	<i>tgdl3vte2</i>	34.9 ± 2.4 ^{abc}	0.8 ± 0.0	0.3 ± 0.4	3.2 ± 0.9 ^c	2.3 ± 0.3 ^{abc}	7.5 ± 0.5 ^{bcd}	11.0 ± 0.3 ^a	40.0 ± 1.6 ^{bcd}
	<i>tgdl4</i>	25.3 ± 3.2 ^{bcd}	1.0 ± 0.3	0.2 ± 0.2	2.1 ± 0.4 ^c	2.3 ± 0.4 ^{abc}	4.8 ± 0.8 ^{ef}	6.9 ± 2.0	57.4 ± 5.2 ^{abc}
	<i>tgdl4vte2</i>	24.1 ± 4.8 ^{bcd}	0.9 ± 0.3	0.2 ± 0.2	2.3 ± 0.2 ^c	1.7 ± 0.4 ^{bc}	4.6 ± 0.6 ^{efg}	6.7 ± 0.2	59.5 ± 5.3 ^{ab}
	<i>fad2</i>	7.5 ± 1.1 ^{de}	4.9 ± 0.5	0.0 ± 0.0	17.9 ± 0.5 ^a	0.5 ± 0.0 ^d	8.7 ± 0.3 ^{bc}	3.6 ± 0.2 ^e	56.9 ± 0.6 ^{abc}
	<i>fad2vte2</i>	2.7 ± 0.7 ^e	2.9 ± 0.4	0.0 ± 0.0	13.1 ± 1.2 ^b	0.4 ± 0.1 ^d	11.3 ± 1.6 ^a	5.1 ± 0.5 ^{de}	64.5 ± 2.1 ^a

Table 3.3 (cont'd)

Lipid	Genotype	Fatty acid composition (mol%)									
		16:0	16:1	16:2	16:3	18:0	18:1	18:2	18:3		
MGDG	<i>Col</i>	4.0 ± 2.7 ^{bc}	2.1 ± 1.3 ^{bc}	0.4 ± 0.6	17.4 ± 2.1 ^a	0.4 ± 0.1 ^b	3.6 ± 1.2 ^{bc}	4.5 ± 1.2	67.5 ± 4.8 ^{ab}		
	<i>vie2</i>	3.5 ± 1.7 ^c	1.7 ± 0.6 ^{bc}	0.4 ± 0.7	17.6 ± 2.5 ^a	0.5 ± 0.2 ^{ab}	3.7 ± 1.4 ^{bc}	5.3 ± 2.6	67.3 ± 3.7 ^{ab}		
	<i>vie1</i>	4.1 ± 3.5 ^{bc}	1.6 ± 0.3 ^{bc}	0.4 ± 0.7	17.0 ± 3.1 ^a	0.5 ± 0.2 ^b	3.5 ± 0.9 ^c	5.8 ± 3.8	67.2 ± 5.2 ^{ab}		
	<i>sve7vie2</i>	4.9 ± 4.1 ^{bc}	1.8 ± 0.8 ^{bc}	0.4 ± 0.6	18.0 ± 4.1 ^a	0.6 ± 0.3 ^{ab}	3.8 ± 2.0 ^{bc}	5.8 ± 4.6	64.6 ± 7.5 ^{abc}		
	<i>igd1</i>	6.7 ± 2.7 ^{bc}	6.5 ± 0.5 ^a	0.6 ± 0.9	17.4 ± 2.6 ^a	0.7 ± 0.2 ^{ab}	14.1 ± 2.4 ^a	4.7 ± 1.9	49.3 ± 5.0 ^c		
	<i>igd1vie2</i>	5.5 ± 0.9 ^{bc}	6.0 ± 0.2 ^a	0.6 ± 1.0	19.0 ± 0.8 ^a	0.6 ± 0.1 ^{ab}	12.5 ± 0.6 ^a	4.1 ± 0.7	51.7 ± 1.8 ^{de}		
	<i>igd2</i>	9.2 ± 3.4 ^{abc}	4.2 ± 3.8 ^{abc}	1.3 ± 1.7	18.7 ± 3.7 ^a	0.9 ± 0.2 ^{ab}	8.0 ± 0.3 ^{abc}	5.5 ± 0.3	52.3 ± 2.6 ^{cde}		
	<i>igd2vie2</i>	7.4 ± 1.4 ^{bc}	4.9 ± 1.0 ^{ab}	0.6 ± 1.1	18.1 ± 2.2 ^a	0.7 ± 0.1 ^{ab}	11.1 ± 2.6 ^{ab}	4.3 ± 0.6	52.8 ± 4.1 ^{cde}		
	<i>igd3</i>	4.4 ± 0.9 ^{bc}	4.6 ± 1.2 ^{ab}	0.6 ± 1.0	19.8 ± 1.9 ^a	0.6 ± 0.0 ^{ab}	10.0 ± 3.0 ^{abc}	4.1 ± 0.8	55.9 ± 3.9		
	<i>igd3vie2</i>	6.4 ± 3.4 ^{bc}	6.1 ± 2.3 ^a	0.9 ± 1.3	17.6 ± 2.8 ^a	0.6 ± 0.1 ^{ab}	11.1 ± 1.8 ^{ab}	4.7 ± 0.5	52.5 ± 4.1 ^{cde}		
	<i>igd4</i>	4.0 ± 1.2 ^{bc}	3.9 ± 1.1 ^{abc}	0.6 ± 1.0	15.6 ± 2.8 ^a	0.6 ± 0.1 ^{ab}	9.1 ± 3.0 ^{abc}	5.0 ± 1.3	61.2 ± 4.5		
	<i>igd4vie2</i>	3.5 ± 1.3 ^c	3.3 ± 0.8 ^{abc}	0.5 ± 0.9	16.8 ± 1.7 ^a	0.5 ± 0.1 ^b	7.6 ± 2.4 ^{abc}	4.7 ± 0.8	63.2 ± 3.7		
	<i>fad2</i>	15.2 ± 0.7 ^a	0.8 ± 0.1 ^c	0.0 ± 0.0	3.1 ± 0.3 ^b	1.0 ± 0.0 ^a	7.6 ± 0.4 ^{abc}	5.9 ± 0.2	66.4 ± 0.9 ^{abc}		
	<i>fad2vie2</i>	10.8 ± 1.4 ^{ab}	0.6 ± 0.0 ^c	0.0 ± 0.0	1.5 ± 0.1 ^b	0.7 ± 0.1 ^{ab}	7.9 ± 0.9 ^{abc}	5.4 ± 0.1	73.1 ± 2.5 ^a		

All genotypes were grown at permissive conditions for 4 weeks when leaf samples were taken at the middle of the light cycle.

Fatty acid composition is expressed as mol % of total fatty acid in a specific lipid species. Data are means ± SD (n=3 or 4).

Non-significant groups are indicated alphabetically (Tukey-Kramer test for multiple comparison, P < 0.05).

Table 3.4 Acyl compositions of PC, PE, DGDG, MGDG in indicated genotypes after 14d LT treatment

Genotype	Fatty acid composition (mol %)							
	16:0	16:1	16:2	16:3	18:0	18:1	18:2	18:3
Col	21.4 ± 3.0^{ab}	0.7 ± 0.3	0.1 ± 0.1	0.2 ± 0.0^c	1.5 ± 0.3^{ab}	6.6 ± 1.2^c	30.3 ± 0.5^c	39.3 ± 4.3^a
<i>vte2</i>	21.9 ± 1.0^a	0.6 ± 0.2	0.1 ± 0.1	0.1 ± 0.1^c	1.5 ± 0.2^{ab}	7.1 ± 0.9^c	39.8 ± 1.6^a	29.1 ± 1.8^{bc}
<i>vte1</i>	19.0 ± 3.2^{ab}	0.6 ± 0.3	0.1 ± 0.1	0.2 ± 0.1^c	1.5 ± 0.2^{ab}	8.2 ± 0.9^c	36.0 ± 2.4^{abc}	34.3 ± 1.2^{ab}
<i>sve7vte2</i>	20.4 ± 1.1^{ab}	0.7 ± 0.4	0.1 ± 0.1	0.1 ± 0.0^c	1.2 ± 0.1^{ab}	9.7 ± 1.7^c	33.2 ± 2.1^{bc}	34.6 ± 1.3^{ab}
<i>tgdl</i>	16.7 ± 0.9^{bc}	0.7 ± 0.2	0.0 ± 0.0	0.8 ± 0.0^{ab}	1.4 ± 0.1^{ab}	23.8 ± 2.1^{bc}	31.7 ± 1.8^c	24.8 ± 1.0^c
<i>tgdlvte2</i>	17.1 ± 1.0^{abc}	0.8 ± 0.2	0.0 ± 0.1	0.7 ± 0.0^{abc}	1.3 ± 0.0^{ab}	23.3 ± 1.9^c	33.4 ± 1.2^{bc}	23.3 ± 1.1^c
<i>tgdl2</i>	18.0 ± 1.4^{abc}	0.6 ± 0.2	0.1 ± 0.0	0.8 ± 0.1^a	1.9 ± 0.2^a	19.4 ± 2.9^{cd}	33.6 ± 2.5^{bc}	25.7 ± 3.2^c
<i>tgdl2vte2</i>	16.5 ± 0.5^{bc}	0.7 ± 0.3	0.0 ± 0.0	0.7 ± 0.1^{abc}	1.4 ± 0.1^{ab}	22.8 ± 2.5^c	32.1 ± 2.6^c	25.7 ± 0.6^c
<i>tgdl3</i>	18.3 ± 2.4^{abc}	0.6 ± 0.2	0.0 ± 0.0	0.7 ± 0.1^{ab}	1.7 ± 0.2^a	18.5 ± 0.7^{cd}	33.5 ± 2.0^{bc}	26.6 ± 1.6^c
<i>tgdl3vte2</i>	18.5 ± 2.3^{abc}	0.7 ± 0.2	0.1 ± 0.0	0.5 ± 0.0^{bcd}	1.6 ± 0.7^{ab}	18.6 ± 0.3^{cd}	36.6 ± 1.1^{abc}	23.4 ± 1.8^c
<i>tgdl4</i>	18.6 ± 1.7^{ab}	0.6 ± 0.3	0.1 ± 0.1	0.5 ± 0.1^{cd}	1.9 ± 0.3^a	15.8 ± 2.2^d	35.1 ± 4.0^{abc}	27.4 ± 3.7^c
<i>tgdl4vte2</i>	19.0 ± 2.0^{ab}	0.7 ± 0.2	0.1 ± 0.1	0.4 ± 0.1^d	1.9 ± 0.5^a	16.4 ± 1.8^d	38.2 ± 2.5^{ab}	23.3 ± 1.9^c
<i>fad2</i>	17.0 ± 0.7^{bc}	0.7 ± 0.0	0.0 ± 0.0	0.1 ± 0.1^c	0.9 ± 0.1^{bc}	28.8 ± 2.4^b	17.6 ± 0.9^d	34.9 ± 2.0^{ab}
<i>fad2vte2</i>	13.6 ± 0.7^c	0.5 ± 0.0	0.0 ± 0.0	0.1 ± 0.1^c	0.5 ± 0.0^c	41.5 ± 1.4^a	17.2 ± 0.7^d	26.6 ± 0.7^c

PC

Table 3.4 (cont'd)

Genotype	Fatty acid composition (mol %)							
	16:0	16:1	16:2	16:3	18:0	18:1	18:2	18:3
<i>Col</i>	22.2 ±2.3	0.5 ±0.2	0.1 ±0.0	0.5 ±0.6 ^{ab}	0.6 ±0.4 ^c	4.2 ±3.1 ^f	36.2 ±0.7 ^b	35.8 ±0.5 ^b
<i>vte2</i>	22.2 ±0.2	0.4 ±0.1	0.1 ±0.0	0.1 ±0.1 ^b	0.9 ±0.0 ^{abc}	5.5 ±0.2 ^{ef}	44.9 ±0.3 ^a	25.8 ±0.3 ^{cde}
<i>vte1</i>	22.6 ±0.7	0.5 ±0.1	0.1 ±0.0	0.1 ±0.1 ^b	1.0 ±0.1 ^{abc}	3.9 ±2.4 ^f	39.7 ±0.8 ^{ab}	32.2 ±1.0 ^{bcd}
<i>sve7vte2</i>	22.5 ±0.8	0.5 ±0.2	0.1 ±0.0	0.3 ±0.1 ^b	0.8 ±0.1 ^{abc}	6.4 ±0.8 ^{def}	36.3 ±2.6 ^b	33.3 ±2.4 ^{bc}
<i>tgdl</i>	18.2 ±2.1	0.5 ±0.1	0.1 ±0.0	0.7 ±0.2 ^{ab}	0.9 ±0.0 ^{abc}	14.4 ±0.4 ^a	41.3 ±0.8 ^{ab}	24.0 ±1.6 ^e
<i>tgdlvte2</i>	18.4 ±0.2	0.6 ±0.1	0.1 ±0.0	0.6 ±0.1 ^{ab}	0.9 ±0.2 ^{abc}	14.4 ±0.1 ^a	43.5 ±0.2 ^{ab}	21.7 ±0.4 ^e
<i>tgdl2</i>	21.7 ±3.2	0.4 ±0.0	0.0 ±0.0	0.7 ±0.2 ^{ab}	1.3 ±0.1 ^a	11.7 ±0.3 ^{abc}	42.3 ±4.7 ^{ab}	21.8 ±2.5 ^e
<i>tgdl2vte2</i>	17.2 ±1.1	0.5 ±0.1	0.0 ±0.0	0.6 ±0.1 ^{ab}	0.9 ±0.1 ^{abc}	13.8 ±0.1 ^{ab}	42.3 ±0.3 ^{ab}	24.6 ±0.8 ^{de}
<i>tgdl3</i>	19.6 ±3.1	0.4 ±0.1	0.1 ±0.0	0.7 ±0.1 ^{ab}	1.0 ±0.1 ^{abc}	11.7 ±0.4 ^{abc}	42.1 ±0.2 ^{ab}	24.3 ±3.0 ^{de}
<i>tgdl3vte2</i>	24.0 ±6.5	0.4 ±0.0	0.0 ±0.0	0.5 ±0.2 ^{ab}	1.1 ±0.5 ^{abc}	12.4 ±1.3 ^{abc}	42.0 ±2.8 ^{ab}	19.5 ±2.8 ^e
<i>tgdl4</i>	20.7 ±0.1	0.4 ±0.1	0.1 ±0.0	0.5 ±0.0 ^{ab}	1.1 ±0.0 ^{abc}	9.9 ±0.4 ^{bcd}	43.3 ±3.9 ^{ab}	24.0 ±3.3 ^e
<i>tgdl4vte2</i>	22.6 ±4.1	0.5 ±0.0	0.1 ±0.0	0.5 ±0.1 ^{ab}	1.2 ±0.1 ^{ab}	8.9 ±0.4 ^{cde}	43.9 ±2.5 ^a	22.3 ±1.8 ^e
<i>fad2</i>	19.0 ±0.6	0.6 ±0.1	0.0 ±0.0	1.1 ±0.4 ^a	0.7 ±0.1 ^{bc}	11.9 ±1.1 ^{abc}	16.6 ±2.0 ^c	50.0 ±2.3 ^a
<i>fad2vte2</i>	15.9 ±1.4	0.5 ±0.1	0.0 ±0.0	0.8 ±0.1 ^{ab}	0.5 ±0.1 ^c	15.4 ±0.7 ^a	14.9 ±0.3 ^c	52.0 ±2.5 ^a

PE

Table 3.4 (cont'd)

Genotype	Fatty acid composition (mol %)							
	16:0	16:1	16:2	16:3	18:0	18:1	18:2	18:3
<i>Col</i>	11.5 ± 1.9 ^d	0.5 ± 0.1 ^{cd}	0.1 ± 0.0	1.6 ± 0.0 ^{de}	0.7 ± 0.1 ^{ef}	1.2 ± 0.2 ^{de}	2.8 ± 0.3 ^b	81.7 ± 2.4 ^a
<i>vte2</i>	14.9 ± 0.5 ^{cd}	0.5 ± 0.1 ^{cd}	0.1 ± 0.0	1.6 ± 0.2 ^{de}	0.9 ± 0.1 ^{def}	1.5 ± 0.1 ^{de}	4.3 ± 0.3 ^{ab}	76.2 ± 0.7 ^{ab}
<i>vte1</i>	11.7 ± 1.2 ^d	0.4 ± 0.1 ^d	0.0 ± 0.0	1.6 ± 0.0 ^e	0.7 ± 0.0 ^{ef}	1.1 ± 0.2 ^e	3.2 ± 0.4 ^b	81.3 ± 1.8 ^a
<i>sve7vte2</i>	11.9 ± 2.6 ^d	0.4 ± 0.1 ^d	0.0 ± 0.0	2.2 ± 0.2 ^{cde}	0.5 ± 0.1 ^{ef}	1.2 ± 0.3 ^{de}	3.1 ± 1.2 ^b	80.5 ± 3.9 ^a
<i>tgdl</i>	35.2 ± 2.2 ^a	0.6 ± 0.1 ^{cd}	0.0 ± 0.0	3.4 ± 0.5 ^{cd}	1.7 ± 0.2 ^{abc}	4.4 ± 0.7 ^{ab}	10.3 ± 2.8 ^{ab}	44.4 ± 1.4 ^{de}
<i>tgdlvte2</i>	36.0 ± 2.1 ^a	0.8 ± 0.2 ^c	0.0 ± 0.0	3.5 ± 0.3 ^c	1.6 ± 0.2 ^{abc}	5.2 ± 0.6 ^a	10.5 ± 1.9 ^{ab}	42.4 ± 1.8 ^e
<i>tgdl2</i>	37.6 ± 0.7 ^a	0.4 ± 0.1 ^{cd}	0.0 ± 0.0	3.0 ± 0.8 ^{cde}	1.9 ± 0.2 ^a	3.8 ± 0.7 ^{abcd}	9.8 ± 4.3 ^{ab}	43.6 ± 3.1 ^{de}
<i>tgdl2vte2</i>	33.9 ± 2.7 ^{ab}	0.5 ± 0.1 ^{cd}	0.0 ± 0.0	2.8 ± 0.1 ^{cde}	1.9 ± 0.6 ^{ab}	5.2 ± 1.5 ^a	12.4 ± 2.9 ^a	43.4 ± 2.1 ^{de}
<i>tgdl3</i>	29.1 ± 1.7 ^b	0.5 ± 0.1 ^{cd}	0.0 ± 0.0	3.9 ± 0.8 ^c	1.3 ± 0.2 ^{bcd}	3.5 ± 1.0 ^{abcd}	10.1 ± 4.6 ^{ab}	51.6 ± 4.4 ^d
<i>tgdl3vte2</i>	33.2 ± 1.2 ^{ab}	0.5 ± 0.0 ^{cd}	0.0 ± 0.0	2.8 ± 0.3 ^{cde}	1.5 ± 0.2 ^{abcd}	4.3 ± 0.6 ^{abc}	12.6 ± 5.6 ^a	45.1 ± 4.5 ^{de}
<i>tgdl4</i>	17.0 ± 2.0 ^c	0.5 ± 0.1 ^{cd}	0.0 ± 0.0	2.4 ± 0.2 ^{cde}	0.9 ± 0.0 ^{def}	2.4 ± 0.5 ^{bcde}	7.0 ± 3.7 ^{ab}	69.8 ± 5.9 ^{bc}
<i>tgdl4vte2</i>	18.7 ± 1.1 ^c	0.6 ± 0.0 ^{cd}	0.0 ± 0.0	2.2 ± 0.2 ^{cde}	1.1 ± 0.1 ^{cde}	3.0 ± 0.3	7.1 ± 2.5 ^{ab}	67.3 ± 3.1 ^{bc}
<i>fad2</i>	5.4 ± 0.6 ^e	1.8 ± 0.1 ^a	0.0 ± 0.0	20.3 ± 1.0 ^a	0.5 ± 0.1 ^f	4.0 ± 0.6 ^{abc}	4.3 ± 0.5 ^{ab}	63.6 ± 0.9 ^c
<i>fad2vte2</i>	3.6 ± 0.9 ^e	1.3 ± 0.2 ^b	0.0 ± 0.0	17.0 ± 1.3 ^b	0.4 ± 0.1 ^f	4.3 ± 1.0 ^{abc}	4.1 ± 0.7 ^{ab}	69.4 ± 1.7 ^{bc}

DGDC

Table 3.4 (cont'd)

Genotype	Fatty acid composition (mol %)							
	16:0	16:1	16:2	16:3	18:0	18:1	18:2	18:3
<i>Col</i>	3.4 ± 3.8 ^{bcd}	1.0 ± 0.9 ^{cde}	0.0 ± 0.0	21.0 ± 2.7 ^{ab}	0.3 ± 0.0 ^b	0.9 ± 0.6 ^d	2.2 ± 1.0 ^{bc}	71.2 ± 3.6 ^{bc}
<i>vie2</i>	3.1 ± 0.7 ^{bcd}	0.7 ± 0.2 ^{de}	0.0 ± 0.0	21.9 ± 1.4 ^{ab}	0.3 ± 0.1 ^b	1.0 ± 0.7 ^d	2.5 ± 0.7 ^{abc}	70.4 ± 1.7 ^{bcd}
<i>vie1</i>	1.7 ± 0.2 ^{cd}	0.6 ± 0.1 ^e	0.0 ± 0.0	22.1 ± 1.1 ^{ab}	0.2 ± 0.0 ^b	0.9 ± 0.6 ^d	2.1 ± 0.5 ^{bc}	72.3 ± 0.1 ^{bc}
<i>svie7vie2</i>	1.2 ± 0.3 ^d	0.5 ± 0.0 ^e	0.0 ± 0.0	23.7 ± 1.3 ^{ab}	0.2 ± 0.1 ^b	0.9 ± 0.5 ^d	1.7 ± 0.4 ^c	71.8 ± 0.5 ^{bc}
<i>tgdl</i>	5.4 ± 0.9 ^{bcd}	1.9 ± 0.1 ^{ab}	0.0 ± 0.0	23.0 ± 0.9 ^{ab}	0.5 ± 0.1 ^{ab}	3.9 ± 0.5 ^{ab}	3.6 ± 0.7 ^{abc}	61.7 ± 0.4 ^{ef}
<i>tgdl1vie2</i>	6.4 ± 1.0 ^{bcd}	2.3 ± 0.3 ^a	0.0 ± 0.0	21.9 ± 0.5 ^{ab}	0.6 ± 0.3 ^{ab}	4.7 ± 0.1 ^a	4.1 ± 1.2 ^{ab}	60.0 ± 0.6 ^f
<i>tgdl2</i>	6.8 ± 4.9 ^{bcd}	0.6 ± 0.1 ^e	0.0 ± 0.0	22.0 ± 1.6 ^{ab}	0.5 ± 0.2 ^{ab}	3.2 ± 0.2 ^{abc}	3.0 ± 0.4 ^{abc}	63.9 ± 4.2 ^{def}
MGDG	8.5 ± 0.4^{ab}	1.8 ± 0.2^{abc}	0.0 ± 0.0	20.7 ± 1.2^{ab}	0.5 ± 0.0^{ab}	3.8 ± 0.6^{ab}	3.9 ± 0.7^{ab}	60.7 ± 0.3^f
<i>tgdl3</i>	3.6 ± 0.2 ^{bcd}	1.5 ± 0.1 ^{abcd}	0.0 ± 0.0	24.3 ± 1.1 ^a	0.4 ± 0.1 ^{ab}	3.0 ± 0.6 ^{bc}	3.5 ± 1.3 ^{abc}	63.7 ± 1.0 ^{def}
<i>tgdl3vie2</i>	4.6 ± 3.5 ^{bcd}	1.2 ± 0.5 ^{bcd}	0.0 ± 0.0	21.4 ± 1.2 ^{ab}	0.4 ± 0.2 ^{ab}	2.4 ± 0.8 ^{bcd}	3.1 ± 0.0 ^{abc}	67.0 ± 6.1 ^{bc}
<i>tgdl4</i>	2.2 ± 0.7 ^{cd}	1.2 ± 0.1 ^{bcd}	0.0 ± 0.0	21.3 ± 0.5 ^{ab}	0.3 ± 0.1 ^b	2.2 ± 0.1 ^{cd}	3.2 ± 0.2 ^{abc}	69.6 ± 1.0 ^{bcd}
<i>tgdl4vie2</i>	3.0 ± 0.3 ^{bcd}	1.6 ± 0.2 ^{abcd}	0.0 ± 0.0	19.9 ± 1.1 ^b	0.3 ± 0.0 ^b	3.0 ± 0.4 ^{bc}	3.7 ± 0.6 ^{abc}	68.4 ± 0.7 ^{bc}
<i>fad2</i>	12.5 ± 0.9 ^a	0.5 ± 0.1 ^e	0.0 ± 0.1	3.4 ± 0.5 ^c	0.9 ± 0.4 ^a	3.4 ± 0.6 ^{abc}	4.2 ± 0.5 ^a	75.1 ± 1.9 ^b
<i>fad2vie2</i>	7.4 ± 1.2 ^{abc}	0.4 ± 0.0 ^e	0.0 ± 0.1	1.8 ± 0.2 ^c	0.4 ± 0.0 ^{ab}	3.3 ± 0.6 ^{abc}	3.2 ± 0.5 ^{abc}	83.5 ± 2.1 ^a

All genotypes were grown at permissive conditions for 4 weeks and then subjected to additional 14d of LT treatment. Leaf

samples were taken at the middle of the light cycle. Fatty acid composition is expressed as mol % of total fatty acid in a specific lipid species. Data are means ± SD (n=3 or 4). Non-significant groups are indicated alphabetically (Tukey-Kramer test for multiple comparison, P < 0.05).

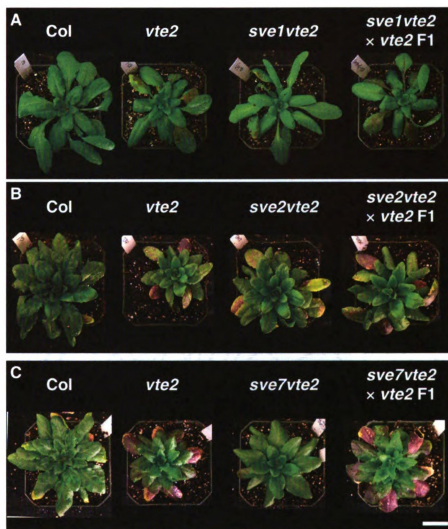


Figure 3.1 Whole plant phenotypes of LT treated Col, *vte2*, *sve1vte2*, *sve2vte2*, *sve7vte2*, and the F1 progeny of *sve1vte2*, *sve2vte2*, *sve7vte2* × *vte2*.

All genotypes were grown under permissive conditions for 4 weeks and then transferred to LT conditions. Representative plants of the indicated genotypes are shown after 14 d (A) and 28 d (B, C) of LT treatment. Bar = 2 cm.

A. Col, *vte2*, *sve1vte2*, *sve1vte2* × *vte2* F1

B. Col, *vte2*, *sve2vte2*, *sve2vte2* × *vte2* F1

C. Col, *vte2*, *sve7vte2*, *sve7vte2* × *vte2* F1

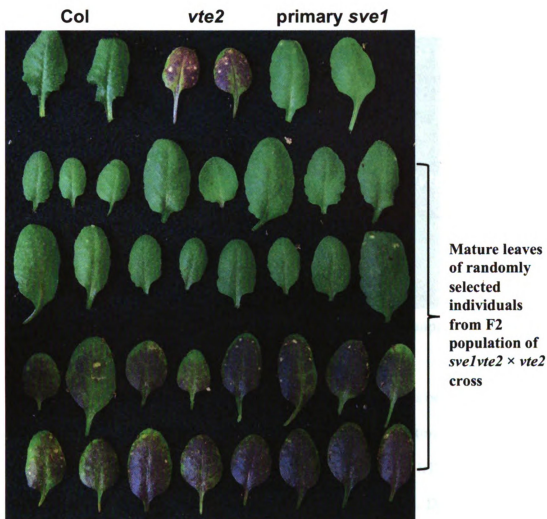


Figure 3.2 A demonstration of leaf phenotypes of F2 population from *sve1vte2* × *vte2* backcross.

All genotypes were grown under permissive conditions for 4 weeks and then transferred to LT conditions for 28 d. 16 mature leaves randomly cut from 32 *sve1*-like and 89 *vte2*-like plants in the 121 F2 population, together with mature leaves of Col, *vte2* and the primary *sve1vte2*, are displayed.

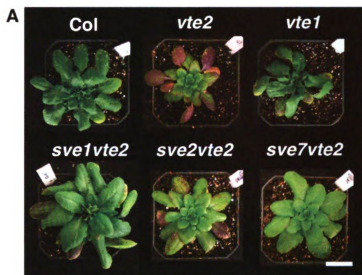


Figure 3.3 LT phenotypes of *sve1vte2*, *sve2vte2* and *sve7vte2* compared with *Col*, *vte2* and *vte1*.

All genotypes were grown under permissive conditions for 4 weeks before transfer to LT.

A Representative whole plant phenotypes after 4 weeks of LT treatment. Bar = 2cm.

B Total soluble sugar content of mature leaves after 2 weeks of LT treatment. Samples were taken from the 9-11th leaves at the end of the light cycle. Data are means \pm SD ($n=5$). Non-significant groups are indicated alphabetically (Tukey-Kramer test, $P<0.05$).

C Photoassimilate export capacity from mature leaves after 7 d of LT treatment. Photoassimilate export capacity was assessed at the middle of the light cycle. Data are means \pm SD ($n=5$). Non-significant groups are indicated alphabetically (Tukey-Kramer test, $P<0.05$).

D Callose deposition after 3 d of LT treatment. Leaves were fixed at the middle of the light cycle and aniline-blue positive fluorescence was examined in the lower portions of leaves ($n\geq 3$, Bar = 1mm).

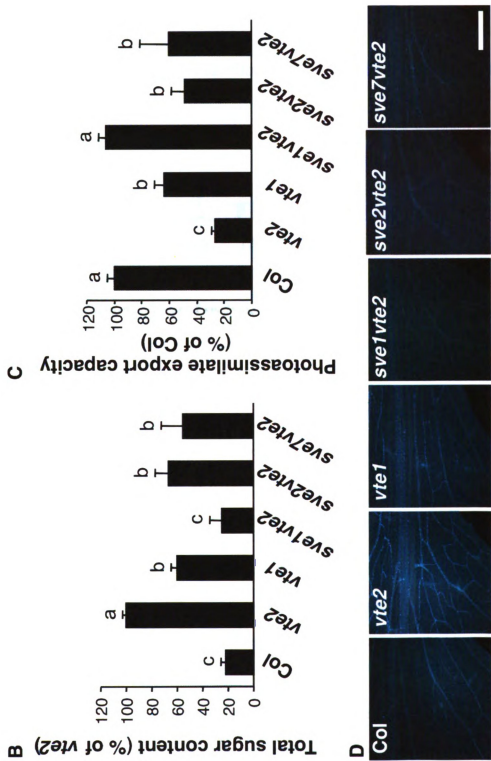


Figure 3.3 (cont'd)

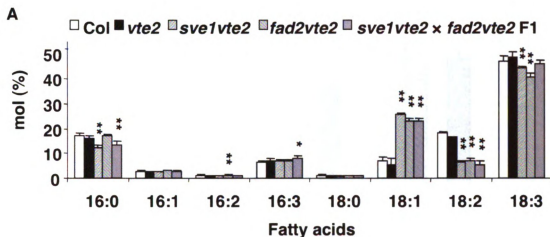


Figure 3.4 Complementation test of *sve1vte2* and *fad2-1vte2*.

Plants were grown 4 weeks under permissive conditions before transfer to LT conditions for the indicated period of time prior to analysis.

A Comparison of leaf fatty acid composition. Leaf samples were taken for fatty acid analysis at the middle of the light cycle before LT treatment. Data are means \pm SD ($n=5$). Significant differences relative to Col are marked with * ($p<0.05$) or ** ($p<0.01$) (Student's t test).

B Comparison of photoassimilate export capacity. Photoassimilate export capacity was assessed using mature leaves at the middle of the light cycle after 7 d at LT. Data are means \pm SD ($n=5$). Significant differences relative to Col are marked with * ($p<0.05$) or ** ($p<0.01$) (Student's t test).

C Comparison of callose deposition. Leaves were fixed at the middle of the light cycle after 3 d at LT and aniline-blue positive fluorescence was examined around the mid-vein ($n\geq 3$, Bar = 1 mm).

D Representative whole plant phenotypes after 4 weeks of LT treatment. Bar = 2 cm.

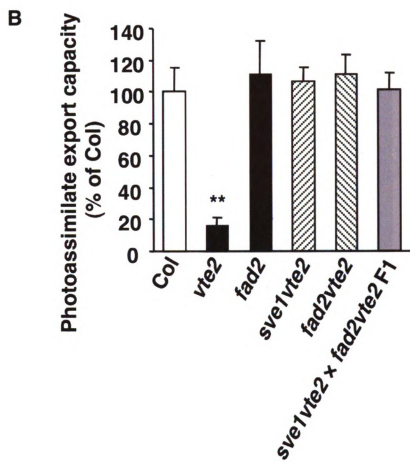


Figure 3.4 (cont'd)

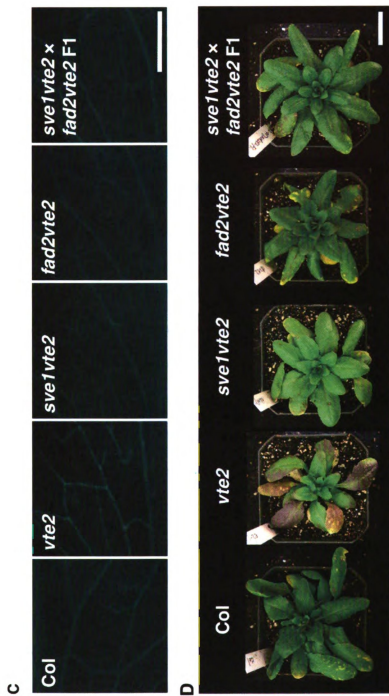


Figure 3.4 (cont'd)

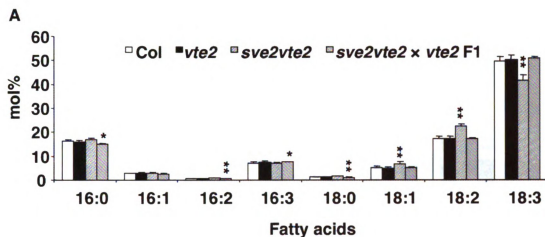


Figure 3.5 *sve2* carries a single recessive mutation in *TGD1*.

Plants were grown 4 weeks under permissive conditions before transfer to LT conditions for the indicated period of time prior to analysis.

A Comparisons of leaf fatty acid composition. Leaf samples were taken from the indicated genotypes at the middle of the light cycle before LT treatment. Data are means \pm SD ($n=5$). Significant differences relative to Col are marked with * ($p<0.05$) or ** ($p<0.01$) (Student's t test).

B Comparison of leaf polar lipid composition. Thin-layer chromatography of polar lipids showing the accumulation of TGDG in *sve2vte2*, *tgdl* and the F1 progeny of an *sve2vte2* × *tgdl* cross. Lipids were visualized by α -naphthol staining. DGDG: digalactosyldiacylglycerol; TGDG: trigalactosyldiacylglycerol.

C Segregation of leaf total sugar content in F2 progeny of an *sve2vte2* × *vte2* cross. Samples were taken from the 9-11th leaves at the end of the light cycle. Data for Col and *vte2* are means \pm SD ($n=5$). Significant differences relative to *vte2* are marked with * ($p<0.05$) or ** ($p<0.01$) (Student's t test).

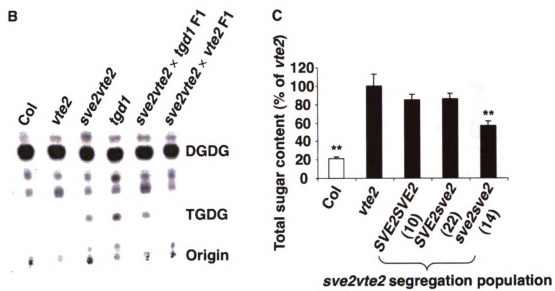


Figure 3.5 (cont'd)

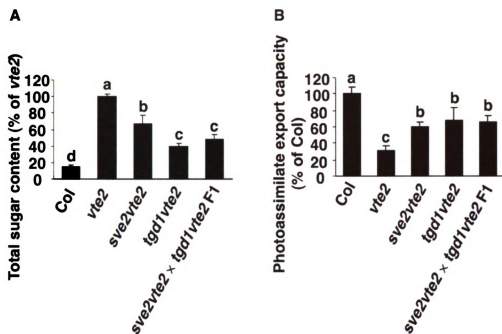


Figure 3.6 Complementation test of *sve2vte2* and *tgdlvte2*.

Plants were grown 4 weeks under permissive conditions before transfer to LT conditions for the indicated periods of time prior to analysis.

A Comparison of leaf total soluble sugar content after 2 weeks of LT treatment. Samples were taken from the 9-11th leaves at the end of the light cycle. Data are means \pm SD ($n=5$). Non-significant groups are indicated alphabetically (Tukey-Kramer test, $P < 0.05$).

B Comparison of photoassimilate export capacity. Photoassimilate export capacity was assessed using mature leaves at the middle of the light cycle after 7 d of LT treatment. Data are means \pm SD ($n=5$).

C Comparison of callose deposition. Leaves were fixed at the middle of the light cycle after 3 d at LT conditions and aniline-blue positive fluorescence was examined around the mid-vein of the leaves ($n \geq 3$, Bar = 1 mm).

D Representative whole plant phenotypes after 4 weeks of LT treatment. Bar = 2 cm.

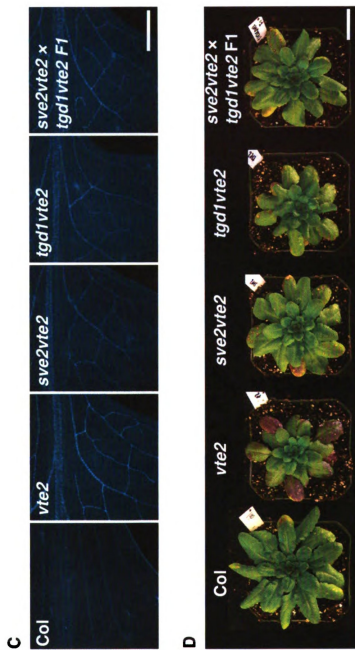


Figure 3.6. (cont'd)

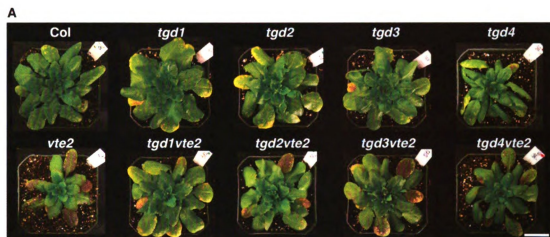


Figure 3.7 *tgd2*, *tgd3* and *tgd4* also suppress the *vte2* LT phenotypes.

Plants were grown 4 weeks under permissive conditions before transfer to LT conditions for the indicated periods of time prior to analysis.

A Representative whole plant phenotypes after 4 weeks of LT treatment. Bar = 2 cm.

B Total soluble sugar content of mature leaves after 2 weeks of LT treatment. Samples were taken from the 9-11th leaves at the end of the light cycle. Data are means \pm SD ($n=5$). Non-significant groups are indicated alphabetically (Tukey-Kramer test, $P<0.05$).

C Photoassimilate export capacity. Photoassimilate export capacity was assessed using mature leaves at the middle of the light cycle after 7 d of LT treatment. Data are means \pm SD ($n=5$). Non-significant groups are indicated alphabetically (Tukey-Kramer test, $P<0.05$).

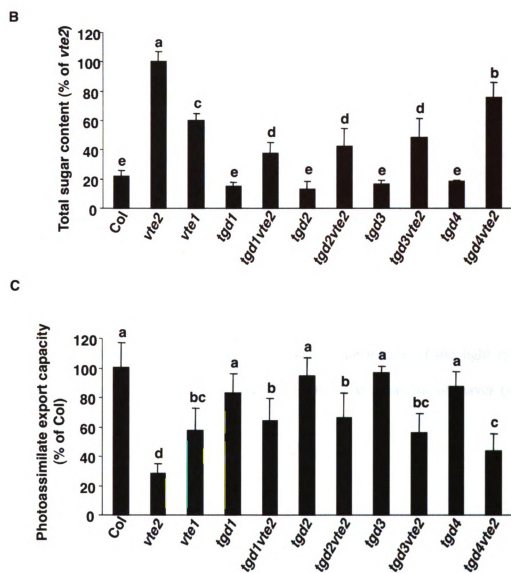


Figure 3.7 (cont'd)

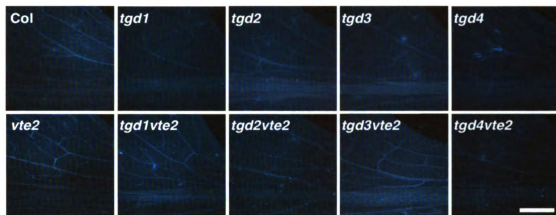


Figure 3.8 *tgd* mutations impact differently on *vte2* LT-induced callose deposition.

All genotypes were grown at permissive conditions for 4 weeks and transferred to LT conditions for 3 additional days. Leaves were fixed at the middle of the light cycle. Aniline-blue positive fluorescence was examined in the lower portions of leaves ($n=3$, Bar = 1 mm).

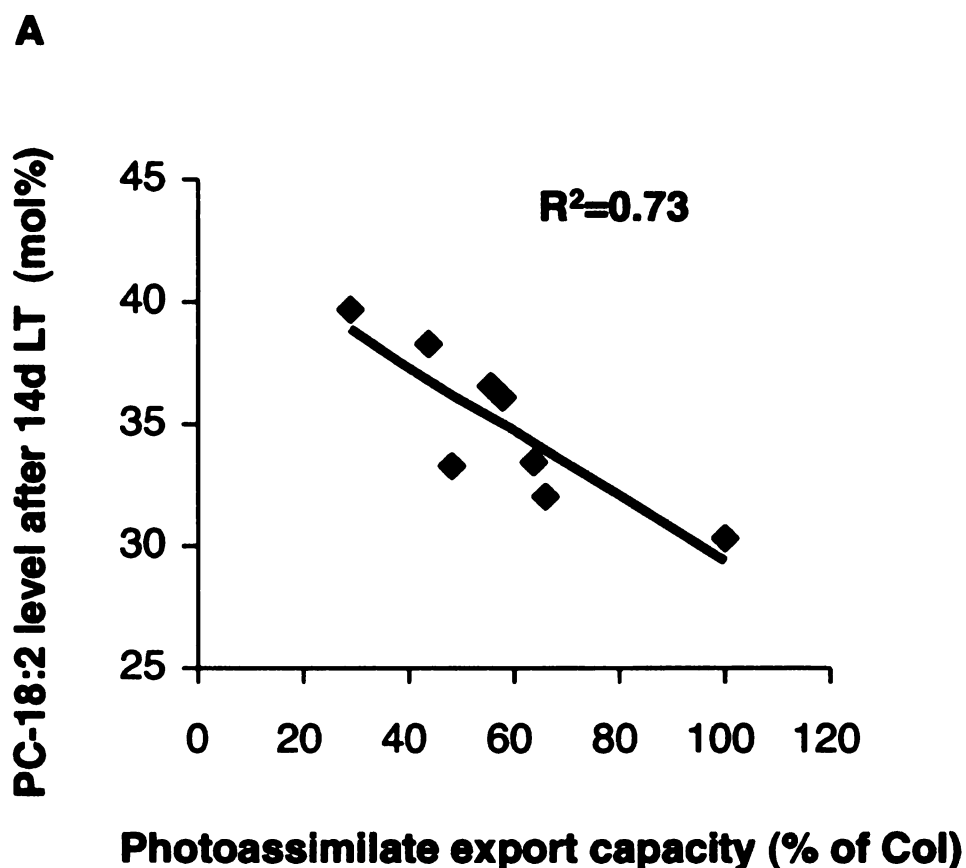


Figure 3.9 Correlation of individual lipid species with photoassimilate export capacity.

Data include *sve7vte2*, *tgdlvte2*, *tgdlvte2*, *tgdlvte2*, *tgdlvte2*, *Col*, *vte2* and *vte1*.

A A scattered plot of PC-18:2 levels (average of $n=3$ or 4) after 14 d LT treatment and photoassimilate export capacity (% of Col, average of $n=5$).

B Coefficient of determination (R^2) of unsaturated 18C fatty acid levels (\blacktriangle 18:1, \blacksquare 18:2, \bullet 18:3) esterified to PC, PE, MGDG and DGDG (average of $n=3$ or 4) after 14 d LT treatment and the photoassimilate export capacity (% of Col, average of $n=5$). R^2 is based on linear regression. Significant R^2 is marked with * ($P<0.05$).

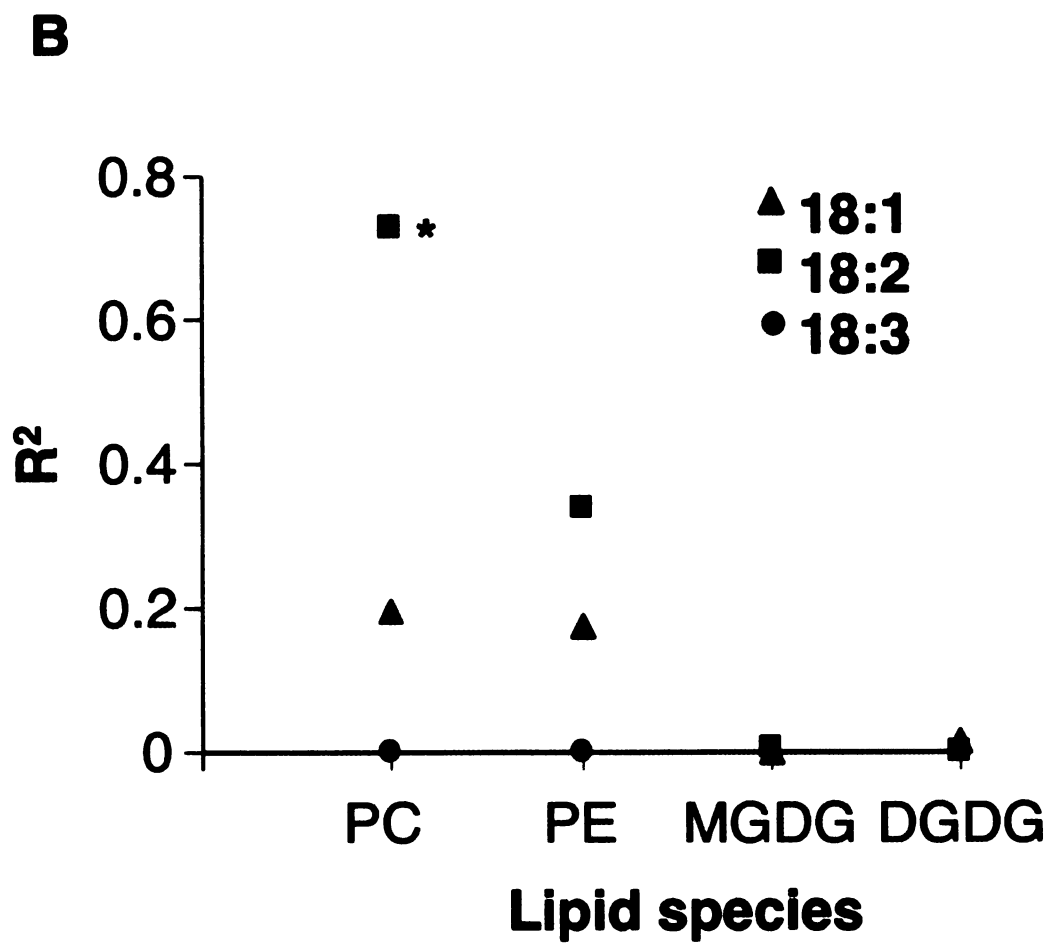


Figure 3.9 (cont'd)

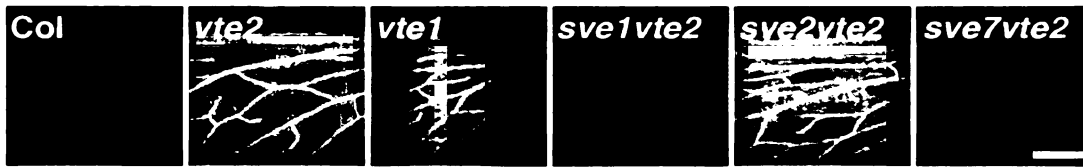


Figure 3.10 Callose deposition in leaf vascular tissues of the indicated genotypes after 7 d of LT treatment.

All genotypes were grown under permissive conditions for 28 d before being transferred to LT conditions. Leaves were fixed at the middle of the light cycle after 7 d of LT conditions and aniline-blue positive fluorescence was examined at the bottom part of the leaves ($n \geq 3$, Bar=1 mm). Representative images are shown.

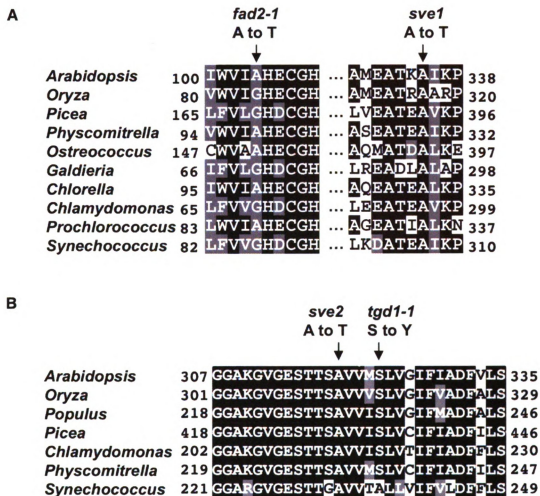


Figure 3.11 Multiple sequence alignment of relevant regions of FAD2 (A) and TGD1 (B) from representative photosynthetic organisms.

Black boxes highlight identical, gray boxes highlight conserved amino acids. Black arrows indicate amino acid substitutions converting A104 to T104 in *fad2-1* and A335 to T335 in *sve1* (A); A319 to T319 in *sve2* and S323 to Y323 in *tgd1-1* (B), respectively.

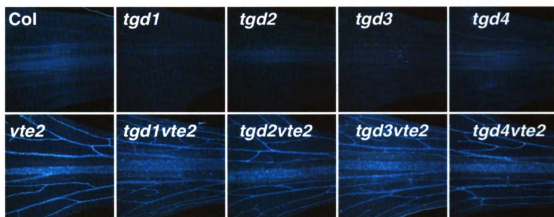


Figure 3.12 Callose deposition in the indicated genotypes after 7 d LT treatment.

All genotypes were grown under permissive conditions for 28 d before being transferred to LT conditions. Leaves were fixed at the middle of the light cycle after 7 d of LT conditions and aniline-blue positive fluorescence was examined at the bottom part of the leaves ($n \geq 3$, Bar=1 mm). Representative images are shown.

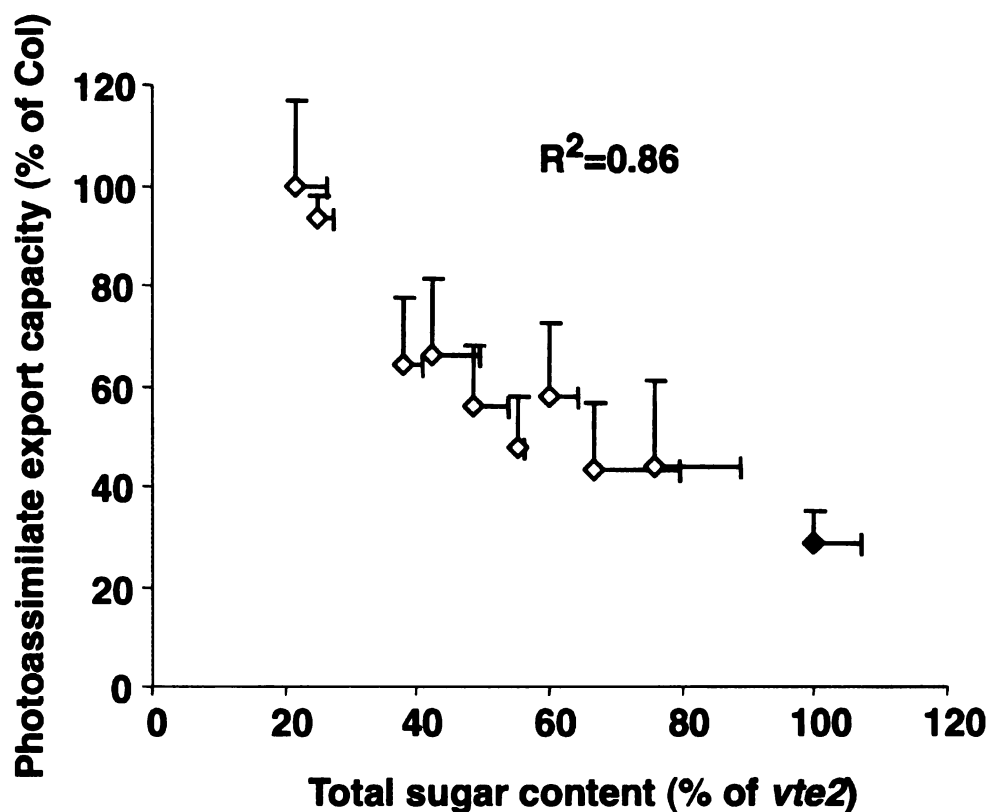


Figure 3.13 Scattered plot of photoassimilate export capacity versus leaf total sugar content.

Data include *vte1*, *sve1vte2*, *sve2vte2*, *sve7vte2*, *tgdlvte2*, *tgdl2vte2*, *tgdl3vte2*, *tgdl4vte2* (gray), Col (white) and *vte2* (black). Photoassimilate export capacity and leaf total sugar content are expressed relative to the 7 d LT treated Col and 14 d LT treated *vte2*, respectively. Unidirectional error bars (\pm SD, n = 4~5) are shown for clarity. Coefficient of determination (R^2) is derived from linear regression.

CHAPTER 4 MICROARRAY ANALYSIS OF THE LOW TEMPERATURE RESPONSE OF THE *ARABIDOPSIS VTE2* MUTANT

ABSTRACT

The contrasting phenotype displayed in germinating seed of *vte2* relative to wild type clearly demonstrated a primary role of tocopherols in limiting the damage of seed PUFA pools from nonenzymatic lipid oxidation. Transcript profiling studies further confirmed the importance of nonenzymatic lipid oxidation in triggering the oxidative and defense responses in germinating seed of *vte2*. While mature plants of *vte2* are biochemically and physiologically indistinguishable from wild type at optimum growth conditions, they develop a series of biochemical and physiological phenotypes, detailed in Chapter 2 and 3, which eventually led to growth inhibition. The identification and characterization of suppressors of the *vte2* LT-induced phenotypes (*sve* loci) in Chapter 2 and 3 have indicated ER lipid metabolism is an early, upstream event and highlights an important role for tocopherols and lipid metabolism in the initiation and development of the *vte2* LT-induced phenotypes. To further understand the response of *vte2* to LT at the transcriptional level, a global transcript profiling study comparing *vte2* and wild type plants under different time period (0h, 48h, 120h) of LT treatment was carried out. Tocopherol deficiency has no impact on global gene expression at permissive conditions but affected a small number (77) of genes after 48h of LT treatment. Comparisons with gene profiles of plants subjected to various stress conditions revealed that some degree of oxidative stress response was likely occurring in 48h-LT-treated *vte2*. Consistent with its biochemical and physiological phenotypes, LT-treated *vte2* also showed enhancement in expression of genes involved in cell wall modification and repression of genes related

with solute transport. Statistical analyses also highlighted several other potentially important target genes for future studies.

INTRODUCITON

The Arabidopsis *vte2* mutant, which is deficient in homogentisate phytyl transferase (HPT) and lacks all forms of tocopherols and pathway intermediates, has significantly reduced seed longevity compared with the wild type (Sattler et al., 2004). During germination, *vte2* seedlings exhibited severe seedling growth defects and contained excessive amounts of the major classes of free radical-mediated lipid peroxidation products: hydroxy fatty acids, malondialdehyde (MDA) and phytoprostanes (Sattler et al., 2006). Sattler et al (2006) performed global transcript profiling on 3-d-old wild type, *vte1* and *vte2* seedlings and defined 160 genes induced by at least 2.5 fold in 3-d-old *vte2* seedlings relative to wild type. Overall this gene list overlapped substantially with gene expression profiles of oxidative and biotic stress (Sattler et al., 2006). These results suggested that the non-enzymatic lipid peroxidation occurring in *vte2* seedlings contributed to triggering the transcriptional response of seedlings to pathogens.

Surprisingly, once past the germination and early seedling development stage, *vte2* mutant plants are biochemically and physiologically indistinguishable from wild type at optimum growth conditions (Maeda et al., 2006), suggesting that tocopherols are dispensable in mature plants. However, when the mutant plants were subjected to low temperature treatment, they displayed series of biochemical and phenotypic phenotypes, as described in detail in Appendix (Maeda et al., 2006). The identification and characterization of suppressors of the *vte2* LT-induced phenotypes (*sve* loci) in Chapter 2 and 3 have further suggested that alteration in ER lipid metabolism is an early event and highlighted an important role for tocopherols and lipid metabolism in the initiation and development of the *vte2* LT-induced phenotypes. However, it is still poorly understood

why tocopherol deficiency would alter ER lipid metabolism at LT conditions and what might be the molecular links between tocopherol deficiency, lipid metabolism and LT adaptation.

In animals, multiple studies have investigated transcriptome level responses to vitamin E in different organs using either experimental animals fed with tocopherol - sufficient and -deficient diets (Barella et al., 2004; Rota et al., 2004; Rota et al., 2005; Nell et al., 2007; Oommen et al., 2007) or α -tocopherol transfer protein knock out mice (α TTP(-/-)), which have extremely low cellular tocopherol contents (Gohil et al., 2003; Vasu et al., 2007; Vasu et al., 2009). While a few studies showed that vitamin E deficiency elicits pronounced changes in the expression of known antioxidant-responsive genes, such as catalase, superoxide dismutase and glutathione S-transferase (Gohil et al., 2003; Jarvis and Robaire, 2004; Hyland et al., 2006), other studies failed to detect significant changes in the expression of these classical antioxidant genes and instead showed alteration of expression in other distinctive groups of genes, such as those involved in testosterone synthesis and cancer development in testes (Rota et al., 2004), hormone metabolism and apoptosis in the hippocampus (Rota et al., 2005), lipid metabolism, inflammation and immune system in the heart (Vasu et al., 2007), transport processes, synaptic vesicular trafficking in particular, in livers (Nell et al., 2007), cytoskeleton modulation in lungs (Oommen et al., 2007) and muscle contractility and protein degradation pathways in muscles (Vasu et al., 2009). The impact of dietary or mutation induced α -tocopherol deficiency may explain the observed whole animal dysfunctions in muscle, neural and reproductive organs that seem to be independent of tocopherol's antioxidant functions.

In plants, no global gene expression profile for the effect of tocopherols in photosynthetic tissues has hitherto been undertaken. Comparing wild type and *vte2* plants at permissive and low temperatures should provide an ideal system to investigate the transcriptome level responses of plants to tocopherol deficiency in plants. DNA microarray analysis with Affymetrix's ATH1 GeneChip® technology was used to investigate the effects of tocopherol deficiency on global gene expression at both permissive and LT conditions. Because our goal was to identify early changes in gene expression that might be directly related to absence of tocopherols at LT, these time points were selected for the experimental design: 0, 48 and 120 hours of LT treatment. Based on the previous time course physiological and biochemical analyses detailed in Appendix (Maeda et al., 2006), at 0h (before LT treatment), *vte2* and Col plants are physiologically and biochemically indistinguishable. After 48h of LT treatment, vascular callose deposition has been induced and photoassimilate export capacity in mature leaves of *vte2* is significantly lower than Col but soluble sugar accumulation between the two do not differ. 120h of LT treatment represents a relatively late response of *vte2* where soluble sugars are significantly higher in the mutant and callose deposition is extensive and wide spread. After 48 h of LT treatment, it should be possible to identify early responses to tocopherol deficiency that are distinct from those due to the elevated sugar levels in *vte2* after 120h of LT treatment. The zero (permissive) 0h time point is a critical control to compare gene expression differences between *vte2* and Col in the absence of LT treatment. The experiment comprised 18 chips and is a factorial design, with three independent biological replicates for Col and *vte2* at each of the three time points.

RESULTS

Data evaluation and preprocessing

Preprocessing, including data evaluation, cleaning and the analytical methods that are applied to obtain reliable estimates of the relative abundance of each gene in a sample, is an essential requirement before any downstream statistical analysis (Russell et al., 2009). The quality of RNA used for GeneChip hybridization can be crucial in determining the quality of the obtained data. Because perfect match (PM) probe intensities should be systematically elevated at the 3' end of a probe set when compared to the 5' end when RNA degradation is sufficiently advanced, the 3'/5' ratios of expression have been used as a global indicator of RNA degradation (Bolstad et al., 2005). When the 3'/5' expression ratios of PM probes were used to evaluate the quality of the 18 arrays (Figure 4.1), all the arrays showed similar slopes, indicating the RNA used for the experiments is of good and comparable quality.

The 3': 5' ratios of the control genes on the chips were also assessed as another quality check. The 3': 5' values of GAPDH and β -actin (Figure 4.2) of all the chips were within the recommended ranges (Affymetrix's recommendation is ~ 1 for GAPDH and < 3 for β -actin). In addition, the percentage of present genes on all the chips were similar, ranging from 49.6 ~ 61.7% (Figure 4.2). The average background of most of the chips ranged from 86.3 ~ 109.8, except for chips C03, v01 and v02 (which represents Col-0h-replicate 3, *vte2*-0h-replicate 1, and *vte2*-0h-replicate 2, respectively) (Figure 4.2), which therefore necessitated up-scaling as indicated by the positive scale factors in Figure 4.2.

Different arrays have different distributions and it is important to assess the effect of background noise and to diagnose outliers. As seen in the boxplot (Figure 4.3) and the

histogram (Figure 4.4) of the chip data, most chips had a similar distribution range, with the exception of chips v01 and v02 which were significantly lower than the others. The low intensity of these chips is probably due to attenuated biochemical reactions during labeling or a reduction in detection efficiency. Therefore the data needed to be preprocessed with background correction and normalization to ensure chip-chip comparisons.

The Robust Multichip Average (RMA) technique for background adjustment, normalization and summarization functions (Irizarry et al., 2003b) as implemented in the affy package was chosen for preprocessing the array data because it performs better than the scaling method and is computationally fast (Russell et al., 2009). It consists of three preprocessing steps: convolution and background correction, quantile normalization, and a summarization based on a multi-array model fit robustly using the median polish algorithm. Because of various problems associated with Mismatch (MM) probes, only PM intensities are used in the RMA convolution method (Bolstad et al., 2003; Irizarry et al., 2003a; Irizarry et al., 2003b). Quantile normalization imposes the same empirical distribution of intensities to each array and summarization combines the multiple probe intensities for each probe set to produce an expression value. The distributions of the chip data after these three steps were similar as shown in the boxplot (Figure 4.5) and histogram (Figure 4.6), suggesting that expression values from different chips are now directly comparable.

To further investigate the relationship of the chips, a cluster dendrogram was generated (Figure 4.7). The chips grouped into three clusters, which are consistent with *the* three time points of low temperature treatment, with the chips for 48h and 120h LT-

treated samples being more closely related than to the 0h data, suggesting that the effect of LT treatment was greater than the differences between the genotypes. The three replicates of genotype in each treatment generally clustered together, suggesting the good biological repetition of the experiments.

Tocopherol deficiency had little impact on global gene expression at permissive conditions

Previous biochemical and physiological analyses have shown that except for an absence of tocopherols, *vte2* mutant plants grown at permissive conditions contain identical levels of chlorophylls, carotenoids, anthocyanins and lipid peroxides, have normal photosynthesis as indicated by maximum photosynthetic efficiency (Fv/Fm) and quantum yield of PSII (Φ_{PSII}), and like wild type, contain identical soluble sugar and starch and have no callose deposition in vasculature tissues (Maeda et al., 2006). Recently it was further shown that under permissive conditions *vte2* plants have fatty acid compositions identical to wild type indicating tocopherol deficiency does not impact the fatty acid and lipid metabolism prior to LT treatment (Maeda et al., 2008).

To investigate if there are any transcriptional changes in *vte2* plants relative to Col before LT treatment, limma analysis was performed to detect differently expressed genes between *vte2* and Col at the 0h time point. Only two genes [*NdhG* (Atcg01080, NADH dehydrogenase ND6) and *AtpI* (Atcg00150, a subunit of ATPase complex CF0)], both of which are encoded by and located in chloroplast, showed significant differences (adjusted P value = 0.05) between *vte2* and Col before LT treatment. For comparison, a different method was used for data analysis with GeneSpring software. To reduce false positives, the data of 6 chips at 0h time point were filtered using the detection call (Present/Absent)

generated by the Affymetrix microarray suite version 5 software (MAS5). 13572 probe sets called “Present” in either Col or *vte2* were further filtered with “2 fold change” between *vte2* and Col and 3 genes were identified. After t test, the same 2 genes as detected by limma analysis (NdhG and AtpI) were identified to be significantly different between the 2 genotypes (False discovery rate < 0.05). The near identical results obtained from the two different analysis methods indicated that lack of tocopherols had little, if any, impact on the global gene expression in *vte2* at permissive conditions.

77 genes are significantly different in 48h-LT-treated vte2 and Col

At 48 hours of LT treatment, 77 probe sets were found to be significantly different (adjusted p value<0.05) between *vte2* and Col using the limma analysis. The genes represented by the probe sets can be grouped into two categories: 49 genes that are significantly induced (Table 4.1), and 28 genes that are significantly repressed in *vte2* relative to Col (Table 4.2). A gene tree was generated to further investigate the expression patterns of the genes across different time points and based on this, the significant genes in *vte2* at 48h of LT treatment were further classified into 4 groups (Figure 4.8). The majority of the genes (43 genes, group I) showed temporary and moderate induction in Col while their induction in *vte2* was higher than Col at 48h of LT treatment and generally remained higher than Col at 120h of LT treatment. Group IV contains 16 genes that were temporarily repressed in 48h-LT-treated Col and were continually repressed in LT-treated *vte2*. Group II (11 genes) are repressed in LT-treated Col but induced in LT-treated *vte2* whereas group III (18 genes) generally had increased expression in LT-treated Col and decreased expression in LT-treated *vte2*. Because groups II and III genes have opposite expression patterns in *vte2* and Col, they may be

u
L
S

i
(
p
an

WR

used as potential “marker genes” differentiating the transcriptional responses between LT-treated *vte2* and Col.

Significantly induced genes in 48h-LT-treated vte2 and possible roles of WRKY

Among the list of 49 significantly upregulated genes in *vte2* after 48h of LT treatment, 6 are annotated as glycosyl transferases (At3g14750, At3g59100, At4g19460), UDP-glucosyl transferase (At3g21780) or glucanases (At1g26450, At1g65610) (Table 4.1). These genes are likely involved in different aspects of cell wall modification, which is consistent with the major modifications of cell wall structure in phloem parenchyma cells of LT-treated *vte2*. Notably, LT treatment induced significant, albeit low, expression of two putative callose synthase genes, *GSL4* (At3g14570) and *GSL11* (At3G59100) in *vte2*. These two members of the 12 *GSL* family in Arabidopsis may contribute to the substantial callose deposition in transfer cells of *vte2* and are investigated further in a later section.

Some of the upregulated genes in LT-treated *vte2* are involved in stress and senescence responses, including a senescence-associated family protein (At4g23410) and three glutathione S-transferases (GSTs), which have well-established roles in xenobiotic and ROS detoxification (Foyer et al., 1997). Furthermore, several upregulated genes are involved in various signaling pathways, including two auxin-responsive genes (At1g59500, At4g27260, both are auxin-responsive GH3 family proteins) and two genes potentially involved in calcium signaling (At3g22910, a calcium-transporting ATPase, and At1g68620, a putative calmodulin-related protein).

Notably, 5 transcription factors are among the induced genes in *vte2*, including three WRKY, one NAM and a zinc finger (C₂H₂ type) family protein (Table 4.1). WRKY

factors belong to the zinc-finger-type class of proteins and these plant-specific transcription factors contain a DNA-binding region of approximately 60 amino acids in length (the WRKY domain), which comprises the absolutely conserved WRKY motif adjacent to a novel zinc-finger motif (Ulker and Somssich, 2004). The WRKY family has 74 members in Arabidopsis and the physiological functions of most are not known, however, some have been implicated in plant stress responses (Eulgem et al., 2000), especially biotic stress responses (Eulgem and Somssich, 2007). The three WRKY factors that were induced in *vte2* relative to Col after 48h LT treatment are WRKY75 (At5g13080), WRKY8 (At5g46350) and WRKY38 (At5g22570). Based on microarray analysis, WRKY 75 has been shown to be involved in pathogen infection (Dong et al., 2003) and senescence (Guo et al., 2004) and is strongly induced during phosphate deprivation in Arabidopsis (Devaiah et al., 2007). WRKY38 was shown to be involved in regulating cold and drought stress response in barley (Mare et al., 2004), is induced by both pathogen infection and SA treatment and thought to function as a negative regulator of plant basal defense in Arabidopsis (Dong et al., 2003; Kim et al., 2008). The function of WRKY8 is currently unknown.

It is possible that some of the induced genes in 48h-LT-treated *vte2* might be regulated by WRKY factors. WRKY family members have been shown to bind to a DNA sequence designated the W box, (C/T)TGAC(T/G) (Eulgem et al., 2000). When the promoter regions of the 46 induced genes (excluding three WRKY from the total of 49 induced genes) in 48h-LT-treated *vte2* were analyzed for this sequence motif, 22 were found to have at least one hit for a W box element in their promoter regions (Table 4.3). Notably, the promoters of all six cell wall-related genes have one or more W-box

sequences and could potentially be regulated by the WRKY transcription factors. Some of the genes involved in stress (two GSTs) and auxin homeostasis (At1g59500) also have the binding sites of W box.

Significantly repressed genes in 48h-LT-treated vte2

One of the significantly repressed gene in *vte2* encodes VTE2/HPT (Table 4.2), the basis of the mutant and key limiting enzyme activity for tocopherol biosynthesis (Collakova and DellaPenna, 2003b). One of the downregulated genes of interest is *MsrB5* (At4g04830), which encodes methionine sulfoxide reductase B5. It is known that a variety of oxidants generated in metabolic stress conditions readily oxidize methionine (Met) residues in proteins to Met sulfoxide (MetSO) (R or S configuration) (Brot and Weissbach, 1991), resulting in modification of protein activity and conformation. MetSO can be reduced back to Met by Met sulfoxide reductase (MSR, EC 1.8.4.6). MSR activity is present in most organisms and has been included in the minimal set of proteins sufficient for cell life (Moskovitz et al., 1995; Mushegian and Koonin, 1996). MsrA enzymes utilize thioredoxin to reduce the S stereoisomer of MetSO back to Met (Moskovitz et al., 1995) while MsrB can catalyze the reduction of the R isomer of MetSO to Met (Lowther et al., 2002; Weissbach et al., 2002). Interestingly, plants have the largest number of Msr isoforms, with five *MsrA* (Sadanandom et al., 2000) and nine *MsrB* genes (Dos Santos et al., 2005) identified in *Arabidopsis*. Certain *Msr* genes displays organ-specific expression patterns and may protect plants from oxidative damage under different conditions (Sadanandom et al., 2000; Bechtold et al., 2004; Romero et al., 2004).

Altogether, 12 genes, five *MsrA* and seven *MsrB*, are represented on the Affymetrix chip. The expression levels of *MsrA3* (cytosolic), *MsrA4* (plastidic) and *MsrB7* (cytosolic) increased continuously, while that of *MsrB1* (plastidic) continuously decrease during LT treatment (Figure 4.9). The expression of *MsrA1*, *MsrA2*, *MsrB1* and *MsrB2* were temporarily repressed at 48h but tended to recover to pre-treatment levels at 120h of LT (Figure 4.9). Among all these *Msr* genes, only *MsrB5*, which likely localizes in the cytosol (Rouhier et al., 2006), showed significantly different expression between *vte2* and Col at 48h of LT treatment. Before LT treatment, *vte2* and Col had similar levels of *MsrB5* expression, however, after 48h of LT treatment, *vte2* showed a more than 3 fold decrease relative to Col, and remained repressed in *vte2* by 120h of LT. The transcript of *MsrB5* was reported to be most abundantly expressed in roots (Rouhier et al., 2006), it would be interesting to locate the transcription signals of *MsrB5* in LT-treated leaf tissue.

The other group of genes that was specifically repressed in 48h-LT-treated *vte2* include four genes in the nodulin drug/metabolite transporter (DMT) superfamily, a family of structurally homologous membrane proteins with diverse transport functions. Three of the four nodulins belong to the MtN21 family, which have 10 putative α -helical transmembrane spanners (TMSs) and are proposed to be localized in plasma membranes (Rouanet and Nasser, 2001). Several members of the DMT family in bacteria have been implicated in transport of various solutes (Ferguson and Krzycki, 1997; Tucker et al., 2003). The functions of nodulins in plants are largely uncharacterized, except for a few involved in bacterial nodulation in plants (Vandewiel et al., 1990; Hohnjec et al., 2009). Considering the enormous deposition of vascular callose and defective export capacity of both sugars and amino acids in LT-treated *vte2* (Maeda et al., 2006) and potato *VTE1*-

RNAi lines (Hofius et al., 2004), repression of the expression of these nodulins might reflect the declined transport of certain solutes from source to sink tissues in tocopherol-deficient plants.

*Different stress responses of the 49 induced genes in *vte2**

To investigate how the 49 induced genes in LT-treated *vte2* respond to other types of stress conditions, their expression patterns in response to various selected abiotic and biotic stress conditions were examined (Figure 4.10). Roughly half of the induced genes in *vte2* were also induced in response to treatment with the necrotrophic fungus *Botrytis cinerea* and the pathogenic leaf bacterium *Pseudomonas syringae* but not with phloem-feeding aphid *Myzus persicae*. Interestingly many of the same genes induced by pathogen treatments were also induced by ozone treatment and less so by hydrogen peroxide treatment. These genes include most of the transcription factors (WRKY75, WRKY 8, NAM and zinc finger family proteins) and some of the stress and signal-related genes (GST, auxin-responsive GH3 family protein). In contrast, very few induced genes in LT-treated *vte2* are responsive to abiotic stress conditions including heat, drought or cold treatments or hormone treatments such as zeatin, IAA, ethylene or ABA. The lack of induction of these genes by cold treatment suggests their response in *vte2* is due to tocopherol deficiency rather than cold stress *per se*.

Previously, the transcriptome of germinating *vte2* seedlings was shown to be substantially influenced by the elevation in nonenzymatic lipid peroxidation in the mutant (Sattler et al., 2006). The transcriptional responses of LT-treated *vte2* were further compared with those of 3-d-old *vte2* seedlings. When the same procedure of preprocessing and statistical analysis was applied for the microarray data of germinating

Col and *vte2* seedlings, 744 genes were identified as significantly different (adjusted $p < 0.05$) in 3-d-old *vte2* seedlings relative to Col (gene list not shown). When the list of 744 genes was compared with the list of 77 significant genes in 48h-LT-treated *vte2* plants, only 12 genes were in common (Table 4.4). The overlapping genes are 10 upregulated genes and two downregulated genes in both lists, including all three induced GSTs, WRKY8 and NAM transcription factors, and a chloroplast TAG lipase (At2g30550). Notably, these genes were also induced by *Botrytis cinerea*, *Pseudomonas syringae* and ozone treatments (Figure 4.10), suggesting that there was at least some degree of oxidative stress response at the transcriptional level in *vte2* at 48h of LT treatment.

Preliminary work on putative callose synthase genes

Previously, callose deposition was observed in phloem vascular parenchyma cells of LT-treated *vte2* as early as 6h of LT treatment, which coincided with the impairment of photoassimilate export in *vte2* (Maeda et al., 2006). There are 12 putative glucan synthase like (*GSL*) genes encoding callose synthases in Arabidopsis (Richmond and Somerville, 2000; Hong et al., 2001). Five *GSL* family members (*GSL1*, *GSL2*, *GSL5*, *GSL8*, *GSL10*) have been shown to be required in microgametogenesis (Dong et al., 2005; Enns et al., 2005; Nishikawa et al., 2005; Toller et al., 2008; Huang et al., 2009). *GSL5* (*PMR4*) was also shown to be responsible for deposition of callose after wounding or pathogen attack (Jacobs et al., 2003; Nishimura et al., 2003). When the *gs15* mutation was introduced into the *vte2* background, the double mutant showed a significant but incomplete reduction of callose deposition relative to *vte2* in response to LT treatment but this did not impact photoassimilate export defect, soluble sugar accumulation and leaf

purple coloration and plant growth inhibition (Maeda, 2006). These data indicate that *GSL5* is responsible for a large portion of callose deposited in LT-treated *vte2*, but that *GSL5*-dependent callose deposition is not the root cause for the subsequent photoassimilate export defect and may be secondary effect brought about by other factors or callose deposition by other *GSL* family members.

Two putative callose synthase genes, *GSL4* (At3g14570) and *GSL11* (At3G59100) were induced in 48h-LT-treated *vte2* (Table 4.1). To investigate if either of these callose synthase like genes is responsible for the *GSL5*-independent callose deposition in LT-treated *vte2*, homozygous mutants of *gsl4* and *gsl11* from available T-DNA inactivation lines were selected and introduced into the *vte2* background. The single *gsl* and *vte2* mutants and *gsl4vte2* and *gsl11vte2* double mutants were subjected to LT treatment to assess their LT phenotypes. Before being transferred to LT conditions, all the single and double mutants appeared visually similar to Col and *vte2* (Figure 4.11, panel A). After prolonged LT treatment (28d), the single mutants appeared similar to Col while both of the double mutants were smaller and purple, similar to *vte2* (Figure 4.11, panel B), suggesting that neither *gsl4* nor *gsl11* mutation alone has any impact on the *vte2* LT phenotype. This is also reflected at the level of vascular callose deposition (Figure 4.12), indicating that *gsl4* or *gsl11* mutation is not responsible for the callose deposited in LT-treated *vte2*. It is possible that *GSL4* and *GSL11* are functionally redundant in this regard or alternatively other *GSL* genes, which are not regulated at the transcriptional level, are responsible for the non-*GSL5*-dependent callose deposition in LT-treated *vte2*. Generating *gsl4gsl11vte2*, *gsl4gsl5vte2* and *gsl11gsl5vte2* triple mutants and a *gsl4gsl5gsl11vte2* quadruple mutant would be required to address this question.

D

A

v

e

r

ex

ce

of

tra

se

ce

th

4.

le

(T

su

in

mi

exp

inv

DISCUSSION

This study indicates that tocopherol deficiency does not impact the transcriptome of *Arabidopsis* at permissive conditions. Compared with the transcriptional responses of *vte2* seedlings after 3d of germination where accumulation of massive amounts of non-enzymatic lipid peroxidation products had a strong impact on the expression of a relatively large amount of genes, relatively very few genes in *vte2* showed different expression relative to Col after 48h of LT treatment.

The biochemical phenotype of 48h-LT-treated *vte2* plants includes phloem transfer cell-specific callose deposition that has started to spread from the petiole to the upper part of the mature leaves and impact on the capacity of source to sink photoassimilate transportation (Maeda et al., 2006). Consistent with these phenotypes, the expression of several genes which are likely involved in the cell wall modification in phloem transfer cells were significantly upregulated in *vte2* (Table 4.1). Further analysis suggested that these cell-wall modifying genes contain W box elements in the promoter regions (Table 4.3) and may be regulated by WRKY transcription factors. In addition, the expression levels of several nodulin genes which may be involved in solute transport, were repressed (Table 4.2), probably as a response to the blockage of phloem transport process.

Previous reports (Maeda et al., 2006; Maeda et al., 2008) and the characterization of suppressors in Chapter 2 and Chapter 3 have highlighted the involvement of tocopherols in ER lipid metabolism under low temperature conditions. Based on these results, it might be expected that some genes related to lipid metabolism might be differentially expressed in *vte2*. Surprisingly, only 2 of the 77 genes differentially expressed in *vte2* are involved in lipid metabolism. Both of them are lipase class 3 family proteins and

proposed to have triacylglycerol lipase activities, with one of them (At2g30550) localized in the chloroplast and the other (At1g30370) in mitochondria. Previous studies have shown that the majority of fatty acid desaturase genes in *Arabidopsis* do not respond to decreases in temperature via changes in transcription (Iba et al., 1993; Okuley et al., 1994; Heppard et al., 1996), or to alterations in the membrane fatty acid composition due to mutations in the desaturase pathway (Falcone et al., 1994). Only the relatively unusual case of the desaturation step catalyzed by *FAD8* (Gibson et al., 1994), and other highly specific examples for particular plant species (Berberich et al., 1998), have been shown to be regulated at the level of transcription by temperature. It seems likely that the effect of tocopherol deficiency on ER lipid metabolism in LT-treated *vte2* plants does not occur primarily through transcriptional regulation but rather at the post-transcriptional and enzymatic activity levels.

Although no obvious elevation of lipid peroxidation was detected in LT-treated *vte2* (Maeda et al., 2006; Maeda et al., 2008), comparisons of the expression of the significantly different genes in *vte2* across various abiotic and biotic treatments (Figure 4.10, Table 4.4) suggests that at least some degree of oxidant stress was occurring in *vte2* after 48h of LT treatment. Because all biochemical assays of lipid oxidation required whole leaf tissue for practical reasons, it is possible that oxidation was occurring only in small fraction of cells (e.g. transfer cells) and that this signal is diluted in whole leaf assays. It is possible that these oxidative stress responses reflected on the level of protein oxidation, as *MsrB5* was significantly repressed in LT-treated *vte2* (Figure 4.9) and such misregulation could induce covalent modification of the functions of related enzymes.

As with biochemical analyses, the experimental materials for this microarray analysis were of necessity taken from whole leaves (see Methods) and it is possible that the transcriptional “signatures” present in a small portion of specialized cell types are diluted and thus difficult to identify in bulk leaf samples. Consistent with this idea, most of the genes differentially expressed in LT-treated *vte2* have low expression levels and attempts to verify their expression by traditional RNA gel blot analysis failed (data not shown). It is possible that transcriptional responses may only be present in certain cell types of *vte2*, especially in its transfer cells where endomembrane biogenesis is largely enhanced and the deposition of callose and abnormal cell wall ingrowths occur. In situ hybridization or laser-microdissection of specific cells especially the vascular parenchyma cells will help to further confirm the expression levels and possible localization specificity of some of the 77 genes identified in this study. Future experimental investigations with real-time PCR and analysis of post-transcriptional processes, such as protein oxidation, will be necessary to elucidate how these genes may be regulated by tocopherols and contribute to the LT-induced phenotype of *vte2*.

MATERIALS AND METHODS

Experimental design

A factorial design comprising of two genotypes (Col, *vte2*) at three different time points (0h, 48h, 120h of LT treatment) was chosen. Three independent biological replicates were included for each genotype at each time point. Experiments for the first two replicates for Col and *vte2* at 0h time point were performed with the first set of plants in May-June of 2005 and the rest of the experiments were finished with a second set of plants during July-Sep of 2006. Fresh seed were used for both sets, plants were grown in the same chamber with identical conditions.

Plants and growth conditions

Arabidopsis thaliana seeds from wild type (ecotype Columbia-0) and *vte2-1* were planted on vermiculite and potting soil mixture and stratified in the dark for 5 days at 4°C before being transferred to permissive conditions with 12 hours of light (100 μ E, 22°C) and 12 hours of dark period (18°C). Plants from both genotypes were randomly assigned to different locations in the chambers. Plants were fertilized with 1 \times Hoagland solution every week. For 0h time point, plants of *vte2* and Col were grown to 4 weeks at permissive temperatures and the 9th to 11th leaves from 3 plants of the same genotype were harvested. For 48h and 120h time points, 4 week old plants were transferred to LT conditions (75 μ E, 7.5 \pm 3°C, 12 hour light) and the 9th to 11th leaves from 3 plants of the same genotype were harvested when plants were treated for 48 and 120 hours, respectively. All leaf materials were harvested directly into tubes filled with liquid nitrogen when plants were at 1 hour of light cycle.

RNA extraction, labeling and hybridization

Total RNA was extracted using the RNAqueous RNA extraction kit and the Plant RNA Isolation Aid (Ambion) according to the manufacturer's protocol. Labeling and hybridization of RNA were conducted using standard Affymetrix protocols by the Michigan State University DNA Microarray Facility. ATH1 Arabidopsis GeneChips (Affymetrix, Santa Clara, CA) were used for measuring changes in gene expression levels. Total RNA was converted into cDNA, which was in turn used to synthesize biotinylated cRNA. The cRNA was fragmented into smaller pieces and then was hybridized to the GeneChips. After hybridization, the chips were automatically washed and stained with streptavidin phycoerythrin using a fluidics station. The chips were scanned by the GeneArray scanner by measuring light emitted at 570nm when excited with 488-nm wavelength light.

Data evaluation and preprocessing

The raw chip data were analyzed with R software (version 2.9, <http://www.r-project.org/>). The RNA degradation plot for all 18 chips was generated using the AffyRNAdeg function in the simpleAffy package. Boxplot and Histogram tools included in the affy and simpleaffy packages were used to investigate the data distribution of the 18 chips. RMA function as implemented in the affy package was used for background adjustment, normalization and summarization. The cluster dendrogram (Figure 4.8) was generated applying hclust function using average linkage clustering of Euclidean distance based on the normalized expression values from 18 chips.

Statistical analysis for significant genes

As we are interested in genes differentially expressed between genotypes at different time points of cold treatment and also the differential response of genotypes to different durations of cold treatments. Considering this complexity, the limma package implemented in Bioconductor of R software was used for statistical analysis, because it is designed to analyze complex experiments involving comparisons between many RNA targets simultaneously. Another consideration is that use of empirical Bayes method in limma can borrow the information across genes making the analysis stable even for experiments with small number of arrays, as in this case. For statistical analysis, the signal intensity data were analyzed with use of a linear statistical model and an empirical Bayes method for assessing differential expression in the limma package (Smyth, 2005). Genes with <5% of adjusted P values were considered significant. Cluster analysis of the 77 significantly different genes in *vte2* at 48h of LT treatment was performed by Pearson's method.

Data of 0h chips were also analyzed with Agilent's GeneSpring analysis platform (version 7.2). The data files generated by the Affymetrix microarray suite version 5 software (MAS5) were imported and subjected to recommended normalization process (the expression values <0.01 were set to 0.01; the data are normalized to 50% percentile per chip and median per gene). The data were then filtered using the detection call (Present/Absent) and probe sets called "Present" in either genotype were further filtered with "2 fold change" between the genotypes. The probe sets after the above advanced filtering were finally analyzed with t test (False discovery rate < 0.05).

The 49 genes which are significantly induced in 48h LT-treated *vte2* relative to wild-type plants were examined using the Meta-Analyzer feature of GENEVESTIGATOR (Zimmermann et al., 2004) to assess their responses to various conditions or treatments. The gene expression responses were calculated as ratios between treatment and negative control samples and the resulting values thus reflect up- or down-regulation of genes. Twelve different conditions were chosen: Biotic stress includes treatments with *Botrytis cinerea* (6 treatment chips + 6 control chips), *Pseudomonas syringae* (9+9) and *Myzus persicae* (3+3). Chemical stress includes hydrogen peroxide (H₂O₂) (3+2) and ozone treatments (3+3). Hormone stress includes treatments with ABA (2+2), ethylene (3+3), IAA (3+3), zeatin (3+3). Abiotic stress includes treatments with cold (6+6), drought (3+1) and heat (2+2). Only high-quality 22K chips were used for the analysis. For Figure 4.12, the data for 0d- and 3d- old seedlings of Col and *vte2* (three biological replicates at each treatment, see (Sattler et al., 2006) were subjected to the same procedure of preprocessing and statistical analysis as described above for *vte2* plants under LT treatments.

Promoter analysis

The conservative four amino acid sequence of W box (TGAC) was used for promoter regulatory sequence analysis using the promoter analysis tool implemented in GeneSpring. 1000bp upstream of 49 induced genes in 48h-LT-treated *vte2* was searched. The promoters containing TGAC were further checked for the presence of the consensus sequence of W box (C/T)TGAC(T/G).

Generating double homozygous mutants and LT treatment

The following T-DNA insertion lines were obtained from the Arabidopsis Biological Resource Center at Ohio State University: SALK_000507 (exon) for *GSL4* (At3g14570) and SALK_019534 (exon) for *GSL11* (At3G59100). Homozygous mutant lines were screened with PCR and crossed into *vte2*. Double homozygous mutants were obtained by PCR screening for the presence of the insertions and *vte2* tocopherol deficiency with HPLC. The *vte2* allele was confirmed by CAPs marker developed for *vte2-1* point mutation (Maeda et al., 2006). Plants of wild type (Col), *vte2*, single mutants of *gsl4*, *gsl11* and double mutants of *vte2gsl4* and *vte2gsl11* were grown for 28 d at permissive conditions and then transferred to LT conditions for various time for evaluation of LT-induced phenotypes.

ACKNOWLEDGEMENTS

We would thank Maria Magallanes-Lundback for performing RNA extraction and labeling and the Research Technology Support Facility (RTSF) at Michigan State University for performing microarray analysis.

TABLES AND FIGURES

Table 4.1 The 49 genes significantly upregulated in *vte2* relative to Col at 48h of LT treatment

M-value (M) is the value of the contrast and represents a \log_2 fold change between 48h-LT-treated *vte2* and Col. adj-P.value is the p-value adjusted for multiple testing with Benjamini and Hochberg's method to control the false discovery rate. B-statistic (B) is the log-odds that the gene is differentially expressed. Description of gene functions was obtained from the Gene Ontology section of The Arabidopsis Information Resources.

AGI number	M	Adj.P. Val	B	Annotated gene function
At1g26450	2.62	0.00	11.64	beta-1,3-glucanase-related
At4g23410	1.53	0.00	10.08	Senescence-associated family protein
At1g68290	2.39	0.00	7.97	bifunctional nuclease, putative
At5g22860	1.38	0.00	7.04	serine carboxypeptidase S28 family protein
At3g14570	1.85	0.00	6.88	glycosyl transferase family 48 protein
At1g59500	1.58	0.00	6.79	auxin-responsive GH3 family protein
At3g17690	1.80	0.00	6.74	cyclic nucleotide-binding transporter 2 / CNBT2
At1g74590	1.50	0.00	6.31	Glutathione S-transferase, putative
At4g20320	1.08	0.00	5.80	CTP synthase, putative / UTP-ammonia ligase, putative
At3g22910	1.82	0.00	5.65	Ca-transporting ATPase, plasma membrane-type, putative (ACA13)
At5g13080	1.88	0.00	5.51	WRKY family transcription factor (WRKY75)
At5g47920	1.06	0.00	5.13	expressed protein
At1g68620	2.08	0.00	4.95	expressed protein
At1g65500	2.13	0.00	4.84	expressed protein
At1g76640	2.52	0.00	4.54	calmodulin-related protein, putative
At2g26020	2.01	0.00	4.40	plant defensin-fusion protein, putative (PDF1.2b)
At1g74055	1.00	0.00	4.18	expressed protein
At1g30370	1.60	0.01	3.80	lipase class 3 family protein
At5g13880	1.45	0.01	3.60	expressed protein
At3g49130	0.94	0.01	3.16	hypothetical protein
At5g46590	1.31	0.01	3.09	no apical meristem (NAM) family protein
At3g21780	0.91	0.01	3.09	UDP-glucosyl transferase family protein
At1g17180	1.21	0.02	2.82	glutathione S-transferase, putative
At1g65610	1.33	0.02	2.70	endo-1,4-beta-glucanase, putative / cellulase, putative
At3g53600	0.70	0.02	2.39	zinc finger (C2H2 type) family protein
At5g13170	1.01	0.02	2.37	nodulin MtN3 family protein

Table 4.1 (cont'd)

AGI number	M	Adj.P. Val	B	Annotated gene function
At5g46350	1.02	0.02	2.34	WRKY family transcription factor (WRKY8)
At5g09470	0.93	0.02	2.26	mitochondrial substrate carrier family protein
At4g35730	1.24	0.02	2.23	expressed protein
At2g29090	1.07	0.03	2.15	cytochrome P450 family protein
At2g30550	0.70	0.03	2.08	lipase class 3 family protein
At4g38420	1.58	0.03	2.02	multi-copper oxidase type I family protein
At4g27260	0.76	0.03	1.98	auxin-responsive GH3 family protein
At3g59100	1.04	0.03	1.81	glycosyl transferase family 48 protein
At4g19460	0.80	0.03	1.80	glycosyl transferase family 1 protein
At3g09270	2.07	0.03	1.73	glutathione S-transferase, putative
At5g22570	1.18	0.03	1.72	WRKY family transcription factor (WRKY38)
At1g32350	1.45	0.04	1.64	alternative oxidase, putative
At5g17330	0.74	0.04	1.54	glutamate decarboxylase 1 (GAD 1)
At4g28550	1.05	0.04	1.43	RabGAP/TBC domain-containing protein
At5g65600	1.27	0.04	1.38	legume lectin family protein / protein kinase family protein
At4g36430	0.79	0.04	1.37	peroxidase, putative
At5g04080	0.63	0.04	1.32	expressed protein
At5g64905	1.78	0.04	1.25	expressed protein
At5g66920	1.09	0.04	1.24	multi-copper oxidase type I family protein
At5g63970	0.97	0.05	1.20	copine-related
At2g23270	0.95	0.05	1.20	expressed protein
At1g19250	0.86	0.05	1.10	flavin-containing monooxygenase family protein
At5g67080	1.69	0.05	1.08	protein kinase family protein

Table 4.2 The 28 genes significantly downregulated in *vte2* relative to Col at 48h of

LT treatment

AGI number	M	Adj. P.Val	B	Annotated Gene function
At2g18950	-2.36	0.00	7.93	HPT: tocopherol phytyltransferase
At5g14740	-0.77	0.00	6.32	carbonate dehydratase 2 (CA2) (CA18)
At3g11930	-1.47	0.00	6.10	Universal stress protein (USP) family protein
At2g36830	-1.01	0.00	5.94	major intrinsic family protein / MIP family protein
At1g04680	-0.74	0.00	5.41	pectate lyase family protein
At1g76800	-1.43	0.00	5.36	nodulin, putative
At4g08300	-2.98	0.00	4.58	nodulin MtN21 family protein
At2g22330	-1.67	0.00	4.44	cytochrome P450, putative
At3g10080	-0.72	0.01	3.86	germin-like protein, putative
At5g44720	-1.05	0.02	2.89	molybdenum cofactor sulfurase family protein
At5g23020	-3.81	0.02	2.88	2-isopropylmalate synthase 2 (IMS2)
At3g47470	-0.84	0.02	2.77	chlorophyll A-B binding protein 4, chloroplast / LHCI type III CAB-4 (CAB4)
At1g51400	-0.88	0.02	2.61	photosystem II 5 kD protein
At4g08290	-1.22	0.02	2.56	nodulin MtN21 family protein
At1g21440	-1.17	0.03	2.18	mutase family protein
At1g01620	-0.83	0.03	2.02	plasma membrane intrinsic protein 1C (PIP1C) / aquaporin PIP1.3 (PIP1.3) / transmembrane protein B (TMPB)
At3g08940	-0.82	0.03	1.95	chlorophyll A-B binding protein (LHCB4.2)
At5g24490	-1.22	0.03	1.91	30S ribosomal protein, putative
At4g04830	-1.57	0.04	1.58	methionine sulfoxide reductase domain-containing protein
At2g37460	-1.93	0.04	1.54	nodulin MtN21 family protein
At4g04040	-0.69	0.04	1.44	pyrophosphate--fructose-6-phosphate 1-phosphotransferase beta subunit, putative
At1g31180	-0.85	0.04	1.41	3-isopropylmalate dehydrogenase, chloroplast, putative
At1g78370	-1.07	0.04	1.40	glutathione S-transferase, putative
At5g02260	-1.23	0.04	1.38	expansin, putative (EXP9)
At5g67070	-0.51	0.04	1.28	rapid alkalization factor (RALF) family protein
At1g13280	-0.94	0.04	1.26	allene oxide cyclase family protein
At3g09580	-0.73	0.05	1.08	amine oxidase family protein
At1g03600	-0.48	0.05	1.08	photosystem II family protein

M-value (M) is the value of the contrast and represents a \log_2 fold change between 48h-LT-treated *vte2* and Col. adj-P.value is the p-value adjusted for multiple testing with Benjamini and Hochberg's method to control the false discovery rate. B-statistic (B) is the log-odds that the gene is differentially expressed. Description of gene functions was obtained from the Gene Ontology section of The Arabidopsis Information Resources.

Table 4.3 Genes containing W box sequence (C/T)TGAC(T/G) in the 1000bp upstream regions.

Probe	AGI ID	Gene function	Distance (bp)	Sequence
248896_at	At5g46350	beta-1,3-glucanase-related	929	TTGACT
			766	TTGACT
			758	TTGACT
			717	CTGACT
252989_at	At4g38420	Multi-copper oxidase type I family protein	879	CTGACT
254575_at	At4g19460	glycosyl transferase family 1 protein	802	TTGACT
			211	TTGACG
248777_at	At5g47920	expressed protein	681	TTGACT
			544	TTGACG
262229_at	At1g68620	expressed protein	664	CTGACT
264685_at	At1g65610	Endo-1,4-beta-glucanase, putative / cellulase	531	TTGACT
251950_at	At3g53600	zinc finger (C ₂ H ₂ type) family protein	521	TTGACT
			509	TTGACT
247026_at	At5g67080	protein kinase family protein	476	CTGACT
251499_at	At3g59100	glycosyl transferase family 48 protein	458	TTGACG
252289_at	At3g49130	hypothetical protein	433	TTGACT
			160	TTGACT
256833_at	At3g22910	Ca ²⁺ ATPase, plasma membrane-type (ACA13)	401	TTGACT
253768_at	At4g28550	beta-1,3-glucanase-related	399	TTGACT
256306_at	At1g30370	Lipase class 3 family protein	375	TTGACT
250211_at	At5g13880	expressed protein	316	TTGACT
261004_at	At1g26450	beta-1,3-glucanase-related	280	TTGACT
245982_at	At5g13170	nodulin MtN3 family protein	195	TTGACT
248855_at	At5g46590	no apical meristem (NAM) family protein	169	TTGACT
262517_at	At1g17180	Glutathione S-transferase, putative	153	CTGACT
260225_at	At1g74590	Glutathione S-transferase, putative	134	TTGACT
247145_at	At5g65600	legume lectin family protein	127	TTGACT
262099_s at	At1g59500	Auxin-responsive GH3 family protein	125	TTGACT
			108	CTGACG
258377_at	At3g17690	cyclic nucleotide-binding transporter 2 / CNBT2 (CNGC19)	124	TTGACG

Table 4.4 Common 12 genes between the 77 significantly different genes in 48h-LT-treated *vte2* plant and 744 significantly different genes in 3-d-old *vte2* seedling.

Data of seedling of LT-treated plants were subjected to the same process of limma analysis for significant genes (see Methods). The overlapping 12 genes between the 744 differentially expressed genes in 3-d-old *vte2* seedlings and 77 differentially expressed genes in 48h-LT-treated *vte2* plants were listed. M-value (M) is the value of the contrast and represents a \log_2 fold change, and adj. P, the p-value adjusted for multiple testing with Benjamini and Hochberg's method to control the false discovery rate, were shown for 48h-LT-treated *vte2* plant and 3-d-old *vte2* seedling, respectively. Descriptions of gene function and cellular component were obtained from the Gene Ontology section of The Arabidopsis Information Resources.

AGI number	48h-LT-treated <i>vte2</i> plant		3-d-old <i>vte2</i> seedling		Gene title	GO molecular function	GO cellular component
	M	adj. p	M	adj. p			
At1g68290	2.39	0.00	2.01	0.00	bifunctional nuclease, putative	nucleic acid binding /// endonuclease activity	endomembrane system
At1g65500	2.13	0.00	4.33	0.00	expressed protein	---	endomembrane system
At1g74590	1.50	0.00	2.19	0.00	glutathione S-transferase	glutathione transferase activity	cytoplasm
At5g46590	1.31	0.01	1.93	0.00	no apical meristem (NAM) family protein	transcription factor activity /// DNA binding	---
At1g17180	1.21	0.02	1.93	0.03	glutathione S-transferase	glutathione transferase activity	cytoplasm
At5g46350	1.02	0.02	1.69	0.00	WRKY family transcription factor (WRKY8)	transcription factor activity /// DNA binding	Nucleus
At3g09270	2.07	0.03	1.29	0.02	glutathione S-transferase	glutathione transferase activity	Cytoplasm
At2g30550	0.07	0.03	1.02	0.05	lipase class 3 family protein	triacylglycerol lipase activity	chloroplast
At4g36430	0.79	0.04	3.20	0.00	peroxidase, putative	peroxidase activity /// calcium ion binding /// oxidoreductase activity	Endomembrane system
At5g64905	1.78	0.04	1.10	0.01	expressed protein	---	---
At1g76800	-1.43	0.00	-0.74	0.02	nodulin, putative	---	---
At3g09580	-0.73	0.05	-0.90	0.02	amine oxidase family protein	oxidoreductase activity	Chloroplast

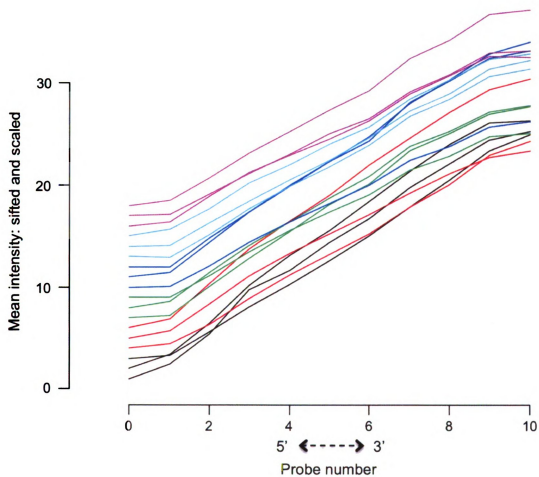


Figure 4.1 RNA degradation plot for the 18 arrays used in this study.

For each array, the probes are ordered from the 5' end of the targeted transcript. Three replicates for each treatment were shown in the same color for clarity.

Figure 4.2 QC plot of 3': 5' ratios for control genes, percentage of present gene calls and background levels.

Dotted horizontal lines separate the plot into rows, one for each chip. Dotted vertical lines provide a scale from -3 to 3. Each row shows the array index (C0.1-3 stands for Col 0h replicates 1-3, C48.1-3 stands for Col 48h replicates 1-3, and C120.1-3 stands for Col 120h replicates 1-3 while v01.1-3 stands for *vte2* 0h replicates 1-3, v48.1-3 stands for *vte2* 48h replicates 1-3, and v120.1-3 stands for *vte2* 120h replicates 1-3, respectively), % present, average background, scale factors (plotted as a red line from the center line of the image. A line to the left corresponds to a down-scaling, to the right, to an up-scaling), 3':5' ratios of GAPDH (blue circles) and β -actin (blue triangles) for an individual chip.

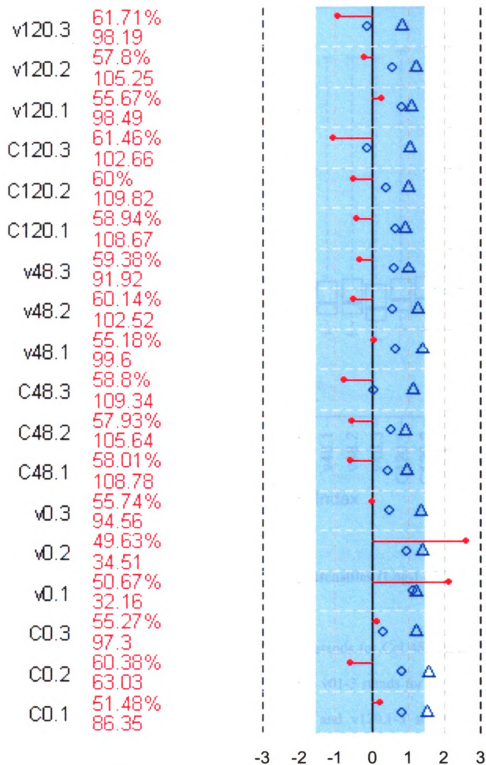


Figure 4.2

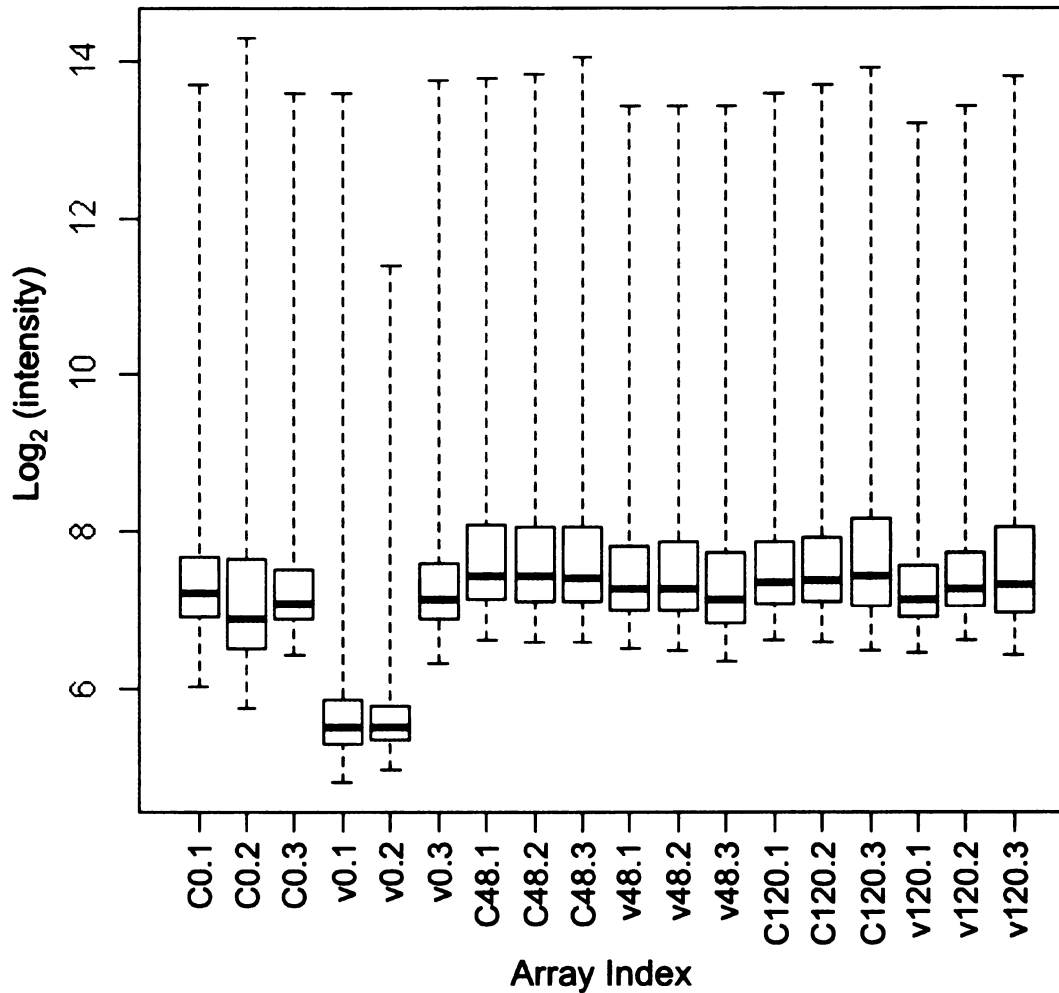


Figure 4.3 Box plot of all perfect match (pm) intensities (Log_2) of unnormalized 18 array data set.

C0.1-3 stands for Col 0h replicates 1-3, C48.1-3 stands for Col 48h replicates 1-3, and C120.1-3 stands for Col 120h replicates 1-3 while v01-3 stands for *vte2* 0h replicates 1-3, v48.1-3 stands for *vte2* 48h replicates 1-3, and v120.1-3 stands for *vte2* 120h replicates 1-3, respectively.

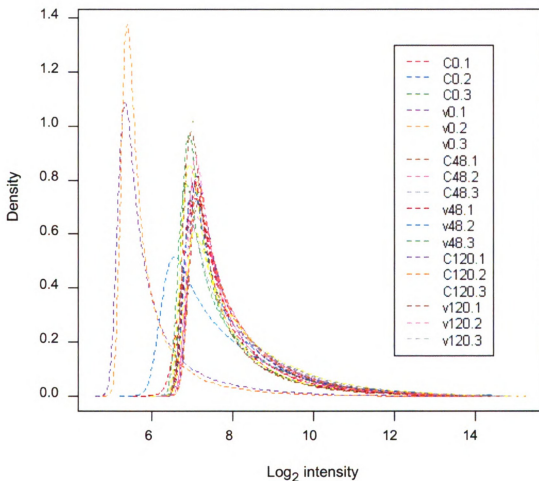


Figure 4.4 Histogram of kernel density estimates of all perfect match (pm) probe intensities (Log_2) of unnormalized 18 array data set.

C0.1-3 stands for Col 0h replicates 1-3, C48.1-3 stands for Col 48h replicates 1-3, and C120.1-3 stands for Col 120h replicates 1-3 while v01-3 stands for *vte2* 0h replicates 1-3, v48.1-3 stands for *vte2* 48h replicates 1-3, and v120.1-3 stands for *vte2* 120h replicates 1-3, respectively.

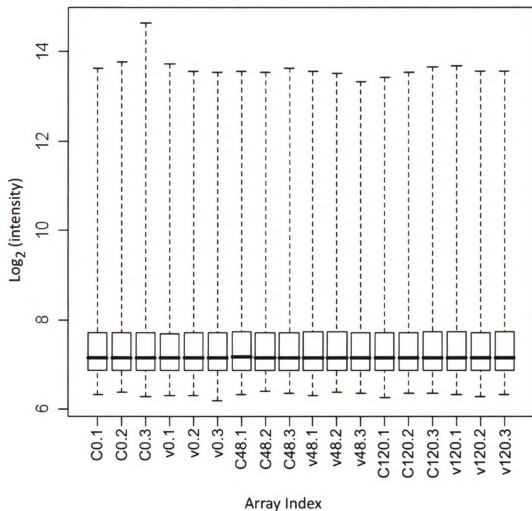


Figure 4.5 Box plot of all perfect match probe intensities (Log_2) of quantile normalized array data.

C0.1-3 stands for Col 0h replicates 1-3, C48.1-3 stands for Col 48h replicates 1-3, and C120.1-3 stands for Col 120h replicates 1-3 while v01-3 stands for *vte2* 0h replicates 1-3, v48.1-3 stands for *vte2* 48h replicates 1-3, and v120.1-3 stands for *vte2* 120h replicates 1-3, respectively.

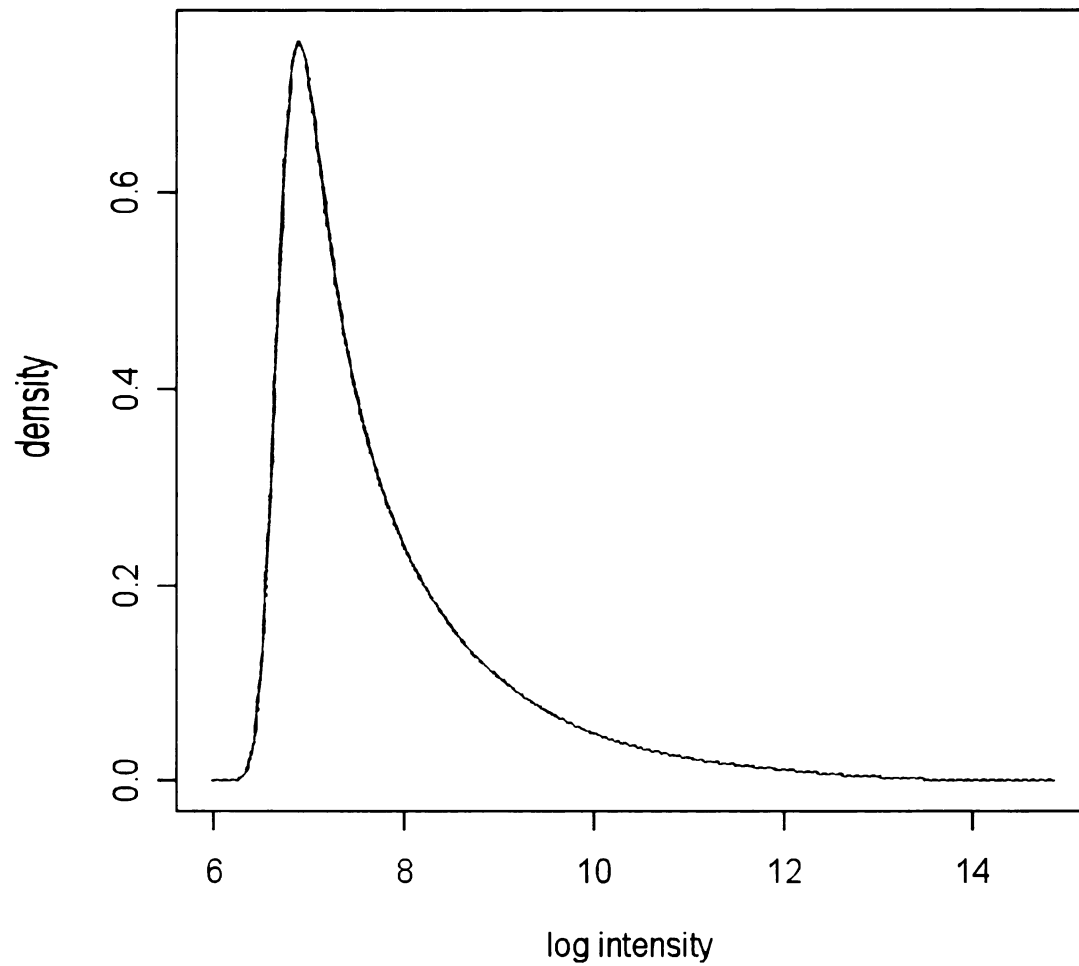


Figure 4.6 Histogram of kernel density estimates of all perfect match probe intensities (Log_2) of quantile normalized 18 array data set.

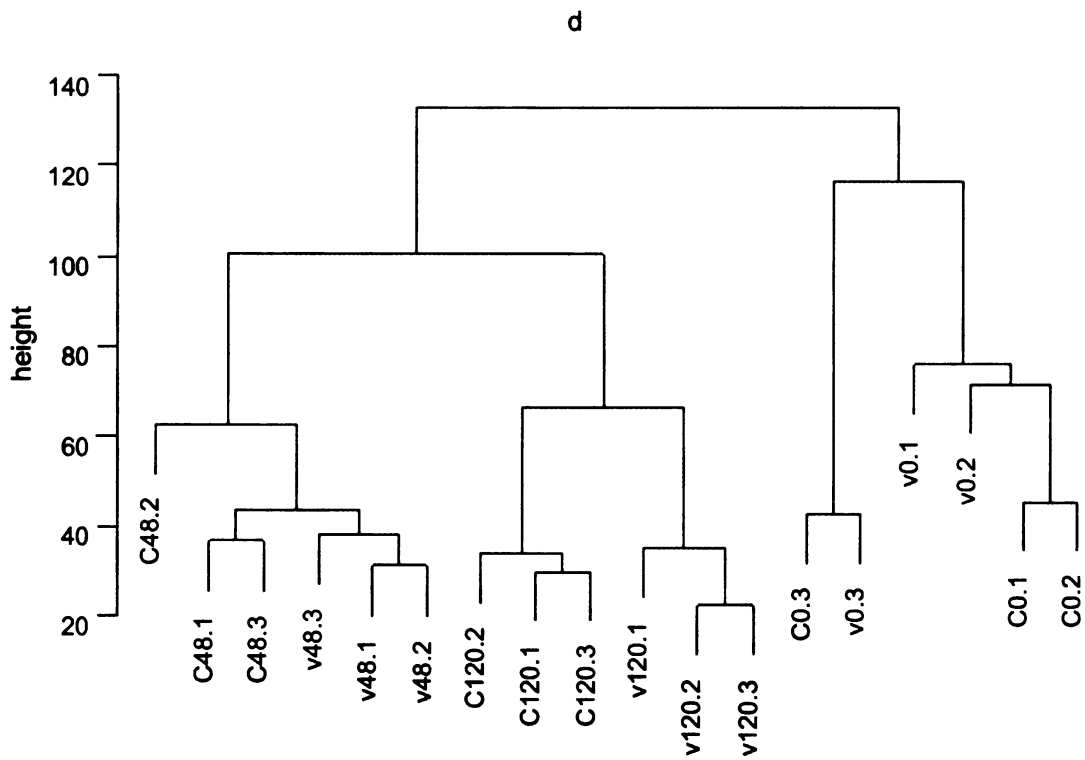


Figure 4.7 Cluster dendrogram of a correlation matrix for all-against-all chip comparisons.

C0.1-3 stands for Col 0h replicates 1-3, C48.1-3 stands for Col 48h replicates 1-3, and C120.1-3 stands for Col 120h replicates 1-3 while v01-3 stands for *vte2* 0h replicates 1-3, v48.1-3 stands for *vte2* 48h replicates 1-3, and v120.1-3 stands for *vte2* 120h replicates 1-3, respectively.

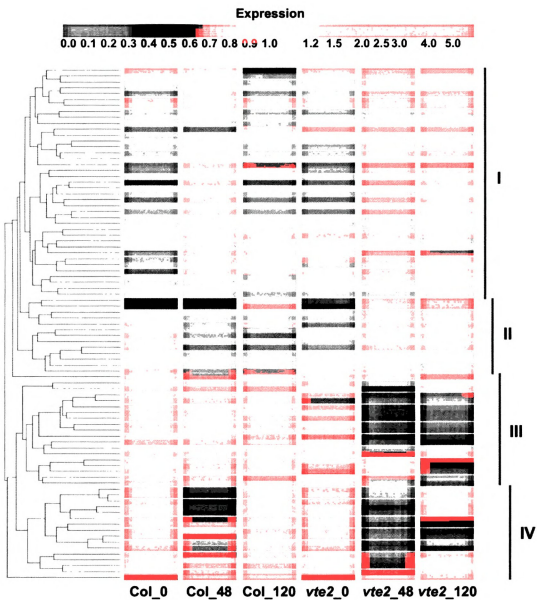


Figure 4.8 A gene tree of the 77 significantly different genes in 48h-LT-treated *vte2* relative to Col.

The color bar represents different levels of expression (\log_2). The groups (labeled as I, II, III and IV) were based on general expression patterns across Col and *vte2* at three time points of LT treatment.

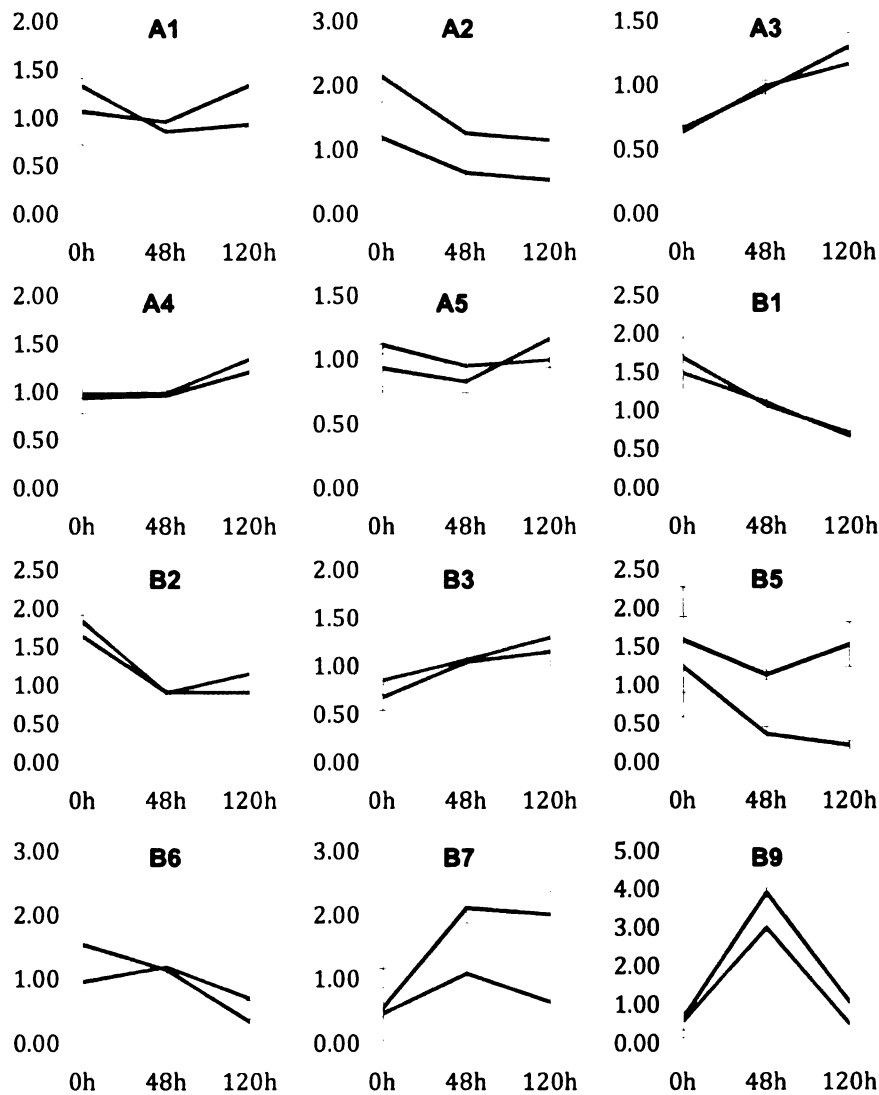


Figure 4.9 Normalized expression levels of *Msr* genes in *Col* (gray) and *vte2* (purple) at different time points of LT treatment.

A1-A5, B1-B3, B5-B7 and B9 represents the individual *MsrA* or *MsrB* genes on the Affymetrix chip, respectively. Based on targeting prediction software, *MsrA1-A3* are cytosolic and *MsrA4* is plastidic. *MsrB1* and *MsrB2* are plastidic, *MsrB3* is addressed to a secretory pathway and the remainder of the *MsrB* genes are likely located in the cytosol. The expression of *MsrB5* in *vte2* (red) is significantly different from *Col* (blue) (adjusted p value <0.05) at 48h of LT treatment and is highlighted. Standard errors are indicated (n=3).

Figure 4.10 A heat map of expression of the significantly upregulated 49 genes in 48h LT-treated *vt2* under different conditions.

Genes (AGI number) significantly induced in 48h LT-treated *vt2* relative to Col plants were examined using the Meta-Analyzer feature of GENEVESTIGATOR to assess their responses to various conditions or treatments relative to each corresponding negative control. The conditions and treatments were sorted by increasing ratios from the left to the right. The color bar represents different levels of expression (\log_2)

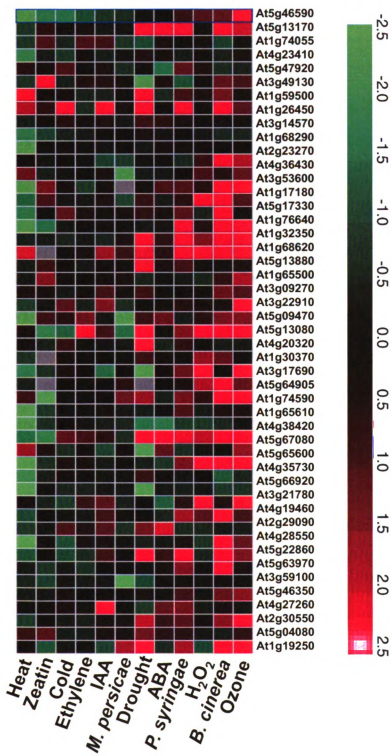


Figure 4.10

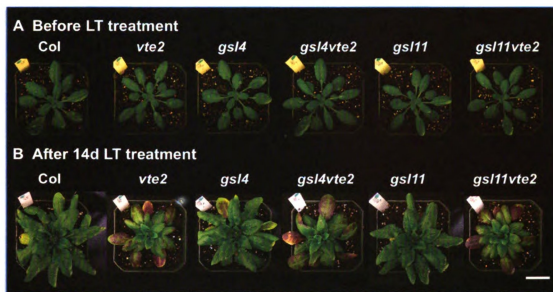


Figure 4.11 Whole plant phenotype of Col, *vte2*, *gsl4*, *gsl4vte2*, *gsl11*, *gsl11vte2*.

All genotypes were grown under permissive conditions for 4 weeks and then transferred to LT conditions. Representative plants of the indicated genotypes are shown before LT treatment (A) and after 28d of LT treatment (B). Bar=2cm.

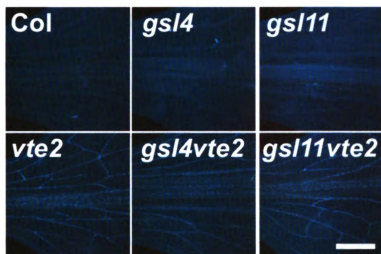


Figure 4.12 Vascular callose deposition in *Col*, *vte2*, *gsl4*, *gsl4vte2*, *gsl11* and *gsl11vte2* after 3 d of LT treatment.

All genotypes were grown under permissive conditions for 4 weeks and then transferred to LT conditions. Samples for callose staining were fixed in the middle of the light cycle after 3 d of LT treatment. Representative images are shown (n=3). Bar = 1mm.

CHAPTER 5 SUMMARY AND FUTURE PERSPECTIVES

Tocopherol levels in plant tend to increase in response to various abiotic stresses including high intensity light, salt, cold, drought, heat, osmotic and heavy metals (Munne-Bosch and Alegre, 2000; Collakova and DellaPenna, 2003b; Muller-Moule et al., 2003; Maeda et al., 2006; Abbasi et al., 2007; Collin et al., 2008). Some phenotypes of tocopherol deficient mutants are consistent with an important role for tocopherols in controlling lipid peroxidation, however in many cases the lack of expected phenotypes consistent with enhanced oxidative stress in tocopherol deficient mutants indicates long held assumptions about the role and function(s) of these compounds in plants are erroneous (Porfirova et al., 2002; Havaux et al., 2005; Kanwischer et al., 2005; Abbasi et al., 2007). For instance, the absence of enhanced lipid peroxidation in *Arabidopsis vite2* plants indicates the photoprotective role of tocopherols is limited and studies indicate many functions of tocopherols may be both stress- and species-specific. However, one common phenotype shared by maize (*sxd1*), potato (VTE1-RNAi) and *Arabidopsis (vite2 ad vite1)* tocopherol deficient lines is disruption in photoassimilate transportation from the source leaves to sink tissues (Russin et al., 1996; Provencher et al., 2001; Hofius et al., 2004; Maeda et al., 2006). This common phenotype between dicotyledous and monocotyledous species suggests that tocopherols are required for the development of full photoassimilate transport capacity, and this function is evolutionarily conserved. However, the mechanism of how tocopherol deficiency induces the photoassimilate export phenotype was elusive. The inducible nature of the phenotypes in *Arabidopsis* has provided a unique and ideal platform to study this aspect of tocopherol functions.

In this thesis work, a suppressor screen of EMS mutagenized *vte2* was carried out to identify second site mutations which impacted the *vte2* LT-induced phenotypes (Chapter 2, Chapter 3). Transcript profiling studies were also performed on mature plants of *vte2* and Col prior to and during LT treatment to assess the whole genome responses (Chapter 4). The unbiased approaches of both studies were aimed at identifying the molecular links between tocopherol deficiency and the *vte2* LT-induced phenotypes.

Seven *suppressors of vte2 LT-induced phenotype (sve loci)* were identified. Preliminary characterization of these primary *sve* loci has provided information for categorizing them and to prioritize and select the three most significant loci for the subsequent studies and as targets for molecular cloning.

sve1 was the strongest suppressor, had a unique fatty acid profile at permissive conditions and was found to be a novel allele of *fad2*, the endoplasmic reticulum-localized oleate desaturase. Coincidentally an independent study aiming to investigate the interactions of various PUFA species and tocopherols (Maeda et al., 2008) also identified *fad2* as a suppressor of the *vte2* LT-induced phenotype. This common finding from both physiological and genetic screen studies reinforces the importance of the ER PC-18:1 desaturation step as an important component in the development of *vte2* LT-phenotypes. The second suppressor, *sve2*, showed partial suppression and also had a fatty acid composition that differed from wild type before the LT treatment. *sve2* was found to contain a unique lipid species, trigalactosyldiacylglycerol (TGDG) and was determined to be a new allele of *trigalactosyldiacylglycerol1 (tgd1)*, a component of the ER-to-plastid lipid ATP-binding cassette (ABC) transporter. Introduction of the other available *tgd* mutations, *tgd2*, *tgd3*, and *tgd4*, into the *vte2* background similarly suppressed the *vte2*

LT phenotypes, indicating a key role for lipid transport in this process. The finding that all *tdg* mutations were *sve* suppressors indicated that the disruption of the ER-plastid lipid trafficking process is responsible for the suppression of *vte2* LT phenotypes. The identification of *sve1* and *sve2* provides clear and unbiased genetic evidence for involvement of ER PUFA/lipid metabolism in the *vte2* LT phenotype. The third *sve* locus, *sve7*, partially suppressed all *vte2* LT phenotypes, but unlike *sve1* and *tdg* mutations, had no detectable impact on fatty acid and lipid metabolism at permissive temperature. *sve7* suggests that processes other than constitutive alteration of fatty acid and lipid metabolism can also impact on the *vte2* LT phenotypes. *sve7* has not been cloned.

Maeda et al (2008) found that the lower 18:3 and higher 18:2 levels consistently observed in LT-treated *vte2* was due to a reduced conversion of 18:2 to 18:3 in ER derived lipids and lipidomics further showed that a large number of lipid species were identified to be altered in *vte2* relative to wild type. However, it was not clear from this work which lipid species alteration was critical for the development of *vte2* LT phenotypes or whether all were equally important. To gain further insight, a detailed study on the changes of the acyl composition of ER- and plastid-derived lipids in suppressors before and after LT treatment was carried out. The common biochemical phenotype shared by all *vte2* suppressing lines (i.e. *sve1*, *sve2*, *sve7*, *tdg2*, *tdg3*, *tdg4* and *vte1*) was an attenuation in the elevation of 18:2 in PC and PE that would otherwise occur in *vte2* at LT. Interestingly, when the levels of 18 carbon fatty acids in individual lipid classes were plotted against the LT photoassimilate export capacity of various genotypes, only PC-18:2 levels were found to be significantly correlated. These results indicate that

the increase in 18:2 esterified to PC plays a key role in the onset of the *vte2* LT phenotype.

ER-produced PC is a key intermediate in lipid metabolism because it is the predominant substrate for ER-localized desaturases (Arondel et al., 1992; Okuley et al., 1994), the precursor of the transport lipid molecules from ER to plastid (Ohlrogge and Browse, 1995; Mongrand et al., 2000; Andersson et al., 2004), subjected to constant acyl editing (Williams et al., 2000; Bates et al., 2007; Bates et al., 2009), and especially PC-18:2 species are the major donors of the DAG moiety for plastidic galactolipid synthesis (Slack et al., 1977; Browse et al., 1986; Somerville and Browse, 1991). Therefore it is likely that an elevated ER PC-18:2 level in LT-treated *vte2* could influence many ER-localized biochemical processes. Such suboptimal or unbalanced fatty acid acyl compositions may affect the formation and function of ER-derived vesicles and thus influence the coordinated and rapid development of transfer cell wall upon LT treatment. In this regard, mutations directly (*sve1*) or indirectly (*sve2* and all *tgd*) decreasing PC-18:2 synthesis may completely or partially restore the unbalanced PUFA composition of ER-derived lipids used for transfer cell wall development.

Global transcript profiling study comparing *vte2* and wild type plants under different time periods (0h, 48h, 120h) of LT treatment showed that tocopherol deficiency has no impact on global gene expression at permissive conditions but affects a limited number of specific genes (77 genes) after 48h of LT treatment. Gene expression profiles were consistent with a degree of oxidative stress response by *vte2* that was not reflected at the biochemical level (Maeda et al., 2006; Maeda et al., 2008). LT-treated *vte2* was also shown to have an enhancement in expression of genes involved in cell wall modification

and repression of genes related with solute transport. These responses seem to be consistent with the biochemical and physiological phenotypes observed in *vte2* at the corresponding time period of LT treatment.

The results from these biochemical, genetic and transcriptome studies are summarized in a genetic model of *vte2* LT-responses (Figure 5.1). This study has made the involvement of tocopherols in ER lipid metabolism clear but the exact mechanism of how tocopherols influence the ER lipid metabolism still remains unknown and there are many questions to be answered to further understand the involved tocopherol functions.

Is PC-18:2 elevation the root cause of the vte2 LT phenotype?

All the characterized lines in this study (*sve1*, *sve2*, *tgd2*, *tgd3*, *tgd4*, *sve7* and *vte1*) suppressed the elevation in PC-18:2 in LT-treated *vte2*. However it remains to be determined whether the PC-18:2 elevation is the root cause of the abnormal transfer cell wall development, vascular callose deposition and the other downstream *vte2* LT phenotypes. Previously the *fad3* single mutant was shown to have reduced export capacity under LT (Maeda et al., 2008), which may be due to the increased 18:2-PC level in *fad3*. If this is the case, it would mean that the PC-18:2 elevation causes the defective photoassimilate export capacity independent of tocopherol status and is a general rather than tocopherol-specific phenomenon. A 35S promoter-driven overexpressor of the ER lineolate desaturase *FAD3* was shown to have reduced 18:2 and increased 18:3 (Arondel et al., 1992) and its analysis for the photoassimilate export phenotype could be informative. Similarly introduction of 35S::*FAD3* into *vte2* and the assessment of the LT phenotype of the single and double mutants could also be informative.

Assessing the acyl composition of ER-derived lipid species in tocopherol-deficient mutants in other plant species, such as maize *sxd1* mutant will also provide an independent assessment of whether the alteration in ER lipid metabolism is a general consequence from tocopherol deficiency, although in this case, the constitutive nature of *sxd1* mutation may make data interpretation difficult.

Are tocopherols located in ER or PLAMs to affect the ER lipid metabolism and vesicle function?

One possible mechanism that tocopherols could affect the ER lipid metabolism is that they are localized to the PLAM regions or even in the ER membranes so that they have access to the ER compartment. Although there are several lines of evidence that tocopherols are present in ER-derived oil bodies in seed (Yamauchi and Matsushita, 1976; Fisk et al., 2006; White et al., 2006), it still remains to be determined if tocopherols are also distributed to extraplastidic sites in photosynthetic tissues. It might be possible to isolate PLAMs, ER and chloroplast and assess the tocopherol content in the different subcellular compartments. However such fractioning is often difficult because tocopherols are easily oxidized during fractioning and the process is also complicated with the likely contamination especially between ER and chloroplast.

General lipid peroxidation is clearly not involved in the *vte2* LT phenotypes (Maeda et al., 2008). Based on the suppressor studies, I have proposed that tocopherols influence the lipid or membrane proteins involved in lipid metabolism via their other biophysical or biochemical properties, which would likely impact processes such as vesicle function and membrane fusion in Arabidopsis transfer cells at LT (Chapter 3). It is difficult to directly test these possibilities. However, it is possible to use the combination of stable isotope

pulse labeling and ESI-MS/MS detection to evaluate the flux of phospholipid species and any alteration of acyl editing process in LT-treated *vte2*. The possible role of tocopherols in vesicle formation and function might be tested in *vte2* at other process or developmental stages which also require massive formation of vesicles, such as during the fast elongation of root.

What is the nature of the other sve loci?

The cloning of *sve1* and *sve2* has provided important insight into the mechanisms of tocopherol function. The third locus, *sve7*, has been backcrossed and characterized in detail but not yet cloned. *sve7* had an incomplete but strong suppression on all the *vte2* LT phenotypes. It would be possible to physically clone the locus by map-based cloning based on its visible and sugar phenotypes. However, the sugar accumulation phenotype has large biological variations and may be technically difficult to assess in a single plant among the segregation populations. Unlike *sve1* or *sve2*, *sve7* did not have any alteration in fatty acid composition before LT treatment. *sve7* is especially interesting as it may be involved in regulating ER lipid metabolism under LT conditions and this feature may help to narrow down the candidate genes for fine mapping process. A fourth interesting *sve* locus is *sve5*, which had partial suppression of all *vte2* LT phenotypes and an abnormal fatty acid composition before LT treatment that is distinct from that of *sve1* and *sve2*. Preliminary backcrossing work on *sve5* suggested that the fatty acid profile is tightly linked to the suppression mutation (data not shown) and thus it may also be possible to map and clone this locus based on its fatty acid profile. Map-based cloning of *sve7* and *sve5* will be pursued by others in the lab after my departure.

How to validate the results from microarray analysis and identify tocopherol target genes?

Studies of global transcript profiling comparing LT-treated *vte2* and wild type have highlighted several potentially important target genes for future studies. Several experiments are ongoing to test the roles of some of these genes.

Although lacking direct experimental evidence for the genes identified, several genes might associate with abnormal transfer cell wall development and callose deposition in *vte2*. Isolation and introduction of single mutations for the induced callose synthase genes (*gsl4*, *gsl11*) into *vte2* background did not yield a clear impact on the *vte2* LT phenotype, but this may be due to genetic redundancy and generation and analysis of the triple mutant (*gsl4gsl11vte2*) and double mutants with other callose synthase genes will further provide information in this regard.

In addition, analysis of differentially expression genes between *vte2* and Col found that six cell wall related genes were induced in 48h-LT-treated *vte2* and subsequent promoter analysis further identified the presence of W-box motif in their promoter regions. It would be interesting to investigate whether the WRKY transcription factors are regulators involved in cell wall modification of transfer cells. WRKY 75 showed the strongest induction among the three induced WRKY factors. The possible regulating roles of WRKY75 involved in *vte2* LT-induced phenotype is being tested by evaluating the phenotypes of homozygous *wrky75* and the double mutant of *wrky75vte2* at both permissive and LT conditions.

Transcript profiling suggested that some degree of oxidative stress response might occur in LT-treated *vte2*, with *MSRB5* being significantly repressed in 48h-LT-treated

vte2 relative to Col. Transcriptional repression of this antioxidant repair enzyme may lead to oxidation and malfunction of certain proteins and it would be interesting to assess protein oxidation in LT-treated *vte2*. The *msrb5* and *msrb5vte2* double mutant have been generated and their roles in seedling germination and plant LT adaptation will be tested.

Enhanced endomembrane biogenesis and the deposition of callose and abnormal cell wall ingrowths were only observed in the phloem parenchyma transfer cells of LT-treated *vte2* and is a remarkably cell type-specific response. In this regard it would be most useful to isolate transfer cells by laser-microscopy dissection to evaluate the expression or apply the *in situ* hybridization to localize the expression of the more interesting genes already identified. Such studies may be able to help identify the transcriptional elements linking tocopherol deficiency and the manifested LT phenotypes in *vte2* and lead to further understanding on tocopherol functions.

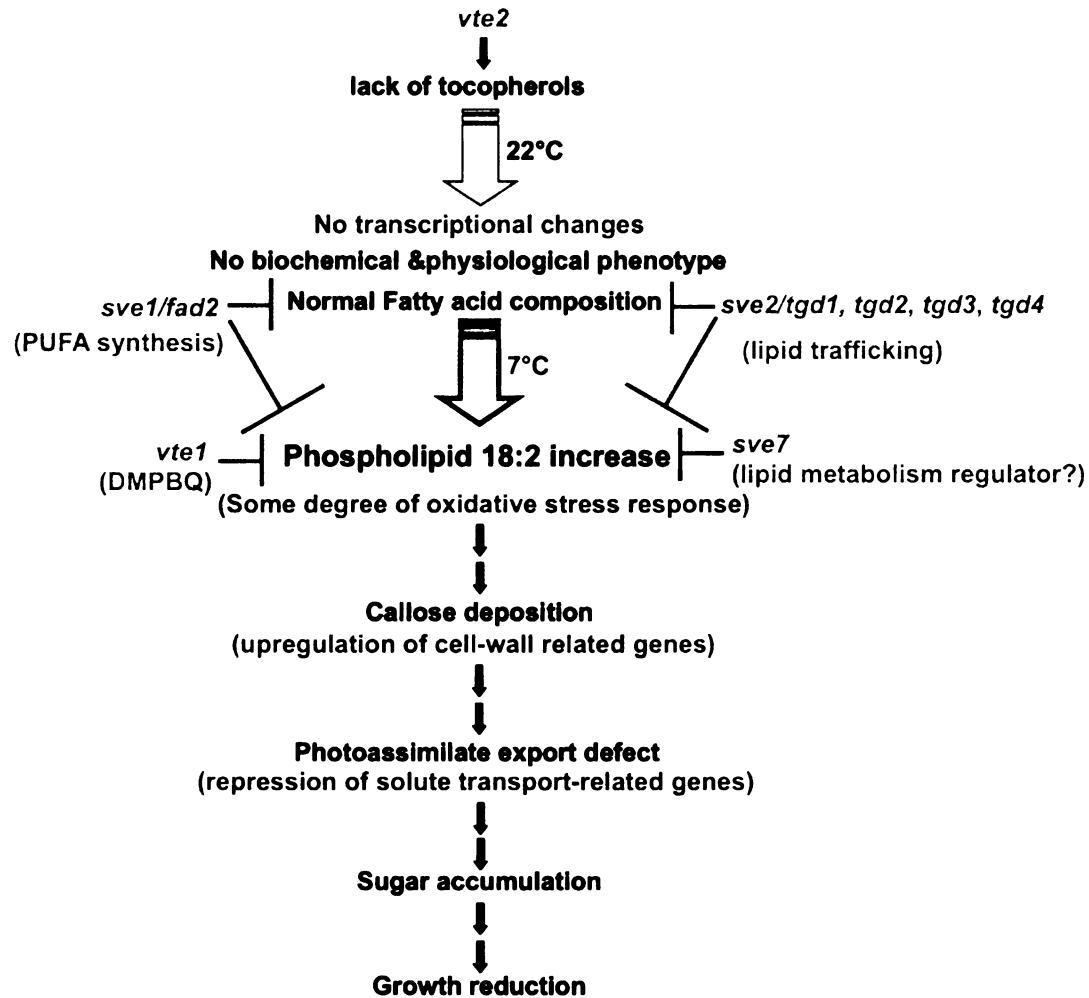


Figure 5.1 A genetic model of *vte2* responses under LT treatment.

The biochemical and physiological responses are in black lettering, transcriptional changes are in green lettering and the suppressors and the (potential) involved process are in red lettering. 22°C and 7°C represents permissive and low temperature conditions, respectively. The *vte2* LT responses are connected with double arrows to indicate multiple steps from one response to the other.

APPENDIX

TOCOPHEROLS PLAY A CRUCIAL ROLE IN LOW TEMPERATURE ADAPTATION AND PHLOEM LOADING IN *ARABIDOPSIS*

The work presented in this section has been published:

Hiroshi Maeda, Wan Song, Tammy L. Sage and Dean DellaPenna

(2006) *Plant Cell* **18**, 2710-2732.

Author's contributions:

Hiroshi Maeda led all the physiological and biochemical assessment except for the diurnal carbohydrate and TEM analyses, which were performed independently by Wan Song and Tammy L. Sage, respectively. Wan Song and Tammy L. Sage also contributed to writing the method part for carbohydrate analysis, and the method and result portion of TEM microscopy analysis. Wan Song also participated the assessment of various biochemical and physiological parameters, including long-term carbohydrate, anthocyanins, tocopherols, carotenoids, lipid peroxides, and maximum photosynthesis efficiency (F_v/F_m) and quantum yield of PSII (Φ_{PSII}). Dean DellaPenna supervised the entire project and involved in all aspects of manuscript writing.

ABSTRACT

To test whether tocopherols (vitamin E) are essential in protection against oxidative stress in plants, a series of *Arabidopsis* *vitamin E* (*vte*) biosynthetic mutants that accumulate different types and levels of tocopherols and pathway intermediates were analyzed under abiotic stress. Surprisingly subtle differences were observed between the tocopherol-deficient *vte2* mutant and wild type during high light, salinity and drought stresses. However, *vte2*, and to a lesser extent *vte1*, exhibited dramatic phenotypes under low temperature, i.e., elevated anthocyanin levels and reduced growth and seed production. That these changes were independent of light level and occurred in the absence of photoinhibition or lipid peroxidation suggests the mechanisms involved are independent of tocopherol functions in photoprotection. Compared to wild-type, *vte1* and *vte2* had reduced rates of photoassimilate export as early as 6 h into low temperature treatment, elevated soluble sugar levels by 60 h, and increased starch and reduced photosynthetic electron transport rate by 14 days. The rapid reduction in photoassimilate export in *vte2* coincides with callose deposition exclusively in phloem parenchyma transfer cell walls adjacent to the companion cell/sieve element complex. Together these results indicate that tocopherols have a more limited role in photoprotection than previously assumed but play crucial roles in low temperature adaptation and phloem loading.

INTRODUCTION

Tocopherols are the best-studied class of lipid soluble antioxidants and are produced only by photosynthetic organisms including all plants and algae, and some cyanobacteria. Structurally, all four tocopherols (α , β , γ and δ -tocopherols) consist of a chromanol head group attached to a phytyl tail and differ only in the number and positions of methyl groups on the chromanol ring (Figure A.1). Tocopherols are amphiphatic molecules and *in vitro* studies using artificial membranes have shown that tocopherols form complexes with specific lipid constituents and physically stabilize membranes (Wassall et al., 1986; Stillwell et al., 1996; Wang and Quinn, 2000; Bradford et al., 2003). Tocopherols can efficiently quench singlet oxygen, scavenge various radicals, particularly lipid peroxy radicals, and thereby terminate lipid peroxidation chain reactions (Liebler and Burr, 1992; Bramley et al., 2000; Schneider, 2005). In animals, vitamin E deficiency results in muscular weakness and neurological dysfunction, which often coincide with elevated lipid peroxidation (Machlin et al., 1977; Yokota et al., 2001). Recent studies have shown that tocopherols also have functions in animals unrelated to their antioxidant activity, such as modulation of cell signaling and transcriptional regulation (Ricciarelli et al., 1998; Jiang et al., 2000; Rimbach et al., 2002; Kempna et al., 2004).

In contrast to the extensive studies of tocopherol functions in animals, we are only beginning to understand tocopherol functions in the photosynthetic organisms in which they are produced. In plants, tocopherols are synthesized and localized in plastid membranes that are also highly enriched in polyunsaturated fatty acids (PUFA) (Bucke, 1968; Soll et al., 1980c; Lichtenthaler et al., 1981; Soll et al., 1985; Soll, 1987; Vidi et al., 2006) and increased tocopherol content has been correlated in the response of

photosynthetic tissues to a variety of abiotic stresses, including high intensity light (HL), salinity, drought and low temperatures (Keles and Oncel, 2002; Bergmuller et al., 2003; Collakova and DellaPenna, 2003b). Such data, together with the evolutionary conservation of tocopherol synthesis among photosynthetic organisms, has led to the assumption that a primary function of tocopherols is to protect photosynthetic membranes from oxidative stresses by acting as lipid-soluble antioxidants (Foyer et al., 2002; Munne-Bosch and Alegre, 2002). While plausible, such hypotheses are based primarily on correlations and circumstantial evidence and have yet to be rigorously tested *in planta*. The isolation of *Arabidopsis* mutants disrupting steps of the tocopherol biosynthetic pathway provides powerful tools to directly investigate tocopherol functions in plants (Figure A.1) (Shintani and DellaPenna, 1998; Collakova and DellaPenna, 2001; Porfirova et al., 2002; Cheng et al., 2003; Sattler et al., 2003a).

The *vt2* (*vitamin E 2*) mutant is defective in homogentisate phytyl transferase (HPT) and lacks all tocopherols and pathway intermediates (Figure A.1, Table A.1). *vt2* mutants are severely impaired in seed longevity and early seedling development due to the massive and uncontrolled peroxidation of storage lipids (Sattler et al., 2004), consistent with loss of the lipid-soluble antioxidant functions of tocopherols (Ham and Liebler, 1995, 1997). Interestingly, the *vt2* mutants that do survive early seedling development become virtually indistinguishable from wild type under standard growth conditions (Sattler et al., 2004), suggesting that unlike seed longevity and germination, tocopherols are dispensable in mature plants in the absence of stress. Consistent with this, constitutive over-expression of *VTE2* in *Arabidopsis* increased total leaf tocopherols 4.5-fold but had no discernible effect relative to wild type on plant growth or chlorophyll and

carotenoid content in the absence of stress or under combined nutrient and HL stress (Collakova and DellaPenna, 2003b).

The *vte1* mutant is defective in tocopherol cyclase activity and deficient in all tocopherols but unlike *vte2*, accumulates the redox active biosynthetic intermediate 2,3-dimethyl-6-phytyl-1,4-benzoquinol (DMPBQ) (Figure A.1, Table A.1, (Sattler et al., 2003a). When grown at 100 to 120 $\mu\text{mol photon m}^{-2} \text{s}^{-1}$ *vte1* plants are virtually identical to wild type at all developmental stages (Porfirova et al., 2002; Sattler et al., 2003a; Sattler et al., 2004). The lipid peroxidation phenotype observed in germinating *vte2* seedlings was not observed in *vte1* indicating the DMPBQ can fully compensate for tocopherols as a lipid-soluble antioxidant in seedlings (Sattler et al., 2004). Under HL stress (5 days at 850 $\mu\text{mol photon m}^{-2} \text{s}^{-1}$; (Porfirova et al., 2002) or a combination of low temperature and HL stress (5 days at 6 to 8°C and 1100 $\mu\text{mol photon m}^{-2} \text{s}^{-1}$) (Havaux et al., 2005), *vte1* was nearly identical to wild type for all parameters measured, including lipid peroxidation, with the exception of a slight decrease in maximum photosynthetic efficiency (Fv/Fm). Only under extreme conditions (24 h at 3°C and continuous 1500-1600 $\mu\text{mol photon m}^{-2} \text{s}^{-1}$) did *vte1* show a more rapid induction of lipid peroxidation than wild type, although this difference was transient and after 48 h of treatment lipid peroxidation was similarly elevated in *vte1* and wild type (Havaux et al., 2005). These studies with *vte1* and *vte2* mutants suggest that a primary function of tocopherols is to control non-enzymatic lipid oxidation, especially during seed storage and early germination, and also probably in photosynthetic tissues but only under the most extreme of combined HL and low temperature stress.

Interestingly, a maize tocopherol cyclase mutant (*sxd1*, *sucrose export defective 1*) was identified several years prior to the identification of *Arabidopsis vte1*, not due to its impact on tocopherol synthesis, but because of accumulation of carbohydrates and anthocyanins in *sxd1* source leaves, which coincided with aberrant plasmodesmata between the bundle sheath and vascular parenchyma cells (Russin et al., 1996). Cloning of the *SXD1* locus did not provide insight into the biochemical activity of the nuclear-encoded chloroplast-localized protein (Provencher et al., 2001) and it is only in retrospect that *SXD1* has been demonstrated to have tocopherol cyclase activity (Porfirova et al., 2002; Sattler et al., 2003a). The maize *sxd1* carbohydrate accumulation phenotype was intriguing as it suggested an unexpected link between the tocopherol pathway and primary carbohydrate metabolism, though the mechanism involved was unclear. A similar carbohydrate phenotype did not occur in the orthologous *Arabidopsis vte1* mutant (Sattler et al., 2003a) but was observed in *VTE1* RNAi knock-down lines in potato (Hofius et al., 2004).

In the current study, we further define and clarify the physiological role(s) of tocopherols in photosynthetic plant tissues by subjecting and analyzing the response of a suite of *Arabidopsis* tocopherol mutants to a variety of abiotic stresses. We report that in contrast to long-held assumptions about tocopherol functions in plants, tocopherol-deficient mutants are remarkably similar to wild type in their response to most abiotic stresses with the notable exception being an increased sensitivity to non-freezing low temperatures. Detailed physiological, biochemical and ultrastructural data demonstrate that the earliest impact of tocopherol deficiency during low temperature treatment is an inhibition of photoassimilate transport associated with dramatic structural changes in

phloem parenchyma transfer cells, a bottleneck for photoassimilate transport. The resulting accumulation of carbohydrates in source leaves impacts the physiology and response of the entire plant to low temperatures.

RESULTS

Tocopherol Biosynthetic (vte) Mutants Used in This Study

vte1-1, *vte1-2* and *vte2-1* are previously isolated and characterized ethyl methanesulfonate mutants in the Columbia (Col) ecotype that are deficient in the tocopherol cyclase and HPT enzymes, respectively (Sattler et al., 2003a; Sattler et al., 2004); Figure A.1). *vte2-2* and *vte4-3* are T-DNA insertion mutants in the Wassilewskija (Ws) ecotype in genes encoding HPT and γ -tocopherol methyltransferase (γ -TMT), respectively. Leaves of all mutants, *vte2-1*, *vte2-2*, *vte1-1*, *vte1-2* and *vte4-3*, lack α -tocopherol, the major tocopherol in wild type *Arabidopsis* leaves (Figure A.1, Table A.1, (Sattler et al., 2003a). *vte2-1* and *vte2-2* lack all tocopherols and pathway intermediates. *vte1-1* and *vte1-2* lack all tocopherols but accumulate the biosynthetic pathway intermediate DMPBQ at a level comparable to α -tocopherol in Col. The *vte4-3* mutant accumulates γ -tocopherol at an equivalent or slightly higher level than α -tocopherol in Ws. Three to five-week-old plants of all mutant genotypes grown under permissive conditions (12 h 120 $\mu\text{mol photon m}^{-2} \text{s}^{-1}$ light at 22°C /12 h darkness at 18°C) were virtually identical to their respective wild type backgrounds, consistent with previous reports that mutations disrupting tocopherol synthesis have little impact on the normal growth of mature plants (Porfirova et al., 2002; Bergmuller et al., 2003; Sattler et al., 2003a; Sattler et al., 2004).

The Response of Tocopherol-Deficient Mutants to High Intensity Light Stress

High intensity light (HL) stress results in excessive excitation of chlorophyll and consequently generates reactive oxygen species (ROS), which in turn attack various biochemical targets in the cell including PUFA-enriched photosynthetic membranes. Tocopherols are most abundant in these photosynthetic membranes (Bucke, 1968; Lichtenthaler et al., 1981; Soll et al., 1985) and leaf tocopherol levels increase up to 18-fold during HL stress in *Arabidopsis* (Collakova and DellaPenna, 2003b; Havaux et al., 2005). Therefore, it has been presumed that the elimination of tocopherols from photosynthetic membranes would have dramatic impacts on plant survival during HL stress. To test this hypothesis, Col, *vte2-1*, *vte1-1*, and *vte1-2* were grown for four weeks under permissive conditions and then subjected to two levels of HL stress, 1000 and 1800 $\mu\text{mol photon m}^{-2} \text{s}^{-1}$ 16 h light/ 8 h darkness at 22°C (hereafter referred to as HL1000 and HL1800, respectively). HL1000 did not result in differential visible or biochemical phenotypes between *vte2-1* and Col (Figure A.14). When Col, *vte2-1*, *vte1-1* and *vte1-2* were subjected to HL1800, which approaches the intensity of full sunlight, this led to bleaching of some mature leaves in all genotypes. *vte2-1* had a slight tendency toward more bleached leaves than Col but this was not reproducible or significant, while *vte1-1* and *vte1-2* reproducibly had as many or more bleached mature leaves than Col or *vte2-1* (Figure A.2A and Figure A.15). *vte2-2* and *vte4-3* subjected to HL1800 responded similarly to Ws, the corresponding wild type (data not shown).

To assess changes in photosynthetic pigment and tocopherol levels in response to HL stress, the 7th to 9th oldest leaves were harvested before and after 4 days of HL1800 for HPLC analysis. Before HL1800 all levels were similar between genotypes except for

slightly lower β -carotene content in *vte2-1* and *vte1-1* relative to Col and the absence of tocopherols in all *vte* genotypes (Table A.4). After 4 days of HL1800, the *vte* mutants generally had lower total and individual chlorophyll levels than Col but these differences were not significant in all cases after 4 days of HL1800, even with $n = 19$ (Figure A.2B, Table A.2, Figure A.15). Total carotenoids were consistently and significantly lower than Col in *vte1-1* and *vte1-2*, but not always in *vte2-1* after 4 days of HL1800. Neoxanthin and violaxanthin were significantly lower in all *vte* mutants, while lutein was significantly lower only in *vte1-1* and *vte1-2*. Interestingly, zeaxanthin was 70 % higher than Col in *vte2-1* but unchanged relative to Col in both *vte1* alleles (Table A.2).

In vivo chlorophyll *a* fluorescence was also analyzed to assess PSII function during HL stress. Typically, when plants are under oxidative stress, PSII is inactivated due to enhanced turnover of the D1 protein, a process termed photoinhibition, and maximum photosynthetic efficiency (Fv/Fm) decreases (Maxwell and Johnson, 2000). Four-week-old Col, *vte2-1*, *vte1-1* and *vte1-2* plants grown under permissive conditions had identical Fv/Fm values of between 0.8 and 0.85, typical values for healthy leaves (Maxwell and Johnson, 2000) (data not shown). After 24 h of HL1800 (8 h HL1800, 8h darkness, and 8h HL1800), a few *vte2-1* leaves showed a dramatic reduction in Fv/Fm (< 0.5), but the majority had values similar to Col and the average Fv/Fm of *vte2-1* was not significantly different from Col, even with $n = 30$ (Figure A.2D, Figure A.15). In contrast, *vte1-1* and *vte1-2* both had more leaves with Fv/Fm < 0.5 and average Fv/Fm values that were significantly lower than Col (Figure A.2D, Figure A.15).

These combined results indicate that the elimination of tocopherols in *vte2* has surprisingly little impact on the response of the photosynthetic apparatus to HL stress in

comparison to Col, with the exception of altered xanthophyll cycle carotenoids. Equally surprising is the fact that though the *vte2* and *vte1* genotypes are identical with regard to their tocopherol deficiencies, *vte1* alleles are slightly more susceptible to HL1800 than *vte2*. As the primary biochemical difference between these two genotypes is that *vte1* mutants accumulate the redox active intermediate DMPBQ while *vte2* mutants do not, the presence of DMPBQ in *vte1* may have negative impacts on HL stress tolerance in *Arabidopsis*.

Tocopherol-Deficient Mutants Exhibit a Low Temperature Sensitive Phenotype.

In searching for a condition that more obviously impacts wild type and the tocopherol-deficient mutants in a differential fashion, *vte2-1* and Col plants were subjected to abiotic stress treatments other than HL, including salinity (100, 150 and 200 mM NaCl), drought, and various low temperature treatments. Like HL stress, the salinity and drought stress conditions used also did not result in obvious phenotypic differences between *vte2-1* and Col (Figure A.14) and further analyses will be required to determine any consequences of tocopherol-deficiency during these stresses. However, when plants were transferred from permissive conditions to non-freezing low temperature conditions, both *vte2-1* and *vte2-2* grew more slowly than their respective wild types, Col and Ws, and their mature leaves changed color to purple (Figure A.3). These phenotypic differences were consistently observed in conditions ranging from 3 to 12°C and light intensities from 15 to 200 $\mu\text{mol photon m}^{-2} \text{s}^{-1}$ (data not shown). Differences were most obvious and consistent under 7.5°C, 12 h 75 $\mu\text{mol photon m}^{-2} \text{s}^{-1}$ light/12h darkness (Figure A.3) and this low temperature regime (hereafter termed 7.5°C-treated) was used

for all subsequent experiments.

Following transfer to 7.5°C, *vte2-1* and Col did not differ in time to bolting (53 ±4 and 51 ±3 days, respectively, after transfer to 7.5°C) or number of leaves produced at the start of bolting (32 ±3 and 31 ±2 leaves, respectively), indicating that the process of vernalization was not affected by the lack of tocopherols. However, after prolonged growth at 7.5°C *vte2-1* siliques were shorter, produced significantly fewer seeds per silique and per plant compared to Col, and 35 % of the seeds in *vte2-1* siliques were aborted compared to less than 1 % in Col siliques (Figure A.3E, Table A.3). These results indicate tocopherols play a crucial role in low temperature adaptation in *Arabidopsis*.

Subjecting *vte1-1* to 7.5°C treatment resulted in a phenotype intermediate between *vte2-1* and Col in terms of overall growth, mature leaf color, silique size, number of seeds/silique, percentage of aborted seed, and seed yield per plant (Figure A.3, Table A.3). These phenotypes in 7.5°C-treated *vte4-3* were virtually indistinguishable from wild type (Ws) (Figure A.3A, Figure A.3B and Figure A.3C). These results indicate that during low temperature adaptation in *Arabidopsis* the quinol biosynthetic intermediate DMPBQ partially compensates for the lack of tocopherols in *vte1-1* while the γ -tocopherol accumulated in *vte4-3* leaves can functionally replace α -tocopherol in this regard.

Photooxidative Damage Is Not Associated with the vte2 Low Temperature Phenotype

To further examine changes during the time course of 7.5°C treatment, *vte2-1* and Col were subject to detailed comparative biochemical analyses. Plants grown for four weeks at permissive conditions were transferred to 7.5°C conditions and the 7th to 9th oldest fully expanded rosette leaves were harvested at various time points for analyses.

The tocopherol content in Col started to increase after 3 days of 7.5°C treatment reaching levels five-fold higher than initial levels by 28 days, while *vte2-1* lacked tocopherols at all time points (Figure A.4A).

Consistent with the purple color of mature leaves of 7.5°C-treated *vte2* mutants (Figure A.3B), *vte2-1* accumulated significantly higher level of anthocyanins than Col after 14 days of 7.5°C (Figure A.4D). In Col anthocyanins were detected only at 7 days. Because anthocyanin accumulation is often associated with plant responses to stress (Leyva et al., 1995; Chalker-Scott, 1999) and tocopherols are well-characterized lipid-soluble antioxidants in animals (Ham and Liebler, 1995, 1997), it seemed plausible that elevated lipid peroxidation might be occurring in *vte2-1* during low temperature treatment. However, the lipid peroxide levels of *vte2-1* and Col analyzed by the ferrous oxidation xylenol orange (FOX) assay were found to be similar and near background levels at all time points (Figure A.4B), indicating that the observed phenotypic differences between 7.5°C-treated *vte2-1* and Col are not associated with a detectable increase in lipid peroxidation.

Given the reported localization of tocopherols and tocopherol biosynthetic enzymes to plastids (Bucke, 1968; Soll et al., 1980c; Lichtenthaler et al., 1981; Soll et al., 1985; Soll, 1987), it seems reasonable to hypothesize that tocopherol deficiency might affect the components and function of the photosynthetic apparatus during 7.5°C treatment. Under permissive growth conditions, the levels of individual and total photosynthetic pigments (chlorophylls and carotenoids) were nearly identical in *vte2-1* and Col (Figure A 4C and Figure A 4E, Table A.5 at 0 day). The chlorophyll and carotenoid content of both *vte2-1* and Col changed in parallel during the first two weeks of 7.5°C treatment and

became significantly different only at 28 days (Figure A.4C and Figure A.4E, Table A.5). It is especially noteworthy that zeaxanthin, a xanthophyll cycle carotenoid that accumulates under HL stress (Muller et al., 2001), was not detectable at any time point in 7.5°C-treated Col and *vt2-1* (Table A.5), suggesting that the plants were not experiencing photooxidative stress under the low temperature conditions used.

To assess the response of the photosynthetic apparatus to 7.5°C, changes in photosynthetic parameters were analyzed. Fv/Fm was unchanged in both Col and *vt2-1* at any time point (Figure A.5A), indicating that photoinhibition is not occurring in either genotype during permissive or 7.5°C conditions. The quantum yield of PSII (Φ_{PSII}) was also identical between Col and *vt2-1* under permissive growth conditions (Figure A.5B at 0 day), suggesting that tocopherol deficiency also does not affect the efficiency of electron transport via PSII in the absence of stress (Genty et al., 1989). During the first 7 days of 7.5°C treatment, Φ_{PSII} responded identically in Col and *vt2-1*: Φ_{PSII} decreased sharply during the first day followed by a gradual recovery by 7 days. However, at 14 days the *vt2-1* Φ_{PSII} was significantly lower than Col and declined further by 28 days, while the Φ_{PSII} of Col remained stable from day 14 and onward (Figure A.5B).

Tocopherol-Deficient Mutants Accumulate Carbohydrates During Low Temperature Treatment

The reduced Φ_{PSII} in *vt2-1* after 14 days could result from feedback inhibition of photosynthesis due to the accumulation of downstream carbon metabolites (Goldschmidt and Huber, 1992; Koch, 1996; Paul and Foyer, 2001; Paul and Peliny, 2003). To assess

this possibility, starch, glucose, fructose and sucrose contents were analyzed during the time course of 7.5°C treatment. Starch represents the main plastidic carbohydrate storage pool, sucrose and fructose are cytosolic pools, while glucose is present in both subcellular compartments. Col and *vte2-1* had identical carbohydrate contents at the end of the light period under permissive growth conditions (Figure A.6 at 0 day). During the first 7 days of 7.5°C treatment starch content increased similarly in both Col and *vte2-1* to approximately 120 μmol glucose equivalents/g FW. After 7 days *vte2-1* starch content steadily increased to 680 μmol glucose equivalents/g FW while Col starch levels decreased to near initial levels (Figure A.6A). Likewise, the glucose, fructose and sucrose content of Col and *vte2-1* increased similarly during the first 3 days of low temperature treatment (Figure A.6B, Figure A.6C and Figure A.6D), likely as a component of the well-documented cold acclimation response(s) in *Arabidopsis* (Wanner and Juntila, 1999; Taji et al., 2002). After 3 days, Col soluble sugar levels decreased, while *vte2-1* continued to rise reaching 35, 43 and 255 times the initial levels of glucose, fructose and sucrose, respectively, after 28 days of low temperature treatment. The timing of the increase and accumulation of carbohydrates in *vte2-1* is consistent with this being the root cause of the reduction in Φ_{PSII} observed after 14 days at 7.5°C (Figure A.5B).

To further investigate any differences in carbohydrate accumulation between *vte2-1* and Col during the initial 5 days of low temperature treatment, diurnal changes in carbohydrate content were analyzed one hour before the end of the light and dark cycles. During the 25 h prior to low temperature treatment (Figure A.7; -25 h, -13 h and -1 h, with 0 h being the transfer of plants to low temperature at the start of the light cycle), starch, glucose, fructose and sucrose content were identical in *vte2-1* and Col. These data

indicate the lack of tocopherols does not have a significant impact on carbohydrate metabolism under permissive growth conditions. Following transfer to low temperature the soluble sugar content increased similarly in *vte2-1* and Col for the first two diurnal cycles with significant differences first being observed between genotypes at the end of the third low temperature light period (59 h in Figure A.7B, Figure A.7C and Figure A.7D). In contrast, starch levels did not become significantly different between genotypes until 14 days of low temperature treatment (Figure A.6A and Figure A.7A). The differential elevation of soluble sugars prior to starch accumulation in *vte2-1* indicates that the increase in cytosolic soluble sugars precedes starch accumulation in the chloroplast and that soluble sugars are not being efficiently metabolized or mobilized in 7.5°C-treated *vte2-1*.

The vte2 and vte1 Cold Sensitive Phenotypes Are Attenuated in Young Leaves

Mature (7th to 9th oldest) and young (13th to 16th oldest) leaves of *vte2-1* and *vte1-1* mutants showed obvious visible differences in their responses to low temperature; young leaves of *vte2-1* and *vte1-1* did not change their color to purple even after two months of 7.5°C treatment (Figure A.3C).-Consistent with this visual observations, mature leaves of *vte1-1* had an anthocyanin content 10 % that of *vte2-1* but still higher than Col, while young *vte2-1* and *vte1-1* leaves accumulated much less anthocyanins compared to their respective mature leaves after 28 days of 7.5°C treatment (Figure A.8A). Fv/Fm was above 0.8 in all cases, indicating that photoinhibition was not occurring in either young or mature leaves of any genotype (data not shown). The Φ_{PSII} of mature *vte2-1* leaves was reduced to 70 % of mature Col leaves, consistent with Figure A.5, while the Φ_{PSII} of

mature *vte1-1* leaves was only slightly decreased relative to mature Col leaves. However, the Φ_{PSII} of mature and young Col leaves and young *vte2-1* and *vte1-1* leaves were not significantly different (Figure A.8B). Levels of all carbohydrates in mature *vte2-1* leaves were greatly elevated in comparison to Col, consistent with Figure A.6. Mature *vte1-1* leaves contained intermediate levels of starch, glucose, fructose and sucrose (51, 53, 68 and 58 % of *vte2-1* levels, respectively) (Figure A.8C to Figure A.8F). Young *vte2-1* and *vte1-1* leaves contained substantially reduced starch, glucose, and sucrose levels compared to their respective mature leaves. These results indicate that the initiation and development of young *vte2-1* and *vte1-1* leaves under 7.5°C conditions attenuates the biochemical phenotypes observed in mature leaves of both genotypes and that the DMPBQ accumulated in *vte1-1* further suppresses these biochemical phenotypes in both mature and young leaves.

Tocopherol-Deficient Mutants Have Reduced Source Leaf Photoassimilate Export Capacity at Low Temperatures

The reduced seed yield (Table A.3) and attenuated carbohydrate accumulation in young leaves relative to mature leaves (Figure A.8) in 7.5°C-treated *vte2-1* suggested impaired translocation of photoassimilates from mature source tissues to young sink tissues. To test this possibility $^{14}\text{CO}_2$ labeling experiments were conducted. Col and *vte2-1* were grown on plates under permissive conditions for three weeks and then transferred to 7.5°C for an additional 7 days. Whole plants were labeled with $^{14}\text{CO}_2$ at 7.5°C, transferred to high humidity in darkness at 7.5°C for 2 h to allow for photoassimilate transport and subsequently exposed to a phosphor screen to visualize the

movement of ^{14}C labeled photoassimilate. Immediately after labeling >99% of the $^{14}\text{CO}_2$ incorporated was present in leaf tissue (data not shown). Col and *vte2-1* incorporated similar amounts of $^{14}\text{CO}_2$ into photosynthate suggesting their carbon fixation rates do not differ, consistent with the similar Φ_{PSII} within the first 7 days at 7.5°C (data not shown and Figure A.5B). Following the 2 h dark period Col had translocated 13.2 % of the ^{14}C labeled photoassimilate fixed in leaves to roots, whereas only 2.7 % was translocated in *vte2-1* (Figure A.9A). These results demonstrate that *vte2-1* translocates significantly less photoassimilate from source to sink than Col after 7 days of 7.5°C-treatment.

Impaired photoassimilate translocation in 7.5°C-treated *vte2-1* could be due to reduced sink strength or impaired photoassimilate export from source leaves (Gottwald 2000, Stitt 1996, Herbers and Sonnewald 1998). To address these possibilities, phloem exudation experiments were conducted (King and Zeevaart 1974). Col and *vte2-1* were grown for four weeks at permissive conditions and transferred to 7.5°C for an additional 0, 1, 3, or 7 days. Mature (7th to 9th oldest) leaves were excised from plants and labeled with $^{14}\text{CO}_2$. The petioles of labeled leaves were then transferred to an EDTA solution to induce phloem exudation and radioactivity in the EDTA solution was determined at various time points (King and Zeevaart, 1974). Again, total $^{14}\text{CO}_2$ fixed in mature leaves were similar in all genotypes at each time point (Figure A.9C). Prior to 7.5°C treatment (0 day), Col, *vte1-1* and *vte2-1* leaves exuded similar amounts of labeled photoassimilates, accounting for approximately 34 % of the total $^{14}\text{CO}_2$ fixed in each genotype. During 7.5°C treatment, the percent exudation by Col slightly decreased after 3

and 7 days (to 27 and 31 % of the total $^{14}\text{CO}_2$ fixed, respectively), whereas that of *vte2-1* was greatly reduced (to 11% and 4% at 3 and 7 days, respectively). Even more intriguingly, exudation in *vte2-1* was significantly lower than Col during the first day of 7.5°C treatment, which corresponds to only 6 h at 7.5°C treatment. The *vte1-1* mutant exuded 17 and 15 % of the total $^{14}\text{CO}_2$ fixed after 3 and 7 days at 7.5°C, respectively, levels intermediate between Col and *vte2-1* (Figure A.9C).

In apoplastic loaders like *Arabidopsis* sucrose is almost the exclusive translocated photoassimilate (Vanbel, 1993). To assess the chemical nature of the labeled compounds exuded from Col and *vte2-1*, phloem exudates were collected and separated by anion-exchange chromatography together with sugar standards. As shown in Figure A.9B, approximately 85 % of the label in Col and *vte2-1* exudates comigrated with the sucrose standard and 10 % with glucose/fructose standards. The high proportion of sucrose indicates that the label collected is almost entirely from phloem exudate rather than sugars from the cytosol of damaged cells.

Overall, the results obtained from $^{14}\text{CO}_2$ labeling experiments indicate that tocopherol deficiency in both *vte1-1* and *vte2-1* results in dramatically reduced capacity of photoassimilate export from source leaves in response to 7.5°C treatment. The rapidity of the reduction in photoassimilate export in 7.5°C-treated *vte2-1* strongly suggests that impairment of photoassimilate export is the root cause of the sugar accumulation phenotype observed in mature leaves of 7.5°C-treated tocopherol-deficient mutants.

Structural Changes in Low Temperature-Treated Tocopherol-Deficient Mutants

Previously, callose was reported to accumulate at the bundle sheath/vascular

parenchyma interface of the maize *sxd1* mutant and in vascular tissue of potato *VTE1*-RNAi lines, both of which are defective in tocopherol cyclase (Botha et al., 2000; Hofius et al., 2004). To determine whether callose deposition also occurs in Col, *vte2-1* and *vte1-1*, leaves were harvested at 0, 1, 3 and 13 days of 7.5°C treatment and aniline blue-positive fluorescence assessed. Under permissive conditions, aniline blue-positive fluorescence was absent or sporadic and no significant differences were observed in any genotypes. Aniline blue-positive fluorescence was also not altered in Col during the entire 7.5°C treatment period (e.g., 13 days at 7.5°C, Figure A.10C). In contrast, aniline blue-positive fluorescence strongly increased in the vascular tissue of 7.5°C-treated *vte2-1* (Figure A.10), and to a slightly lesser extent *vte1-1* (Figure A.16). In both *vte2-1* and *vte1-1*, fluorescence initially appeared in a limited number of vascular cells in the petiole as early as 6 h after transfer to 7.5°C conditions (Figures A.10D and Figures A.10F, Figures A.16A and Figures A.16B). The number of aniline blue fluorescing cells in the vasculature and their fluorescent intensity subsequently increased in an acropetal fashion in both *vte2-1* and *vte1-1* during the course of 7.5°C treatment (Figure A.10, Figure A.16). Intriguingly, the induction, intensity and acropetal spread of vasculature-specific aniline blue positive fluorescence in *vte2-1* at 7.5°C was unaffected by light levels ranging from 1 to 800 $\mu\text{mol photon m}^{-2} \text{s}^{-1}$ (Figure A.11A to Figure A.11F). Aniline blue positive fluorescence was not observed in the vasculature of Col at any light level at 7.5°C (data not shown) and was also absent from the vasculature of both Col and *vte2-1* subjected to HL1800 at 22°C for up to 4 days (Figure A.11G and Figure A.11H and data not shown).

To confirm whether or not aniline blue-positive fluorescence was cell specific and

could be attributed to callose deposition, serial sections of 0 and 14 day 7.5°C-treated Col and *vte2-1* vascular tissue were examined at the level of the transmission electron microscope (TEM). The spatial organization of cells and types of cells comprising the phloem and xylem of both Col and *vte2-1* were identical to what has been previously described for *Arabidopsis* (Haritatos et al., 2000, data not shown). Notably, at day 0 phloem vascular parenchyma cells of both Col and *vte2-1* contained transfer cell wall ingrowths adjacent to sieve elements and companion cells (e.g. Figure A.12A). 7.5°C-treatment of Col for 14 days did not result in obvious ultrastructural changes in any vascular cell type except for a noticeable increase in phloem parenchyma transfer cell differentiation and transfer cell wall deposition exclusively adjacent to sieve elements and companion cells in all vascular tissue (Figure A.12B) although to a lesser degree in the midvein.

During the same time course of 7.5°C-treatment in *vte2-1*, changes in cell fine structure occurred exclusively within the phloem parenchyma transfer cells of all vascular traces. Phloem parenchyma transfer cells in 14 day-treated *vte2-1* exhibited irregularly thickened cell wall depositions with ultrastructural features characteristic of callose (Nishimura et al., 2003); Figure A.12C to Figure A.12F). Large callosic-like masses that dissected the cell lumen corresponded in shape to aniline blue-positive fluorescent regions (compare Figure A.12C and Figure A.12E to Figures A.10F, Figures A.10I and Figures A.10L). The callosic-like wall material also formed a sheath around the cells (Figure A.12D), was deposited over transfer cell wall ingrowths (Figure A.12F) and between the end walls of adjoining transfer cells including plasmodesmata (data not shown). Immunolocalization using monoclonal antibodies against callose confirmed the

presence of callose at each location (Figure A.12G to Figure A.12J) and at plasmodesmata between the phloem parenchyma transfer cells and bundle sheath (Figure A.12K). No immunolabelling was present in controls using secondary antibody only (Figure A.12D to Figure A.12F) and immunolabelling was rare to absent in all cell types of untreated Col and *vte2-1* and in 14-day 7.5°C-treated Col, including phloem parenchyma transfer cells (e.g. Figure A.12L).

Serial sections of vascular tissue from Col and *vte2-1* treated at 7.5°C for 3 and 7 days were subsequently examined at the level of the TEM to determine the spatial and temporal development of callose deposition within phloem parenchyma cells. At 3 days, phloem parenchyma transfer cell wall deposition in Col was confined to the sieve element or companion cell boundary (data not shown) but in *vte2-1* wall deposition was present around the entire transfer cell periphery (Figure A.13A). Cell wall deposition in 3 day-treated *vte2-1* resulted in abnormally thickened and irregular shaped ingrowths with callose-like depositions adjacent to sieve elements and companion cells (Figure A.13A) that grew increasingly prominent by day 7 (data not shown). In 3-day 7.5°C-treated *vte2-1* positive immunolocalization with monoclonal antibodies to callose was present exclusively at the phloem parenchyma transfer cell wall-sieve element boundary (Figure A.13B) and included phloem parenchyma transfer cell-sieve element plasmodesmatal connections (Figure A.13C). In contrast to 14 days, plasmodesmata between bundle sheath and phloem vascular parenchyma cells in 3 day 7.5°C-treated *vte2-1* were continuous and immunonegative for callose (compare Figure A.12K and Figure A.13D).

DISCUSSION

The chemistry of tocopherols as lipid soluble antioxidants and terminators of PUFA free radical chain reactions has been well established from analyses in artificial membranes and animal-derived membrane systems (Liebler and Burr, 1992; Ham and Liebler, 1995). It has long been assumed that similar chemistry occurs in the tocopherol-containing PUFA-enriched membranes of photosynthetic organisms, and this assumption has recently been supported by studies of tocopherol deficient photosynthetic organisms (Sattler et al., 2004; Havaux et al., 2005; Maeda et al., 2005). During the first several days of germination, a period of high oxidative metabolism, *Arabidopsis vte2* seedlings contain levels of oxidized lipids >100-fold higher than wild type or *vte1*, which were indistinguishable (Sattler et al., 2004 and Sattler et al 2006). Thus, a chemical role for tocopherols (or DMPBQ in *vte1*) in limiting lipid peroxidation appears to be conserved between photosynthetic organisms and animals. By 18 days of growth the lipid peroxide levels of *vte2* seedlings had decreased to near that of wild type and *vte1* (Sattler et al., 2004) and became indistinguishable from wild type and *vte1* after four weeks of growth (Figure A.4B), consistent with tocopherols being dispensable in mature photosynthetic tissues in the absence of stress (Porfirova et al., 2002; Bergmuller et al., 2003; Sattler et al., 2003a; Sattler et al., 2004).

While a chemical role for tocopherols in controlling lipid peroxidation at specific points of the plant life cycle now seems clear, the physiological roles of tocopherols during plant stresses do not. In the current study, we have utilized a suite of *Arabidopsis vte* mutants that accumulate different types and levels of tocopherols and pathway intermediates (Table A.1) to directly assess tocopherol specific functions in photosynthetic tissues *in planta* in response to abiotic stress treatments.

A Limited Role for Tocopherols in Protecting Arabidopsis Plants from High Intensity

Light Stress.

Tocopherols have long been assumed to play crucial roles in HL protection presumably by acting as singlet oxygen quenchers and lipid peroxy radical scavengers (Fryer, 1992; Munne-Bosch and Alegre, 2002; Trebst et al., 2002). In the current study the biochemical and photosynthetic responses of the tocopherol-deficient *vte2* mutant exposed to HL1000 and HL1800 at 22°C for up to eleven days was surprisingly similar to wild type (Figure A.2, Figures A.14 and Figures A.15). Likewise, the mutation corresponding to *Arabidopsis vte2* in the cyanobacterium *Synechocystis* sp. PCC6803 (*slr1736*) had a similarly limited impact on growth and photosynthesis under permissive growth conditions and during HL stress (Collakova and DellaPenna, 2001; Maeda et al., 2005). In both organisms it is only when HL stress has been combined with other stresses, in combination with lipid peroxidation inducing chemicals in the *Synechocystis slr1736* mutant (Maeda et al., 2005) or in combination with low temperatures (2-3°C) in *Arabidopsis vte2* and *vte1* mutants that differential impacts on photosynthetic parameters or lipid oxidation are observed (Havaux et al., 2005). These combined data indicate that tocopherols are not essential for adaptation and tolerance of photosynthetic tissues subjected to HL stress alone. Such a conclusion runs counter to long-held presumptions that a primary function of tocopherols is to protect photosynthetic tissues against HL stress (Fryer, 1992; Munne-Bosch and Alegre, 2002).

One possible explanation for this surprisingly limited role of tocopherols during HL stress is that other mechanisms compensate for their absence. The zeaxanthin level of HL1800 *vte2* was nearly twice that of Col (Table A.2). *vte2* (and *vte1*) also had a higher

xanthophyll de-epoxidation state (A+Z/A+Z+V) after HL1800 treatment (Table A.2), as did *vte1* during HL stress combined with low or high temperatures (Havaux et al., 2005). Growth of a tocopherol-deficient *Synechocystis* mutant was also much more susceptible than wild type to treatment with a biosynthetic inhibitor of carotenoid synthesis during HL stress (Maeda et al., 2005). Similarly, a double mutant of *vte1* and *npq1* (*non-photochemical quenching 1*), which cannot accumulate zeaxanthin in response to HL and hence cannot induce non-photochemical quenching (Niyogi et al., 1998), was reported more susceptible than either single mutant to the combination of HL and low temperature stress (Havaux et al., 2005). Conversely, the young *npq1* leaves were also tolerant to short and long term HL stress (up to HL1800) and accumulated higher level of tocopherols than wild type (Havaux et al., 2000; Golan et al., 2006). These data suggest that tocopherols and carotenoids, particularly zeaxanthin, have overlapping functions in protecting photosynthetic organisms against HL stress.

In prior studies it was demonstrated that, although *vte1* and *vte2* are both tocopherol deficient, the two genotypes behaved quite differently during early seedling development: *vte2* exhibited a >100 fold increase in non-enzymatic lipid peroxidation during germination, whereas lipid peroxidation in *vte1* was identical to wild type (Sattler et al., 2004; 2006). In the current study *vte1* was again found to behave differently from *vte2*. In response to HL1800 stress *vte1* had a slightly, but reproducibly, higher degree of photoinhibition and higher level of photobleaching than either *vte2* or wild type (Figure A.2, Table A.2 and Figure A.15), suggesting the *vte1* mutation negatively impacts HL stress tolerance beyond its tocopherol deficiency. Why would *vte1* respond so differently from *vte2* during germination and HL1800 given that both mutant genotypes are

tocopherol deficient? The most likely explanation resides in the singularly unique biochemical feature of *vte1*: it accumulates the redox active quinol biosynthetic intermediate DMPBQ in place of tocopherols. DMPBQ is absent from *vte2* and Col (Table A.1 and Sattler et al., 2003) and its presence in *vte1* can clearly have significant, unintended experimental consequences that are independent of the tocopherol deficiency in *vte1*. Thus, when attempting to define tocopherol functions based on *vte* mutant phenotypes one must be careful to delineate genuine tocopherol functions, which would occur in both *vte1* and *vte2*, from potentially confounding artifacts due to the presence of DMPBQ, which would only occur in *vte1*. Such DMPBQ-dependent artifacts can have negative (HL1800), positive (seedling germination) or partially positive (low temperature adaptation) consequences depending on the treatment condition and phenotype assessed. These concerns are not relevant for *vte2*.

Arabidopsis Tocopherol-Deficient Mutants Exhibit a Cold Sensitive Phenotype Independent of Photooxidative Damage

In contrast to the equivocal results of HL, salinity and drought stress treatments with tocopherol-deficient photosynthetic organisms (Figure A.2, Figure A.14 and Figure A.15, (Porfirova et al., 2002; Havaux et al., 2005; Maeda et al., 2005)), both tocopherol-deficient *vte1* and *vte2* genotypes were found susceptible to non-freezing low temperature treatments in comparison to their respective wild types (Figure A.3). These results clearly indicate that tocopherols play a critical role in the responses of mature *Arabidopsis* plants to non-freezing low temperatures. Given the well-defined role of tocopherols as lipid soluble antioxidants, we initially hypothesized that tocopherol-deficiency at low temperature would result in increased photooxidative damage relative to wild type and

that this might lead to the low temperature sensitive phenotype observed in *vte2*. However, the hallmarks of photooxidative stress and photoinhibition: decreased Fv/Fm and chlorophyll levels and increased zeaxanthin accumulation and lipid peroxidation (Havaux and Niyogi, 1999; Maxwell and Johnson, 2000; Broin and Rey, 2003) were not observed during the first two weeks of low temperature treatment (Figure A.4B, Figure A.4C, Figure A.5A, and Table A.5), the timeframe during which the *vte2* carbohydrate accumulation phenotype fully develops (Figure A.6 and Figure A.7). Likewise, Φ_{PSII} , though altered by low temperature, was identical between wild type and *vte2* during the first week of low temperature treatment (Figure A.5B). These data indicate that the tocopherol-deficiency has no discernable impact on photosynthesis under the low temperature conditions used and that the low temperature sensitive phenotype of *vte2* is not associated with increased photooxidative damage or photoinhibition due to the absence of tocopherols.

Tocopherols Are Required for Photoassimilate Export from Source Leaves During Low Temperature Adaptation

A well-documented response of plants to low temperatures is the accumulation of soluble sugars and other osmoprotectants, which are critical components for the process of cold acclimation leading to freezing tolerance (Wanner and Junttila, 1999; Gilmour et al., 2000). The subsequent recovery of photosynthesis and sucrose metabolism is an important component of low temperature adaptation in that it provides carbon to sustain growth under low temperatures (Strand et al., 1997; Strand et al., 1999). During the first two days of low temperature treatment, soluble sugar levels increased similarly in both *vte2* and wild type (Figure A.7), suggesting tocopherols have little impact on the initial

accumulation of soluble sugars in response to low temperature. However, the accumulation of sucrose and other soluble sugars was much higher in *vte2* than wild type after 60 h of low temperature treatment (Figure A.7B - Figure A.7D), although the rates of photosynthesis and carbon fixation were indistinguishable between the two genotypes until 14 days at low temperature (Figure A.4B and Figure A.9C). *vte2* also reduced soluble sugar levels more slowly at night than wild type after 3 days of low temperature treatment (Figure A.7B- Figure A.7D). These results suggest that tocopherol deficiency affects carbohydrate utilization/mobilization rather than the supply of fixed carbon from photosynthesis during low temperature adaptation.

¹⁴CO₂-labeling experiments demonstrated that in comparison to wild type, low temperature-treated *vte2* translocated significantly less ¹⁴C-labeled photoassimilates from leaves (source tissue) to roots (sink tissue, Figure A.9A). The long distance transport of photoassimilates occurs through phloem and the transport rate is determined either by the rate of export from source leaves to phloem (loading) or by removal into sink tissues (unloading) (Vanbel, 1993; Stitt, 1996; Herbers and Sonnewald, 1998). Phloem exudation experiments with excised leaves showed that *vte2* source leaves exported significantly less ¹⁴C labeled photoassimilates than wild type as early as 6 h following transfer to low temperature (Figure A.9C). The rapidity of this reduction in photoassimilate export in comparison to the elevated sugar accumulation in *vte2* starting at 60 h (compare Figure A.9 and Figure A.7) indicates that impaired photoassimilate export is an early, upstream event in the *vte2* low temperature phenotype and the likely root cause of the elevated sugar accumulation in low temperature-treated *vte2*. Taken together, these analyses demonstrate that tocopherols are required for proper regulation of photoassimilate export

from source leaves and thereby play a critical role in low temperature adaptation in *Arabidopsis*.

Previous studies of the maize *sxd1* mutant and potato *VTE1*-RNAi lines (both affecting tocopherol cyclase activity) had suggested a linkage between carbohydrate metabolism and tocopherol biosynthesis, as in both cases carbohydrates accumulated to high levels in mature leaves at normal growth temperatures (19 to 30°C, (Russin et al., 1996; Provencher et al., 2001; Hofius et al., 2004). The absence of this phenotype in *Arabidopsis vte1* and *vte2* at 22°C raised questions of the universality of any interaction between tocopherol synthesis and carbohydrate metabolism (Sattler et al., 2003a), Figure A.6 and Figure A.7 at 0 day). We now know that tocopherol-deficient *Arabidopsis* mutants do indeed exhibit a phenotype that is analogous to *sxd1* but which is inducible only at low temperatures. Thus, the linkage between tocopherol biosynthesis and carbohydrate metabolism is conserved among all tocopherol-deficient mutants identified in higher plants to date (maize *sxd1*, potato *VTE1*-RNAi and low temperature-treated *Arabidopsis vte1* and *vte2*).

Although the maize *sxd1* mutant and potato *VTE1*-RNAi line suggested tocopherol chromanol ring cyclization was somehow related to regulation of carbohydrate metabolism, it was unclear whether the phenotype was due to the lack of tocopherols or accumulation of the redox active quinol intermediate DMPBQ (Sattler et al., 2003a; Hofius et al., 2004). Analysis of the full suite of *Arabidopsis vte* mutants now allows a conclusive answer to this question. Given that *vte2* lacks DMPBQ (Table A.1) and exhibits a more severe carbohydrate accumulation phenotype than *vte1* (Figure A.8), we can conclude that it is the absence of tocopherols rather than accumulation of DMPBQ

that causes the carbohydrate accumulation phenotype. The reduced severity of the carbohydrate accumulation phenotype in *vte1* suggests that DMPBQ partially suppresses the low temperature-inducible *vte2* carbohydrate accumulation phenotype.

Tocopherol Deficiency Results in a Cell Specific Response by Phloem Parenchyma

Transfer Cells at Low Temperature

The carbohydrate accumulation phenotype of maize *sxd1* was reported to be associated with altered structural features within vascular tissue. Plasmodesmata at the *sxd1* bundle sheath/vascular parenchyma boundary were reported occluded by wall materials (Russin et al., 1996; Provencher et al., 2001) and subsequently suggested to correspond to aniline blue-positive fluorescence (Botha et al., 2000). This structural aberration in *sxd1* plasmodesmata was posited to be the basis of the *sxd1* carbohydrate accumulation phenotype because it would lead to a block in the symplastic movement of photoassimilate. Callose was also observed in vascular tissue of potato *VTE1*-RNAi plants by light microscopy with monoclonal antibodies against β -1,3 glucan (Hofius et al., 2004). In the absence of high-resolution microscopy, Hofius et al. (2004) also suggested this vascular-associated callose somehow interrupts photoassimilate transport. However, in both the *sxd1* and potato *VTE1*-RNAi studies it was impossible to determine whether callose deposition was a cause or effect of carbohydrate accumulation. A critical observation from the present study is that the low temperature-inducible photoassimilate export defect in *Arabidopsis* tocopherol-deficient mutants is temporally associated with callose deposition in a specific vascular tissue cell type (compare Figure A.9C and Figure A.10). These results are significant as they provide a direct link between defective photoassimilate export and callose deposition (or events tightly associated with callose

deposition) in tocopherol-deficient mutants and exclude the possibility that callose deposition is a secondary effect caused by carbohydrate accumulation.

The low temperature-inducible callose deposition in *Arabidopsis vte2* selectively occurred in phloem parenchyma transfer cells (Figure A.12 and Figure A.13). Importantly, initial callose deposition was site specific within these cells and resulted in a callose boundary between the phloem parenchyma transfer cell and sieve element/companion cell complex where transfer cell wall ingrowths occur (Figure A.13). We saw no evidence of callose deposition or occlusion of plasmodesmata at the bundle sheath-vascular parenchyma boundary during induction of the export defective phenotype in *vte2* (e.g., 3 days of low temperature treatment, Figure A.13D). However, by 14 days of low temperature treatment, when *vte2* contains high levels of starch and anthocyanins (Figure A.4D and Figure A.6A) and more closely resembles the phenotype of maize *sxd1*, the entire parenchyma transfer cell became encased in a callose sheath associated with abnormally shaped transfer cell wall ingrowths and it is at this point that callose deposition is also observed in *vte2* plasmodesmata at the bundle sheath-vascular parenchyma boundary (Figure A.12K). When one compares the development, polarity and morphology of transfer cell walls in 7.5°C-treated *vte2* with Col (e.g. compare Figure A.12G and Figure A.12L), it becomes clear that tocopherols play an important role in transfer cell wall synthesis at low temperatures.

Results from previous structural studies on the minor vein structure of *Arabidopsis* have suggested that phloem parenchyma transfer cells are the site of apoplastic unloading of photoassimilates arriving symplastically from bundle sheath cells (Haritatos et al., 2000). The coincidence in reduction of photoassimilate export with callose deposition in

these spatially distinct subcellular sites in the *vte2* mutant during low temperature treatment (Figure A.9, Figure A.10 and Figure A.13) provides direct support for the role of transfer cells in photoassimilate export from source leaves via delivery to the phloem apoplast. This callose deposition (or events associated with the callose deposition) in phloem parenchyma transfer cells of 7.5°C-treated *vte2* would form a barrier to symplast-to-apoplast but not symplast-to-symplast transport. The limited export that still occurs in 7.5°C-treated *vte2* source leaves (Figure A.9) may be due to apoplastic unloading from bundle sheath cells and subsequent loading to the sieve element/companion cell complex (Haritatos et al., 2000). The special characteristics of phloem parenchyma transfer cells that lead them, in comparison to other cell types in the leaf, to be so specifically and differentially impacted by tocopherol-deficiency during low temperature treatment remains to be determined.

Tocopherol Functions in Plant Stress Physiology

In the current study the tocopherol-deficient *vte2* mutant was found to be remarkably similar to wild type in its response to most abiotic stresses with the notable exception of non-freezing low temperature treatments. Tocopherol-deficiency specifically results in abnormal phloem parenchyma transfer cell wall development at low temperature. This leads to rapid impairment of photoassimilate export that profoundly impacts cellular metabolism and whole plant physiology during both short and long term low temperature treatments. That this occurs in both *vte2* and *vte1* strongly argues that tocopherols play a crucial, previously unrecognized role in low temperature adaptation, specifically in phloem loading. Several studies have suggested that vascular tissues, including vascular parenchyma, are metabolically distinct, sensitive to changing environmental conditions

and hence critical sites for stress responses (Orozco-Cardenas et al., 2001; Hibberd and Quick, 2002; Fryer et al., 2003; Koiwai et al., 2004; Narvaez-Vasquez and Ryan, 2004). Our data are consistent with this thesis and suggest tocopherols have important function(s) in regulating the response of these specific cell types to environmental stress, such as low temperatures.

Our findings that photooxidative damage and photoinhibition are not associated with the *vte2* low temperature phenotype and that HL1800 (which approaches full sunlight) at 22°C has little impact on *vte2* compared to wild type suggest a more limited role for tocopherols in protecting plants from photooxidative stress than has been assumed. This seems in direct contradiction with a recent report using *Arabidopsis vte* mutants that concluded tocopherols protect *Arabidopsis* against photoinhibition and photooxidative stress (Havaux et al., 2005). However, the conclusions of this prior work were based entirely on the differential responses of wild type and *vte* mutants exposed to low temperatures (2-8°C) in combination with HL (1000 to 1600 $\mu\text{mol photon m}^{-2} \text{s}^{-1}$) for durations of up to seven days. We now know that such low temperature treatments would rapidly block photoassimilate export in tocopherol-deficient genotypes, but not in wild type, independent of any light regime imposed (Figure A.9 to Figure A.11) and likely confound any interpretations with respect to previously proposed HL-specific tocopherol functions. Thus, the photoprotective functions of tocopherols in plants remain an open question and a critical reassessment is needed to clarify this issue.

METHODS

Growth Conditions and HL and Low Temperature Treatment

Seeds were stratified for four to seven days (4°C), planted in a vermiculite and soil mixture fertilized with 1 x Hoagland solution, and grown in a chamber under permissive conditions: 12h, 120 $\mu\text{mol photon m}^{-2} \text{ s}^{-1}$ light at 22°C / 12h darkness at 18°C with 70 % relative humidity. Plants were watered every other day and with 0.5 x Hoagland solution once a week. For HL treatments, four-week-old plants were transferred in the middle of the light cycle to 1800 $\mu\text{mol photon m}^{-2} \text{ s}^{-1}$ 16h light / 8h darkness at 22°C. For low temperature treatments, three to four-week-old plants were transferred at the beginning of light cycle to 12h 75 $\mu\text{mol photon m}^{-2} \text{ s}^{-1}$ light / 12h darkness at 7.5°C ($\pm < 3^\circ\text{C}$).

Tocopherol, Anthocyanin, Chlorophyll and Carotenoid Analyses

Leaf samples (12-15 mg) were harvested directly into liquid nitrogen at the end of the light cycle and lipids extracted in the presence of 0.01 % (w/v) butylated hydroxytoluene (BHT) using tocol as an internal standard as described (Collakova and DellaPenna, 2001). After phase separation, the aqueous phase was transferred to a new tube, acidified by adding an equal volume of 1N HCl and anthocyanin content measured spectrophotometrically at 520 nm as described (Merzlyak and Chivkunova, 2000). The lipid phase was used for reverse-phase HPLC analyses to identify and quantify each tocopherol, chlorophyll and carotenoid species as described previously (Collakova and DellaPenna, 2001; Tian and DellaPenna, 2001).

Lipid Peroxide Analysis

Lipid peroxide content was measured using the ferrous oxidation-xylenol orange (FOX) assay as previously described (Sattler et al., 2004) with the following modifications. Leaf samples (25-30 mg) harvested at the end of light cycle were immediately extracted with 200 μ L of methanol containing 0.01 % (w/v) BHT, 200 μ L of dichloromethane, and 50 μ L of 150 mM acetic acid using three 3-mm glass beads and a commercial paint shaker. After shaking for 4 min, 100 μ L of water and 100 μ L of dichloromethane were added for phase separation. Half of the organic phase was incubated with an equal volume of 50 mM triphenyl phosphine in methanol for 30 min to reduce lipid peroxides and half was incubated with an equal volume of methanol for 30 min. The triphenyl phosphine-treated and untreated samples (100 μ L) were incubated with 900 μ L of FOX reagent [90% (v/v) methanol, 4 mM BHT, 25 mM sulfuric acid, 250 μ M ferrous ammonium sulfate, 100 μ M xylenol orange] at room temperature for exactly 20 min and A_{560} was measured. Lipid peroxide content was calculated based on a standard curve of hydrogen peroxide as previously described (DeLong et al., 2002).

Chlorophyll Fluorescence Measurements

In vivo chlorophyll *a* fluorescence was measured in the middle of the light cycle using a pulse amplitude modulation (PAM) fluorometer FMS2 (PP Systems, Haverhill, MA). Attached leaves were dark adapted for at least 15 minutes prior to measurements and fluorescence parameters were determined according to (Maxwell and Johnson, 2000). Quantum yield of PSII (Φ_{PSII}) was calculated as $(F'm - F_t) / F'm$, where $F'm$ and F_t are maximum fluorescence and steady state fluorescence in the light, respectively.

Carbohydrate Analyses

Soluble sugar (glucose, fructose and sucrose) and starch levels of leaves were quantified as described (Jones et al., 1977; Lin et al., 1988) with minor modifications. Unshaded leaf tissue (<50mg) was harvested, immediately frozen in liquid nitrogen and extracted twice with 700 μL of 80% ethanol at 80°C. The ethanol extract was evaporated and redissolved in 200 μL of distilled water (Jones et al., 1977). For starch analysis, the extracted leaf residue was ground in 200 μL 0.2N KOH and boiled at 95°C for 45 min. After cooling, the sample was neutralized to pH 5 with 50 μL of 1N acetic acid, centrifuged and 50 μL of supernatant mixed with 492.5 μL of 0.2 M sodium acetate (pH 4.8), 150 μL of H_2O , 4 μL of α -amylase (4 units) and 3.5 μL of amyloglucosidase (2 units) and incubated at 37°C overnight. Glucose, fructose and sucrose levels in the soluble sugar extract and the glucose level of the digested starch extract were determined enzymatically (Jones et al., 1977).

$^{14}\text{CO}_2$ Labeling Experiments

For phloem exudation experiments, approximately 20 mature leaves (7th to 9th oldest) were detached in the middle of the day, 0.5 cm of petiole was re-cut under water, the petiole of each leaf was submerged in water and placed in a tightly sealed 10 L glass chamber. $^{14}\text{CO}_2$ was generated in the chamber by adding 3 mL of 0.25 N H_2SO_4 to 0.1 mCi (7 μmol) $\text{NaH}^{14}\text{CO}_3$ and unlabeled 93 μmol NaHCO_3 to give a carbon dioxide concentration of 522 ppm. After labeling for 30 min at 120 $\mu\text{mol photon m}^{-2} \text{ s}^{-1}$, the petiole of each leaf was submerged in 0.45 mL of 20 mM disodium-

ethylenediaminetetraacetic acid (EDTA) (pH 7.0) and kept in the dark with high humidity to induce phloem exudation (King and Zeevart 1974). All of the aforementioned procedures were performed at 7.5°C for low temperature-treated leaf samples. Exudation of radiolabel into the EDTA solution was then periodically measured over the course of 10 h by liquid scintillation counting (Tri-Carb 2800TR; PerkinElmer, Wellesley, MA, USA). After 10 h of exudation, radiolabel remaining in the leaves was determined by liquid scintillation counting. Total radiolabel fixed per leaf was calculated by adding total radiolabel exuded and remaining in each leaf.

For analyzing translocation of radiolabeled photoassimilates in whole plants, plants were grown on 1/2 MS plates under permissive conditions for 3 weeks and transferred to low temperature conditions for seven days with lids partially ajar to supply atmospheric CO₂. Whole plants were labeled at 7.5°C for 40 min as described above, placed in darkness at 7.5°C and high humidity for 2 h to allow for translocation. Roots were excised from leaves and both exposed to a phosphor screen to visualize the location of radioactivity (Storm; GE Healthcare, UK).

Carbohydrate analysis of phloem exudate was performed by high-pH anion exchange chromatography (HPAEC). Excised leaves were treated as described for phloem exudation experiments except at the end of the initial 2 h exudation period the petiole of each leaf was transferred to 0.45 mL water for 4 h to collect exudates for analysis. The water exudates were dried under vacuum, dissolved in 50 µL water and 20 µL of the sample was mixed with 5 µL of standards (25 nmol glucose, 50 nmol fructose, 125 nmol sucrose and 100 nmol raffinose) and injected onto the HPAEC. The mixtures were separated on a CarboPac PA-10 column (DIONEX, Sunnyvale, CA, USA) using a 30 min

linear gradient of 20 to 140 mM NaOH with a flow rate of 1 mL min⁻¹. One mL fractions were collected and radioactivity was determined by liquid scintillation counting, while sugar standards were detected by pulsed amperometric detection.

Fluorescence and Transmission Electron Microscopy

Leaves were prepared for aniline blue fluorescence microscopy (n = 2 leaves/plant, 4-6 plants/sample time; (Martin, 1959) and transmission electron microscopy (TEM; n = 1 leaf/plant, 2-3 plants/sample time; (Sage and Williams, 1995) at the same sampling times as above for export studies. The presence or absence of callose was determined using immunolocalization at the level of the TEM as described by Lam et al. (2001) with monoclonal antibodies to β -1, 3 glucan (Biosupplies, Australia). Primary and secondary (anti-mouse IgG gold conjugate 18 nm, Jackson ImmunoResearch, West Grove, PA, USA) antibody dilutions were 1: 100 and 1:20 respectively. Incubation time in the 1^o and 2^o antibodies were 2 and 1 h, respectively. Controls were run by omitting 1^o antibody. Images were captured on the Leica MZ 16F fluorescence microscope (Wetzlar, Germany) and the Phillips 201 TEM equipped with an Advantage HR Camera System (Advanced Microscopy Techniques Corp. Danvers, MA, USA).

Statistical Analysis

One-factor ANOVA was used for the data in Table A.2 and Figure A.2 using genotype as a factor. Two-factor ANOVA was used for the data in Figure A.9C using days of cold treatment and genotype as factors. When significance was observed (P < 0.05), pair-wise comparison of least square means was evaluated. SAS software was used for these analyses (SAS Institute, Cary, NC, USA). Student *t* test was used for the rest of the data to compare statistical significance of mutants relative to Col (P < 0.05) using

Microsoft Excel.

Accession Numbers

Sequence data for the *Arabidopsis thaliana* tocopherol biosynthetic enzymes described in this article can be found in the GenBank nucleotide sequence database under the following accession numbers: *VTE1* (At4g32770), [NM119430](#); *VTE2* (At2g18950), [NM179653](#); *VTE4* (At1g64970), [NM105171](#).

ACKNOWLEDGMENTS

We thank Maria Magallanes-Lundback for isolation of the *vte4-3* allele, Kathy Sault for technical assistance with microscopy, Ashok Ragavendran at MSU CANR Biometry Group for assistance with statistical analyses and Drs. Andreas Weber, Dr. Lars Voll and members of the DellaPenna lab for their critical advice, discussions and manuscript review. This work was supported by NSF grant MCB-023529 to D.D.P. and a Connaught Award and NSERC of Canada Discovery Grant to T.L.S.

TABLES AND FIGURES

Table A.1 Tocopherol and DMPBQ Content in Leaves of Wild Types and Tocopherol Biosynthetic Mutants Grown Under Permissive Conditions.

	α^a	β	γ	δ	total	DMPBQ
Col	15.6 ±3.0	0 ^b	0.6 ±0.1	0	16.2 ±3.0	0
vte2-1^c	0	0	0	0	0	0
vte1-1^c	0	0	0	0	0	19.6 ±1.3
vte1-2^c	0	0	0	0	0	17.3 ±1.8
Ws	12.3 ±2.2	0	0	0	12.3 ±2.2	0
vte2-2^d	0	0	0	0	0	0
vte4-3^d	0	0	17.7 ±1.2	0	17.7 ±1.2	0

Plants were grown for four weeks under permissive conditions and mature leaves were harvested for analysis. Data are means ±SD (n = 3 or 4) and are expressed as pmol/mg FW.

^a α , β , γ and δ indicate α , β , γ and δ -tocopherol, respectively.

^b 0 indicates the compound was below detection (typically ≤ 0.1 pmol/mg FW).

^c Col background.

^d Ws background.

Table A.2 Content of Photosynthetic Pigments and Tocopherols of Col and the *vte2* and *vte1* Mutants After HL1800 Treatment at 22°C.

	After HL1800			
	Col	<i>vte2-1</i>	<i>vte1-1</i>	<i>vte1-2</i>
Total tocopherols	1.58 ±0.25^a	0 ±0^b	0 ±0^b	0 ±0^b
Total chlorophylls	17.28 ±1.01	16.60 ±1.37	16.51 ±1.84	16.21 ±2.05
Chla	12.25 ±0.87	11.69 ±1.04	11.61 ±1.38	11.52 ±1.58
Chlb	5.02 ±0.26	4.90 ±0.35	4.90 ±0.51	4.69 ±0.50
Chla/Chlb	2.44 ±0.16	2.38 ±0.09	2.37 ±0.13	2.45 ±0.14
Total carotenoids	5.37 ±0.35^a	4.98 ±0.36^b	4.85 ±0.54^b	4.75 ±0.70^b
β-car	0.66 ±0.08	0.64 ±0.07	0.63 ±0.09	0.64 ±0.11
Lutein	2.45 ±0.14^a	2.39 ±0.15^{ab}	2.26 ±0.22^{bc}	2.20 ±0.27^c
N	0.57 ±0.03^a	0.51 ±0.04^b	0.51 ±0.06^b	0.50 ±0.07^b
V	1.01 ±0.12^a	0.57 ±0.10^c	0.78 ±0.17^b	0.77 ±0.22^b
A	0.39 ±0.04^{ab}	0.39 ±0.04^a	0.36 ±0.04^{bc}	0.36 ±0.04^c
Z	0.28 ±0.05^b	0.48 ±0.06^a	0.30 ±0.06^b	0.29 ±0.03^b
A+Z+V	1.69 ±0.13^a	1.44 ±0.12^b	1.44 ±0.18^b	1.42 ±0.26^b
A+Z/A+Z+V	0.40 ±0.05^c	0.61 ±0.05^a	0.46 ±0.07^b	0.47 ±0.07^b

Plants were grown for four weeks under permissive growth conditions (120 μmol photon m⁻² s⁻¹) and pigment contents were analyzed after 4 days of HL (1800 μmol photon m⁻² s⁻¹) treatment. Data are means ±SD (μg/cm², n = 19). When significance is observed between genotypes (ANOVA, P < 0.05), pair-wise comparison of least square means is evaluated and non-significant groups are indicated by *a*, *b* or *c* with *a* being the highest group. N, neoxanthin; β-car, β-carotene; V, violaxanthin; A, antheraxanthin; Z, zeaxanthin; Chlb, chlorophyll *b*; Chla, chlorophyll *a*.

Table A.3 Yields and Abortion Rates of Seed Produced During Low Temperature (7.5°C) Treatment.

	Col	vte2-1	vte1-1
seeds / siliqua	31.1 ±1.6	19.5 ±3.4**	27.3 ±2.5*
aborted seeds / siliqua	0.1 ±0.4	6.8 ±2.4**	2.0 ±1.0*
percentage abortion (%)	0.4	34.6**	7.3*
yield (mg seeds / plant)	373 ±77	87 ±27**	223 ^a

Data are means ±SD (n = 3 for yields, n = 7 for aborted seed). Student's *t* tests relative to Col (*P < 0.05, **P < 0.01).

^a An average of duplicate plants (225.7 and 219.4 mg seeds/plant)

Table A.4 Content of Photosynthetic Pigments and Tocopherols of Col and the *vte2* and *vte1* Mutants Grown at Permissive condition

	Before HL1800			
	Col	<i>vte2-1</i>	<i>vte1-1</i>	<i>vte1-2</i>
Total tocopherols	0.11 ±0.01^a	0 ±0^b	0 ±0^b	0 ±0^b
Total chlorophylls	21.90 ±1.14	20.51 ±1.70	20.15 ±1.12	21.26 ±1.19
Chla	15.26 ±0.77	14.25 ±1.18	14.02 ±0.79	14.78 ±0.84
Chlb	6.64 ±0.37	6.25 ±0.53	6.13 ±0.33	6.49 ±0.35
Chla/Chlb	2.30 ±0.03	2.28 ±0.02	2.29 ±0.01	2.28 ±0.02
Total carotenoids	3.56 ±0.23	3.32 ±0.28	3.28 ±0.18	3.44 ±0.22
β-car	0.61 ±0.05^a	0.57 ±0.03^b	0.55 ±0.03^b	0.59 ±0.05^{ab}
Lutein	1.85 ±0.13	1.72 ±0.16	1.70 ±0.10	1.79 ±0.12
N	0.59 ±0.03	0.55 ±0.05	0.54 ±0.03	0.57 ±0.03
V	0.51 ±0.04	0.48 ±0.05	0.49 ±0.03	0.50 ±0.03
A	0 ±0	0 ±0	0 ±0	0 ±0
Z	0 ±0	0 ±0	0 ±0	0 ±0
A+Z+V	0.51 ±0.04	0.48 ±0.05	0.49 ±0.03	0.50 ±0.03
A+Z/A+Z+V	0 ±0	0 ±0	0 ±0	0 ±0

Plants were grown for four weeks under permissive growth conditions (22°C, 120 μmol photon m⁻² s⁻¹) and mature leaves were analyzed. Data are means ±SD (μg/cm², n = 7).

When significance is observed between genotypes (ANOVA, P < 0.05), pair-wise comparison of least square means is evaluated and non-significant groups are indicated by *a* or *b* with *a* being the highest group. N, neoxanthin; β-car, β-carotene; V, violaxanthin; A, antheraxanthin; Z, zeaxanthin; Chlb, chlorophyll *b*; Chla, chlorophyll *a*.

Table A.5 Content of Individual Photosynthetic Pigments of Col and the *vte2* Mutant During Low Temperature (7.5°C) Treatment.

Days in cold	Lutein		β-car		N		V	
	Col	<i>Vte2-1</i>	Col	<i>vte2-1</i>	Col	<i>vte2-1</i>	Col	<i>vte2-1</i>
0	154 ±16	165 ±10	66 ±10	79 ±6	43 ±3	46 ±2	37 ±3	40 ±3
1	148 ±7	167 ±21	65 ±4	73 ±14	39 ±2	45 ±6	27 ±3	31 ±5
2	154 ±7	170 ±8	64 ±7	72 ±8	42 ±2	43 ±3	34 ±2	41 ±3
5	167 ±8	168 ±9	63 ±3	66 ±4	40 ±1	42 ±3	46 ±3	50 ±3
7	160 ±11	160 ±11	58 ±4	58 ±4	42 ±3	42 ±3	46 ±8	46 ±8
14	159 ±13	146 ±26	61 ±3	54 ±13	45 ±2	40 ±9	46 ±4	40 ±6
28	184 ±14	105 ±9**	86 ±13	48 ±7**	55 ±3	27 ±5**	46 ±3	30 ±1**

Days in cold	A		Z		total Car		Chlb	
	Col	<i>vte2-1</i>	Col	<i>vte2-1</i>	Col	<i>vte2-1</i>	Col	<i>vte2-1</i>
0	1 ±0	1 ±0	0 ±0	0 ±0	301 ±32	330 ±21	363 ±23	388 ±18
1	4 ±1	4 ±2	0 ±0	0 ±0	283 ±14	319 ±43	320 ±11	359 ±41
2	3 ±0	2 ±1	0 ±0	0 ±0	297 ±18	329 ±19	316 ±6	317 ±30
5	2 ±2	2 ±1	0 ±0	0 ±0	319 ±14	327 ±18	258 ±7	262 ±16
7	4 ±1	4 ±1	0 ±0	0 ±0	309 ±25	309 ±25	246 ±17	246 ±17
14	2 ±2	5 ±2	0 ±0	0 ±0	313 ±23	286 ±54	251 ±9	209 ±39
28	2 ±1	3 ±1	0 ±0	0 ±0	374 ±30	213 ±19**	304 ±27	138 ±21**

Table A.5 (continued)

Days in cold	Chla		Total Chl		Chla/Chlb	
	Col	<i>vte2-1</i>	Col	<i>vte2-1</i>	Col	<i>vte2-1</i>
0	842 ±75	931 ±48	1205 ±98	1319 ±65	2.32 ±0.06	2.40 ±0.04
1	759 ±34	854 ±107	1079 ±45	1212 ±148	2.37 ±0.03	2.38 ±0.03
2	753 ±38	790 ±68	1069 ±44	1107 ±98	2.39 ±0.07	2.49 ±0.03
5	593 ±18	613 ±30	851 ±24	875 ±46	2.30 ±0.02	2.34 ±0.05
7	559 ±32	559 ±32	805 ±49	805 ±49	2.28 ±0.03	2.28 ±0.03
14	581 ±18	499 ±95	832 ±26	708 ±134	2.32 ±0.03	2.39 ±0.02
28	729 ±89	357 ±49**	1033 ±114	495 ±69**	2.39 ±0.12	2.60 ±0.18**

Values are expressed as pmol/mg FW. Data are means ±SD (n = 4 or 5). Student's *t* tests of *vte2-1* relative to Col (* P < 0.05, ** P < 0.01). N, neoxanthin; β-car, β-carotene; V, violaxanthin; A, antheraxanthin; Z, zeaxanthin; total Car, total carotenoids; Chlb, chlorophyll *b*; Chla, chlorophyll *a*; total Chl, total chlorophylls.

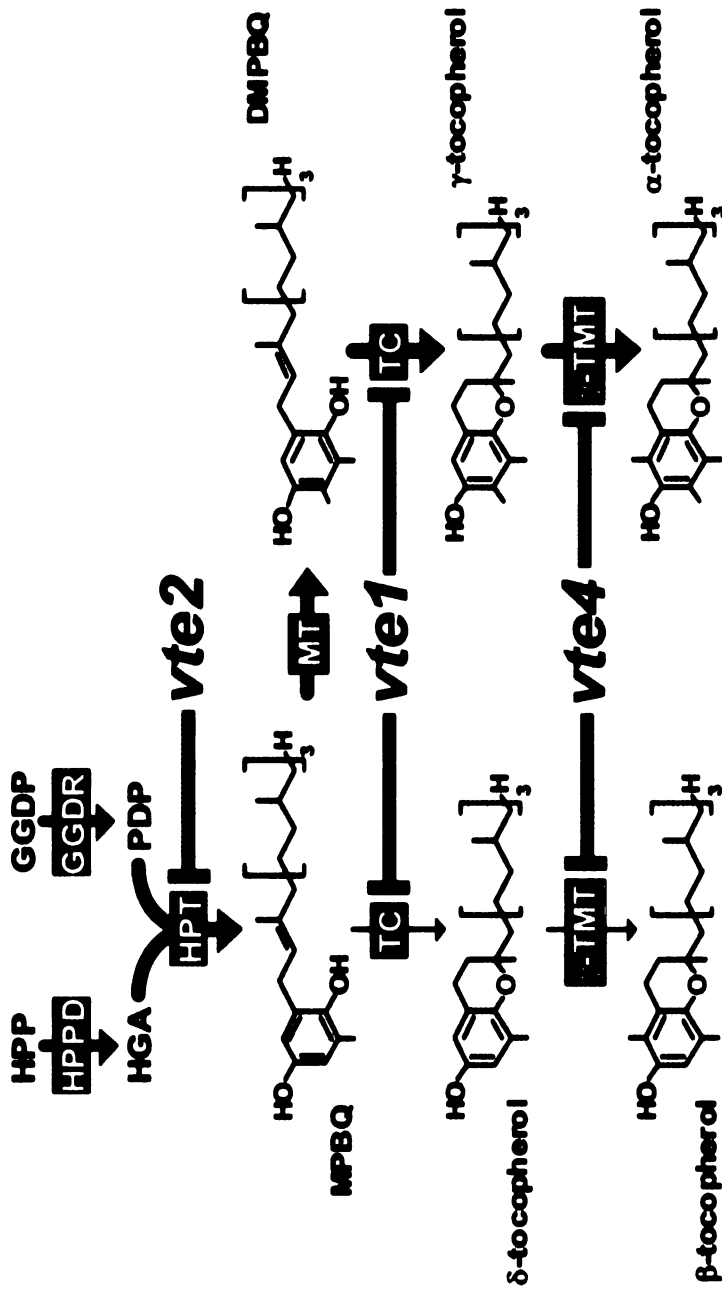


Figure A.1 Tocopherol Biosynthetic Pathway and *vte* Mutations in *Arabidopsis thaliana*.

Enzymes are indicated by black boxes and mutations by gray letters and lines. Bold arrows show the primary biosynthetic route in wild type leaves.

HPP, hydroxyphenylpyruvate; GGDP, geranylgeranyl-diphosphate; PDP, phytyl-diphosphate; HGA, homogentisic acid; MPBQ, 2-methyl-6-phytyl-1,4-benzoquinol; DMPBQ, 2,3-dimethyl-6-phytyl-1,4-benzoquinol; HPPD, HPP dioxygenase; GGDR, GGDP reductase; HPT, HGA phytyltransferase; TC, tocopherol cyclase; MT, MPBQ methyltransferase; γ -TMT, γ -tocopherol methyltransferase; *vte1*, *vte2* and *vte4*, mutants of TC, HPT and γ -TMT, respectively.

Figure A.2 Phenotypic and Photosynthetic Responses of Col and the *vte2* and *vte1* Mutants to HL stress.

Plants were grown under permissive conditions for four weeks and then transferred to HL stress in the middle of the day. When significance is observed between genotypes (ANOVA, $P < 0.05$), pair-wise comparison of least square means is evaluated and non-significant groups are indicated by *a*, *b* or *c* with *a* being the highest group.

(A) Six representative plants after 3 days of HL1800. Bars = 2 cm.

(B) and **(C)** Individual values of total chlorophyll **(B)** and carotenoid

(C) contents from 19 leaves after 4 days of HL1800.

(D) Individual values of Fv/Fm from 30 leaves after 24 h of HL1800.

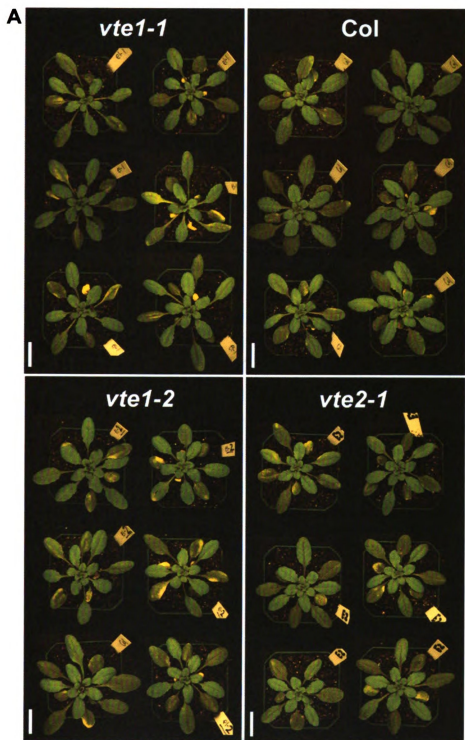


Figure A.2

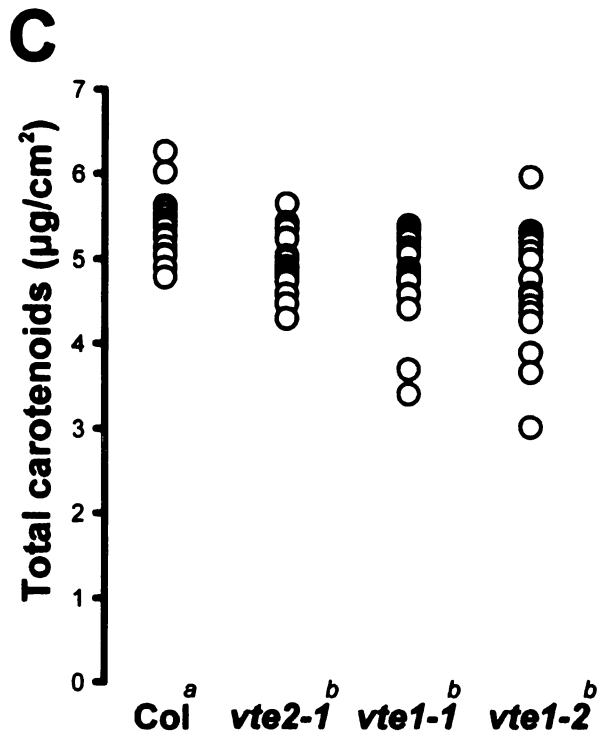
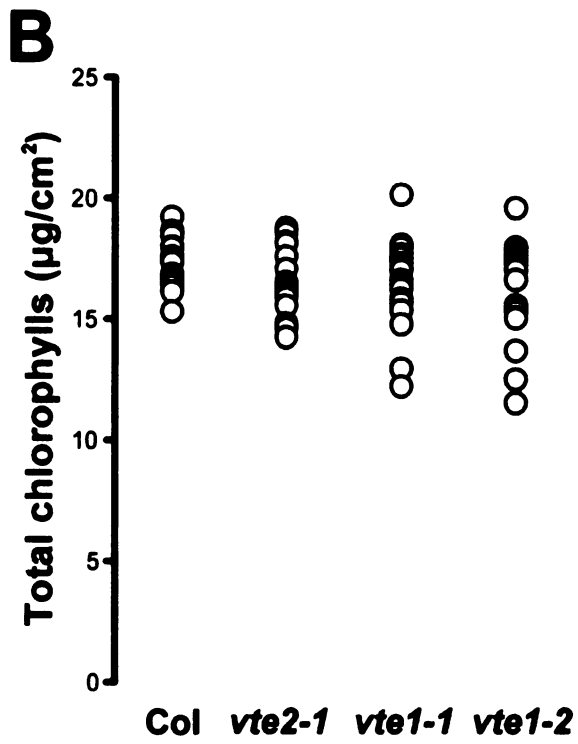


Figure A.2 (cont'd)

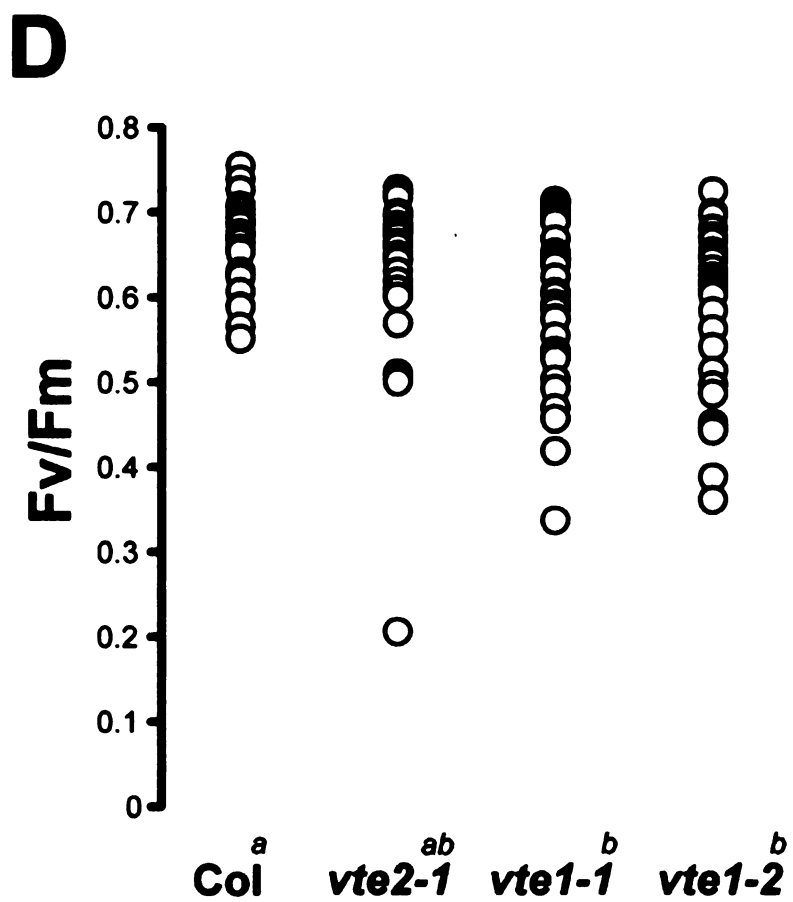


Figure A.2 (cont'd)

Figure A.3 Visible Phenotype of *vte* Mutants During Extended Low Temperature Treatment.

Plants were grown under permissive conditions for three weeks and then subjected to 7.5°C treatment for the indicated time periods. **(A) to (D)** Representative plants of three-week-old wild type (Col and Ws), *vte1-1* and *vte2-1* (Col background), *vte2-2* and *vte4-3* (Ws background) after 0 day (A), one month (B), two months (C) and four months (D) of 7.5°C treatment. Bars = 2 cm. **(E)** Representative siliques from Col, *vte1-1* and *vte2-1* plants after five months of low temperature treatment. Bar = 0.2 cm. Arrows denote aborted seeds in *vte1-1* and *vte2-1* siliques.

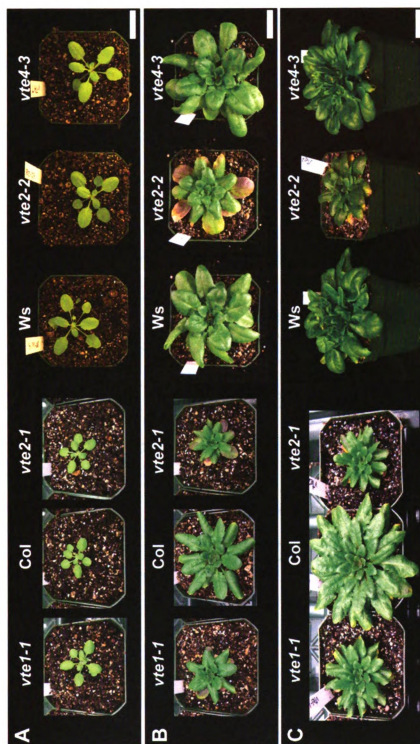


Figure A.3



Figure A.3 (cont'd)

Figure A.4 Tocopherol, Lipid Peroxide, Anthocyanin, and Photosynthetic Pigment Content of Col and the *vte2* Mutant During Four Weeks of Low Temperature Treatment.

Col (closed circles) and *vte2-1* (open squares) were grown under permissive conditions for four weeks and then transferred to 7.5°C conditions at the beginning of the light cycle for the indicated time. Data are means \pm SD (n = 3 or 4). Student's *t* tests of *vte2-1* relative to Col at each time point (*P < 0.05, **P < 0.01).

- (A) Total tocopherols;
- (B) Lipid peroxides;
- (C) Total chlorophylls;
- (D) Anthocyanins;
- (E) Total carotenoid

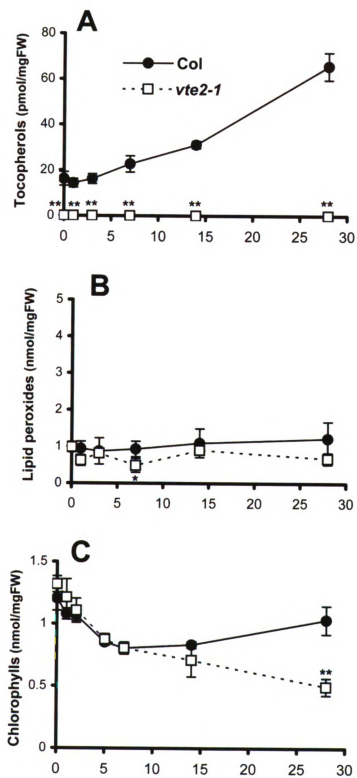


Figure A.4

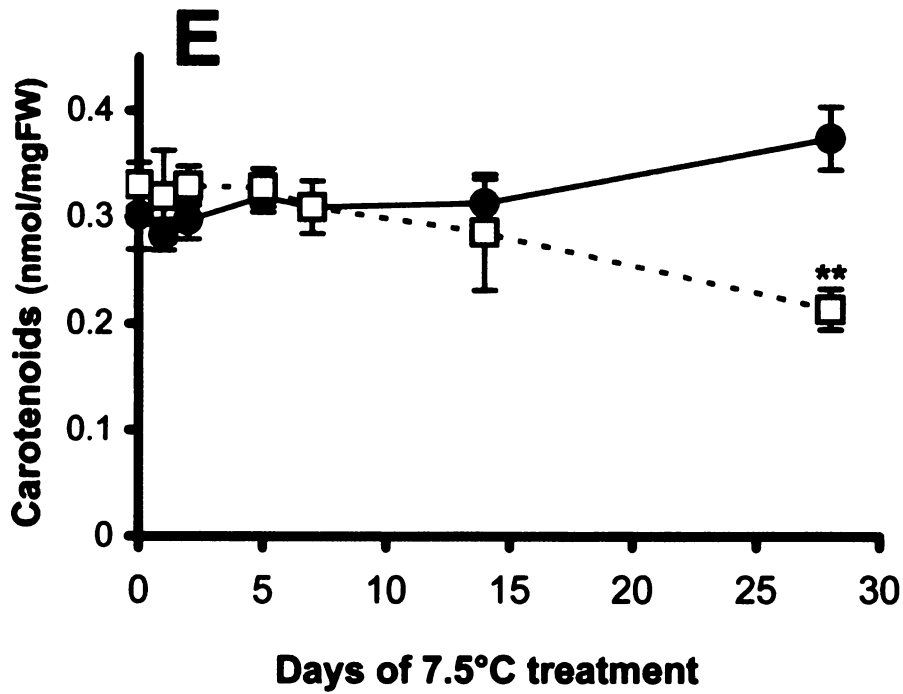
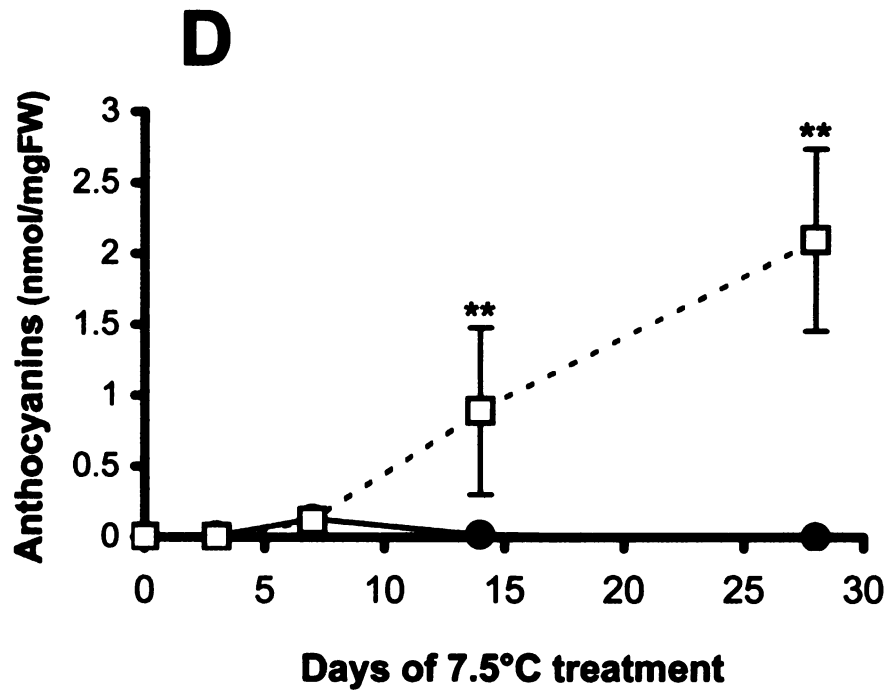


Figure A.4 (cont'd)

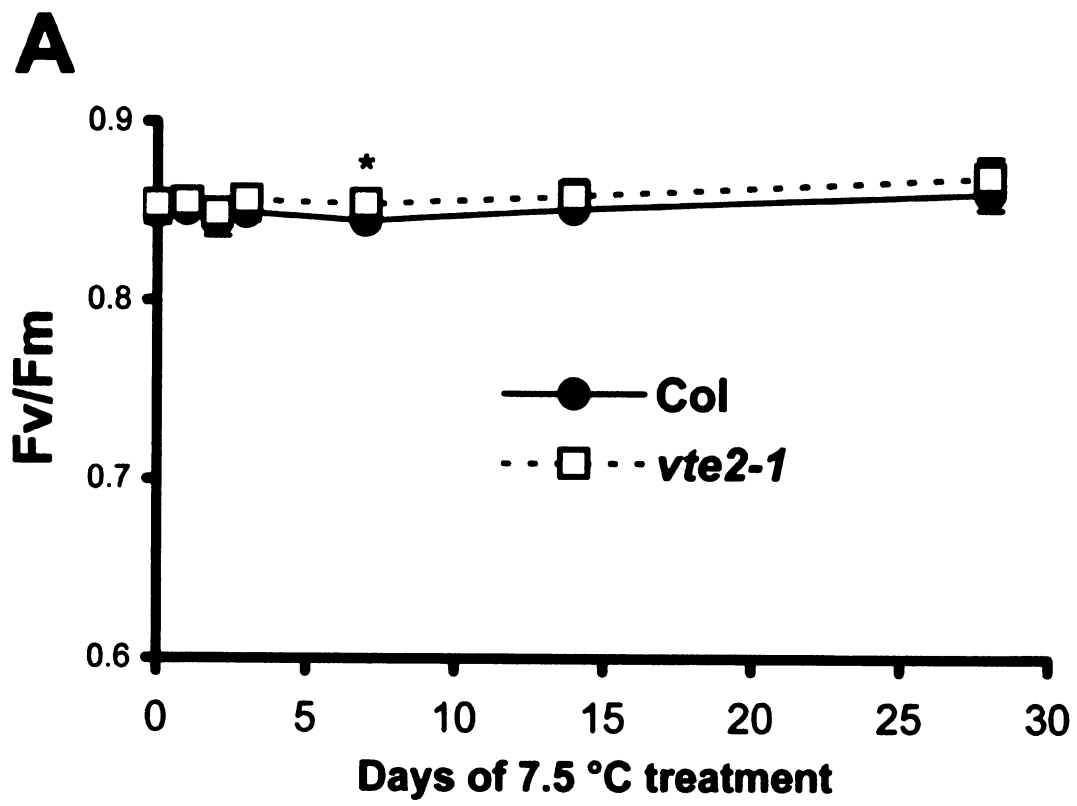


Figure A.5 Photosynthetic Status of Col and the *vte2* Mutant During Four Weeks of Low Temperature Treatment.

Col (closed circles) and *vte2-1* (open squares) were grown under permissive conditions for four weeks and then transferred to 7.5°C conditions at the beginning of the light cycle for the indicated time. Analysis was conducted in the middle of the light cycle. Data are means \pm SD (n = 4). Student's *t* tests of *vte2-1* relative to Col at each time point (*P < 0.05).

(A) Maximum photosynthetic efficiency (Fv/Fm)

(B) Quantum yield of PSII (Φ_{PSII})

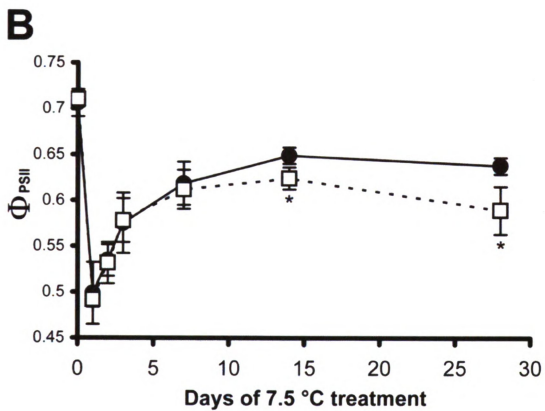


Figure A. 5 (cont'd)

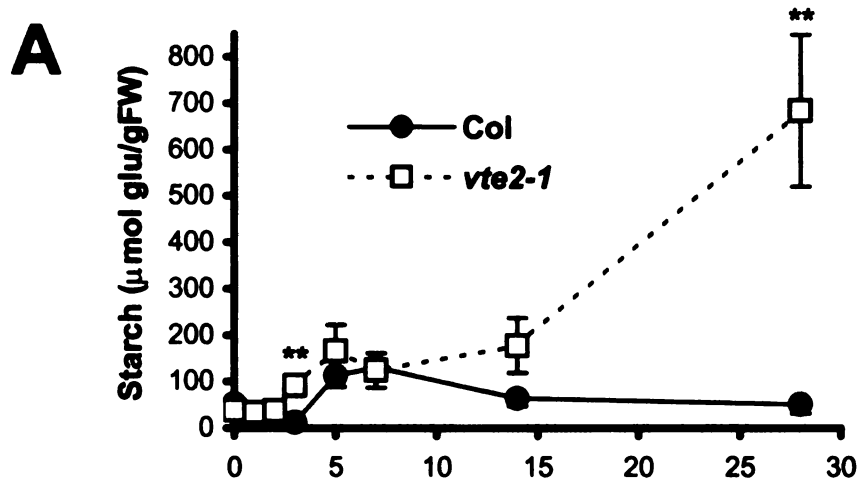


Figure A.6 Changes in Starch and Soluble Sugar levels in Col and the *vte2* Mutant During Four Weeks of Low Temperature Treatment.

Col (closed circles) and *vte2-1* (open squares) were grown under permissive conditions for four weeks and then transferred to 7.5°C conditions at the beginning of the light cycle for the indicated time. Samples were harvested at the end of light cycles. 0 days of cold treatment indicates the end of the light cycle of the day prior to initiating 7.5°C treatment. Starch is expressed as μmol glucose equivalents / g FW. Data are means \pm SD (n = 3 or 4). Student's *t* tests of *vte2-1* relative to Col at each time point (*P < 0.05, **P < 0.01).

(A) Starch

(B) Glucose

(C) Fructose

(D) Sucrose

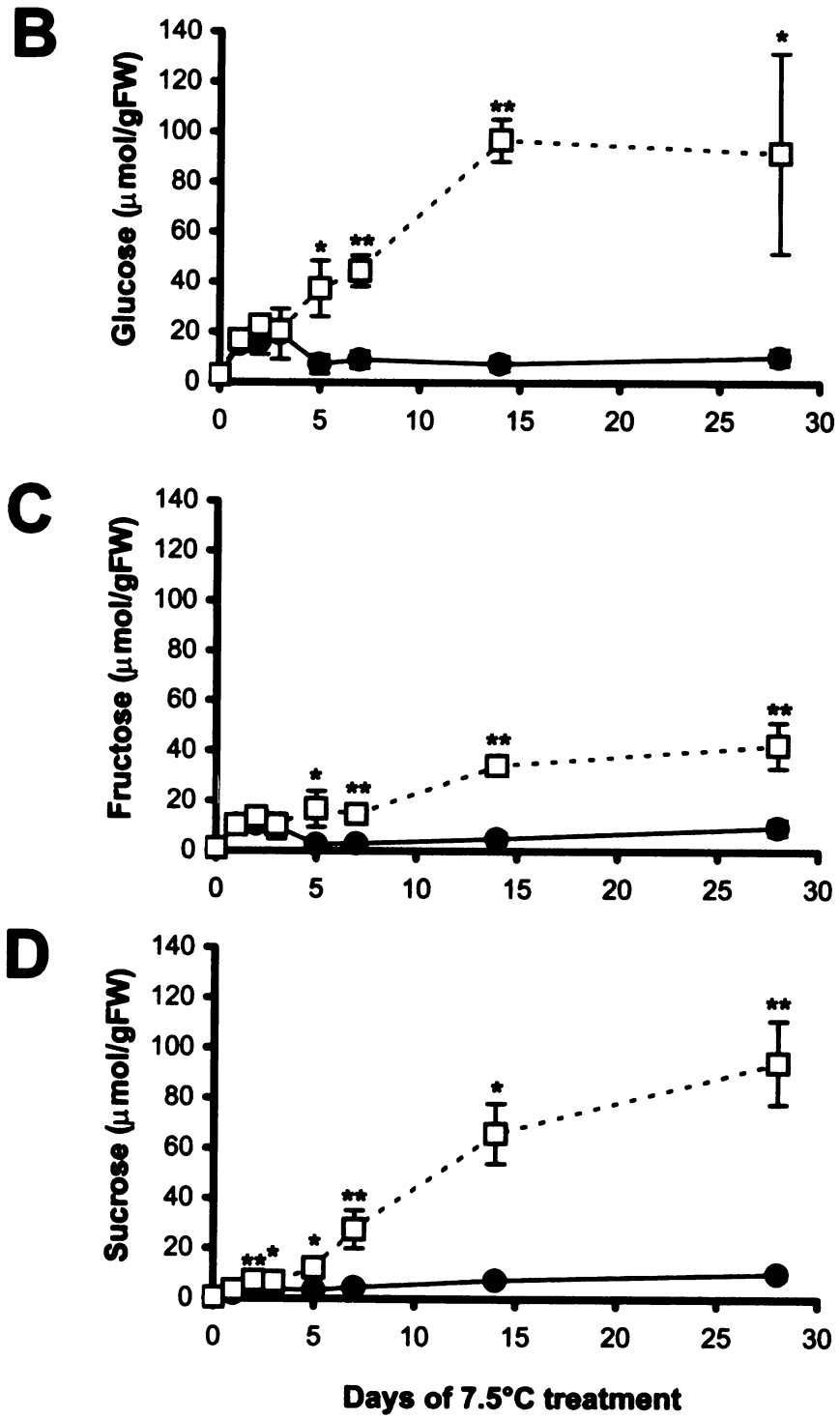


Figure A.6 (cont'd)

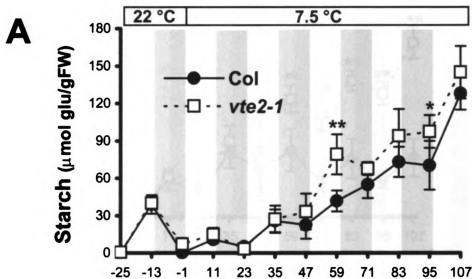


Figure A.7 Diurnal Changes in Starch and Soluble Sugar levels in Col and the *vte2* Mutant During the First Four Days of Low Temperature Treatment.

Col (closed circles) and *vte2-1* (open squares) were grown under permissive conditions for four weeks and then transferred to 7.5°C conditions at the beginning of the light cycle for the indicated time. Samples were harvested at the end of dark and light cycles. Gray shadows indicate 12 h dark cycles. 0 h of cold treatment indicates the beginning of the first light cycle of low temperature treatment. Starch is expressed as $\mu\text{mol glucose equivalents / g FW}$. Data are means \pm SD (n = 5). Student's *t* tests of *vte2-1* relative to Col at each time point (* $P < 0.05$, ** $P < 0.01$).

- (A) Starch
- (B) Glucose
- (C) Fructose
- (D) Sucrose

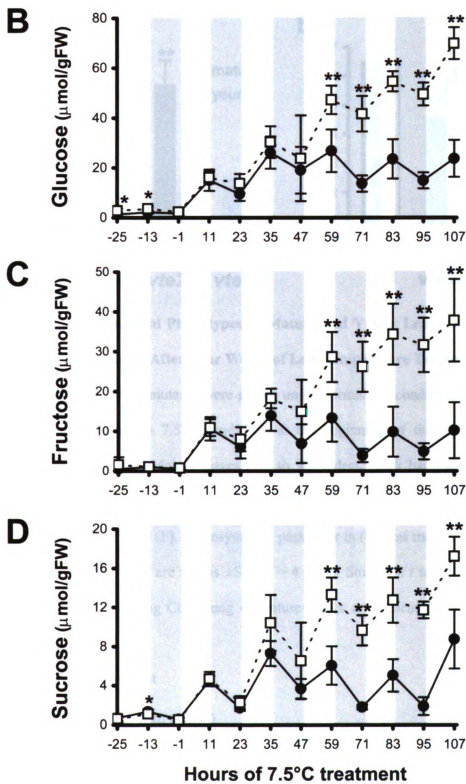


Figure A.7 (cont'd)

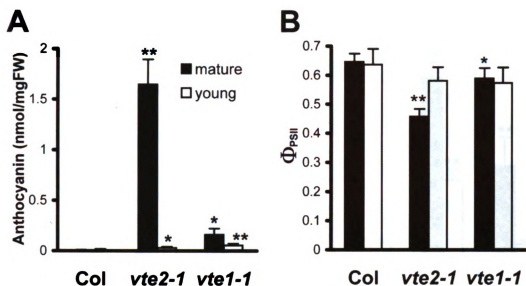


Figure A.8 Biochemical Phenotypes in Mature and Young Leaves of Col, and the *vte2* and *vte1* Mutants After Four Weeks of Low Temperature Treatment.

Col, *vte2-1* and *vte1-1* mutants were grown under permissive conditions for four weeks and then transferred to 7.5°C conditions at the beginning of the light cycle for an additional four weeks. Mature leaves (7th to 9th oldest, black bars) and young leaves (13th to 16th oldest, white bars) were harvested at the end of the light cycle for analyses in (A), (C), (D), (E) and (F). Photosynthetic parameter in (B) was measured in the middle of the light cycle. Data are means \pm SD (n = 4 or 5). Student's *t* tests of mutant leaves relative to corresponding Col young or mature leaves are indicated (*P < 0.05; **P < 0.01)

(A) Anthocyanin content

(B) Quantum yield of PSII (Φ_{PSII})

(C) Starch content expressed as mmol glucose equivalents / g FW

(D) to (F) Glucose, fructose and sucrose content, respectively.

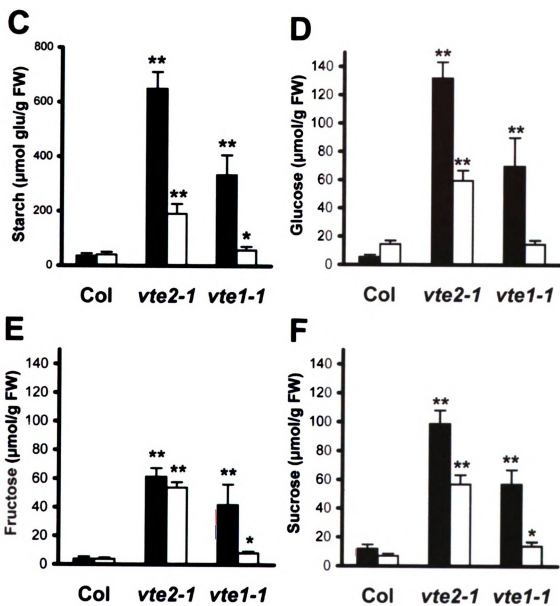


Figure A.8 (cont'd)

Figure A.9 Translocation and Export of ^{14}C Labeled Photoassimilates in Low Temperature-Treated Col and the *vte2* and *vte1* Mutants.

(A) ^{14}C labeled photoassimilate translocation of Col and *vte2-1* treated for 7 days at 7.5°C. Percent label detected in leaves (top) and roots (bottom) are indicated as means \pm SD (n = 3). Student's *t* tests relative to Col (*P < 0.05, **P < 0.01).

(B) HPLC analysis of phloem exudates collected from mature leaves of Col and *vte2-1* treated for 10 days at 7.5°C. The HPLC trace of sugar standards is shown as dotted grey lines. The percentage of label detected in the glucose/fructose or sucrose fractions are indicated as means \pm SD (n = 3). Glu, glucose; Fru, fructose; Suc, sucrose; Raf, raffinose.

(C) Phloem exudation of ^{14}C labeled photoassimilates from Col and *vte2-1* and *vte1-1* mature leaves during 7 days of 7.5°C treatment. Total ^{14}C fixed per mg fresh weight of each sample at the indicated time following transfer to 7.5°C is shown below each graph. Data are means \pm SD (n = 6 to 8). Two-factor ANOVA using end points (values at 10 h of exudation) indicates interactions are significant (P < 0.05, days of 7.5°C treatment and genotype as factors). The pair-wise comparisons of least square means between genotypes at 1, 3 and 7 days of 7.5°C treatment are indicated as *a*, *b* or *c*, while 0 day is not significant. N.A., data not available

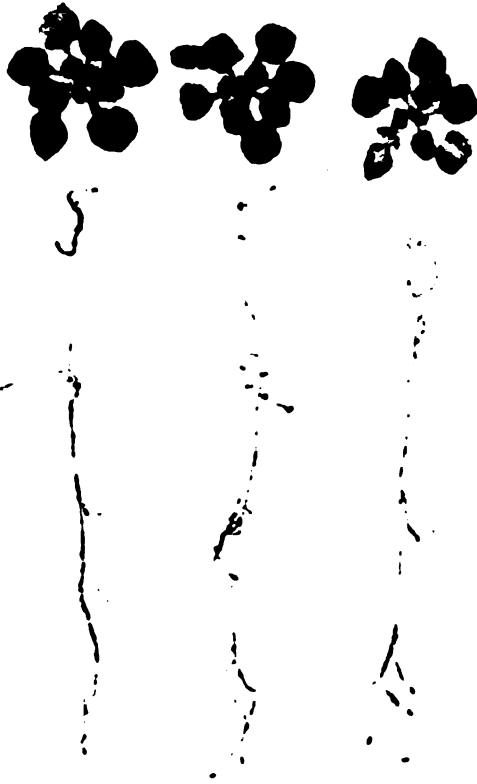
A

Col

vte2-1

86.8 ± 2.4 %

97.3 ± 0.8 %*



13.2 ± 2.4 %



2.7 ± 0.8 %*

Figure A.9

B

	Glu+Fru	Suc	
Col	11.0 ± 2.8	85.8 ± 4.0	(% dpm)
vte2-1	8.9 ± 5.1	83.2 ± 9.8	

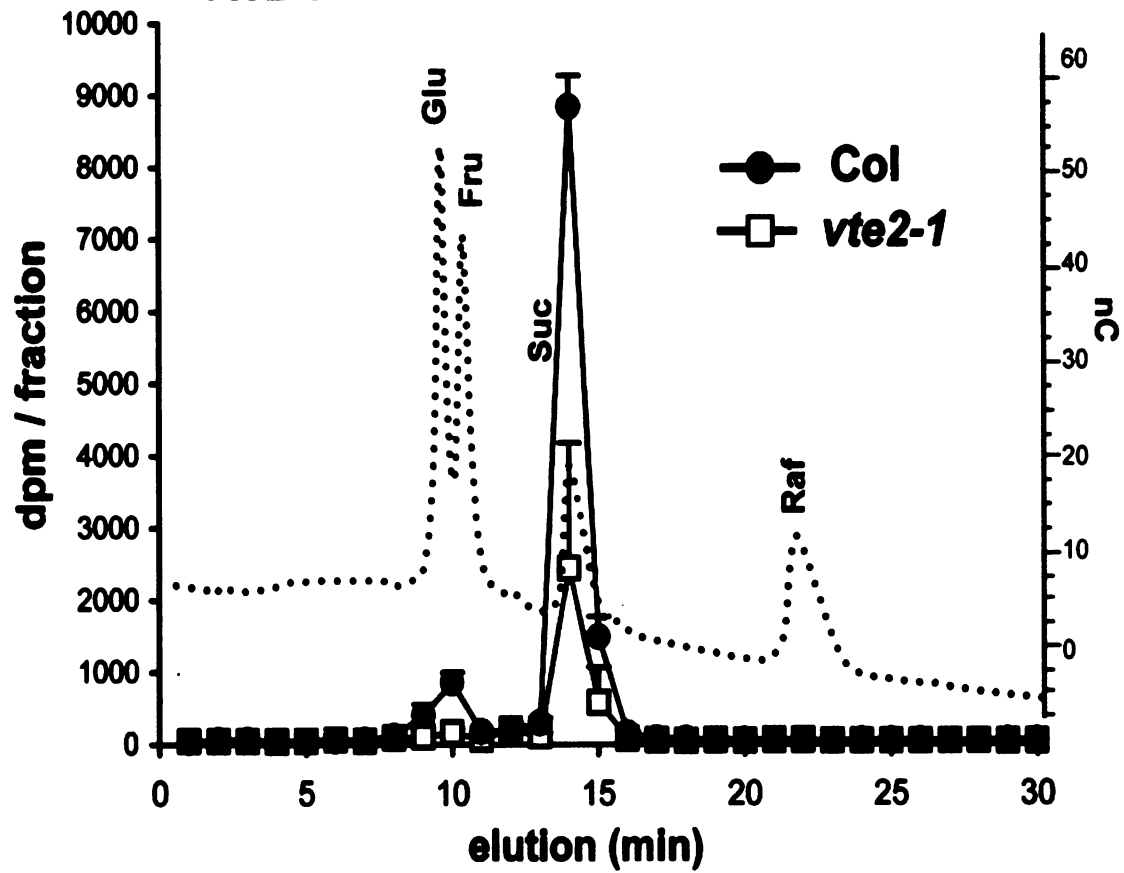
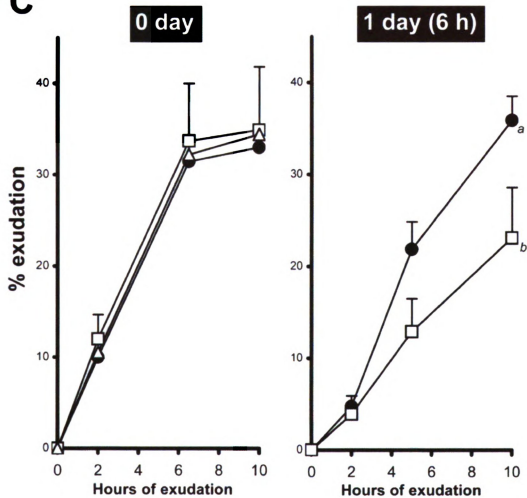


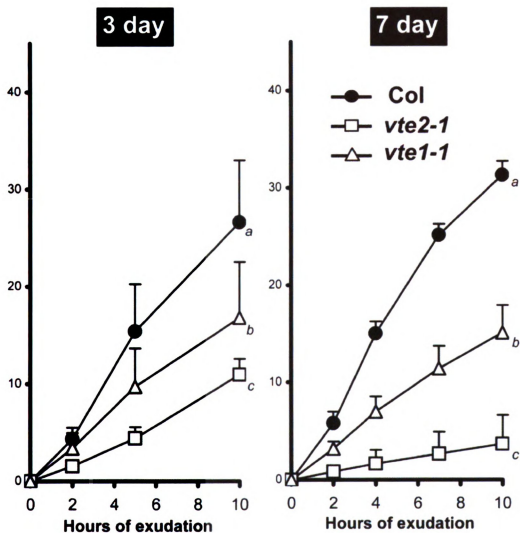
Figure A.9 (cont'd)

C**¹⁴C fixed (dpm/mgFW)**

Col 13868 ± 1177
vte2-1 15195 ± 1197
vte1-1 14491 ± 1370

7839 ± 1090
 7716 ± 1080
N.A.

Figure A. 9 (cont'd)



5915 ± 180

5381 ± 209**

6314 ± 305*

5192 ± 490

4898 ± 847

5167 ± 336

Figure A. 9 (cont'd)

Figure A.10 Aniline Blue Positive Fluorescence in Leaves of Col and the *vte2* Mutant During Low Temperature Treatment.

Col (C) and *vte2-1* (all panels except C) were grown under permissive conditions for four weeks and then transferred to 7.5°C at the beginning of the light cycle. Leaves were harvested in the middle of the day before 7.5°C treatment (0 day; A and B) and after 1 day (6 h; D to F), 3 days (G to I) and 13 days (C and J to L) of 7.5°C treatment and aniline blue positive fluorescence were observed at leaf petioles (A, D, G and J), the lower half of leaves (B, C, E, H and K) and vein junctions (F, I and L). Arrows in (D and F) denote highly fluorescent spots that initially appear in side veins of *vte2-1* petioles after 6 h of 7.5°C treatment. Bars = 50 µm for F, I and L and 500 µm for all other panels.

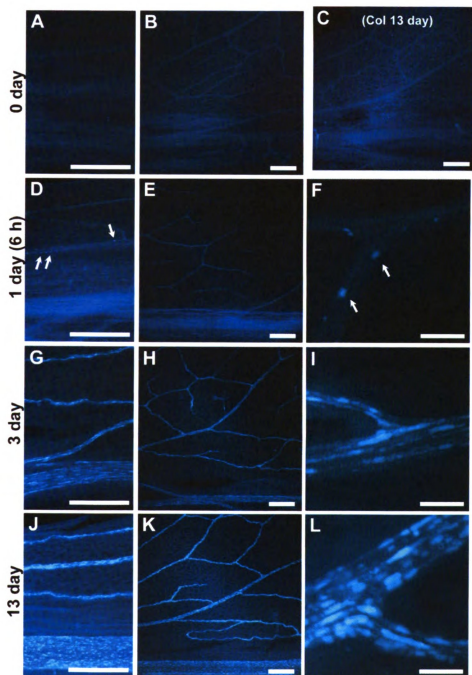


Figure A.10

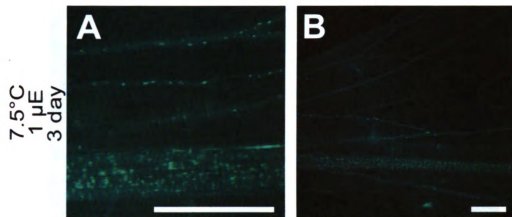


Figure A.11 Aniline Blue Positive Fluorescence in Leaves of the *vte2* Mutant at Various Light Intensities under Permissive and Low Temperature Conditions.

vte2-1 were grown under permissive conditions for four weeks and then transferred at the beginning of the light cycle to 7.5°C 12h light/12 h darkness at the indicated light levels (A to F) and in the middle of the day to HL1800 at 22°C (G and H). Leaves were harvested in the middle of the day. Aniline blue positive fluorescence was observed at leaf petioles (A, C, E and G) and the lower half of leaves (B, D, F and H). Bars = 500 μm .

(A) and (B) 7.5°C at 1 $\mu\text{mol photon m}^{-2} \text{s}^{-1}$ for 3 days (54h).

(C) and (D) 7.5°C at 75 $\mu\text{mol photon m}^{-2} \text{s}^{-1}$ for 2 days (30 h).

(E) and (F) 7.5°C at 800 $\mu\text{mol photon m}^{-2} \text{s}^{-1}$ for 2 days (30h)

(G) and (H) 22°C at 1800 $\mu\text{mol photon m}^{-2} \text{s}^{-1}$ for 4 days (72h).

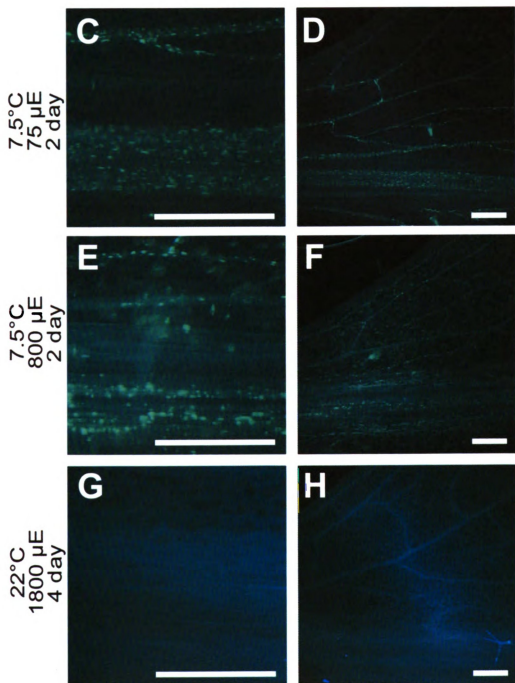


Figure A.11 (cont'd)

Figure A.12 Cellular Structure and Immunodetection of Callose in Col and *vte2-1* Before and After 14 Days of Low Temperature Treatment.

(G) to (L) are immunolabeled with anti- β -1,3 glucan antibody. (D) to (F) are controls with only 2^o antibody. Single arrows denote phloem parenchyma transfer cell wall ingrowths. Double arrows denote abnormal thickening of phloem parenchyma transfer cell wall ingrowths. Single asterisks (*) mark massive wall ingrowths of phloem parenchyma transfer cells. Double asterisks (**) mark wall ingrowths immunolabeled with anti- β -1,3 glucan. Paradermal (C and G) and transverse (E and I) sections show entire phloem parenchyma transfer cell occluded with callose. Paradermal (C and G) and transverse (D and H) sections show the peripheral callose sheath of phloem parenchyma transfer cells. Note callose at boundary between phloem parenchyma transfer cell and sieve element (F and J). Plasmodesmata between bundle sheath (upper cell) and phloem parenchyma transfer cell immunolabeled with anti- β -1,3 glucan (K). b, bundle sheath; c, companion cell; s, sieve element; v, vascular parenchyma. Bars = 1 μ m (all panels except C) and 5 μ m (C)

(A) *vte2-1* before 7.5°C treatment.

(B) to (L) *vte2-1* (C to K) and Col (B and L) after 14 days of 7.5°C treatment.

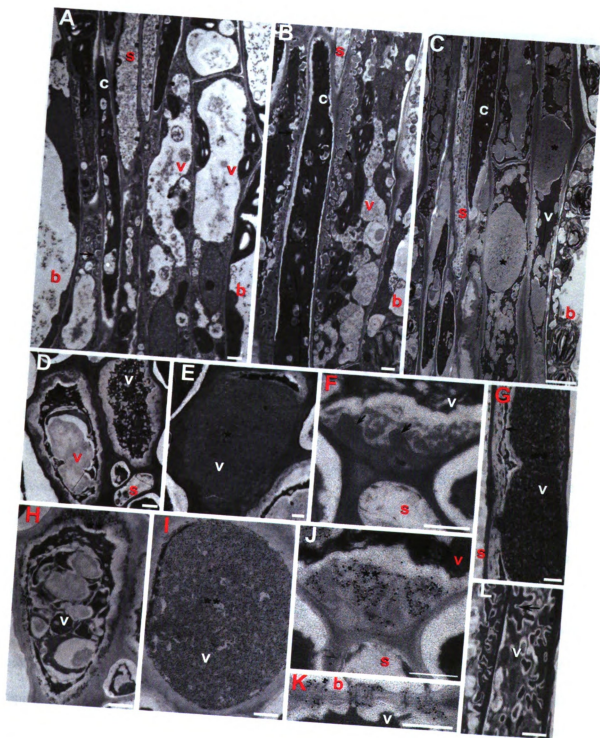


Figure A.12

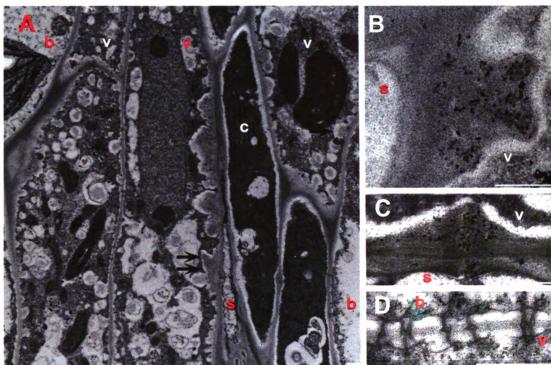


Figure A.13 Cellular Structure and Immunodetection of Callose in *vie2-1* After 3 Days of Low Temperature Treatment.

(B) to (D) are immunolabeled with anti- β -1,3 glucan antibody. Single arrows denote phloem parenchyma transfer cell wall ingrowths adjacent to bundle sheath. Double arrows denote abnormal thickening of phloem parenchyma transfer cell wall ingrowths adjacent to companion cell. Note that transfer cell wall ingrowths are present around the entire phloem parenchyma transfer cell (A). Transverse section of wall ingrowths immunolabeled with anti- β -1,3 glucan at phloem parenchyma transfer cell and sieve element boundary (B) and plasmodesmata between phloem parenchyma transfer cell (upper cell) and sieve element (C). Plasmodesmata between bundle sheath (upper cell) and phloem parenchyma cell are continuous, lack callose-like wall depositions and are immunonegative for anti- β -1,3 glucan (D). b, bundle sheath; c, companion cell; s, sieve element; v, vascular parenchyma transfer cell. Bars = 0.5 μ m

Figure A.14 Phenotypes of the *vte2* Mutant and Col During HL, Drought and Salinity Stress.

The *vte2* mutant and Col were grown at permissive conditions for four to five weeks prior to the indicated stress treatments.

(A) Four-week-old plants were grown under permissive conditions and then transferred to HL1000 stress (16 h 1000 mmol photon m⁻² s⁻¹ light/8h darkness at 22°C) in the middle of the day. The graph shows the Fv/Fm of Col and *vte2-1* grown under permissive conditions or after 24 h of HL1000. The image shows representative plants of Col and *vte2-1* after 11 days of HL1000.

(B) Five-week-old plants grown under permissive conditions were subjected to drought stress. The image shows representative plants of Col and *vte2-1* that had water withheld for 10 days.

(C) Four-week-old plants grown under permissive conditions were subjected to salinity stress. The image shows representative Col and *vte2-1* plants that were watered with 200 mM NaCl every other day for three weeks.

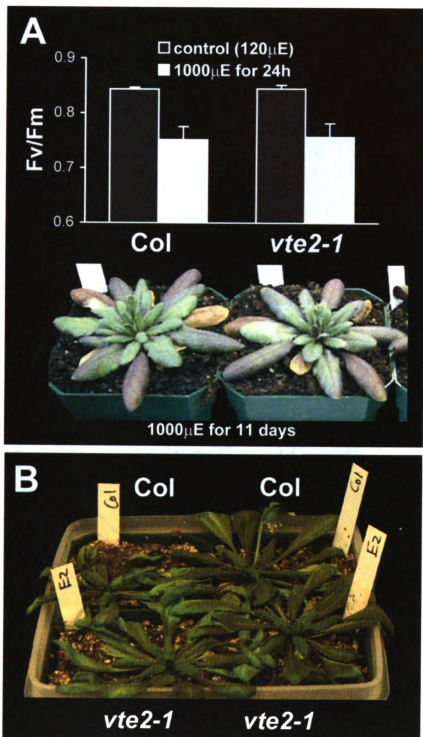


Figure A. 14

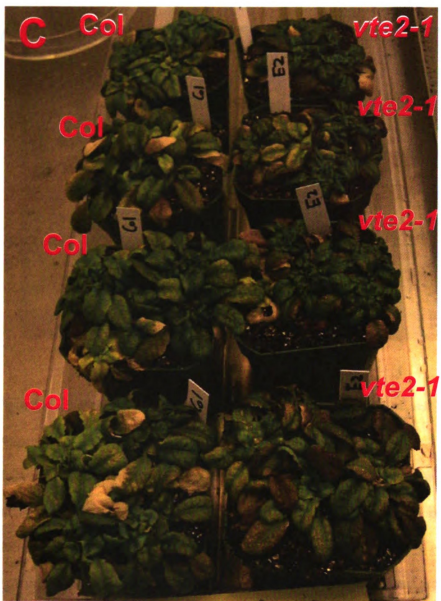


Figure A.14 (cont'd)

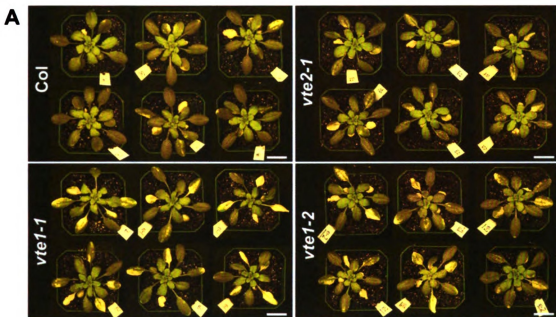


Figure A.15 Phenotypic and Photosynthetic Responses of Col and the *vte2* and *vte1* Mutants to HL stress.

Plants were grown under permissive conditions for four weeks and then transferred to HL stress in the middle of the day. When significance is observed between genotypes (ANOVA, $P < 0.05$), pair-wise comparison of least square means is evaluated and non-significant groups are indicated by *a*, *b* or *c* with *a* being the highest group.

(A) Six representative plants after 3 days of HL1800. Bars = 2 cm.

(B) and (C) Individual values of total chlorophyll (B) and carotenoid (C) contents from 19 leaves after 4 days of HL1800.

(D) Individual values of Fv/Fm from 19 leaves after 24 h of HL1800.

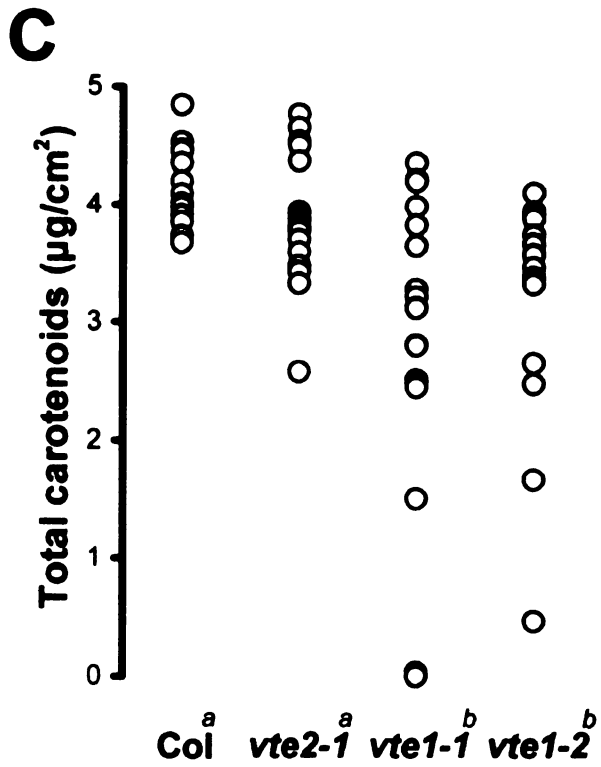
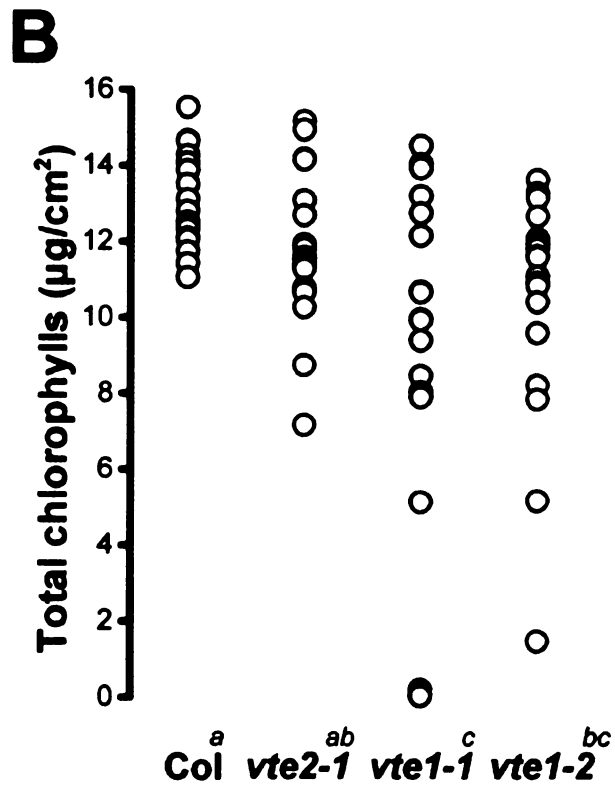


Figure A.15 (cont'd)

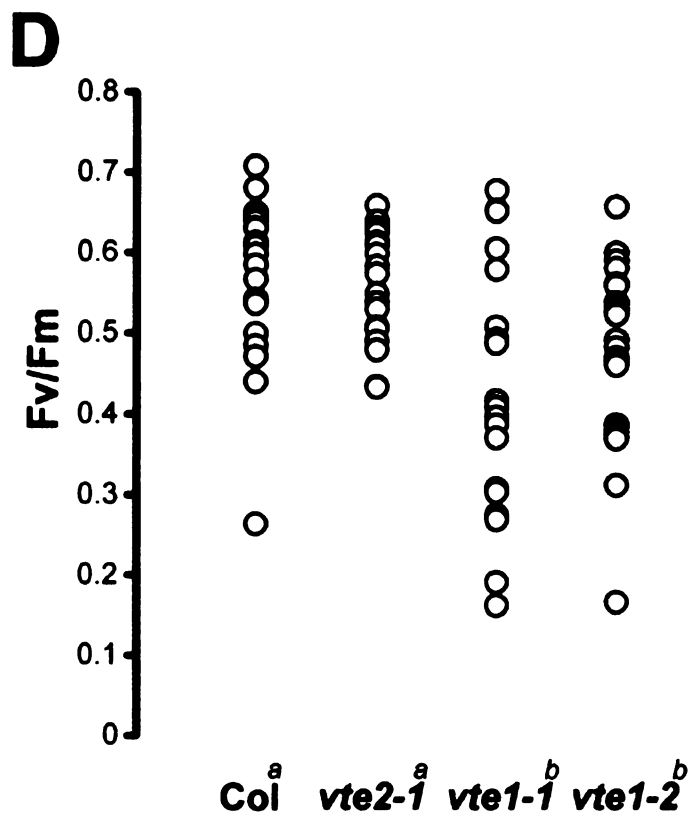


Figure A.15 (cont'd)

Figure A.16 Aniline Blue Positive Fluorescence in Leaves of the *vte2* and *vte1* Mutant During Low Temperature Treatment.

vte2-1 (A, C and E) and *vte1-1* (B, D and F) were grown under permissive conditions for four weeks and then transferred to 7.5°C at the beginning of the light cycle. Leaves were harvested in the middle of the day after 1 day (6 h) (A and B), 2 days (C and D) and 3 days (E and F) of 7.5°C treatment and aniline blue positive fluorescence were observed at leaf petioles (A and B), the lower half of leaves (C to F). Arrows in (A and B) denote fluorescence spots initially appeared at side veins of petioles. Bars = 500 µm.

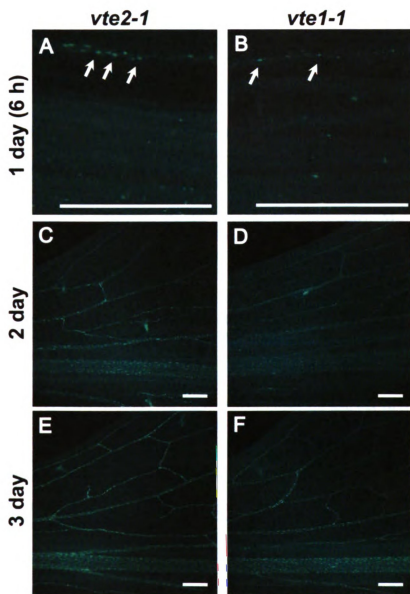


Figure A.16

LITERATURE CITED

- Abbasi, A.R., Hajirezaei, M., Hofius, D., Sonnewald, U., and Voll, L.M.** (2007). Specific roles of alpha- and gamma-tocopherol in abiotic stress responses of transgenic tobacco. *Plant Physiology* **143**, 1720-1738.
- Abbasi, A.R., Saur, A., Hennig, P., Tschiersch, H., Hajirezaei, M., Hofius, D., Sonnewald, U., and Voll, L.M.** (2009). Tocopherol deficiency in transgenic tobacco (*Nicotiana tabacum* L.) plants leads to accelerated senescence. *Plant Cell and Environment* **32**, 144-157.
- Abdrakhamanova, A., Wang, Q.Y., Khokhlova, L., and Nick, P.** (2003). Is microtubule disassembly a trigger for cold acclimation? *Plant and Cell Physiology* **44**, 676-686.
- Agarwal, M., Hao, Y.J., Kapoor, A., Dong, C.H., Fujii, H., Zheng, X.W., and Zhu, J.K.** (2006). A R2R3 type MYB transcription factor is involved in the cold regulation of CBF genes and in acquired freezing tolerance. *Journal of Biological Chemistry* **281**, 37636-37645.
- Ahuja, J.K.C., Goldman, J.D., and Moshfegh, A.J.** (2004). Current status of vitamin E nutriture. *Vitamin E and Health* **1031**, 387-390.
- Andersson, M.X., Kjellberg, J.M., and Sandelius, A.S.** (2004). The involvement of cytosolic lipases in converting phosphatidyl choline to substrate for galactolipid synthesis in the chloroplast envelope. *Biochimica Et Biophysica Acta-Molecular and Cell Biology of Lipids* **1684**, 46-53.
- Andersson, M.X., Goksor, M., and Sandelius, A.S.** (2007). Optical manipulation reveals strong attracting forces at membrane contact sites between endoplasmic reticulum and chloroplasts. *J Biol Chem* **282**, 1170-1174.
- Arango, Y., and Heise, K.P.** (1998). Localization of alpha-tocopherol synthesis in chromoplast envelope membranes of *Capsicum annuum* L. fruits. *Journal of Experimental Botany* **49**, 1259-1262.

- Aratri, E., Spycher, S.E., Breyer, I., and Azzi, A.** (1999). Modulation of alpha-tropomyosin expression by alpha-tocopherol in rat vascular smooth muscle cells. *Febs Letters* **447**, 91-94.
- Aronel, V., Lemieux, B., Hwang, I., Gibson, S., Goodman, H.M., and Somerville, C.R.** (1992). Map-based cloning of a gene controlling omega-3-fatty-acid desaturation in *Arabidopsis*. *Science* **258**, 1353-1355.
- Atkinson, J., Epand, R.F., and Epand, R.M.** (2008). Tocopherols and tocotrienols in membranes: A critical review. *Free Radical Biology and Medicine* **44**, 739-764.
- Aubert, S., Gout, E., Bligny, R., MartyMazars, D., Barrieu, F., Alabouvette, J., Marty, F., and Douce, R.** (1996). Ultrastructural and biochemical characterization of autophagy in higher plant cells subjected to carbon deprivation: Control by the supply of mitochondria with respiratory substrates. *J Cell Biol* **133**, 1251-1263.
- Awai, K., Xu, C.C., Tamot, B., and Benning, C.** (2006). A phosphatidic acid-binding protein of the chloroplast inner envelope membrane involved in lipid trafficking. *Proc Natl Acad Sci U S A* **103**, 10817-10822.
- Baluska, F., Samaj, J., Wojtaszek, P., Volkmann, D., and Menzel, D.** (2003). Cytoskeleton-plasma membrane-cell wall continuum in plants. Emerging links revisited. *Plant Physiology* **133**, 482-491.
- Barella, L., Muller, P.Y., Schlachter, M., Hunziker, W., Stocklin, E., Spitzer, V., Meier, N., de Pascual-Teresa, S., Minihane, A.M., and Rimbach, G.** (2004). Identification of hepatic molecular mechanisms of action of alpha-tocopherol using global gene expression profile analysis in rats. *Biochimica Et Biophysica Acta-Molecular Basis of Disease* **1689**, 66-74.
- Barkan, L., Vijayan, P., Carlsson, A.S., Mekhedov, S., and Browse, J.** (2006). A suppressor of *fab1* challenges hypotheses on the role of thylakoid unsaturation in photosynthetic function. *Plant Physiology* **141**, 1012-1020.
- Bates, P.D., Ohlrogge, J.B., and Pollard, M.** (2007). Incorporation of newly synthesized fatty acids into cytosolic glycerolipids in pea leaves occurs via acyl editing. *J Biol Chem* **282**, 31206-31216.

- Bates, P.D., Durrett, T.P., Ohlrogge, J.B., and Pollard, M.** (2009). Analysis of acyl fluxes through multiple pathways of triacylglycerol synthesis in developing soybean embryos. *Plant Physiol.* **150**, 55-72.
- Bechtold, U., Murphy, D.J., and Mullineaux, P.M.** (2004). *Arabidopsis* peptide methionine sulfoxide reductase2 prevents cellular oxidative damage in long nights. *Plant Cell* **16**, 908-919.
- Bell, J.G., McEvoy, J., Tocher, D.R., and Sargent, J.R.** (2000). Depletion of alpha-tocopherol and astaxanthin in Atlantic salmon (*Salmo salar*) affects autoxidative defense and fatty acid metabolism. *J Nutr* **130**, 1800-1808.
- Benning, C.** (2009). Mechanisms of lipid transport involved in organelle biogenesis in plant cells. *Annu. Rev. Cell Dev. Biol.*, 4.1-4.21.
- Berberich, T., Harada, M., Sugawara, K., Kodama, H., Iba, K., and Kusano, T.** (1998). Two maize genes encoding omega-3 fatty acid desaturase and their differential expression to temperature. *Plant Molecular Biology* **36**, 297-306.
- Bergmuller, E., Porfirova, S., and Dormann, P.** (2003). Characterization of an *Arabidopsis* mutant deficient in gamma-tocopherol methyltransferase. *Plant Molecular Biology* **52**, 1181-1190.
- Bolstad, B.M., Irizarry, R.A., Astrand, M., and Speed, T.P.** (2003). A comparison of normalization methods for high density oligonucleotide array data based on variance and bias. *Bioinformatics* **19**, 185-193.
- Bolstad, B.M., Collin, F., Brettschneider, J., Simpson, K., Cope, L., A., I.R., and Speed, T.P.** (2005). Quality Assessment of Affymetrix GeneChip Data. In *Bioinformatics and Computational Biology Solutions Using R and Bioconductor*, V.J.C. Robert Gentleman, Wolfgang Huber, Rafael A. Irizarry and Sandrine Dudoit, ed (New York: Springer), pp. 33-47.
- Boscoboinik, D., Szewczyk, A., Hensey, C., and Azzi, A.** (1991). Inhibition of cell-proliferation by alpha-tocopherol - role of protein-kinase-C. *J Biol Chem* **266**, 6188-6194.
- Botha, C.E.J., Cross, R.H.M., van Bel, A.J.E., and Peter, C.I.** (2000). Phloem loading in the sucrose-export-defective (SXD-1) mutant maize is limited by callose

- deposition at plasmodesmata in bundle sheath-vascular parenchyma interface. *Protoplasma* **214**, 65-72.
- Boumann, H.A., Damen, M.J.A., Versluis, C., Heck, A.J.R., de Kruijff, B., and de Kroon, A.I.P.M.** (2003). The two biosynthetic routes leading to phosphatidylcholine in yeast produce different sets of molecular species. Evidence for lipid remodeling. *Biochemistry* **42**, 3054-3059.
- Bouvier, F., Rahier, A., and Camara, B.** (2005). Biogenesis, molecular regulation and function of plant isoprenoids. *Prog Lipid Res* **44**, 357-429.
- Bradford, A., Atkinson, J., Fuller, N., and Rand, R.P.** (2003). The effect of vitamin E on the structure of membrane lipid assemblies. *Journal of Lipid Research* **44**, 1940-1945.
- Bramley, P.M., Elmadfa, I., Kafatos, A., Kelly, F.J., Manios, Y., Roxborough, H.E., Schuch, W., Sheehy, P.J.A., and Wagner, K.H.** (2000). Vitamin E. *Journal of the Science of Food and Agriculture* **80**, 913-938.
- Brigelius-Flohe, R.** (2009). Vitamin E: The shrew waiting to be tamed. *Free Radic. Biol. Med.* **46**, 543-554.
- Brigelius-Flohe, R., and Traber, M.G.** (1999). Vitamin E: function and metabolism. *Faseb Journal* **13**, 1145-1155.
- Broin, M., and Rey, P.** (2003). Potato plants lacking the CDSP32 plastidic thioredoxin exhibit overoxidation of the BAS1 2-cysteine peroxiredoxin and increased lipid peroxidation in thylakoids under photooxidative stress. *Plant Physiology* **132**, 1335-1343.
- Brot, N., and Weissbach, H.** (1991). Biochemistry of methionine sulfoxide residues in proteins. *Biofactors* **3**, 91-96.
- Brown, D.A., and London, E.** (1998). Functions of lipid rafts in biological membranes. *Annu. Rev. Cell Dev. Biol.* **14**, 111-136.
- Browse, J., and Somerville, C.** (1991). Glycerolipid synthesis - biochemistry and regulation. *Annual Review of Plant Physiology and Plant Molecular Biology* **42**, 467-506.

- Browse, J., Warwick, N., Somerville, C.R., and Slack, C.R.** (1986a). Fluxes through the prokaryotic and eukaryotic pathways of lipid synthesis in the 16:3 plant *Arabidopsis thaliana*. *Biochem. J.* **235**, 25-31.
- Browse, J., Mcconn, M., James, D., and Miquel, M.** (1993). Mutants of *Arabidopsis* deficient in the synthesis of alpha-linolenate - biochemical and genetic characterization of the endoplasmic-reticulum linoleoyl desaturase. *J Biol Chem* **268**, 16345-16351.
- Bucke, C.** (1968). Distribution and stability of alpha-tocopherol in subcellular fractions of broad bean leaves. *Phytochemistry* **7**, 693-700.
- Burton, G.W., and Ingold, K.U.** (1981). Autoxidation of biological molecules. 1. The antioxidant activity of vitamin-E and related chain-breaking phenolic antioxidants *in vitro*. *J Am Chem Soc* **103**, 6472-6477.
- Buttriss, J.L., and Diplock, A.T.** (1988). The alpha-tocopherol and phospholipid fatty acid content of rat liver subcellular membranes in vitamin e and selenium deficiency. *Biochim. Biophys. Acta* **963**, 61-69.
- Cachia, O., El Benna, J., Pedruzzi, E., Descomps, B., Gougerot-Pocidalo, M.A., and Leger, C.L.** (1998). alpha-tocopherol inhibits the respiratory burst in human monocytes - Attenuation of p47(phox) membrane translocation and phosphorylation. *J Biol Chem* **273**, 32801-32805.
- Caro, A., and Puntarulo, S.** (1996). Effect of in vivo iron supplementation on oxygen radical production by soybean roots. *Biochimica Et Biophysica Acta-General Subjects* **1291**, 245-251.
- Carpinelli, M.R., Hilton, D.J., Metcalf, D., Antonchuk, J.L., Hyland, C.D., Mifsud, S.L., Di Rago, L., Hilton, A.A., Willson, T.A., Roberts, A.W., Ramsay, R.G., Nicola, N.A., and Alexander, W.S.** (2004). Suppressor screen in Mpl(-/-) mice: c-Myb mutation causes supraphysiological production of platelets in the absence of thrombopoietin signaling. *Proc Natl Acad Sci U S A* **101**, 6553-6558.
- Chalker-Scott, L.** (1999). Environmental significance of anthocyanins in plant stress responses. *Photochemistry and Photobiology* **70**, 1-9.

- Chamberlain, R.S., and Spanner, D.C.** (1978). The effect of low temperatures on the phloem transport of radioactive assimilates in the stolon of *Saxifraga sarmentosa* L. *Plant, Cell and Environment*, 285-290.
- Chandra, V., Jasti, J., Kaur, P., Betzel, C., Srinivasan, A., and Singh, T.P.** (2002). First structural evidence of a specific inhibition of phospholipase A(2) by alpha-tocopherol (vitamin E) and its implications in inflammation: Crystal structure of the complex formed between phospholipase A(2) and alpha-tocopherol at 1.8 angstrom resolution. *J Mol Biol* **320**, 215-222.
- Chen, Z., and Rand, R.P.** (1997). The influence of cholesterol on phospholipid membrane curvature and bending elasticity. *Biophysical Journal* **73**, 267-276.
- Chen, Z., Fuller, N., and Rand, R.P.** (1997). Effects of cholesterol and lysolipids on phospholipid membrane curvature and bending elasticity. *Biophys. J.* **72**, Mp254-Mp254.
- Cheng, Z.G., Sattler, S., Maeda, H., Sakuragi, Y., Bryant, D.A., and DellaPenna, D.** (2003). Highly divergent methyltransferases catalyze a conserved reaction in tocopherol and plastoquinone synthesis in cyanobacteria and photosynthetic eukaryotes. *Plant Cell* **15**, 2343-2356.
- Chinnusamy, V., Ohta, M., Kanrar, S., Lee, B.H., Hong, X.H., Agarwal, M., and Zhu, J.K.** (2003). ICE1: a regulator of cold-induced transcriptome and freezing tolerance in *Arabidopsis*. *Genes & Development* **17**, 1043-1054.
- Choi, J.Y., Riekhof, W.R., Wu, W.I., and Voelker, D.R.** (2006). Macromolecular assemblies regulate non-vesicular phosphatidylserine traffic in yeast. *Biochemical Society Transactions* **34**, 404-408.
- Churchward, M.A., Rogasevskaja, T., Hofgen, J., Bau, J., and Coorsen, J.R.** (2005). Cholesterol facilitates the native mechanism of Ca²⁺-triggered membrane fusion. *J Cell Sci* **118**, 4833-4848.
- Cohn, W.** (1997). Bioavailability of vitamin E. *Eur J Clin Nutr* **51**, S80-S85.
- Collakova, E., and DellaPenna, D.** (2001). Isolation and functional analysis of homogentisate phytyltransferase from *Synechocystis* sp PCC 6803 and *Arabidopsis*. *Plant Physiol.* **127**, 1113-1124.

- Collakova, E., and DellaPenna, D.** (2003a). Homogentisate phytyltransferase activity is limiting for tocopherol biosynthesis in *Arabidopsis*. *Plant Physiol.* **131**, 632-642.
- Collakova, E., and DellaPenna, D.** (2003b). The role of homogentisate phytyltransferase and other tocopherol pathway enzymes in the regulation of tocopherol synthesis during abiotic stress. *Plant Physiology* **133**, 930-940.
- Collin, V.C., Eymery, F., Genty, B., Rey, P., and Havaux, M.** (2008). Vitamin E is essential for the tolerance of *Arabidopsis thaliana* to metal-induced oxidative stress. *Plant Cell and Environment* **31**, 244-257.
- Collins, R.T., and Cohen, S.M.** (2005). A genetic screen in *Drosophila* for identifying novel components of the Hedgehog signaling pathway. *Genetics* **170**, 173-184.
- Cook, D., Fowler, S., Fiehn, O., and Thomashow, M.F.** (2004). A prominent role for the CBF cold response pathway in configuring the low-temperature metabolome of *Arabidopsis*. *Proc Natl Acad Sci U S A* **101**, 15243-15248.
- Dasilva, E.J., and Jensen, A.** (1971). Content of alpha-tocopherol in some blue-green algae. *Biochimica Et Biophysica Acta* **239**, 345-&.
- de Kroon, A.I.P.M.** (2007). Metabolism of phosphatidylcholine and its implications for lipid acyl chain composition in *Saccharomyces cerevisiae*. *Biochimica Et Biophysica Acta-Molecular and Cell Biology of Lipids* **1771**, 343-352.
- DellaPenna, D.** (1999). Nutritional genomics: Manipulating plant micronutrients to improve human health. *Science* **285**, 375-379.
- DellaPenna, D.** (2005a). A decade of progress in understanding vitamin E synthesis in plants. *J Plant Physiol* **162**, 729-737.
- DellaPenna, D.** (2005b). Progress in the dissection and manipulation of vitamin E synthesis. *Trends Plant Sci* **10**, 574-579.
- DellaPenna, D., and Pogson, B.J.** (2006). Vitamin synthesis in plants: Tocopherols and carotenoids. *Annu. Rev. Plant Biol.* **57**, 711-738.

- DellaPenna, D., and Last, R.L.** (2006). Progress in the dissection and manipulation of plant vitamin E biosynthesis. *Physiologia Plantarum* **126**, 356-368.
- DeLong, J.M., and Steffen, K.L.** (1997). Photosynthetic function, lipid peroxidation, and alpha-tocopherol content in spinach leaves during exposure to UV-B radiation. *Can J Plant Sci* **77**, 453-459.
- DeLong, J.M., Prange, R.K., Hodges, D.M., Forney, C.F., Bishop, M.C., and Quilliam, M.** (2002). Using a modified ferrous oxidation-xylenol orange (FOX) assay for detection of lipid hydroperoxides in plant tissue. *Journal of Agricultural and Food Chemistry* **50**, 248-254.
- Demmig-Adams, B., and Adams, W.W.** (2002). Antioxidants in photosynthesis and human nutrition. *Science* **298**, 2149-2153.
- Devaiah, B.N., Karthikeyan, A.S., and Raghothama, K.G.** (2007). WRKY75 transcription factor is a modulator of phosphate acquisition and root development in *Arabidopsis*. *Plant Physiology* **143**, 1789-1801.
- Dilley, R.A., and Crane, F.L.** (1963). Subcellular distribution of alpha-tocopherol in spinach and lilac leaf tissue. *Plant Physiology* **38**, 452-&.
- Doherty, C.J., Van Buskirk, H.A., Myers, S.J., and Thomashow, M.F.** (2009). Roles for *Arabidopsis* CAMTA transcription factors in cold-regulated gene expression and freezing tolerance. *Plant Cell* **21**, 972-984.
- Dong, J., Chen, C., and Chen, Z.** (2003). Expression profiles of the Arabidopsis WRKY gene superfamily during plant defense response. *Plant Mol Biol*, 21-37.
- Dong, X.Y., Hong, Z.L., Sivaramakrishnan, M., Mahfouz, M., and Verma, D.P.S.** (2005). Callose synthase (CalS5) is required for exine formation during microgametogenesis and for pollen viability in *Arabidopsis*. *Plant Journal* **42**, 315-328.
- Dormann, P.** (2007). Functional diversity of tocochromanols in plants. *Planta* **225**, 269-276.

- Dormann, P., HoffmannBenning, S., Balbo, I., and Benning, C.** (1995). Isolation and characterization of an *Arabidopsis* mutant deficient in the thylakoid lipid digalactosyl diacylglycerol. *Plant Cell* **7**, 1801-1810.
- Dos Santos, C.V., Cuine, S., Rouhier, N., and Rey, P.** (2005). The *Arabidopsis* plastidic methionine sulfoxide reductase B proteins. Sequence and activity characteristics, comparison of the expression with plastidic methionine sulfoxide reductase A, and induction by photooxidative stress. *Plant Physiology* **138**, 909-922.
- Douglas, C.E., Chan, A.C., and Choy, P.C.** (1986). Vitamin e inhibits platelet phospholipase A2. *Biochim. Biophys. Acta* **876**, 639-645.
- Enns, L.C., Kanaoka, M.M., Torii, K.U., Comai, L., Okada, K., and Cleland, R.E.** (2005). Two callose synthases, GSL1 and GSL5, play an essential and redundant role in plant and pollen development and in fertility. *Plant Molecular Biology* **58**, 333-349.
- Eriksson, M., Moseley, J.L., Tottey, S., del Campo, J.A., Quinn, J., Kim, Y., and Merchant, S.** (2004). Genetic dissection of nutritional copper signaling in chlamydomonas distinguishes regulatory and target genes. *Genetics* **168**, 795-807.
- Erin, A.N., Spirin, M.M., Tabidze, L.V., and Kagan, V.E.** (1983). Formation of complexes of alpha-tocopherol with fatty acids - the possible mechanism of stabilization of biomembranes by vitamin e. *Biochemistry-Moscow* **48**, 1597-1602.
- Erin, A.N., Gorbunov, N.V., Brusovanik, V.I., Tyurin, V.A., and Prilipko, L.L.** (1986). Stabilization of synaptic membranes by alpha-tocopherol against the damaging action of phospholipases - possible mechanism of biological action of vitamin e. *Brain Research* **398**, 85-90.
- Eulgem, T., and Somssich, I.E.** (2007). Networks of WRKY transcription factors in defense signaling. *Current Opinion in Plant Biology* **10**, 366-371.
- Eulgem, T., Rushton, P.J., Robatzek, S., and Somssich, I.E.** (2000). The WRKY superfamily of plant transcription factors. *Trends in Plant Science* **5**, 199-206.
- Evans, H.M., and Bishop, K.S.** (1922). On the existence of a hitherto unrecognized dietary factor essential for reproduction. *Science* **56**, 650-651.

- Falcone, D.L., Gibson, S., Lemieux, B., and Somerville, C. (1994).** Identification of a gene that complements an *Arabidopsis* mutant deficient in chloroplast omega-6 desaturase activity. *Plant Physiology* **106**, 1453-1459.
- Ferguson, D.J., and Krzycki, J.A. (1997).** Reconstitution of trimethylamine-dependent coenzyme M methylation with the trimethylamine corrinoid protein and the isozymes of methyltransferase II from *Methanosarcina barkeri*. *Journal of Bacteriology* **179**, 846-852.
- Fisk, I.D., White, D.A., Carvalho, A., and Gray, D.A. (2006).** Tocopherol - An intrinsic component of sunflower seed oil bodies. *J. Am. Oil Chem. Soc.* **83**, 341-344.
- Foyer, C.H., LopezDelgado, H., Dat, J.F., and Scott, I.M. (1997).** Hydrogen peroxide- and glutathione-associated mechanisms of acclimatory stress tolerance and signalling. *Physiologia Plantarum* **100**, 241-254.
- Foyer, C.H., Vanacker, H., Gomez, L.D., and Harbinson, J. (2002).** Regulation of photosynthesis and antioxidant metabolism in maize leaves at optimal and chilling temperatures: review. *Plant Physiology and Biochemistry* **40**, 659-668.
- Fryer, M.J. (1992).** The antioxidant effects of thylakoid vitamin-E (alpha-tocopherol). *Plant Cell and Environment* **15**, 381-392.
- Fryer, M.J., Ball, L., Oxborough, K., Karpinski, S., Mullineaux, P.M., and Baker, N.R. (2003).** Control of Ascorbate Peroxidase 2 expression by hydrogen peroxide and leaf water status during excess light stress reveals a functional organisation of *Arabidopsis* leaves. *Plant Journal* **33**, 691-705.
- Fukuzawa, K. (2008).** Dynamics of lipid peroxidation and antioxidant of alpha-tocopherol in membranes. *Journal of Nutritional Science and Vitaminology* **54**, 273-285.
- Giaquinta, R.T., and Geiger, D.R. (1973).** Mechanism of inhibition of translocation by localized chilling. *Plant Physiology* **51**, 372-377.
- Gibson, S., Arondel, V., Iba, K., and Somerville, C. (1994).** Cloning of a temperature-regulated gene encoding a chloroplast omega-3 desaturase from *Arabidopsis thaliana*. *Plant Physiology* **106**, 1615-1621.

- Gilmour, S.J., Sebolt, A.M., Salazar, M.P., Everard, J.D., and Thomashow, M.F.** (2000). Overexpression of the Arabidopsis CBF3 transcriptional activator mimics multiple biochemical changes associated with cold acclimation. *Plant Physiology* **124**, 1854-1865.
- Goetz, J.G., and Nabi, I.R.** (2006). Interaction of the smooth endoplasmic reticulum and mitochondria. *Biochemical Society Transactions* **34**, 370-373.
- Gohil, K., Schock, B.C., Chakraborty, A.A., Terasawa, Y., Raber, J., Farese, R.V., Packer, L., Cross, C.E., and Traber, M.G.** (2003). Gene expression profile of oxidant stress and neurodegeneration in transgenic mice deficient in alpha-tocopherol transfer protein. *Free Radical Biology and Medicine* **35**, 1343-1354.
- Goldschmidt, E.E., and Huber, S.C.** (1992). Regulation of photosynthesis by end-product accumulation in leaves of plants storing starch, sucrose, and hexose sugars. *Plant Physiology* **99**, 1443-1448.
- Gorbunov, N.V., Kagan, V.E., Alekseev, S.M., and Erin, A.N.** (1991). Role of the isoprenoid chain of lateral mobility of alpha-tocopherol in the lipid bilayer. *Bull. Exp. Biol. Med.* **112**, 946-949.
- Gotoda, T., Arita, M., Arai, H., Inoue, K., Yokota, T., Fukuo, Y., Yazaki, Y., and Yamada, N.** (1995). Adult-onset spinocerebellar dysfunction caused by a mutation in the gene for the alpha-tocopherol-transfer protein. *New England Journal of Medicine* **333**, 1313-1318.
- Grasses, T., Grimm, B., Koroleva, O., and Jahns, P.** (2001). Loss of alpha-tocopherol in tobacco plants with decreased geranylgeranyl reductase activity does not modify photosynthesis in optimal growth conditions but increases sensitivity to high-light stress. *Planta* **213**, 620-628.
- Gray, G.R., and Heath, D.** (2005). A global reorganization of the metabolome in Arabidopsis during cold acclimation is revealed by metabolic fingerprinting. *Physiologia Plantarum* **124**, 236-248.
- Grusak, M.A., and DellaPenna, D.** (1999). Improving the nutrient composition of plants to enhance human nutrition and health. *Annu Rev Plant Physiol Plant Mol Biol* **50**, 133-161.

- Guo, Y., Cai, Z., and Gan, S.** (2004). Transcriptome of *Arabidopsis* leaf senescence. *Plant Cell and Environment* **27**, 521-549.
- Hajnoczky, G., Csordas, G., and Yi, M.** (2002). Old players in a new role: mitochondria-associated membranes, VDAC, and ryanodine receptors as contributors to calcium signal propagation from endoplasmic reticulum to the mitochondria. *Cell Calcium* **32**, 363-377.
- Ham, A.J.L., and Liebler, D.C.** (1995). Vitamin e oxidation in rat liver mitochondria. *Biochemistry* **34**, 5754-5761.
- Ham, A.J.L., and Liebler, D.C.** (1997). Antioxidant reactions of vitamin E in the perfused rat liver: Product distribution and effect of dietary vitamin E supplementation. *Archives of Biochemistry and Biophysics* **339**, 157-164.
- Hannah, M.A., Wiese, D., Freund, S., Fiehn, O., Heyer, A.G., and Hinch, D.K.** (2006). Natural genetic variation of freezing tolerance in *Arabidopsis*. *Plant Physiology* **142**, 98-112.
- Haritatos, E., Medville, R., and Turgeon, R.** (2000). Minor vein structure and sugar transport in *Arabidopsis thaliana*. *Planta* **211**, 105-111.
- Hartel, H., Dormann, P., and Benning, C.** (2000). DGD1-independent biosynthesis of extraplastidic galactolipids after phosphate deprivation in *Arabidopsis*. *Proc Natl Acad Sci U S A* **97**, 10649-10654.
- Harwood, J.L.** (1996). Recent advances in the biosynthesis of plant fatty acids. *Biochimica Et Biophysica Acta-Lipids and Lipid Metabolism* **1301**, 7-56.
- Havaux, M.** (1998). Carotenoids as membrane stabilizers in chloroplasts. *Trends Plant Sci* **3**, 147-151.
- Havaux, M., and Niyogi, K.K.** (1999). The violaxanthin cycle protects plants from photooxidative damage by more than one mechanism. *Proc Natl Acad Sci U S A* **96**, 8762-8767.
- Havaux, M., Eymery, F., Porfirova, S., Rey, P., and Dormann, P.** (2005). Vitamin E protects against photoinhibition and photooxidative stress in *Arabidopsis thaliana*. *Plant Cell* **17**, 3451-3469.

- Hazel, J.R.** (1995). Thermal adaptation in biological-membranes - Is homeoviscous adaptation the explanation. *Annual Review of Physiology* **57**, 19-42.
- Heppard, E.P., Kinney, A.J., Stecca, K.L., and Miao, G.H.** (1996). Developmental and growth temperature regulation of two different microsomal omega-6 desaturase genes in soybeans. *Plant Physiology* **110**, 311-319.
- Herbers, K., and Sonnewald, U.** (1998). Molecular determinants of sink strength. *Current Opinion in Plant Biology* **1**, 207-216.
- Herrmann, K.M., and Weaver, L.M.** (1999). The shikimate pathway. *Annu Rev Plant Physiol Plant Mol Biol* **50**, 473-503.
- Hibberd, J.M., and Quick, W.P.** (2002). Characteristics of C-4 photosynthesis in stems and petioles of C-3 flowering plants. *Nature* **415**, 451-454.
- Hofius, D., Hajirezaei, M.R., Geiger, M., Tschiersch, H., Melzer, M., and Sonnewald, U.** (2004). RNAi-mediated tocopherol deficiency impairs photoassimilate export in transgenic potato plants. *Plant Physiology* **135**, 1256-1268.
- Hohnjec, N., Lenz, F., Fehlberg, V., Vieweg, M.F., Baier, M.C., Hause, B., and Kuster, H.** (2009). The signal peptide of the *Medicago truncatula* modular nodulin MtNOD25 operates as an address label for the specific targeting of proteins to nitrogen-fixing symbiosomes. *Molecular Plant-Microbe Interactions* **22**, 63-72.
- Hong, Z.L., Delauney, A.J., and Verma, D.P.S.** (2001). A cell plate specific callose synthase and its interaction with phragmoplastin. *Plant Cell* **13**, 755-768.
- Horvath, G., Wessjohann, L., Bigirimana, J., Jansen, M., Guisez, Y., Caubergs, R., and Horemans, N.** (2006). Differential distribution of tocopherols and tocotrienols in photosynthetic and non-photosynthetic tissues. *Phytochemistry* **67**, 1185-1195.
- Hosomi, A., Arita, M., Sato, Y., Kiyose, C., Ueda, T., Igarashi, O., Arai, H., and Inoue, K.** (1997). Affinity for alpha-tocopherol transfer protein as a determinant of the biological activities of vitamin E analogs. *Febs Letters* **409**, 105-108.
- Hsu, J.C.** (1996). *Multiple Comparisons: Theory and Methods*. (London: Chapman & Hall).

- Huang, L.J., Chen, X.Y., Rim, Y., Han, X., Cho, W.K., Kim, S.W., and Kim, J.Y.** (2009). *Arabidopsis* glucan synthase-like 10 functions in male gametogenesis. *Journal of Plant Physiology* **166**, 344-352.
- Hugly, S., and Somerville, C.** (1992). A role for membrane lipid polyunsaturation in chloroplast biogenesis at low temperature. *Plant Physiology* **99**, 197-202.
- Humphrey, T.V., Bonetta, D.T., and Goring, D.R.** (2007). Sentinels at the wall: cell wall receptors and sensors. *New Phytologist* **176**, 7-21.
- Hurry, V., Strand, A., Furbank, R., and Stitt, M.** (2000). The role of inorganic phosphate in the development of freezing tolerance and the acclimatization of photosynthesis to low temperature is revealed by the *pho* mutants of *Arabidopsis thaliana*. *Plant Journal* **24**, 383-396.
- Hurry, V., Druart, N., Cavaco, A., Gardestrom, P., and Strand, A.** (2002). Photosynthesis at low temperatures: a case study with *Arabidopsis*. In *Plant Cold Hardiness*, E.T.P. Li Paul H, ed (New York, Boston, Dordrecht, London, Moscow: Kluwer Academic/Plenum Publishers), pp. 161-179.
- Hyland, S., Muller, D., Hayton, S., Stoecklin, E., and Barella, L.** (2006). Cortical gene expression in the vitamin E-deficient rat: Possible mechanisms for the electrophysiological abnormalities of visual and neural function. *Annals of Nutrition and Metabolism* **50**, 433-441.
- Iba, K., Gibson, S., Nishiuchi, T., Fuse, T., Nishimura, M., Arondel, V., Hugly, S., and Somerville, C.** (1993). A gene encoding a chloroplast omega-3-fatty-acid desaturase complements alterations in fatty-acid desaturation and chloroplast copy number of the *fad7* mutant of *Arabidopsis thaliana*. *J Biol Chem* **268**, 24099-24105.
- Irizarry, R.A., Hobbs, B., Collin F., Beazer-Barclay, Y.D., Antonellis, K.J., Scherf, U., and T.P., S.** (2003b). Exploration, normalization, and summaries of high density oligonucleotide array probe level data. *Biostatistics*, 249-264.
- Ishizaki-Nishizawa, O., Fujii, T., Azuma, M., Sekiguchi, K., Murata, N., Ohtani, T., and Toguri, T.** (1996). Low-temperature resistance of higher plants is significantly enhanced by a nonspecific cyanobacterial desaturase. *Nature Biotechnology* **14**, 1003-1006.

- Jacobs, A.K., Lipka, V., Burton, R.A., Panstruga, R., Strizhov, N., Schulze-Lefert, P., and Fincher, G.B.** (2003). An *Arabidopsis* callose synthase, GSL5, is required for wound and papillary callose formation. *Plant Cell* **15**, 2503-2513.
- James, D.W., and Dooner, H.K.** (1990). Isolation of EMS-induced mutants in *Arabidopsis* altered in seed fatty-acid composition. *Theor Appl Genet* **80**, 241-245.
- Jander, G., Norris, S.R., Rounsley, S.D., Bush, D.F., Levin, I.M., and Last, R.L.** (2002). *Arabidopsis* map-based cloning in the post-genome era. *Plant Physiol.* **129**, 440-450.
- Jervis, K.M., and Robaire, B.** (2004). The effects of long-term vitamin E treatment on gene expression and oxidative stress damage in the aging brown Norway rat epididymis. *Biology of Reproduction* **71**, 1088-1095.
- Jiang, Q., Elson-Schwab, I., Courtemanche, C., and Ames, B.N.** (2000). Gamma-tocopherol and its major metabolite, in contrast to alpha-tocopherol, inhibit cyclooxygenase activity in macrophages and epithelial cells. *Proc Natl Acad Sci U S A* **97**, 11494-11499.
- Jiang, Q., Christen, S., Shigenaga, M.K., and Ames, B.N.** (2001). Gamma-Tocopherol, the major form of vitamin E in the US diet, deserves more attention. *Am. J. Clin. Nutr.* **74**, 714-722.
- Jiang, Z.Y., Hunt, J.V., and Wolff, S.P.** (1992). Ferrous ion oxidation in the presence of xylenol orange for detection of lipid hydroperoxide in low-density-lipoprotein. *Anal. Biochem.* **202**, 384-389.
- Johnson, G., and Williams, J.P.** (1989). Effect of growth temperature on the biosynthesis of chloroplastic galactosyldiacylglycerol molecular species in *Brassica napus* leaves. *Plant Physiol.* **91**, 924-929.
- Jones, M.G.K., Outlaw, W.H., and Lowry, O.H.** (1977). Enzymic assay of 10^{-7} to 10^{-14} moles of sucrose in plant-tissues. *Plant Physiology* **60**, 379-383.
- Kagan, V.E.** (1989). Tocopherol stabilizes membrane against phospholipase-a, free fatty-acids, and lysophospholipids. *Ann. N. Y. Acad. Sci.* **570**, 121-135.

- KamalEldin, A., and Appelqvist, L.A.** (1996). The chemistry and antioxidant properties of tocopherols and tocotrienols. *Lipids* **31**, 671-701.
- Kanwischer, M., Porfirova, S., Bergmuller, E., and Dormann, P.** (2005). Alterations in tocopherol cyclase activity in transgenic and mutant plants of *Arabidopsis* affect tocopherol content, tocopherol composition, and oxidative stress. *Plant Physiol.* **137**, 713-723.
- Kaplan, F., Kopka, J., Sung, D.Y., Zhao, W., Popp, M., Porat, R., and Guy, C.L.** (2007). Transcript and metabolite profiling during cold acclimation of *Arabidopsis* reveals an intricate relationship of cold-regulated gene expression with modifications in metabolite content. *Plant Journal* **50**, 967-981.
- Keles, Y., and Oncel, I.** (2002). Response of antioxidative defence system to temperature and water stress combinations in wheat seedlings. *Plant Science* **163**, 783-790.
- Kempna, P., Reiter, E., Arock, M., Azzi, A., and Zingg, J.M.** (2004). Inhibition of HMC-1 mast cell proliferation by vitamin E - Involvement of the protein kinase B pathway. *Journal of Biological Chemistry* **279**, 50700-50709.
- Khodakovskaya, M., McAvoy, R., Peters, J., Wu, H., and Li, Y.** (2006). Enhanced cold tolerance in transgenic tobacco expressing a chloroplast omega-3 fatty acid desaturase gene under the control of a cold-inducible promoter. *Planta* **223**, 1090-1100.
- Kim, K.C., Lai, Z.B., Fan, B.F., and Chen, Z.X.** (2008). Arabidopsis WRKY38 and WRKY62 transcription factors interact with histone deacetylase 19 in basal defense. *Plant Cell* **20**, 2357-2371.
- Kjellberg, J.M., Trimborn, M., Andersson, M., and Sandelius, A.S.** (2000). Acyl-CoA dependent acylation of phospholipids in the chloroplast envelope. *Biochimica Et Biophysica Acta-Molecular and Cell Biology of Lipids* **1485**, 100-110.
- Knight, H., Trewavas, A.J., and Knight, M.R.** (1996). Cold calcium signaling in *Arabidopsis* involves two cellular pools and a change in calcium signature after acclimation. *Plant Cell* **8**, 489-503.
- Knox, J.P., and Dodge, A.D.** (1985). Singlet oxygen and plants. *Phytochemistry* **24**, 889-896.

- Koch, K.E.** (1996). Carbohydrate-modulated gene expression in plants. *Annual Review of Plant Physiology and Plant Molecular Biology* **47**, 509-540.
- Kodama, H., Hamada, T., Horiguchi, G., Nishimura, M., and Iba, K.** (1994). Genetic enhancement of cold tolerance by expression of a gene for chloroplast omega-3-fatty-acid desaturase in transgenic tobacco. *Plant Physiology* **105**, 601-605.
- Kodama, H., Horiguchi, G., Nishiuchi, T., Nishimura, M., and Iba, K.** (1995). Fatty acid desaturation during chilling acclimation is one of the factors involved in conferring low-temperature tolerance to young tobacco leaves. *Plant Physiology* **107**, 1177-1185.
- Koiwai, H., Nakaminami, K., Seo, M., Mitsuhashi, W., Toyomasu, T., and Koshiba, T.** (2004). Tissue-specific localization of an abscisic acid biosynthetic enzyme, AAO3, in *Arabidopsis*. *Plant Physiology* **134**, 1697-1707.
- Kol, M.A., Kuster, D.W.D., Boumann, H.A., de Cock, H., Heck, A.J.R., de Kruijff, B., and de Kroon, A.I.P.M.** (2004). Uptake and remodeling of exogenous phosphatidylethanolamine in *E. coli*. *Biochimica Et Biophysica Acta-Molecular and Cell Biology of Lipids* **1636**, 205-212.
- Krapp, A., and Stitt, M.** (1995). An evaluation of direct and indirect mechanisms for the sink regulation of photosynthesis in spinach - Changes in gas exchange, carbohydrates, metabolites, enzyme activities and steady-state transcript levels after cold-girdling source leaves. *Planta* **195**, 313-323.
- Krause, G.H., and Weis, E.** (1984). Chlorophyll fluorescence as a tool in plant physiology. 2. Interpretation of fluorescence signals. *Photosynthesis Research* **5**, 139-157.
- Kruk, J., and Strzalka, K.** (1995). Occurrence and function of alpha-tocopherol quinone in plants. *J Plant Physiol* **145**, 405-409.
- Kunst, L., Browse, J., and Somerville, C.** (1989). A mutant of *Arabidopsis* deficient in desaturation of palmitic acid in leaf lipids. *Plant Physiology* **90**, 943-947.
- Lee, B.H., Henderson, D.A., and Zhu, J.K.** (2005). The *Arabidopsis* cold-responsive transcriptome and its regulation by ICE1. *Plant Cell* **17**, 3155-3175.

- Leegood, R.C., and Furbank, R.T.** (1986). Stimulation of photosynthesis by 2-percent oxygen at low temperatures is restored by phosphate. *Planta* **168**, 84-93.
- Lemieux, B., Miquel, M., Somerville, C., and Browse, J.** (1990). Mutants of *Arabidopsis* with alterations in seed lipid fatty acid composition. *Theor Appl Genet* **80**, 234-240.
- Levine, T.** (2004). Short-range intracellular trafficking of small molecules across endoplasmic reticulum junctions. *Trends Cell Biol* **14**, 483-490.
- Leyva, A., Jarillo, J.A., Salinas, J., and Martinezapater, J.M.** (1995). Low-temperature induces the accumulation of phenylalanine ammonia lyase and chalcone synthase messenger-Rnas of *Arabidopsis thaliana* in a light-dependent manner. *Plant Physiology* **108**, 39-46.
- Li, X., Zhang, Y.L., Clarke, J.D., Li, Y., and Dong, X.N.** (1999). Identification and cloning of a negative regulator of systemic acquired resistance, SNIII, through a screen for suppressors of npr1-1. *Cell* **98**, 329-339.
- Lichtenthaler, H.K., Prenzel, U., Douce, R., and Joyard, J.** (1981a). Localization of prenylquinones in the envelope of spinach-chloroplasts. *Biochimica Et Biophysica Acta* **641**, 99-105.
- Liebler, D.C.** (1993). The role of metabolism in the antioxidant function of vitamin-e. *Critical Reviews in Toxicology* **23**, 147-169.
- Liebler, D.C., and Burr, J.A.** (1992). Oxidation of vitamin-E during iron-catalyzed lipid-peroxidation - Evidence for electron-transfer reactions of the tocopheroxyl radical. *Biochemistry (Mosc.)* **31**, 8278-8284.
- Liebler, D.C., and Burr, J.A.** (2000). Antioxidant reactions of alpha-tocopherolhydroquinone. *Lipids* **35**, 1045-1047.
- Lin, T.P., Caspar, T., Somerville, C., and Preiss, J.** (1988). Isolation and characterization of a starchless mutant of *Arabidopsis thaliana* (L) Heynh lacking ADP-glucose pyrophosphorylase activity. *Plant Physiology* **86**, 1131-1135.

- Lowther, W.T., Weissbach, H., Etienne, F., Brot, N., and Matthews, B.W.** (2002). The mirrored methionine sulfoxide reductases of *Neisseria gonorrhoeae* pilB. *Nature Structural Biology* **9**, 348-352.
- Lu, B.B., Xu, C.C., Awai, K., Jones, A.D., and Benning, C.** (2007b). A small ATPase protein of *Arabidopsis*, TGD3, involved in chloroplast lipid import. *J Biol Chem* **282**, 35945-35953.
- Macdonald, J.I.S., and Sprecher, H.** (1991). Phospholipid fatty acid remodeling in mammalian cells. *Biochimica Et Biophysica Acta* **1084**, 105-121.
- Machlin, L.J., Filipski, R., Nelson, J., Horn, L.R., and Brin, M.** (1977). Effects of a prolonged vitamin-E-deficiency in rat. *Journal of Nutrition* **107**, 1200-1208.
- Maeda, H.** (2006). Vitamin E functions in photosynthetic organisms. In Department of Molecular Biology and Biochemistry (East Lansing: Michigan State University).
- Maeda, H., and DellaPenna, D.** (2007). Tocopherol functions in photosynthetic organisms. *Current Opinion in Plant Biology* **10**, 260-265.
- Maeda, H., Sakuragi, Y., Bryant, D.A., and DellaPenna, D.** (2005). Tocopherols protect *Synechocystis* sp strain PCC 6803 from lipid peroxidation. *Plant Physiology* **138**, 1422-1435.
- Maeda, H., Song, W., Sage, T.L., and DellaPenna, D.** (2006). Tocopherols play a crucial role in low-temperature adaptation and phloem loading in *Arabidopsis*. *Plant Cell* **18**, 2710-2732.
- Maeda, H., Sage, T.L., Isaac, G., Welti, R., and DellaPenna, D.** (2008). Tocopherols modulate extraplastidic polyunsaturated fatty acid metabolism in *Arabidopsis* at low temperature. *Plant Cell* **20**, 452-470.
- Mahoney, C.W., and Azzi, A.** (1988). Vitamin-E inhibits protein kinase-C activity. *Biochem. Biophys. Res. Commun.* **154**, 694-697.
- Mare, C., Mazzucotelli, E., Crosatti, C., Francia, E., Stanca, A.M., and Cattivelli, L.** (2004). Hv-WRKY38: a new transcription factor involved in cold- and drought-response in barley. *Plant Mol Biol*, 399-416.

- Martin, F.W.** (1959). Staining and observing pollen tubes in the style by means of fluorescence. *Stain Technology* **34**, 125-128.
- Maxwell, K., and Johnson, G.N.** (2000). Chlorophyll fluorescence - a practical guide. *Journal of Experimental Botany* **51**, 659-668.
- McConn, M., and Browse, J.** (1996). The critical requirement for linolenic acid is pollen development, not photosynthesis, in an *Arabidopsis* mutant. *Plant Cell* **8**, 403-416.
- McCurdy, D.W., Patrick, J.W., and Offler, C.** (2008). Wall ingrowth formation in transfer cells: novel examples of localized wall deposition in plant cells. *Curr Opin Plant Biol*, 653-661.
- Merzlyak, M.N., and Chivkunova, O.B.** (2000). Light-stress-induced pigment changes and evidence for anthocyanin photoprotection in apples. *Journal of Photochemistry and Photobiology B-Biology* **55**, 155-163.
- Miquel, M., and Browse, J.** (1992). *Arabidopsis* mutants deficient in polyunsaturated fatty acid synthesis-biochemical and genetic characterization of a plant oleoyl-phosphatidylcholine desaturase. *Journal of Biological Chemistry* **267**, 1502-1509.
- Miquel, M., James, D., Dooner, H., and Browse, J.** (1993). *Arabidopsis* requires polyunsaturated lipids for low temperature survival. *Proc Natl Acad Sci U S A* **90**, 6208-6212.
- Mongrand, S., Cassagne, C., and Bessoule, J.J.** (2000). Import of lysophosphatidylcholine into chloroplasts likely at the origin of eukaryotic plastidial lipids. *Plant Physiol.* **122**, 845-852.
- Monroy, A.F., and Dhindsa, R.S.** (1995). Low temperature signal transduction - Induction of cold acclimation-specific genes of alfalfa by calcium at 25-degrees-C. *Plant Cell* **7**, 321-331.
- Monroy, A.F., Sarhan, F., and Dhindsa, R.S.** (1993). Cold-induced changes in freezing tolerance, protein phosphorylation, and gene expression - Evidence for a role of calcium. *Plant Physiology* **102**, 1227-1235.

- Moskovitz, J., Rahman, M.A., Strassman, J., Yancey, S.O., Kushner, S.R., Brot, N., and Weissbach, H.** (1995). *Escherichia coli* peptide methionine sulfoxide reductase gene regulation of expression and role in protecting against oxidative damage. *Journal of Bacteriology* **177**, 502-507.
- Muller, P., Li, X.P., and Niyogi, K.K.** (2001). Non-photochemical quenching. A response to excess light energy. *Plant Physiology* **125**, 1558-1566.
- Muller-Moule, P., Havaux, M., and Niyogi, K.K.** (2003). Zeaxanthin deficiency enhances the high light sensitivity of an ascorbate-deficient mutant of *Arabidopsis*. *Plant Physiology* **133**, 748-760.
- Munne-Bosch, S.** (2005a). The role of alpha-tocopherol in plant stress tolerance. *J Plant Physiol* **162**, 743-748.
- Munne-Bosch, S.** (2005b). Linking tocopherols with cellular signaling in plants - RNAi-mediated tocopherol deficiency impairs photoassimilate export in transgenic potato plants. *New Phytol* **166**, 363-366.
- Munne-Bosch, S., and Alegre, L.** (2000). Changes in carotenoids, tocopherols and diterpenes during drought and recovery, and the biological significance of chlorophyll loss in *Rosmarinus officinalis* plants. *Planta* **210**, 925-931.
- Munne-Bosch, S., and Alegre, L.** (2002). The function of tocopherols and tocotrienols in plants. *Critical Reviews in Plant Sciences* **21**, 31-57.
- Munne-Bosch, S., and Falk, J.** (2004). New insights into the function of tocopherols in plants. *Planta* **218**, 323-326.
- Murakami, Y., Tsuyama, M., Kobayashi, Y., Kodama, H., and Iba, K.** (2000). Trienoic fatty acids and plant tolerance of high temperature. *Science* **287**, 476-479.
- Murata, N., and Los, D.A.** (1997). Membrane fluidity and temperature perception. *Plant Physiology* **115**, 875-879.
- Mushegian, A.R., and Koonin, E.V.** (1996). A minimal gene set for cellular life derived by comparison of complete bacterial genomes. *Proc Natl Acad Sci U S A* **93**, 10268-10273.

- Narvaez-Vasquez, J., and Ryan, C.A.** (2004). The cellular localization of prosystemin: a functional role for phloem parenchyma in systemic wound signaling. *Planta* **218**, 360-369.
- Nell, S., Bahtz, R., Bossecker, A., Kipp, A., Landes, N., Bumke-Vogt, C., Halligan, E., Lunec, J., and Brigelius-Flohe, R.** (2007). PCR-verified microarray analysis and functional in vitro studies indicate a role of alpha-tocopherol in vesicular transport. *Free Radical Research* **41**, 930-942.
- Nguema-Ona, E., Bannigan, A., Chevalier, L., Baskin, T.I., and Driouich, A.** (2007). Disruption of arabinogalactan proteins disorganizes cortical microtubules in the root of *Arabidopsis thaliana*. *Plant Journal* **52**, 240-251.
- Nishida, I., and Murata, N.** (1996). Chilling sensitivity in plants and cyanobacteria: The crucial contribution of membrane lipids. *Annual Review of Plant Physiology and Plant Molecular Biology* **47**, 541-568.
- Nishikawa, S.I., Zinkl, G.M., Swanson, R.J., Maruyama, D., and Preuss, D.** (2005). Callose (beta-1,3 glucan) is essential for *Arabidopsis* pollen wall patterning, but not tube growth. *BMC Plant Biology* **5**.
- Nishimura, M.T., Stein, M., Hou, B.H., Vogel, J.P., Edwards, H., and Somerville, S.C.** (2003). Loss of a callose synthase results in salicylic acid-dependent disease resistance. *Science* **301**, 969-972.
- Niyogi, K.K., Grossman, A.R., and Bjorkman, O.** (1998). *Arabidopsis* mutants define a central role for the xanthophyll cycle in the regulation of photosynthetic energy conversion. *Plant Cell* **10**, 1121-1134.
- Offler, C.E., McCurdy, D.W., Patrick, J.W., and Talbot, M.J.** (2002). Transfer cells: cells specialized for a special purpose. *Annu. Rev. Plant Biol.*, 431-454.
- Ohlrogge, J., and Browse, J.** (1995). Lipid Biosynthesis. *Plant Cell* **7**, 957-970.
- Okayasu, T., Kameda, K., Ono, T., and Imai, Y.** (1977). Effects of dietary Vitamin B-2 and Vitamin E on delta-9-desaturase and catalase activities in rat liver microsomes. *Biochim. Biophys. Acta* **489**, 397-402.

- Okuley, J., Lightner, J., Feldmann, K., Yadav, N., Lark, E., and Browse, J.** (1994). *Arabidopsis FAD2* gene encodes the enzyme that is essential for polyunsaturated lipid synthesis. *Plant Cell* **6**, 147-158.
- Oommen, S., Vasu, V.T., Leonard, S.W., Traber, M.G., Cross, C.E., and Gohil, K.** (2007). Genome wide responses of murine lungs to dietary alpha-tocopherol. *Free Radical Research* **41**, 98-U50.
- Orozco-Cardenas, M.L., Narvaez-Vasquez, J., and Ryan, C.A.** (2001). Hydrogen peroxide acts as a second messenger for the induction of defense genes in tomato plants in response to wounding, systemin, and methyl jasmonate. *Plant Cell* **13**, 179-191.
- Orvar, B.L., Sangwan, V., Omann, F., and Dhindsa, R.S.** (2000). Early steps in cold sensing by plant cells: the role of actin cytoskeleton and membrane fluidity. *Plant Journal* **23**, 785-794.
- Palta, J.P., Whitaker, B.D., and Weiss, L.S.** (1993). Plasma-membrane lipids associated with genetic variability in freezing tolerance and cold-acclimation of *Solanum* species. *Plant Physiology* **103**, 793-803.
- Paul, M.J., and Foyer, C.H.** (2001). Sink regulation of photosynthesis. *Journal of Experimental Botany* **52**, 1383-1400.
- Paul, M.J., and Peliny, T.K.** (2003). Carbon metabolite feedback regulation of leaf photosynthesis and development. *Journal of Experimental Botany* **54**, 539-547.
- Pichler, H., Gaigg, B., Hrastnik, C., Achleitner, G., Kohlwein, S.D., Zellnig, G., Perktold, A., and Daum, G.** (2001). A subfraction of the yeast endoplasmic reticulum associates with the plasma membrane and has a high capacity to synthesize lipids. *Eur J Biochem* **268**, 2351-2361.
- Polisensky, D.H., and Braam, J.** (1996). Cold-shock regulation of the *Arabidopsis* TCH genes and the effects of modulating intracellular calcium levels. *Plant Physiology* **111**, 1271-1279.
- Porfirova, S., Bergmuller, E., Tropf, S., Lemke, R., and Dormann, P.** (2002). Isolation of an *Arabidopsis* mutant lacking vitamin E and identification of a cyclase essential for all tocopherol biosynthesis. *Proc Natl Acad Sci U S A* **99**, 12495-12500.

- Pratico, D., Tangirala, R.K., Rader, D.J., Rokach, J., and FitzGerald, G.A. (1998).** Vitamin E suppresses isoprostane generation *in vivo* and reduces atherosclerosis in ApoE-deficient mice. *Nature Medicine* **4**, 1189-1192.
- Provencher, L.M., Miao, L., Sinha, N., and Lucas, W.J. (2001).** Sucrose export defective1 encodes a novel protein implicated in chloroplast-to-nucleus signaling. *Plant Cell* **13**, 1127-1141.
- Rautenkranz, A.A.F., Li, L.J., Machler, F., Martinoia, E., and Oertli, J.J. (1994).** Transport of ascorbic and dehydroascorbic acids across protoplast and vacuole membranes isolated from barley (*Hordeum vulgare* L Cv Gerbel) Leaves. *Plant Physiol.* **106**, 187-193.
- Ricciarelli, R., Zingg, J.M., and Azzi, A. (2000).** Vitamin E reduces the uptake of oxidized LDL by inhibiting CD36 scavenger receptor expression in cultured aortic smooth muscle cells. *Circulation* **102**, 82-87.
- Ricciarelli, R., Maroni, P., Ozer, N., Zingg, J.M., and Azzi, A. (1999).** Age-dependent increase of collagenase expression can be reduced by alpha-tocopherol via protein kinase C inhibition. *Free Radical Biology and Medicine* **27**, 729-737.
- Ricciarelli, R., Tasinato, A., Clement, S., Ozer, N.K., Boscoboinik, D., and Azzi, A. (1998).** alpha-Tocopherol specifically inactivates cellular protein kinase C alpha by changing its phosphorylation state. *Biochem. J.* **334**, 243-249.
- Richmond, T.A., and Somerville, C.R. (2000).** The cellulose synthase superfamily. *Plant Physiology* **124**, 495-498.
- Rimbach, G., Minihane, A.M., Majewicz, J., Fischer, A., Pallauf, J., Virgli, F., and Weinberg, P.D. (2002).** Regulation of cell signalling by vitamin E. *Proc Nutr Soc* **61**, 415-425.
- Robinson, J.M. (1988).** Does O₂ photoreduction occur within chloroplasts *in vivo*? *Physiol Plant* **72**, 666-680.
- Romero, H.M., Berlett, B.S., Jensen, P.J., Pell, E.J., and Tien, M. (2004).** Investigations into the role of the plastidial peptide methionine sulfoxide reductase in response to oxidative stress in *Arabidopsis*. *Plant Physiology* **136**, 3784-3794.

- Rota, C., Barella, L., Minihane, A.M., Stocklin, E., and Rimbach, G.** (2004). Dietary alpha-tocopherol affects differential gene expression in rat testes. *IUBMB Life* **56**, 277-280.
- Rota, C., Rimbach, G., Minihane, A.M., Stoecklin, E., and Barella, L.** (2005). Dietary vitamin E modulates differential gene expression in the rat hippocampus: Potential implications for its neuroprotective properties. *Nutritional Neuroscience* **8**, 21-29.
- Rouanet, C., and Nasser, W.** (2001). The PecM protein of the phytopathogenic bacterium *Erwinia chrysanthemi*, membrane topology and possible involvement in the efflux of the blue pigment indigoidine. *Journal of Molecular Microbiology and Biotechnology* **3**, 309-318.
- Roughan, P.G., and Slack, C.R.** (1982). Cellular organization of glycerolipid metabolism. *Annual Review of Plant Physiology and Plant Molecular Biology* **33**, 97-132.
- Rouhier, N., Vieira Dos Santos, C., Tarrogo, L., and Rey, P.** (2006). Plant methionine sulfoxide reductase A and B multigenic families. *Photosynthesis Research*, 247-262.
- Routaboul, J.M., and Browse, J.** (2002). Trienoic fatty acids and plant tolerance of temperature. *Ocl-Oleagineux Corps Gras Lipides* **9**, 43-47.
- Ruby, J.R., Dyer, R.F., and Skalko, R.G.** (1969). Continuities between mitochondria and endoplasmic reticulum in mammalian ovary. *Zeitschrift Fur Zellforschung Und Mikroskopische Anatomie* **97**, 30-&.
- Russell, S., Meadows, L.A., and Russell, R.R.** (2009). *Microarray technology in practice.* (Amsterdam, Boston, Heidelberg, London, New York, Oxford, Paris, San Diego, San Francisco, Singapore, Sydney, Tokyo: Elsevier).
- Russin, W.A., Evert, R.F., Vanderveer, P.J., Sharkey, T.D., and Briggs, S.P.** (1996). Modification of a specific class of plasmodesmata and loss of sucrose export ability in the sucrose export defective1 maize mutant. *Plant Cell* **8**, 645-658.
- Sadanandom, A., Poghosyan, Z., Fairbairn, D.J., and Murphy, D.J.** (2000). Differential regulation of plastidial and cytosolic isoforms of peptide methionine sulfoxide reductase in *Arabidopsis*. *Plant Physiology* **123**, 255-263.

- Sage, T.L., and Williams, E.G.** (1995). Structure, ultrastructure, and histochemistry of the pollen tube pathway in the milkweed *Asclepias exaltata* L. Sexual Plant Reproduction **8**, 257-265.
- Salgado, J., Villalain, J., and Gomezfernandez, J.C.** (1993). Alpha-tocopherol interacts with natural micelle-forming single-chain phospholipids stabilizing the bilayer phase. Arch. Biochem. Biophys. **306**, 368-376.
- SanchezMigallon, M., Aranda, F.J., and GomezFernandez, J.C.** (1996). Interaction between alpha-tocopherol and heteroacid phosphatidylcholines with different amounts of unsaturation. Biochimica Et Biophysica Acta-Biomembranes **1279**, 251-258.
- Sangwan, V., Foulds, I., Singh, J., and Dhindsa, R.S.** (2001). Cold-activation of *Brassica napus* BN115 promoter is mediated by structural changes in membranes and cytoskeleton, and requires Ca²⁺ influx. Plant Journal **27**, 1-12.
- Sattler, S.E., Cahoon, E.B., Coughlan, S.J., and DellaPenna, D.** (2003a). Characterization of tocopherol cyclases from higher plants and cyanobacteria. Evolutionary implications for tocopherol synthesis and function. Plant Physiology **132**, 2184-2195.
- Sattler, S.E., Gilliland, L.U., Magallanes-Lundback, M., Pollard, M., and DellaPenna, D.** (2004). Vitamin E is essential for seed longevity, and for preventing lipid peroxidation during germination. Plant Cell **16**, 1419-1432.
- Sattler, S.E., Mene-Saffrane, L., Farmer, E.E., Krischke, M., Mueller, M.J., and DellaPenna, D.** (2006). Nonenzymatic lipid peroxidation reprograms gene expression and activates defense markers in *Arabidopsis* tocopherol-deficient mutants. Plant Cell **18**, 3706-3720.
- Schmid, P.C., Deli, E., and Schmid, H.H.O.** (1995). Generation and remodeling of phospholipid molecular species in rat hepatocytes. Archives of Biochemistry and Biophysics **319**, 168-176.
- Schneider, C.** (2005). Chemistry and biology of vitamin E. Mol Nutr Food Res **49**, 7-30.
- Schwender, J., Seemann, M., Lichtenthaler, H.K., and Rohmer, M.** (1996). Biosynthesis of isoprenoids (carotenoids, sterols, prenyl side-chains of chlorophylls

and plastoquinone) via a novel pyruvate/glyceraldehyde 3-phosphate non-mevalonate pathway in the green alga *Scenedesmus obliquus*. *Biochem. J.* **316**, 73-80.

Sharkey, T.D., Stitt, M., Heineke, D., Gerhardt, R., Raschke, K., and Heldt, H.W. (1986). Limitation of photosynthesis by carbon metabolism. 2. O²-insensitive CO₂ uptake results from limitation of triose phosphate utilization. *Plant Physiology* **81**, 1123-1129.

Shih, J.C.H., Jonas, R.H., and Scott, M.L. (1977). Oxidative deterioration of muscle proteins during nutritional muscular dystrophy in chicks. *Journal of Nutrition* **107**, 1786-1791.

Shintani, D., and DellaPenna, D. (1998). Elevating the vitamin E content of plants through metabolic engineering. *Science* **282**, 2098-2100.

Shintani, D.K., Cheng, Z.G., and DellaPenna, D. (2002). The role of 2-methyl-6-phytylbenzoquinone methyltransferase in determining tocopherol composition in *Synechocystis* sp PCC6803. *FEBS Lett* **511**, 1-5.

Simons, K., and Toomre, D. (2000). Lipid rafts and signal transduction. *Nat Rev Mol Cell Biol* **1**, 31-39.

Slack, C.R., Roughan, P.G., and Balasingham, N. (1977). Labeling studies *in vivo* on metabolism of acyl and glycerol moieties of glycerolipids in developing maize leaf. *Biochemical Journal* **162**, 289-296.

Smyth, G.K. (2005). Limma: Linear models for microarray data. In *Bioinformatics and Computational Biology Solutions Using R and Bioconductor*, V.C. R. Gentleman, S. Dudoit, R. Irizarry, and W. Huber, ed (New York: Springer), pp. 397-420.

Soll, J. (1987). Alpha-tocopherol and plastoquinone synthesis in chloroplast membranes. *Methods Enzymol* **148**, 383-392.

Soll, J., Douce, R., and Schultz, G. (1980a). Site of biosynthesis of alpha-tocopherol in spinach chloroplasts. *FEBS Lett* **112**, 243-246.

Soll, J., Kemmerling, M., and Schultz, G. (1980b). Tocopherol and plastoquinone synthesis in spinach chloroplasts subfractions. *Arch. Biochem. Biophys.* **204**, 544-550.

- Soll, J., Douce, R., and Schultz, G.** (1980c). Site of biosynthesis of alpha-tocopherol in spinach-chloroplasts. *Febs Letters* **112**, 243-246.
- Soll, J., Schultz, G., Joyard, J., Douce, R., and Block, M.A.** (1985). Localization and synthesis of prenylquinones in isolated outer and inner envelope membranes from spinach-chloroplasts. *Archives of Biochemistry and Biophysics* **238**, 290-299.
- Somerville, C., and Browse, J.** (1991). Plant Lipids - Metabolism, Mutants, and Membranes. *Science* **252**, 80-87.
- Stillwell, W., Ehringer, W., and Wassall, S.R.** (1992). Interaction of alpha-tocopherol with fatty acids in membranes and ethanol. *Biochimica Et Biophysica Acta* **1105**, 237-244.
- Stillwell, W., Dallman, T., Dumauual, A.C., Crump, F.T., and Jenki, L.J.** (1996). Cholesterol versus alpha-tocopherol: Effects on properties of bilayers made from heteroacid phosphatidylcholines. *Biochemistry* **35**, 13353-13362.
- Stitt, M.** (1991). Rising CO₂ levels and their potential significance for carbon flow in photosynthetic cells. *Plant Cell and Environment* **14**, 741-762.
- Stitt, M.** (1996). Plasmodesmata play an essential role in sucrose export from leaves: A step toward an integration of metabolic biochemistry and cell biology. *Plant Cell* **8**, 565-571.
- Stitt, M., Grosse, H., and Woo, K.C.** (1988). Interactions between sucrose synthesis and CO₂ fixation. 2. Alterations of fructose 2,6-bisphosphate during photosynthetic oscillations. *Journal of Plant Physiology* **133**, 138-143.
- Strand, A., Hurry, V., Gustafsson, P., and Gardestrom, P.** (1997). Development of *Arabidopsis thaliana* leaves at low temperatures releases the suppression of photosynthesis and photosynthetic gene expression despite the accumulation of soluble carbohydrates. *Plant Journal* **12**, 605-614.
- Strand, A., Hurry, V., Henkes, S., Huner, N., Gustafsson, P., Gardestrom, P., and Stitt, M.** (1999a). Acclimation of *Arabidopsis* leaves developing at low temperatures. Increasing cytoplasmic volume accompanies increased activities of enzymes in the Calvin cycle and in the sucrose-biosynthesis pathway. *Plant Physiology* **119**, 1387-1397.

- Sung, D.Y., Kaplan, F., Lee, K.J., and Guy, C.L. (2003).** Acquired tolerance to temperature extremes. *Trends in Plant Science* **8**, 179-187.
- Suzuki, I., Los, D.A., Kanesaki, Y., Mikami, K., and Murata, N. (2000).** The pathway for perception and transduction of low-temperature signals in *Synechocystis*. *Embo Journal* **19**, 1327-1334.
- Suzuki, I., Kanesaki, Y., Mikami, K., Kanehisa, M., and Murata, N. (2001).** Cold-regulated genes under control of the cold sensor Hik33 in *Synechocystis*. *Molecular Microbiology* **40**, 235-244.
- Tahtiharju, S., Sangwan, V., Monroy, A.F., Dhindsa, R.S., and Borg, M. (1997).** The induction of kin genes in cold-acclimating *Arabidopsis thaliana*. Evidence of a role for calcium. *Planta* **203**, 442-447.
- Taji, T., Ohsumi, C., Seki, M., Iuchi, S., Yamaguchi-Shinozaki, K., and Shinozaki, K. (2002).** Important roles of drought- and cold-inducible genes for galactinol synthase in stress tolerance in *Arabidopsis thaliana*. *Plant and Cell Physiology* **43**, S233-S233.
- Tanaka, K., Fukuda, R., Ono, Y., Eguchi, H., Nagasawa, S., Nakatani, Y., Watanabe, H., Nakanishi, H., Taguchi, R., and Ohta, A. (2008).** Incorporation and remodeling of extracellular phosphatidylcholine with short acyl residues in *Saccharomyces cerevisiae*. *Biochimica Et Biophysica Acta-Molecular and Cell Biology of Lipids* **1781**, 391-399.
- Tasinato, A., Boscoboinik, D., Bartoli, G.M., Maroni, P., and Azzi, A. (1995).** d-alpha-tocopherol inhibition of vascular smooth muscle cell proliferation occurs at physiological concentrations, correlates with protein kinase C inhibition, and is independent of its antioxidant properties. *Proc Natl Acad Sci U S A* **92**, 12190-12194.
- Thion, L., Mazars, C., Thuleau, P., Graziana, A., Rossignol, M., Moreau, M., and Ranjeva, R. (1996).** Activation of plasma membrane voltage-dependent calcium-permeable channels by disruption of microtubules in carrot cells. *FEBS Letters* **393**, 13-18.
- Thomashow, M.F. (1999).** Plant cold acclimation: Freezing tolerance genes and regulatory mechanisms. *Annual Review of Plant Physiology and Plant Molecular Biology* **50**, 571-599.

- Thomashow, M.F.** (2001). So what's new in the field of plant cold acclimation? Lots! *Plant Physiology* **125**, 89-93.
- Thomashow, M.F., Stockinger, E.J., Jaglo-Ottosen, K.R., Gilmour, S.J., and Zarka, D.G.** (1997). Function and regulation of *Arabidopsis thaliana* COR (cold-regulated) genes. *Acta Physiologiae Plantarum* **19**, 497-504.
- Tian, L., and DellaPenna, D.** (2001). Characterization of a second carotenoid beta-hydroxylase gene from *Arabidopsis* and its relationship to the LUT1 locus. *Plant Molecular Biology* **47**, 379-388.
- Toller, A., Brownfield, L., Neu, C., Twell, D., and Schulze-Lefert, P.** (2008). Dual function of *Arabidopsis* glucan synthase-like genes GSL8 and GSL10 in male gametophyte development and plant growth. *Plant Journal* **54**, 911-923.
- Towfighi, J.** (1981). Effects of chronic vitamin-e-deficiency on the nervous system of the rat. *Acta Neuropathologica* **54**, 261-267.
- Traber, M.G., Burton, G.W., and Hamilton, R.L.** (2004). Vitamin E trafficking. *Vitamin E and Health* **1031**, 1-12.
- Trebst, A., Depka, B., and Hollander-Czytko, H.** (2002). A specific role for tocopherol and of chemical singlet oxygen quenchers in the maintenance of photosystem II structure and function in *Chlamydomonas reinhardtii*. *FEBS Letters* **516**, 156-160.
- Tucker, A.M., Winkler, H.H., Driskell, L.O., and Wood, D.O.** (2003). S-adenosylmethionine transport in *Rickettsia prowazekii*. *Journal of Bacteriology* **185**, 3031-3035.
- Uemura, M., and Steponkus, P.L.** (1997). Effect of cold acclimation on the lipid composition of the inner and outer membrane of the chloroplast envelope isolated from rye leaves. *Plant Physiol.* **114**, 1493-1500.
- Uemura, M., Joseph, R.A., and Steponkus, P.L.** (1995). Cold acclimation of *Arabidopsis thaliana* - Effect on plasma-membrane lipid composition and freeze-induced lesions. *Plant Physiology* **109**, 15-30.
- Ulker, B., and Somssich, I.E.** (2004). WRKY transcription factors: from DNA binding towards biological function. *Current Opinion in Plant Biology* **7**, 491-498.

- Urano, S., Yano, K., and Matsuo, M.** (1988). Membrane-stabilizing effect of Vitamin E - effect of alpha-tocopherol and its model compounds on fluidity of lecithin liposomes. *Biochem. Biophys. Res. Commun.* **150**, 469-475.
- Valentin, H.E., Lincoln, K., Moshiri, F., Jensen, P.K., Qi, Q.G., Venkatesh, T.V., Karunanandaa, B., Baszis, S.R., Norris, S.R., Savidge, B., Gruys, K.J., and Last, R.L.** (2006). The Arabidopsis vitamin E pathway gene 5-1 mutant reveals a critical role for phytol kinase in seed tocopherol biosynthesis. *Plant Cell* **18**, 212-224.
- Vanbel, A.J.E.** (1993). Strategies of phloem loading. *Annual Review of Plant Physiology and Plant Molecular Biology* **44**, 253-281.
- Vandewiel, C., Norris, J.H., Bochenek, B., Dickstein, R., Bisseling, T., and Hirsch, A.M.** (1990). Nodulin gene expression and Enod2 localization in effective, nitrogen-fixing and ineffective, bacteria-free nodules of alfalfa. *Plant Cell* **2**, 1009-1017.
- Vasu, V.T., Hobson, B., Gohil, K., and Cross, C.E.** (2007). Genome-wide screening of alpha-tocopherol sensitive genes in heart tissue from alpha-tocopherol transfer protein null mice (ATTP(-/-)). *FEBS Letters* **581**, 1572-1578.
- Vasu, V.T., Ott, S., Hobson, B., Rashidi, V., Oommen, S., Cross, C.E., and Gohil, K.** (2009). Sarcolipin and ubiquitin carboxy-terminal hydrolase 1 mRNAs are over-expressed in skeletal muscles of alpha-tocopherol deficient mice. *Free Radical Research* **43**, 106-116.
- Vidi, P.A., Kanwischer, M., Baginsky, S., Austin, J.R., Csucs, G., Dormann, P., Kessler, F., and Brehelin, C.** (2006). Tocopherol cyclase (VTE1) localization and vitamin E accumulation in chloroplast plastoglobule lipoprotein particles. *Journal of Biological Chemistry* **281**, 11225-11234.
- Vogel, J.T., Zarka, D.G., Van Buskirk, H.A., Fowler, S.G., and Thomashow, M.F.** (2005). Roles of the CBF2 and ZAT12 transcription factors in configuring the low temperature transcriptome of *Arabidopsis*. *Plant Journal* **41**, 195-211.
- Wallis, J.G., and Browse, J.** (2002). Mutants of *Arabidopsis* reveal many roles for membrane lipids. *Prog Lipid Res* **41**, 254-278.
- Wang, Q.Y., and Nick, P.** (2001). Cold acclimation can induce microtubular cold stability in a manner distinct from abscisic acid. *Plant and Cell Physiology* **42**, 999-1005.

- Wang, X.M., Li, W.Q., Li, M.Y., and Welti, R.** (2006). Profiling lipid changes in plant response to low temperatures. *Physiologia Plantarum* **126**, 90-96.
- Wang, X.Y., and Quinn, P.J.** (2000). The location and function of vitamin E in membranes (review). *Molecular Membrane Biology* **17**, 143-156.
- Wanner, L.A., and Junttila, O.** (1999). Cold-induced freezing tolerance in Arabidopsis. *Plant Physiology* **120**, 391-399.
- Wassall, S.R., Thewalt, J.L., Wong, L., Gorrissen, H., and Cushley, R.J.** (1986). Deuterium NMR-study of the Interaction of alpha-tocopherol with a phospholipid model membrane. *Biochemistry* **25**, 319-326.
- Wasteneys, G.O., and Galway, M.E.** (2003). Remodelling the cytoskeleton for growth and form: An overview with some new views. *Annual Review of Plant Biology* **54**, 691-722.
- Weigel, D., Ahn, J.H., Blazquez, M.A., Borevitz, J.O., Christensen, S.K., Fankhauser, C., Ferrandiz, C., Kardailsky, I., Malancharuvil, E.J., Neff, M.M., Nguyen, J.T., Sato, S., Wang, Z.Y., Xia, Y.J., Dixon, R.A., Harrison, M.J., Lamb, C.J., Yanofsky, M.F., and Chory, J.** (2000). Activation tagging in Arabidopsis. *Plant Physiol.* **122**, 1003-1013.
- Weiss, L.S., Whitaker, B.D., and Palta, J.P.** (1993). Temporal changes in plasma membrane lipids during cold-acclimation of potato species differing in acclimation capacity. *Plant Physiology* **102**, 84-84.
- Weissbach, H., Etienne, F., Hoshi, T., Heinemann, S.H., Lowther, W.T., Matthews, B., St John, G., Nathan, C., and Brot, N.** (2002). Peptide methionine sulfoxide reductase: Structure, mechanism of action, and biological function. *Archives of Biochemistry and Biophysics* **397**, 172-178.
- Welti, R., Li, W.Q., Li, M.Y., Sang, Y.M., Biesiada, H., Zhou, H.E., Rajashekar, C.B., Williams, T.D., and Wang, X.M.** (2002). Profiling membrane lipids in plant stress responses - Role of phospholipase D alpha in freezing-induced lipid changes in Arabidopsis. *Journal of Biological Chemistry* **277**, 31994-32002.
- Whistanc, G., and Threlfal, D.** (1970). Biosynthesis of phytoquinones - homogentisic acid - a precursor of plastoquinones, tocopherols and alpha-tocopherolquinone in higher plants, green algae and blue-green algae. *Biochemical Journal* **117**, 593-&.

- White, D.A., Fisk, I.D., and Gray, D.A.** (2006). Characterisation of oat (*Avena sativa* L.) oil bodies and intrinsically associated E-vitamins. *J Cereal Sci* **43**, 244-249.
- Williams, J.P., Khan, M.U., and Wong, D.** (1992). Low temperature-induced fatty acid desaturation in *Brassica napus* - Thermal deactivation and reactivation of the process. *Biochimica Et Biophysica Acta* **1128**, 275-279.
- Williams, J.P., Khan, M.U., Mitchell, K., and Johnson, G.** (1988). The effect of temperature on the level and biosynthesis of unsaturated fatty acids in diacylglycerols of *Brassica napus* leaves. *Plant Physiol.* **87**, 904-910.
- Williams, J.P., Imperial, V., Khan, M.U., and Hodson, J.N.** (2000). The role of phosphatidylcholine in fatty acid exchange and desaturation in *Brassica napus* L. leaves. *Biochemical Journal* **349**, 127-133.
- Wise, R.R., and Naylor, A.W.** (1987). Chilling-enhanced photooxidation-evidence for the role of singlet oxygen and superoxide in the breakdown of pigments and endogenous antioxidants. *Plant Physiol.* **83**, 278-282.
- Wolff, S.P.** (1994). Ferrous Ion Oxidation in Presence of Ferric Ion Indicator Xylenol Orange for Measurement of Hydroperoxides. *Oxygen Radicals in Biological Systems, Pt C* **233**, 182-189.
- Wu, J.R., and Browse, J.** (1995). Elevated levels of high-melting-point phosphatidylglycerols do not induce chilling sensitivity in an *Arabidopsis* mutant. *Plant Cell* **7**, 17-27.
- Wu, J.R., Lightner, J., Warwick, N., and Browse, J.** (1997). Low-temperature damage and subsequent recovery of *fab1* mutant *Arabidopsis* exposed to 2 degrees C. *Plant Physiology* **113**, 347-356.
- Xin, Z., and Browse, J.** (2000). Cold comfort farm: the acclimation of plants to freezing temperatures. *Plant Cell and Environment* **23**, 893-902.
- Xin, Z.G., and Browse, J.** (1998). *eskimo1* mutants of *Arabidopsis* are constitutively freezing-tolerant. *Proc Natl Acad Sci U S A* **95**, 7799-7804.
- Xiong, L.M., Schumaker, K.S., and Zhu, J.K.** (2002). Cell signaling during cold, drought, and salt stress. *Plant Cell* **14**, S165-S183.

- Xu, C.C., Fan, J.L., Cornish, A.J., and Benning, C. (2008).** Lipid trafficking between the endoplasmic reticulum and the plastid in *Arabidopsis* requires the extraplastidic TGD4 protein. *Plant Cell* **20**, 2190-2204.
- Xu, C.C., Fan, J.L., Riekhof, W., Froehlich, J.E., and Benning, C. (2003a).** An *Arabidopsis* chloroplast outer envelope permease/flippase, TGD1, involved in interorganelle lipid trafficking. *FASEB J* **17**, A1319-a1319.
- Xu, C.C., Fan, J.L., Riekhof, W., Froehlich, J.E., and Benning, C. (2003b).** A permease-like protein involved in ER to thylakoid lipid transfer in *Arabidopsis*. *EMBO J.* **22**, 2370-2379.
- Xu, C.C., Fan, J., Froehlich, J.E., Awai, K., and Benning, C. (2005).** Mutation of the TGD1 chloroplast envelope protein affects phosphatidate metabolism in *Arabidopsis*. *Plant Cell* **17**, 3094-3110.
- Yamauchi, R., and Matsushita, S. (1976).** Tocopherol contents of vegetables and fruits. *J. Agric. Chem. Soc. Japan* **50**, 569-570.
- Yokota, T., Igarashi, K., Uchihara, T., Jishage, K., Tomita, H., Inaba, A., Li, Y., Arita, M., Suzuki, H., Mizusawa, H., and Arai, H. (2001a).** Delayed-onset ataxia in mice lacking alpha-tocopherol transfer protein: Model for neuronal degeneration caused by chronic oxidative stress. *Proc Natl Acad Sci U S A* **98**, 15185-15190.
- Yoshiba, Y., Aoki, C., Iuchi, S., Nanjo, T., Seki, M., Sekiguchi, F., Yamaguchi-Shinozaki, K., and Shinozaki, K. (2001).** Characterization of four extensin genes in *Arabidopsis thaliana* by differential gene expression under stress and non-stress conditions. *DNA Research* **8**, 115-122.
- Zarka, D.G., Vogel, J.T., Cook, D., and Thomashow, M.F. (2003).** Cold induction of *Arabidopsis* CBF genes involves multiple ICE (Inducer of CBF expression) promoter elements and a cold-regulatory circuit that is desensitized by low temperature. *Plant Physiology* **133**, 910-918.
- Zimmermann, P., Hirsch-Hoffmann, M., Hennig, L., and Gruissem, W. (2004).** GENEVESTIGATOR. *Arabidopsis* microarray database and analysis toolbox. *Plant Physiology* **136**, 2621-2632.
- Zingg, J.M., and Azzi, A. (2004).** Non-antioxidant activities of vitamin E. *Curr Med Chem* **11**, 1113-1133.

MICHIGAN STATE UNIVERSITY LIBRARIES



3 1293 03063 1422